

F L U I D F L O W D I V E R S I O N

A Summary and Bibliography of Literature

by

St. Anthony Falls Hydraulic Laboratory  
University of Minnesota

Project Report No. 1

Submitted by  
Lorenz G. Straub  
Director

Prepared by  
Alvin G. Anderson

August, 1947

Prepared for the  
David Taylor Model Basin  
Navy Department  
Washington, D.C.

Under Bureau of Ships Contract NObS-34208  
Task Order 1

## P R E F A C E

Under Contract NObs-34208 between the University of Minnesota and the Bureau of Ships, Task Order 1 was submitted on July 31, 1946, by the David Taylor Model Basin. It called for services to be rendered by the St. Anthony Falls Hydraulic Laboratory under the following specifications:

"Analyze the fundamental mechanics of altering or diverting fluid flow streams, review the existing literature relating to the problem, prepare a selected bibliography with collected papers, correlate and extend the existing theory, perform exploratory tests and prepare a program for the advancement of this knowledge founded on theoretical considerations and allied empirical confirmation.

"This program is intended to provide a general study of the problem of directing or diverting fluid flows with special emphasis on the use of guide vane systems and with the eventual purpose of determining and presenting fundamental information suitable for use in other more specific research or practical engineering applications."

The investigations at the David Taylor Model Basin in the design of hydraulic facilities and devices embodying the directional diversion of flowing water disclosed that there was inadequate information available on which to base economical designs offering a reasonable assurance of desired flow control. This task order was the result.

This report is a summary and bibliography of the subject as specified in the contract. It has been written by Alvin G. Anderson. He was assisted by Meir Pilch and Owen Lamb in library research, by William Dingman in preparation of the illustrations, and by Mary H. Marsh in manuscript preparation. The study was prepared under the supervision of Dr. Lorenz G. Straub, Director of St. Anthony Falls Hydraulic Laboratory, and John F. Ripken, Assistant Professor of Hydraulics.

C O N T E N T S

	Page
Summary of Literature . . . . .	1
Introduction . . . . .	1
I. Flow Through Conduit Bends . . . . .	2
A. General . . . . .	2
B. Development of Secondary Currents . . . . .	2
C. Velocity Distribution . . . . .	3
D. Pressure Distribution . . . . .	7
E. Laminar-Turbulent Critical . . . . .	8
F. Effect of Aspect Ratio on Secondary Currents . . . . .	9
G. Transition from Curved Flow to Straight Flow after a Bend . . . . .	10
H. Energy Loss caused by Bends . . . . .	11
I. Effect of Reynolds Number on the Bend Coefficient . . . . .	15
J. Effect of Curvature Ratio on Bend Coefficient . . . . .	15
K. Effect of Roughness on the Bend Coefficient . . . . .	17
L. Effect of Deflection Angle on the Bend Coefficient . . . . .	17
M. Effect of Aspect Ratio on the Bend Coefficient . . . . .	17
N. Effect of Combinations of Bends on the Bend Coefficient . . . . .	19
II. Flow Through Conduit Bends with Guide Vanes . . . . .	20
A. General . . . . .	20
B. Effect of Vane Shape upon Velocity Distribution . . . . .	21
C. Effect of Vane Shape of the Pressure Loss . . . . .	22
D. Effect of Spacing on Velocity Distribution and Pressure Loss . . . . .	23
E. Effect of Angle of Attack on Velocity Distribution and Pressure Loss . . . . .	25
F. Pressure Distribution around the Vane Profile . . . . .	25
G. Irregularly Spaced Vanes . . . . .	25
H. Corner Expansions . . . . .	25
I. Theoretical Investigations . . . . .	26
III. Flow in Open-Channel Bends . . . . .	27
A. General . . . . .	27
B. Transverse Slope . . . . .	28
C. Observations on Secondary Currents . . . . .	29
D. Cross-Sectional Shape in Erodible Beds . . . . .	30
E. Head Loss caused by Open-Channel Bends . . . . .	31
F. Supercritical Flow in Open-Channel Bends . . . . .	31
Conclusion . . . . .	33
Bibliography . . . . .	34
I. Flow Through Conduit Bends . . . . .	35
II. Flow Through Conduit Bends with Guide Vanes . . . . .	53
III. Flow in Open-Channel Bends . . . . .	58
Appendix, Abstracts . . . . .	62
Index to Abstracts . . . . .	62
I. Flow Through Conduit Bends . . . . .	64
II. Flow Through Conduit Bends with Guide Vanes . . . . .	162
III. Flow in Open-Channel Bends . . . . .	210

# S U M M A R Y   O F   L I T E R A T U R E

## INTRODUCTION

A knowledge of the motion of a fluid as it undergoes a change in direction, and of the energy and pressure variations which accompany the directional diversion has many applications in engineering practice. The designing of duct and piping systems requires a knowledge of the pressure losses incurred in the flow of a fluid around a bend. In large installations, it may be necessary to investigate means of reducing the pressure losses in elbows from the standpoint of power requirements. In installations such as wind tunnels and water tunnels constructed for aerodynamic and hydrodynamic research, the requirements for uniform velocity distribution and parallel flow downstream from the bend are greater than pressure considerations, and a knowledge of the effects of guide vanes on flow around a corner is important. The efficiency of pumps, turbines, propellers, and fans is influenced by the relationships between curvature of the streamlines and the resulting pressures and velocities.

In natural streams and in artificial channels, bends are the cause of unsymmetrical velocity distribution, of local changes in slopes, and of secondary currents. Meandering of streams in erodible beds is the result of forces generated by bends, and a knowledge of these forces is necessary to the design of artificial channels.

The literature indicates that research into the mechanics of flow around bends has been carried on for several centuries but that it has intensified only during the last few decades. The early works were directed mainly toward measurement of the losses of pressure caused by bends in conduits for the purpose of supplying specific design data. More recently, encouraged by the greatly increased use of wind tunnels, the emphasis in research has been placed upon the development of guide vanes for the dual purpose of reducing the losses and of improving the velocity distribution downstream of bends. Guide vane study has been encouraged further by the application of airfoil theory to the design of turbines and pumps.

This report is a partial fulfillment of Task Order #1 dated July 31, 1946, under terms of Contract NObs-34208 between the University of Minnesota and the Bureau of Ships, Navy Department. The specifications stated in

part "...review the existing literature relating to the problem (of diverting fluid flow streams), prepare a selected bibliography with collected papers..." The report is limited to an examination of the literature pertaining to directional flow diversion by means of stationary boundaries such as pipe bends, tunnel corners, and open channel bends. In addition, there is discussed the related problem of flow through vanes of turbines, pumps, fans, and propellers to the extent that the boundaries of the flow, for purposes of analysis, can be considered as stationary. The review also extends to papers covering research and analysis leading to the development of guide vanes for improving conditions at corners.

## I. FLOW THROUGH CONDUIT BENDS

### A. General

Theory and experiment show that when a fluid flows under pressure in a straight horizontal conduit of constant cross section, the pressure decreases in the direction of flow in consequence of the energy loss resulting from fluid friction. A fluid layer of molecular thickness adheres to the wall and remains at rest with respect to it. Thus, when the flow pattern is fully established, the velocity at any cross section increases from zero at the wall to a maximum at the center in a curve symmetrical about the axis of the conduit. If the flow is laminar, the velocity profile is parabolic and the loss of energy is brought about by the internal friction within the viscous fluid. If the flow is turbulent, the loss of energy is greater and results mainly from the turbulent mixing of the fluid, the viscous resistance being small compared to the resistance caused by the turbulent mixing. The velocity profile is flatter near the center and steeper near the walls than in laminar flow.

### B. Development of Secondary Currents

If the conduit is curved, the velocity profile will no longer be symmetrical about the axis of the conduit. The centrifugal forces resulting from the change in direction of the fluid motion create a transverse pressure gradient, in which the maximum pressure occurs at the outer wall and the minimum pressure at the inner wall, with a proportional decrease in velocity near the outer wall and an increase in velocity near the inner wall of the curve. Because of turbulent or viscous resistance, however, the velocities

near the walls are less than those in the central portion of the conduit, and as a result the differences in centrifugal force give rise to secondary currents. The secondary currents develop into two vortices symmetrically placed on each side of the central diameter in the plane of the bend. In a horizontal bend the fluid flows toward the inside of the bend along the top and bottom walls and thence back toward the outer wall along the central diameter. The superposition of the two vortices upon the main flow results in a double spiral that passes through the bend. The flow pattern at the boundaries of the bend is shown schematically in Fig. 1.

The secondary currents in bends have been observed by many investigators and detailed observations as to their form have been made. Taylor [103]\* observed the motion for laminar flow by introducing dye through the wall of a glass helix at a point where curvilinear flow had become established. The dye followed the wall toward the inside of the bend, moved to the outside along a diameter of the duct which lay in the plane of the bend, and then returned again to the inner side by flowing along the wall. In 1910 Eustice [37] studied the laminar-turbulent critical in bent tubes by the use of dye streams, and demonstrated the existence of secondary currents. The delineation was not clear in most cases because the dye was introduced in the body of the fluid. By introducing air into the stream through minute holes in the wall, Lell [72] was able to show the existence of spiral currents in the bend. On the basis of Lell's work, Zur Nedden [124] developed a theory for the cause of the spiral currents based on the Bernoulli equation and on the assumption of potential flow around the bend, applied to a thin layer near the top and bottom of a horizontal bend. Hinderks [61] recorded the spiral flow for turbulent conditions by painting the inside of split bends and allowing the fluid to flow over the partially dried paint. The flow pattern on the boundary was thus etched into the paint and direction could be ascertained.

### C. Velocity Distribution

Analysis by potential flow theory of the velocity distribution in the plane of the bend, neglecting the effect of the spiral currents, results in a velocity distribution in which the velocity is inversely proportional to the radius of curvature.

---

\*Numbers in brackets refer to corresponding items in the Bibliography.

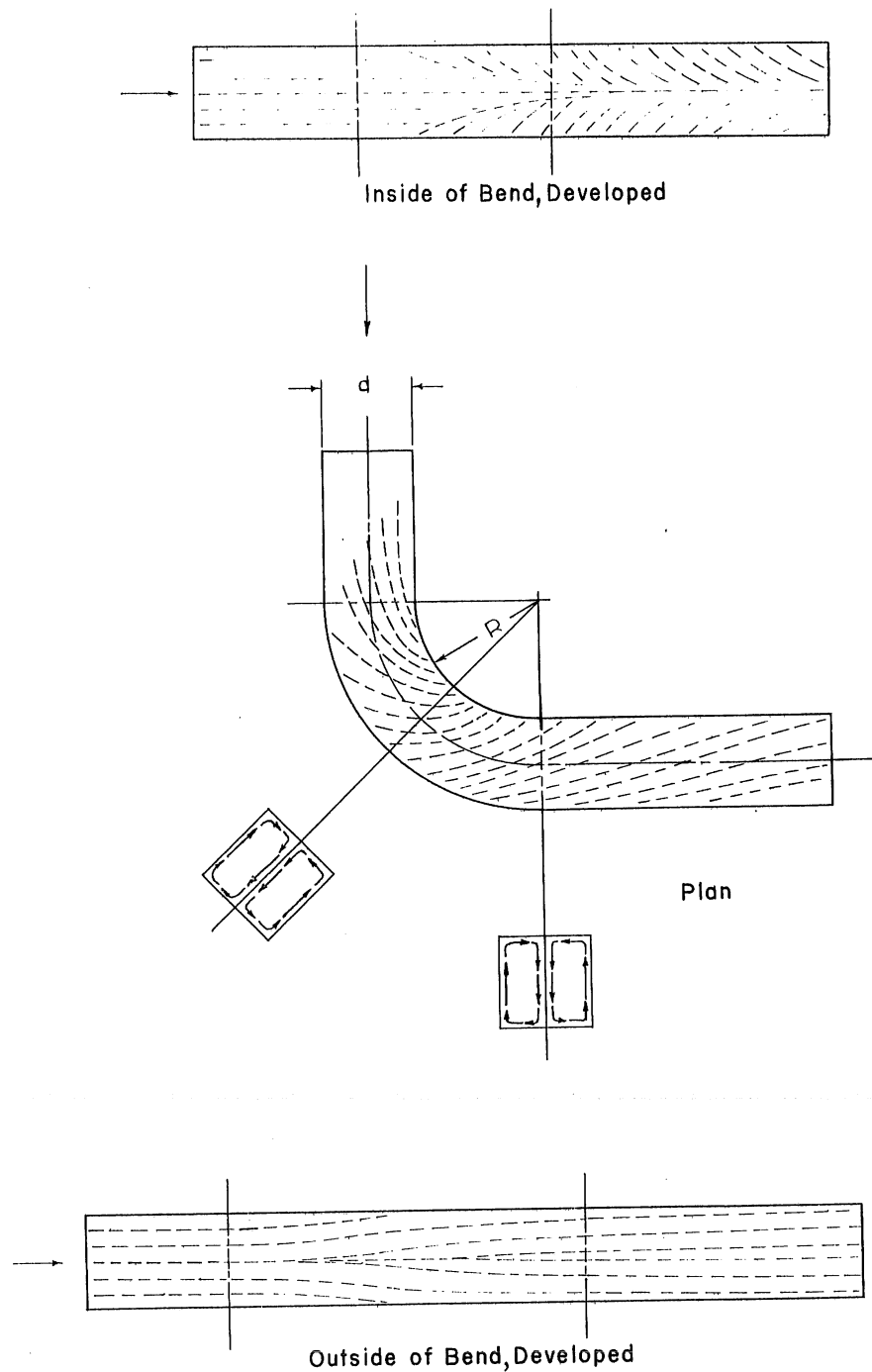


Fig.1—Schematic Diagram of Secondary Currents in a 90° Bend,  $\frac{R}{d} = 2.0$

Neglecting rotational effects and assuming that the streamlines follow concentric circles around the bend, the radial pressure gradient which balances the centrifugal force is

$$\frac{\partial P}{\partial r} = \rho \frac{V^2}{R} \quad (1)$$

where  $R$  is the radius of curvature,  $P$  is the pressure,  $V$  is the tangential velocity, and  $\rho$  is the density of the fluid. If the total energy is the same for each streamline, then

$$P + \rho V^2/2 = \text{constant} \quad (2)$$

Differentiation of equation (2) with respect to  $R$  and substitution in equation (1) results by integration in an expression of the velocity in terms of the radius of curvature of

$$VR = \text{constant} \quad (3)$$

Measurements by Wattendorf [110] in a deep, narrow channel indicated qualitative agreement with equation (3). The conduit was 5 cm wide and 90 cm deep with a 20-cm radius of curvature of the inner wall. The 18:1 ratio of depth to breadth was chosen largely in order to avoid as much as possible the formation of longitudinal vortices so that the motion in the central region could be considered two dimensional. Measurements of velocity at 30° intervals around the bend showed the transition from the normal profile of the straight section to the distorted profile resulting from the curvature. The velocity profiles are shown in Fig. 2, p. 139. The shape of the profiles remained constant after 150° of the curve had been traversed, at which point it was considered that the curvilinear flow was fully developed. In this region the theoretical velocity profile,  $VR = \text{constant}$ , was tangent to the measured velocity curve a short distance from the outer side, and departed only slightly from the measured velocity profile throughout the central portion of the channel. Near the walls the velocity decreased from the theoretical as the boundary shear influence increased.

The flow conditions are quite different in conduit bends where the depth-width ratio is smaller and secondary currents are generated. The secondary currents modify the distribution of velocity so that the profile approaches the theoretical distribution for only a short distance beyond the

beginning of the curvature. For the remaining distance around the bend, the profile appears to be the result of the secondary current effect and the potential distribution effect. In measurements of velocity along the diameter at the midpoint in the plane of the bend, Robertson [93] (Figs. 1 and 2, p. 123), showed that the velocity profile was similar to the theoretical profile, except near the walls. Yarnell's [120] measurements in six-inch pipe bends also indicated that the velocity along the inner side of the bend increased for a  $90^\circ$  or  $180^\circ$  bend, but the thread of maximum velocity in the bend gradually moved toward the outer side as the water traveled around the bend. Yarnell's work also showed that nonuniform velocity distribution in the approach channel caused abnormal velocity distribution in the bend, but the velocity still tended to increase at the inner side of the bend and to decrease along the outer side for the first part of the curve. Because of the nature of the secondary currents which move to the outside at the center of the conduit in the plane of the bend and toward the inner side along the upper and lower boundaries, the maximum velocity would be found on the outer side of the bend. Observations by Hinderks [61] indicate that the spiral currents are not evident along the outer wall until the flow reaches a point past the midsection of the bend, while along the inner wall the converging flow towards the central plane of the bend is apparent for some distance upstream of the bend. It appears that the secondary currents do not greatly influence the development of potential flow in the first part of the bend, but that they do alter significantly the distribution pattern as the flow passes around the bend.

All of these observations have been made in bends that are relatively short, that is, in  $90^\circ$  or  $180^\circ$  bends with small values of  $R/d$ , (the ratio of the mean radius of curvature to the diameter of the conduit). Therefore, in many cases the flow in the bend is in a transition stage and, because of the shortness of the bend, the flow enters the second transition stage from the bend to the straight pipe before the curvilinear flow is fully established. The measurements of Adler [3] at the end of a  $90^\circ$  bend of 1-cm inside diameter, for which the ratios of the radius of the conduit to the radius of curvature of the bend were  $1/50$ ,  $1/100$ , and  $1/200$ , showed the maximum value of the velocity profile to be between the centerline and the outside wall of the bend for both laminar and turbulent flow at Reynolds numbers ranging from 1900 to about 12,000. This is shown in Fig. 2, p. 66. The location of the measuring point was well beyond the transition segment according to the criterion of Keulegan and Beij [66], so that presumably the flow pattern was fully developed.

Comparison of the measurements of Wattendorf [110] and Adler [3] suggests that the shape of the velocity profile, at least in turbulent flow, is influenced greatly by the presence of the secondary currents. For the deep, narrow conduit where secondary currents are negligible, the velocity profile approximates that resulting from potential flow considerations. For circular conduits, or those with depth-width ratios near unity, however, the secondary currents strongly influence the velocity profile so that the point of maximum velocity shifts from a point between the centerline and the inner wall to a point between the centerline and outer wall.

#### D. Pressure Distribution

For potential flow, equation (1) represents the pressure gradient transverse to the flow in the plane of the bend. Integration of equation (1) between  $R_1$  and  $R_2$ , the radii to the inner and outer walls, and using equation (3) for the velocity distribution leads to

$$P_2 - P_1 = \frac{\rho}{2} V_o^2 R_o^2 \left( \frac{1}{R_1^2} - \frac{1}{R_2^2} \right) \quad (4)$$

where  $P_2$  and  $P_1$  are the pressures at the outer and inner walls respectively and  $R_o$  is the radius where the mean velocity  $V_o$  occurs. When  $R_2 - R_1$  is small compared to  $R_o$ , (large radius ratio), equation (4) may be expressed in approximate form as given by Lorenz [74] as

$$P_2 - P_1 = \rho \frac{V_o^2}{R_o} (R_2 - R_1) \quad (5)$$

Numerous observations of the pressures on the boundaries of conduit bends have been made. In the case of the theoretical velocity distribution, the pressure on the outside wall increases to the maximum and the pressure on the inside decreases to a minimum because of the increased velocity, in accordance with the Bernoulli equation for total energy. In Yarnell's [120] experiments, the pressure on the outside increased rather regularly to the maximum at the midpoint of the bend and then decreased to the normal pipe pressure in the downstream tangent. The pressure on the inside of the bend decreased sharply to a minimum at approximately  $22 \frac{1}{2}^\circ$  around the bend and after this point gradually increased again to that of the downstream tangent.

The longitudinal increase of pressure from the beginning of the bend on the outer wall and downstream of the midpoint on the inner wall indicates that these areas will constitute zones of separation for sufficiently high rates of flow.

For the  $45^\circ$  bend the maximum and the minimum pressures on the outer and inner walls, respectively, occurred at approximately  $22\ 1/2^\circ$ , the midpoint of the bend. Similar results were obtained by Yarnell and Woodward [122] and Kumabe [69] using rectangular cross sections with  $180^\circ$  and  $90^\circ$  deflection angles respectively. Fig. 1, p. 161, as presented by Zur Nedden [124] shows the pressure distribution in the plane of the bend based on experiments of von Cordier [108].

#### E. Laminar-Turbulent Critical

Laminar flow through bends has been more amenable to theoretical analysis than turbulent flow. However, even the theoretical analysis is so complicated by the presence of secondary currents that progress toward a complete solution has been slow. By integrating approximately the equations of motion, Dean [32] derived an expression relating the resistance in a curved pipe to that in a similar straight pipe.

By the use of this similarity criterion White [114] was able to correlate the results of his experiments on pipes of different curvatures and sizes. The results were plotted on a single curve, using as ordinates the ratio of the resistance coefficients, and as abscissas Dean's criterion,  $Re (d/2R)^{1/2}$ , where  $Re$  is Reynolds number,  $d$  is the pipe diameter, and  $R$  is the radius of the bend. At certain values, different for each bend, the curves diverged from the main curve and the ratio of the resistances increased more rapidly. White [114] deduced that this departure was connected with a change in the type of motion in the pipe and presumably the divergence occurred at the point where turbulence could be maintained in the pipe. The Reynolds number corresponding to this change was considerably above the critical Reynolds number for turbulent flow in straight pipes. Based upon this deduction, it was further concluded that for large disturbances the flow in curved pipes is more stable than the flow in straight pipes. By direct observation Taylor [103] demonstrated that the onset of turbulence in a curved pipe occurs at a higher Reynolds number than in a straight pipe. By introducing a dye through the wall of a glass helix some distance downstream from

the entrance so that entrance effects were eliminated, he was able to demonstrate the spiral currents for laminar flow and to determine the Reynolds number at which the flow became turbulent.

By reducing the entrance disturbances with a bell-mouthed entrance, Keulegan and Beij [66] were able to maintain laminar flow in a straight tube up to a Reynolds number of 9200 with correspondingly high values for the transition from laminar to turbulent flow in bends of various curvatures. Fig. 1, p. 104, which includes data from other investigators, shows the critical Reynolds number in terms of curvature ratio,  $d/2R$ .

According to potential flow theory, the streamlines past a corner are in the form of hyperbolas symmetrical about the bisector of the bend. The flow pattern through a conduit is established if two streamlines are chosen as the boundaries of the conduits. In this case, the inside and outside walls of the bend are hyperbolic in shape, and approach the tangents symmetrically. A solution for the potential flow past a corner was carried out by Szczeniowski [102] and applied to conduits where the entrance and exit velocities were the same; the solution was also obtained for increased or decreased velocity at the exit. Previously Grether [57] had compared experimentally a rectangular bend whose shape in the plane of the bend coincided with two theoretical streamlines and a simple bend of the same cross section in the form of a circular arc in the plane of the bend. It would be expected that a bend whose boundaries are defined by streamlines would cause the least resistance to the flow through the bend, inasmuch as the flow could follow the mathematical streamlines. Tests of the two bends indicated that as long as the flow was below the laminar-turbulent critical the resistance of the equipotential bend was less than the resistance of the circular bend. When the velocity was above the critical, however, the resistance of the equipotential bend became greater than that of the circular bend. A possible explanation is that in the turbulent flow the streamline pattern is destroyed, while for laminar flow the streamlines more nearly coincide with those calculated on the basis of potential flow. The presence of spiral currents precluded the possibility of potential flow in the bend. The spiral currents are the result of the resistance to flow along the walls.

#### F. Effect of Aspect Ratio on Secondary Currents

Resistance measurements on flow around a bend indicate that the aspect ratio has an important effect. The aspect ratio, which applies to

conduits of rectangular cross section, is the ratio of depth normal to the plane of the bend to the width in the plane of the bend. Wattendorf [110] found that by making the aspect ratio of the bend as much as 18:1 the influence of secondary currents was negligible as far as measurement of velocity and the pressure along the centerline of the bend were concerned. The conclusion suggested is that for large aspect ratios the intensity of the spiral currents is decreased and the influence of the spiral currents upon the velocity pattern is less marked. For bends with deflection angles of  $90^\circ$  and large aspect ratios, it is probable that the spirals do not develop fully. Thus the influence of spiral flow is not as apparent as it is for bends with a small aspect ratio.

#### G. Transition from Curved Flow to Straight Flow after a Bend

In practice the bend is usually followed by a straight conduit, which implies a transition from the distorted flow pattern of the bend to the symmetrical one of the straight pipe. The mechanics of the transition and the distance required to establish developed flow in the straight conduit depend on the flow pattern in the bend and the configuration and roughness of the boundary. Little experimental and analytical work has been done to determine the rate of decay of the induced spiral currents.

In experimental work on the resistance of bends, pressure measurements are usually observed at a point a considerable distance along the downstream tangent where it is assumed that the normal profile has again been established. On the basis of a fully developed, viscous, velocity profile characteristic of the bend, Keulegan and Beij [66] determined empirically an equation relating the effective pipe resistance coefficient in the downstream tangent to the distance along the tangent from the bend. From this equation the transition length could be calculated. Lack of experimental data prevented verification of the calculated length.

Measurement of the hydraulic gradient along the entire conduit, including the upstream and downstream tangent, allows a determination of the length of the transition section. The point on the gradient, downstream of the bend, where the slope of the gradient again becomes constant and presumably of the same slope as that of the upstream tangent may be taken as the end of the transition segment. The difference in elevation of the two gradients, the upstream gradient being extended downstream at its constant slope,

is a measure of the loss caused by the bend. The distance required for the downstream gradient to reach the same slope as the upstream tangent is a measure of the transition distance. The length of the transition segment is connected with the decay of the spiral currents generated in the bend. Dissipation of the secondary currents commences at the end of the bend, with the disappearance of the forces which cause the spirals. The distance along the tangent required for the complete decay of the spiral flow presumably depends upon the intensity of the currents, which in turn depends upon the characteristics of the flow, the properties of the fluid, and the geometry of the boundary. In general, as the velocity increases, the transition length becomes greater. Yarnell's [120] measurements indicated lengths from 10 to 20 diameters for velocities increasing from 5 ft per sec to 12 ft per sec around a 6-in.  $90^\circ$  standard bend. The maximum transition length for a  $90^\circ$  miter bend was only 10 diameters, while for a  $180^\circ$  reversed curvature bend and several special bends over 50 diameters of straight pipe was required for the spiral currents to decay.

#### H. Energy Loss caused by Bends

The generation of spiral currents and separation of the flow at the inner wall result in energy loss in addition to that caused by boundary friction alone, as in a straight conduit. In bends of constant cross section, the energy loss is usually expressed as the pressure loss which occurs from the beginning of the bend to some point downstream where the effect of the bend has been entirely eliminated, in excess of that pressure loss which would have existed had the conduit been straight. The total loss between two points may then be expressed as the sum of the frictional loss that would occur in a straight pipe of the same axial length as the bend, and the excess loss caused by the presence of the bend. This pressure loss may be expressed as

$$-\frac{\Delta P}{\gamma} = H_s + H_b$$

where  $H_s = \lambda_s \frac{\ell}{d} \frac{V^2}{2g}$ , and

$H_b = \zeta \frac{V^2}{2g}$ , so that

$$-\frac{\Delta P}{\gamma} = \lambda_s \frac{\ell}{d} \frac{V^2}{2g} + \zeta \frac{V^2}{2g} \quad (6)$$

where  $\Delta P$  = the total pressure loss,

$\gamma$  = the specific weight of the fluid,

$H_s$  = the head loss in a straight pipe of the same character with its axial length equal to the distance along the centerline of the bend between measuring points,

$H_b$  = the excess loss of head in the bend,

$V$  = the mean velocity in the conduit,

$g$  = acceleration of gravity,

$\lambda_s$  = coefficient of resistance for a straight pipe with characteristic velocity distribution for straight pipe,

$\ell$  = length of conduit between measuring points,

$d$  = diameter of the conduit, and

$\zeta$  = the bend coefficient.

When the normal resistance to the flow in a corresponding straight pipe is subtracted from the total pressure loss, the excess loss, as exemplified by  $\zeta$ , depends mainly upon the properties of the bend and perhaps to a lesser extent upon the characteristics of the flow. Dimensional analysis suggests that the expression for the loss of head resulting from a bend of circular cross section may be expressed as

$$H_b = C \phi \left( \frac{R}{d}, \frac{k}{r}, Re, \alpha \right) \frac{V^2}{2g} \quad \text{or} \quad (7)$$

$$\zeta = C \phi \left( \frac{R}{d}, \frac{k}{r}, Re, \alpha \right) \quad (8)$$

The functional expression for  $\zeta$  probably should include a parameter describing the turbulence level of the flow. The form that the parameter should take to be the most useful is uncertain, however, and the difficulty of determining quantitatively the intensity of turbulence in a bend is such that no data on its influence on the energy loss are available. For this reason, a turbulence level parameter was omitted from the general expression.

When the conduit is not circular in cross section, another variable, a shape factor, enters the expression for  $\zeta$ . For rectangular cross sections, the ratio of the width of the cross section normal to the plane of the bend to the depth of the conduit in the plane of the bend is called the aspect ratio. When bends of rectangular cross section are being considered, the aspect ratio should be included in the function, so that

$$\zeta = C \phi' \left( \frac{R}{d}, \frac{k}{r}, Re, \alpha, \frac{w}{d} \right) \quad (9)$$

where, in addition to the terms previously defined,

$R$  = radius of the centerline of the bend in the plane of the bend,

$k$  = a roughness parameter with dimension of length,

$r$  = the radius of the conduit =  $d/2$ ,

$Re$  = Reynolds number =  $Vd/\nu$ ,

$\nu$  = kinematic viscosity,

$\alpha$  = the deflection angle of the bend,

$c$  = constant,

$w$  = width of the bend normal to the plane of the bend, and

$d$  = diameter of the conduit in the plane of the bend.

The variation of  $\zeta$  for various bends and various velocities, particularly in relation to the curvature ratio,  $R/d$ , has been the subject of many investigations because of its practical importance to hydraulic design. However, agreement of the results of the various investigators has not been good, probably because of extreme variability of conditions that exist in the flow of a fluid through a bend and the lack of an analytical expression for the function.

In the case of laminar flow in long bends, Dean's criterion for the similarity between the flow in a bend and the flow in a corresponding straight pipe can be stated as follows: for a given mean velocity in two pipes of the same dimensions, one straight and the other curved, the ratio of the resistance depends upon a parameter given by the product of the Reynolds number and the square root of the curvature ratio; that is  $Re (d/2R)^{1/2}$  (Keulegan and Beij [66]). On this basis, White [114] was able to correlate results of his experiments with those of Grindley and Gibson [58] pertaining to flow through helices of greatly different degrees of curvature into a single curve. This is shown in Fig. 1, p. 114.

The results of Adler [3] and Keulegan and Beij [66] fall on the same curve with remarkable agreement. Adler derived an expression for the resistance coefficient based on the boundary layer theory for larger values of  $Re (d/2R)^{1/2}$  that agrees with the experimental data. The results of these experiments are plotted in Fig. 1, p. 66, in which  $\lambda_c/\lambda_s$  is plotted as the ordinate with  $Re (d/2R)^{1/2}$  as the abscissa. The resistance coefficient,  $\lambda_c$ , is that which exists in a long bend beyond the transition segment where the curvilinear flow is fully established. The pressure loss in a length of

curve is given as

$$\Delta P = \lambda_c \frac{\ell}{d} \rho \frac{V^2}{2} \quad (10)$$

where  $\ell$  = the length along the curve, and

$d$  = the diameter of the conduit.

When the transition segment is included, the resistance coefficient, of course, increases from that characteristic of the straight pipe to that characteristic of the curved pipe. In this case the effective coefficient, applicable to a segment of curve which includes the transition segment, will be a function of the length of the curve ( $d/2R$ ). Keulegan and Beij [66] established a relationship on the basis of their experiments on long bends for the effective resistance coefficient. They obtained

$$\lambda_x = \lambda_c - \frac{d}{x} \frac{\lambda_c - \lambda_s}{(0.0059 + 0.844 (\frac{d}{2R})^{1/2})} \quad (11)$$

where  $\lambda_x$  is the effective resistance coefficient corresponding to a length  $x$  of the bend.

It is apparent that for the conditions of laminar flow in long bends of circular cross section in which the curvilinear flow is fully established, the variables  $k/r$ ,  $\alpha$ , and  $w/d$  do not appear in the general function, equation (8), for  $\zeta$ . For laminar flow the roughness of the conduit does not affect the resistance; since the flow is fully established, the entrance and exit transitions as exemplified by the angle  $\alpha$  do not appear and for a circular conduit the aspect ratio is a constant.

When turbulent flow exists in a bend of circular cross section and of definite deflection angle, conditions that exist in the majority of cases, the other dimensionless variables of the  $\zeta$ -function also influence the bend coefficient to varying degrees. Analogous to the flow in straight pipes, it may be expected that the influence of the Reynolds number would depend upon the relative roughness,  $k/r$ , as well as upon the degree of development of an established flow pattern which, in turn, would be influenced by the curvature ratio,  $R/d$ , and the deflection angle,  $\alpha$ . As a result of the complex interrelationships, the functional form of  $\zeta$  is not very clear although numerous experiments have been performed to determine the excess loss caused by the several factors separately.

### I. Effect of Reynolds Number on the Bend Coefficient

For bends with rough walls it appears that the Reynolds number has little influence on the value of the bend coefficient. Experiments by Beij [13] and Hofmann [62] on rough  $90^\circ$  bends of various  $R/d$  show that  $\zeta$  is practically constant for each value of  $R/d$  within a range of Reynolds numbers from about 40,000 to 300,000. For smooth surfaces, however, the bend coefficient decreases as the Reynolds number increases up to about 150,000 (Hofmann [62]). Wasielewski's experiments [109] on smooth bends with deflection angles of less than  $90^\circ$  also showed marked effect of Reynolds numbers below 120,000; above this, however, the bend coefficient remained nearly constant.

### J. Effect of Curvature Ratio on Bend Coefficient

In Fig. 2 are shown the results of experiments involving the variation of the bend coefficient for  $90^\circ$  bends. As far as possible the normal flow friction in similar straight pipes has been subtracted from the total loss so that  $\zeta$  includes only the excess loss caused by the bends.

In spite of considerable variation, a general tendency is apparent in the high values of  $\zeta$  for the shorter bend where the change in direction is abrupt and in the decreasing values of  $\zeta$  as the bend becomes longer or "easier". Most of the experiments indicate a minimum value of  $\zeta$  for an  $R/d$  between 3 and 5 and increasing values of  $\zeta$  for an  $R/d$  greater than 5. The result of Hofmann [62] is an exception to this, in that the minimum occurs at a somewhat larger value of  $R/d$ . The curves also show that  $\zeta$  increases again for larger values of  $R/d$  with a tendency toward a second minimum as  $R/d$  increases to values approaching a straight pipe, when  $\zeta$  must necessarily approach zero. The second maximum may possibly be explained in terms of the several factors that influence the value of the bend coefficient. As the  $R/d$  increases, the length of bend in which secondary flow can develop increases also with corresponding dissipation of energy. Also, as the  $R/d$  increases, the forces generating the spiral currents would be decreased with consequent reduction in dissipation of energy. It seems plausible that the first effect would be paramount for moderately high values of  $R/d$ , causing an increase in  $\zeta$ , while as  $R/d$  increases still further, the second effect tending to reduce  $\zeta$  would become more important as the bend approaches a straight pipe.

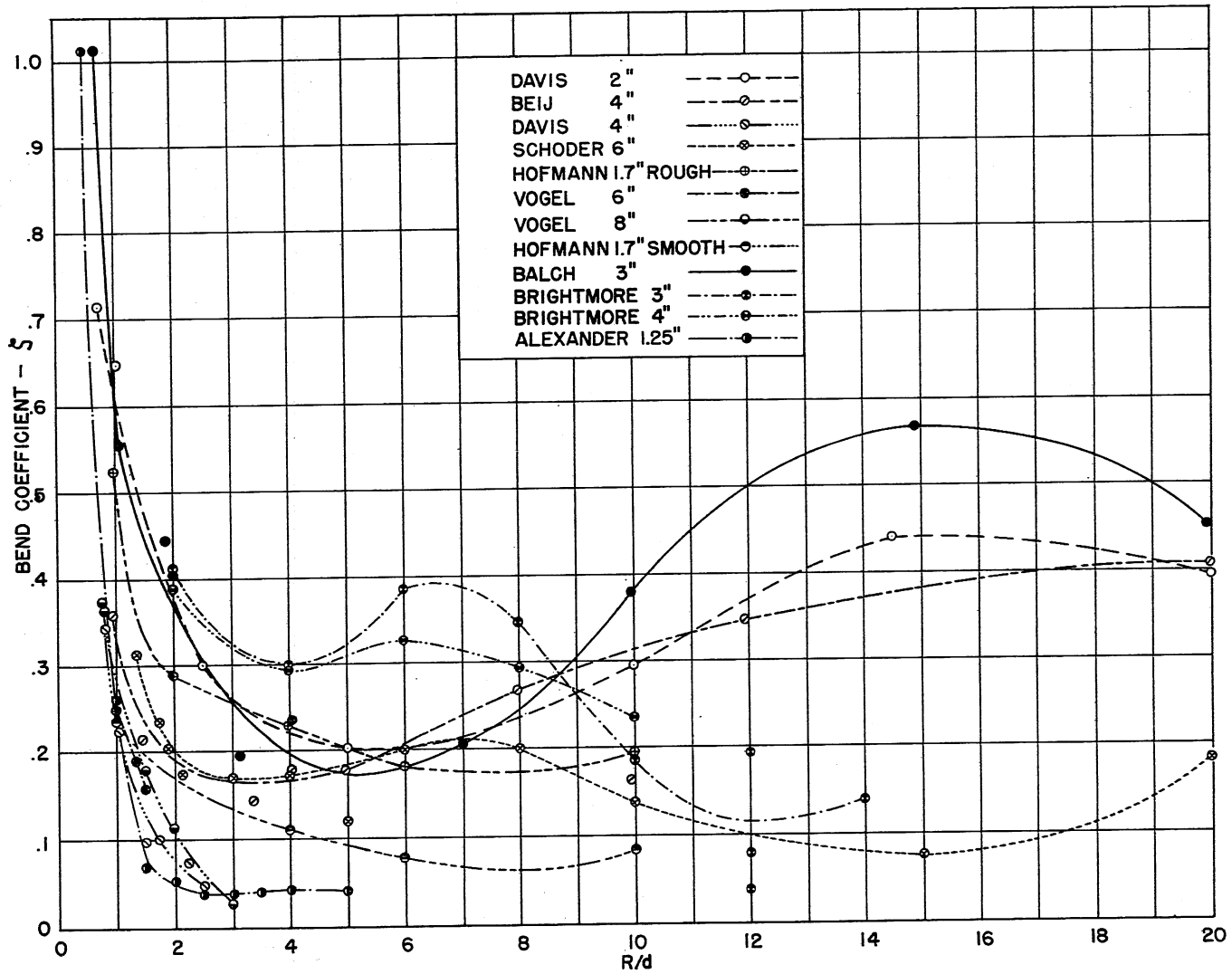


Fig.2-Relation of Bend Coefficient  $S$  to Radius Ratio Determined by Various Investigators

### K. Effect of Roughness on the Bend Coefficient

The influence of the roughness of the bend is apparent from an examination of Hofmann's data [62] for smooth and rough bends. The smooth bends were constructed by carefully machining the split halves, and the rough bends were made by coating the inside of the bend with a mixture of sand and paint. The effect of the roughness, as shown in Fig. 3, p. 100, is to increase the bend coefficient above that for smooth bends even though the resistance of a corresponding rough straight pipe has been subtracted from the total head loss. Beij [13] studied the effect of roughness of the bend by comparing the bend coefficients found by other investigators for  $90^\circ$  bends of circular cross section with the value of  $k/r$  as determined in their experiments on different conduits. He determined the value of  $k/r$  from the value of  $\lambda$ , the friction factor for straight pipes corresponding in roughness to the bends, by means of the expression

$$\frac{k}{r} = 280 \lambda^3$$

It is apparent from Fig. 4, p. 73, that greater roughness of the walls increases the bend coefficient.

### L. Effect of Deflection Angle on the Bend Coefficient

As might be expected, the resistance of a bend would depend on the degree to which the flow was deflected--the greater the deflection angle, the greater the resistance. Experiments indicate that, other things being equal, the bend coefficient is roughly proportional to the deflection angle. The results of Kirchbach [68], Schubart [97], Bouchayer [16], Davies and Puranik [27], and Wasielewski [109] are plotted in Fig. 3, for large Reynolds numbers.

### M. Effect of Aspect Ratio on the Bend Coefficient

In all of the above-mentioned experiments the bends tested have been of a circular or square cross section, in which case the aspect ratio also influenced the bend coefficient by its effect on the development of spiral currents. Wattendorf [110] found that for large aspect ratios, (18:1), the flow in the central region could be considered two dimensional.

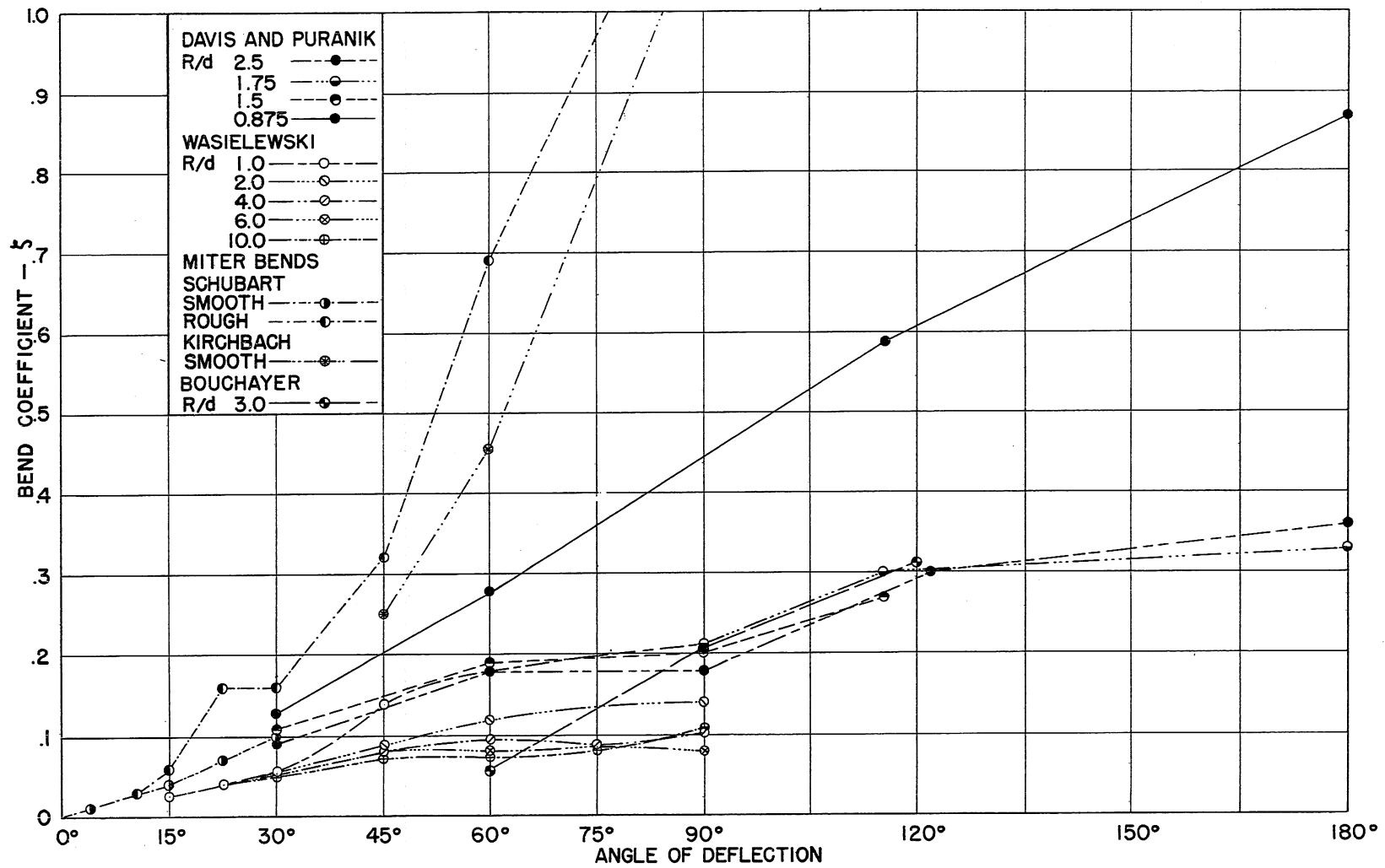


Fig.3-Relation of Bend Coefficient,  $S$ , to Deflection Angle,  $\alpha$ , Determined by Various Investigators

The decrease in the intensity of the spiral vortices causes a corresponding decrease in the bend coefficient. Experiments involving air ducts for ventilating systems have shown a very marked reduction in the bend coefficient resulting from an increase in the aspect ratio of the duct from one to six. Data obtained by Wirt are shown in Fig. 2, p. 148.

#### N. Effect of Combinations of Bends on the Bend Coefficient

The form of the relationship is further complicated when several units are installed in tandem in the same system, as would be the case when two elbows are separated by spacers of varying lengths. Such combinations are quite common in practice. Here another variable, the length of the spacer, is introduced; this influences the state of flow at the entrance to the second bend. However, the influence is effective only if the second bend is close enough to the first so that the flow enters the second bend with a certain amount of residual vorticity. Kirchbach [68] determined that for two  $45^\circ$  miter bends, placed so as to effect a  $90^\circ$  turn, the optimum distance between the bends was  $1.5 d$ . The total bend coefficient corresponding to this spacing is about 0.3, as compared to 0.472 for two  $45^\circ$  miter bends taken separately, or to 1.15 for one  $90^\circ$  miter bend.

To be mentioned also are Freeman's experiments [49] on standard elbows of many sizes and piping arrangements. Schubart [97] also made numerous experiments on the losses through combinations of miter bends with both rough and smooth walls.

## II. FLOW THROUGH CONDUIT BENDS WITH GUIDE VANES

### A. General

Theory indicates and experimental results show that the distribution of velocities in a bend cross section are far from uniform and that the pressure loss increases rapidly as the radius of the bend, compared to the duct diameter, becomes smaller than a certain minimum, ( $R/d = 3$  to  $4$ ). Experimental evidence also indicates that the pressure loss decreases as the aspect ratio of the conduit increases. Guide vanes increase both the radius ratio and the aspect ratio by dividing the flow into narrow compartments. Used to direct the flow around a corner, guide vanes have beneficial effects that largely eliminate the adverse velocity distribution and the large pressure loss by altering the conditions that cause them. The guide vanes may vary in shape from simple bent plates or partitions to elaborate airfoils in cascade. Experimental evidence in connection with the pressure loss suggests that in sharp bends the increased pressure loss is largely caused by the existence of secondary currents that are generated in deflecting the flow and by separation at the inner and outer corners of the bend. These secondary currents as well as the separation are also effective in developing a non-uniform velocity distribution. The installation of guide vanes in the corner may eliminate the secondary currents to a large extent and serve to prevent separation, with the consequent improvement in the velocity distribution as well as in decreased pressure loss. On the other hand, guide vanes present additional surface area to the flow with the consequent increase in skin friction. However, unless the number of vanes becomes excessive or, their chords very long, the effect of the additional friction is negligible compared to the improvement of the velocity distribution and the decrease in pressure loss resulting from the presence of the vanes.

The development of wind and water tunnels and large conduit installations, where uniformity of velocity distribution and minimum pressure drop are of prime importance, or where sharp corners are required, has resulted in accelerated research, both experimental and theoretical, into the design of guide vanes best suited to satisfy these conditions. Experimental research has dealt largely with the effects of specific forms of vanes to determine the arrangements that provide the most suitable flow conditions and minimum pressure drop. Theoretical research has dealt with the development

of vane shapes and settings to provide specified flow patterns on the basis of hydrodynamic considerations.

The suitability of a cascade of guide vanes depends upon the requirements to be satisfied. In general these requirements can be divided into velocity distribution, pressure drop, and the angle of deflection. In some installations a minimum pressure drop may be of greatest importance; in others, such as research apparatus, the velocity distribution and deflection angle are the controlling conditions. In general, however, all three may be important. The most suitable guide vane is that which provides the most uniform velocity distribution without angularity in the downstream flow and with a minimum pressure drop. Much of the experimental work carried out has been directed to determining the effect of shape and setting upon the three criteria and to measure the forces on the vanes. The effects upon the velocity distribution, pressure drop, and deflection are the result of a combination of separate conditions from which the optimum condition must be determined.

#### B. Effect of Vane Shape upon Velocity Distribution

The effect of vane shape upon the velocity distribution and the pressure drop hinges upon the flow pattern through the vane system. In an abrupt corner the diagonal is longer than the diameter or side of the upstream and downstream conduit; therefore, if the axis of the cascade joins the inner and outer corner the space between the vanes may be a variable. For thin plate vanes bent on the arc of a circle such that the ends of the arc are parallel to the axis of the upstream and downstream conduits, the distance between the vanes will be greater at the midpoint than at the upstream and downstream ends of the arc. The vanes may be thickened so that this distance is constant throughout the arc length, maintaining sharp leading and trailing edges. In practice, however, the leading and trailing edges must have a finite thickness. Vanes of many shapes intermediate between the thin or bent plate vane and the thickened vane, in which the distance between vanes is constant, may be used to create a flow diversion.

Klein, Tupper, and Green [133], measured the downstream velocity distribution and the pressure drop caused by vanes in a  $90^\circ$  corner. The vanes tested are shown in Fig. 1, p. 177. Four of the vanes were constructed of sheet iron bent to various radii and two were of thickened sections similar to airfoils. The downstream velocity distribution for vanes 1, 3, 4, and 5 are shown in Fig. 2, p. 177. The distribution curves are very similar and

the authors concluded that, although vanes 4 and 5 were superior to the others, the downstream distribution of velocity of all the vanes was greatly superior to the distribution without vanes. The profile of vane 4 is the arc of a quarter circle, while vane 5 is thickened and is similar to the vanes used in the Gottingen wind tunnel. These results indicate that the thickness of the vanes is not important in regard to velocity distribution.

Tests by Kröber [134] on thin plate vanes designed from aerodynamic considerations also indicated a uniform velocity distribution as shown in Fig. 4a, p. 186. Available evidence indicates that the velocity distribution does not depend upon the thickness of the vanes as such and that the velocity becomes more uniform as the vanes are placed closer together.

By placing a metal sheet coated with a thin layer of lamp black and kerosene in the downstream airflow perpendicular to the vanes, Klein, Tupper, and Green attempted to determine the direction of the air as it left the vanes. Although the method was not entirely satisfactory, they found that vane 1 deflected the air current considerably more than  $90^\circ$ , causing a high velocity downstream of the inner corner. Similar tests on vane 3 indicated that the flow was quite smooth and the deflection was approximately  $90^\circ$ . Collar [126] found that the deflection of the airstream varied somewhat with the Reynolds number of the flow. For some vanes the deflection decreased and for other vanes the deflection increased as the Reynolds number increased (Table I, p. 163). The vane profiles that Collar used in his experiments are shown in Figs. 1 to 5, p. 164.

### C. Effect of Vane Shape on the Pressure Loss

The pressure drop through the vanes appears to depend not only on the vane shape but also on the vane spacing and the angle of attack of the vane to the flow. As would be expected for vanes far apart, the pressure drop would be high, approaching as the limit that of a bend without vanes. As the spacing is decreased the development of secondary currents is restricted more and more to the region near the walls, where the vanes join the conduit boundary. It would appear that the best flow conditions would exist if the vanes are placed close together, but as the number of vanes in a given conduit is increased, the added skin friction caused by the vanes themselves increases. There is, therefore, an optimum spacing or spacing-chord ratio for each vane profile at which the pressure loss is a minimum. When the spacing-chord ratio is greater than the minimum, the increase in pressure drop is due to secondary currents and possibly to separation along the convex

boundary of the vane. When the spacing-chord ratio is less than the minimum, the added pressure loss is due to the increased skin friction on the surfaces of the vanes themselves. The experiments of Klein, Tupper, and Green [133] show the minimum resistance was obtained for vane 4, a thin vane bent to the arc of a quarter circle. However, as shown in Fig. 4, p. 178, the measured resistances for the thickened vanes were only slightly larger than for the thin vanes 3 and 4. The resistance of the vane is measured as the ratio of the pressure drop to the upstream dynamic pressure. Kröber [134] found that the minimum resistance coefficient for his thin vanes was 0.134. On the other hand, for the vanes he tested, Collar [126] obtained very low resistance coefficients, as low as 0.05 for profile C at a Reynolds number of approximately  $1.8 \times 10^5$ . The coefficient was greater at lower Reynolds numbers, increasing to 0.105 for a Reynolds number of approximately  $5 \times 10^4$ . The experimental evidence concerning the effect of vane thickness upon the minimum resistance is not very definite and direct comparison is difficult. Klein, Tupper, and Green tested both thick and thin vanes with the same experimental apparatus and found that the resistance was nearly the same for both thick and thin vanes; Kröber tested only thick vanes and obtained lower resistances, while Collar tested only thickened vanes and obtained still lower values for the resistance coefficient. The evidence suggests that the shape of the profile, including the thickness, is important in reducing the resistance. The thin profiles of Klein, Tupper, and Green were constructed as combinations of circular arcs and tangents. Kröber's vane had a varying radius of curvature dictated by aerodynamic considerations. The thick sections of Klein, Tupper, and Green were of two types, one based largely upon the section used in the Gottingen tunnel; the other was an RAF 30-section arranged along a circular arc. Those of Collar had boundaries consisting of circular arcs such that there was no constriction or expansion of the flow in passing through the vanes.

#### D. Effect of Spacing on Velocity Distribution and Pressure Loss

The influence of the spacing-chord ratio on velocity distribution and pressure loss has already been suggested. As the spacing-chord ratio decreases, the secondary currents are restricted more and more to the region near the conduit walls, and the difference in velocity between the inner and outer walls in each compartment in the vane system decreases. Hence, the velocity distribution becomes more uniform as the spacing-chord ratio decreases.

Klein, Tupper, and Green [133] found that, as a general rule, the most uniform velocity distribution is obtained with the closest vane spacing.

It might also be expected that the pressure loss would decrease as the vanes were spaced closer together, since the ratio of radius of curvature to spacing would increase. It has been found, however, in the case of conduits that the resistance decreases rapidly at first as the radius ratio and the aspect ratio increase, but that the decrease in resistance is negligible when the radius ratio and the aspect ratio increase beyond a certain value. In addition to this, the increase in the number of vanes presented to the flow increases the surface area and results in increasing total surface friction resistance.

The combination of these influences suggests the existence of an optimum vane spacing for each type of vane, at which the pressure loss and the resistance coefficient would be a minimum, with a greater pressure drop developing as the spacing became greater or less. The results of experiment indicate a minimum pressure drop occurs for spacing-chord ratios in the neighborhood of 0.3 to 0.5, the exact value depending on the shape and characteristics of the vane being tested. Klein, Tupper, and Green [133] made a rather extensive series of experiments on different vanes at various spacing-chord ratios and found that a minimum value of the resistance coefficient occurred for each vane. The value of the spacing-chord ratio for minimum resistance was 0.3 for vane 4, a thin circular arc vane, and 0.35 for vane 5, a streamlined modified airfoil. For the thin circular arc, the minimum resistance was slightly lower, being 20 per cent of the impact velocity pressure, while that for the airfoil vane was about 21 per cent.

The exact spacing of the vanes in Kröber's experiments [134] is not explicitly stated, but his equation for the chord gives  $t/S = 2\sqrt{2}/C_a$  as the ratio of chord length to spacing. Taking his value for  $C_a$ , the lift coefficient of the airfoil, as being equal to 1.35, the spacing-chord ratio becomes about 0.48. The coefficient of resistance for a  $90^\circ$  bend was 0.134, using vanes of the first approximation, presumably at the spacing-chord ratio of 0.48. Collar's experiments were performed only at one spacing, 1.0 inch. The chord length of his vanes was 2.0 in., except for profile C, which was less because of the rounded leading edge. In this case the spacing-chord ratio was 0.5 for profiles A and B and greater than 0.5 for profile C.

#### E. Effect of Angle of Attack on Velocity Distribution and Pressure Loss

The angle of attack of the vane is the angle between its chord and the direction of the upstream velocity. For symmetrical vanes in a  $90^\circ$  corner this angle is usually  $45^\circ$  so that the velocity downstream of the vanes will presumably leave the vanes parallel to the axis of the downstream conduit. For unsymmetrical vanes, the shape of the vane determines the angle of attack that will produce the most uniform velocity distribution with the minimum of angularity and pressure drop. Klein, Tupper, and Green found that for vane 5, the pressure drop was relatively insensitive to small changes in the angle of attack from  $45^\circ$ .

#### F. Pressure Distribution around the Vane Profile

The pressure distribution and magnitude is important from the structural viewpoint for determining the forces which act on the vane and the location of the resultant or the center of pressure. Relatively little information is available on the pressure distribution on a vane as used in a cascade. Klein, Tupper, and Green measured the pressure distribution on one vane in the cascade. The results for vane 5 are shown in Fig. 6, p. 178. The pressure distribution about thin vanes of the Kröber type are shown in Fig. 4b, p. 186, taken from Kröber's paper. The pressure distribution and the lift and drag acting on the individual airfoil in a cascade have been measured by Shimoyama [151]. In this case, however, the deflection of the current was very slight, since the airfoils tested were not designed specifically to deflect the flow through any given angle.

#### G. Irregularly Spaced Vanes

When velocity distribution and angularity of the flow following a corner is not critical, the pressure drop may be greatly reduced by the installation of irregularly spaced vanes whose purpose is to reduce or eliminate the separation at the inner corner of the bend. Frey [130] has developed a vane system of this kind in which the vanes are placed in such a position that separation is prevented. His experiments indicate that the loss can be greatly reduced by this process.

#### H. Corner Expansions

Attempts have been made to incorporate an expansion with a sharp bend in a conduit and still provide a uniform velocity distribution by the

use of vanes. Collar [126] found that an expansion of 1.2 was too large, even with specially designed thickened vanes, to prevent separation on the suction side of the vane, with consequent irregular velocity distribution. MacPhail [135] found similar results in his experiments on corner expansions, but was able to improve the velocity distribution downstream of the vanes by the use of screens through which the water flowed.

### I. Theoretical Investigations

The theoretical investigations of cascades of vanes have dealt principally with the design of blades for hydraulic machinery, such as axial flow pumps and turbines. The methods used have generally been those of aerodynamics, utilizing airfoil theory to describe the flow through the cascades by the introduction of interference factors to translate data pertaining to isolated airfoils to a cascade of such airfoils. The problem has also been attacked hydrodynamically by transforming the known flow patterns past a series of laminae to other patterns which represent the potential flow through vanes with a given deflection.

A parallel flow superposed upon a vortex will undergo a deflection in direction. The magnitude of the deflection will depend upon the circulation of the vortex. Kröber [134] used this method to determine the properties of a vane that would deflect a parallel flow through a given deflection. The vanes were replaced by a series of vortices of such strength that the flow would be deflected by the given amount. It was assumed that the center of pressure for each vane coincided with the center of a corresponding vortex. In this way he obtained a flow net for the flow around the corner (Fig. 1, p. 185). Any airfoil which subsequently replaced the vortex must possess the same circulation as the vortex which created the deflection. Kröber chose an airfoil which had been deduced theoretically so that the lift coefficient could be given in a formula. By choosing a proper value of the lift coefficient, and assuming that the velocity far in front and far behind the vane was the same as the velocity of the parallel flow far in front of the untransformed airfoil, the airfoil was transformed from the parallel flow to the deflected flow directly, by making the center of pressure of the airfoil coincide with the center of the vortex.

Other investigators have proceeded directly from the hydrodynamic equations to determine possible airfoil shapes that would provide a given deflection by utilizing the procedures of conformal transformation. Weinig [154] developed the concept of an equivalent grid of straight line profiles,

for which the flow is known when placed at the no-lift angle of attack and can be determined for other angles of attack. Further transformations of this flow resulted in a corresponding flow around a series of cylinders, which were then, by a generalization of the Joukowski method, transformed to the flow around bodies similar to airfoils. Merchant and Collar [139] followed a similar procedure utilizing a cascade of ovals. Other papers dealing with the hydrodynamics of cascades include those of Collar [128], Pistoiesi [147], and Numachi [141].

### III. FLOW IN OPEN CHANNEL BENDS

#### A. General

The scale of the flow around open channel bends covers a much wider range than that of flow in conduit bends because it must include natural waterways, in which wide meanders may occur, as well as artificial channels of all sizes. It appears from observation and experiment that the phenomena of flow in open channel bends corresponds to that in the lower half of a conduit bend. The transverse free surface slope at the bend in the open channel, the result of centrifugal forces, corresponds to the transverse pressure gradient in a conduit bend. If the friction on the bed is neglected the transverse velocity distribution is given by  $VR = \text{constant}$ , so that the velocity at any radius in the bend is inversely proportional to the radius. This leads to the conclusion that the velocity is greatest near the convex side and least near the concave side. Actually, however, the friction on the sides and bottom alters these relationships by the generation of helicoidal currents, so that the maximum velocity is found near the convex side at the beginning of the bend and near the concave side in the downstream portions of the bend. This is similar to the velocity distribution in one half of a conduit bend.

James Thomson [176] was probably the first to describe the secondary currents in an open channel bend and to verify them by experiment. In a small model of a bend he was able to delineate currents in various parts of the cross section by the use of small particles, dye streams, and threads.

Secondary currents are brought into being by the centrifugal force as modified by the drag generated on the sidewalls and bottom. Because of the drag on the bottom, the velocity in the region near the bed is reduced and the particles are subjected to smaller centrifugal forces than are those in the regions of higher velocity in the upper portion of the stream. The transverse pressure gradient which balances the centrifugal forces is manifested

in a transverse slope, higher at the outer bank and lower at the inner bank. Near the bed the forces resulting from the pressure gradient are greater than the centrifugal forces and the particles are forced toward the inner bank. Near the surface, where the velocity is the greatest, the centrifugal forces outweigh the forces resulting from the pressure gradient at that point, and the particles tend to flow toward the outside bank. The result is a secondary current which flows toward the inner bank along the bottom and toward the outer bank near the surface. This secondary current is superposed upon the main current around the bend so that the resultant is somewhat of a spiral current.

#### B. Transverse Slope

Woodward [179] calculated the transverse slope caused by the flow around the bend with different results, depending on assumptions regarding the transverse velocity distribution. For constant velocity the difference in elevation of the water surface at the outer and inner bank is given as

$$\Delta h = \frac{V^2 b}{g R_o} \quad (12)$$

where  $\Delta h$  = the difference in elevation of the water surface at the outer and inner bank,

$V$  = the velocity of the water (assumed constant across the cross section),

$b$  = breadth of the stream,

$g$  = acceleration resulting from gravity, and

$R_o$  = radius of curvature of the center of the stream.

If a potential velocity distribution exists,  $VR = \text{constant}$ , the difference in elevation of the water surface at the outer and inner bank could be expressed as

$$\Delta h = \frac{V_o^2 R_o}{2g} \left( \frac{1}{R_1^2} - \frac{1}{R_2^2} \right) \quad (13)$$

where  $V_o$  = the velocity at a radius  $R_o$ , assumed to be the radius of the centerline, and

$R_1$  and  $R_2$  = radii of the convex and concave sides, respectively.

If the radius is large compared to the width of the stream, this expression for the difference in elevation becomes approximately that for constant velocity. Chatley [157] measured the transverse slope of the Whangpoo River at

Pootung Point and compared the results obtained with several formulas for the transverse slope. He found that the difference in elevation of the water surface at the banks of the bend agreed reasonably well with that calculated by assuming a constant velocity. He observed, however, that a closer approximation could be obtained from actual velocity measurements by calculating the difference in elevation for narrow strips. Blue, Herbert, and Lancefield [156] also observed the transverse slope in connection with observations on the Iowa River, as did Eakin [158] on a bend in the Mississippi River. Blue, Herbert, and Lancefield found the best agreement with measurement when it was assumed that the velocity distribution was parabolic, with a maximum velocity at the center and zero velocity at the banks.

### C. Observations on Secondary Currents

Since the time of James Thomson [176], numerous observations have been made on bends of natural streams to establish the existence and magnitude of the secondary currents and the transverse slope resulting from the centrifugal forces.

To determine the secondary currents in a bend in the Mississippi River, Eakin [158] traced the path of pea coal and limestone particles that were dumped into the water at several points, and observed the direction and magnitude of the velocity by means of meters and special direction-finding apparatus. He concluded that his observations of current direction and of movement of the identifiable sediment all join to indicate the existence of systematic cross-sectional components of motion, in thorough keeping with the theory of the secondary currents. Blue, Herbert, and Lancefield [156] measured the velocity, direction of the velocity, and direction of currents at a bend in the Iowa River. They concluded that the secondary currents were of the nature described by Thomson in 1876, and that near the bed the current was most pronounced toward the inner bank in the region just downstream of the midpoint of the bend. The maximum velocity was found near the inner bank above the bend and near the outer bank below the bend.

The intensity of the secondary currents probably depends upon the ratio of width to depth, as well as upon the radius of curvature and the length of the curve. The width-depth ratio of the bend upon which Blue, Herbert, and Lancefield made their observations was approximately 40, while the width-depth ratio of the bend on the Mississippi River where Eakin made his observations was approximately 100.

Model experiments of a bend led Vogel and Thompson [177] to question the theory of helicoidal flow propounded by Thomson. Their observations showed that sediment moved toward the inner bank, where some of it was deposited, but their measurements of current direction indicated that the flow was sensibly parallel all around the curve. They have made the point that for large width-depth ratios of the order to 200 to 1, such as are found in the lower Mississippi, the tendency for transverse currents to develop may exist but they are not as readily apparent.

Other experiments by Mockmore [171] on an open channel bend of  $180^\circ$  also indicated very clearly that spiral currents do exist in a bend in the manner enunciated by James Thomson. His measurements further demonstrated that in the first half of the bend the velocity is greater near the convex bank than the concave bank, and that it varied across the channel in close agreement with the law of a free vortex.

#### D. Cross-Sectional Shape in Erodible Beds

For an open channel with fixed bed and walls, the channel shape remains uniform and constant with changes in velocity and intensity of secondary currents. With a movable bed, however, the shape of the channel changes at various points around the bend because of the secondary currents. Sediment transported on a diagonal across the stream toward the inner bank shows a tendency to deposit on the inside of the curve beginning just downstream of the midpoint of the bend. The depth is greater near the outside of the bend since the transverse currents scour the bed until an equilibrium is reached. The shape of the cross profile of a natural watercourse in a bend has been subject to a considerable amount of study and observation with resulting empirical formulas for determining the depth at any point in the cross section. Ripley [174] presented several formulas based upon observations of numerous bends. Chatley [157] made a critical study of available formulas and compared them with observations on the Whangpoo River in China.

The change in shape of the cross section of an open channel bend with erodible bed and banks is probably connected with an equilibrium condition of minimum head loss. Some evidence of this is available in the results of experiments by Yen and Howe [180]. They found that decreased head loss resulted when the channel at the bend was made narrower and deeper. It may be, however, that the reduced head loss resulted from a decrease in the intensity of the secondary currents.

### E. Head Loss Caused by Open Channel Bends

The head loss caused by a bend in an open channel appears to depend upon the same variables as the head loss in a conduit bend. Experimental evidence concerning the losses in open channel bends is relatively meager, but experiments of Raju [172] on two 90° bends show a tendency for the bend coefficient to decrease with increasing radius-width ratio, similar to that in conduit bends. The magnitude of the bend coefficient appears to be about the same as that for smooth conduit bends for low radius-width ratios, but the resistance is somewhat less than that for conduit bends as the ratio of radius of curvature to width of channel increases. This is shown in Fig. 4, p. 219. In open channels, as in conduit bends, the aspect ratio, in this case the depth-width ratio, affects the losses by influencing the development of secondary currents. Yen and Howe [180] found that the bend coefficient for a 90° bend of a uniform width of 11 in. and a 5-ft radius of curvature was approximately 0.380, a value much higher than the 0.04 found by Raju in a similar bend in which the width was 300 mm and the radius of curvature was 1500 mm.

### F. Supercritical Flow in Open Channel Bends

As is well known, the flow in an open channel may be of two types, "streaming" flow, when the depth is greater than the critical depth, and "shooting" flow, when the depth is less than critical depth. The experiments and observations described above pertain only to streaming flow. Experimental and theoretical study of shooting flow around bends in open channels is limited. Such flow is characterized by extreme differences in water surface elevation on the outside and the inside of the bend, causing disturbances which continue for long distances downstream of the bend. An important study of such flow is that of Knapp and Ippen [167], in which the problem was investigated both experimentally and theoretically. They found that the longitudinal profile along the wall at the beginning of the curve could be described satisfactorily by the equation

$$h = \frac{v^2}{g} \sin^2 \left( \beta_0 + \frac{\theta}{2} \right) \quad (3)$$

where  $h$  = the depth of flow,  
 $v$  = the velocity, assumed constant,  
 $\beta_0$  = the wave angle, and  
 $\theta$  = the angle of turn.

The first maximum water surface elevation occurs at an angle  $\theta_0$  from the beginning of the turn, such that

$$\theta_0 = \tan^{-1} \frac{b}{(R + \frac{b}{2}) \tan \beta_0} \quad (4)$$

where  $b$  = channel width, and

$R$  = radius of curvature of the bend.

Some success was achieved in reducing the profile maxima in existing flumes by the use of sills designed to produce a counter disturbance, and by transition curves and banking of the bend in the case of proposed flumes.

## CONCLUSION

The review of the literature has included published papers on the flow around bends in conduits without guide vanes, the flow through guide vanes and cascades, and the flow around bends in open channels.

The literature on bends in conduits shows that a great deal of experimentation has been performed on some of the individual factors that influence the magnitude of the bend coefficient. Considerable progress toward an analytical solution has been made in the case of laminar flow in long bends or coils. The problem becomes more complex when the additional variables of turbulent flow and the shorter bends used in practice are considered. Many of the earlier experiments considered only separate factors without taking into account the effects of the other variables. Because of the uncertainty about the magnitude of the remaining factors, there are limitations at present to the extent that the results of different investigators may be correlated. It would be desirable to conduct further research in which the separate factors are varied systematically while the other conditions are maintained at known constant values. At the same time an analytical approach to the form of the bend coefficient function would aid in interpreting the experimental results.

The design of guide vanes has profited considerably as a result of theoretical studies of the flow phenomena through cascades by the application of airfoil theory and the methods of hydrodynamics. The need for experimental investigations on the practical application of theoretical vane shapes to establish design data is of considerable urgency. The results of such studies would be immediately useful in design problems.

Knowledge concerning the flow around bends in open channels faces the same problems as does the flow in conduit bends, with the additional variables of a free surface and, in the case of natural waterways, a variation in cross section and a movable bed. It appears that success with the problem depends upon the systematic study of the separate factors by the elimination of the uncontrolled variables.

B I B L I O G R A P H Y

In the preparation of this bibliography an attempt has been made to include all reports and articles contributing to the knowledge of directional diversion of fluids by use of rigid stationary boundaries. The bibliography is divided into three sections, each of which covers a phase of directional diversion that appears to be more or less self-contained. In each section the flow phenomena is essentially different from that treated in other sections. The first section includes the literature pertaining to the flow without guide vanes through conduit bends, in which the fluid is completely enclosed and may flow under pressure. The second section includes the literature pertaining to guide vanes developed for use in conduit bends. This division was made because the nature of the flow through a bend with guide vanes is essentially different from the flow without guide vanes. The third division of the bibliography includes the literature on flow in open channel bends.

The literature and existing bibliographies in English were examined, and references to articles in other languages have been included. It is believed that the list of English and German articles is fairly complete and that no important papers in other languages were omitted. The bibliography includes reports on the flow through conduit bends, through cascades of vanes used to deflect the flow, and through open channel bends. The literature on the deflection of fluids by moving boundaries such as turbines, pumps, and propellers is not included, except for those references which are generally applicable to the flow through cascades. The directional diversions involved in turbines, pumps, and propellers are necessarily the subject of a separate study.

## I. Flow Through Conduit Bends

- [1] Addison, Herbert, "Experiments on the Flow of Water in Pipe-Bends," 1936-37 JOURNAL OF THE INSTITUTION OF CIVIL ENGINEERS, Vol. 6, Paper No. 5084, pp. 561-564, 1936-37, 1 fig., 1 table. Tests were made on bends, single and compound, of 6-cm square cross section with smooth and rough walls.
- [2] Addison, Herbert, "The Use of Pipe Bends as Flow Meters," ENGINEERING (London), Vol. 145, pp. 227-229, March 4, 1938, 10 figs., 3 tables. On the assumption of free vortex flow equations are developed for the velocity in terms of the transverse pressure difference. Tests were made to establish a discharge coefficient.
- \*[3] Adler, M., "Strömung in Gekrümmten Rohren" (Flow in Curved Pipes), 1934 ZEITSCHRIFT VON ANGEWANDTE MATHEMATIK UND MECHANIK, Vol. 14, pp. 257-275, October, 1934, 23 figs. A theoretical treatment, supported by experimental data, of the resistance to laminar flow of curved pipes as a function of  $Re(a/R)^{1/2}$  based upon Prandtl's boundary layer theory. The work of Dean is extended to higher Reynolds numbers in the laminar range.
- \*[4] Alexander, C. W. L., "Resistance Offered to the Flow of Water in Pipes by Bends and Elbows," PROCEEDINGS OF THE INSTITUTION OF CIVIL ENGINEERS, Vol. 159, Paper No. 526, pp. 341-364, 1905, 14 figs., 3 tables. This paper reports experimental results on loss of head in 1 1/4-in. smooth 90° bends for  $R/d$  varying between 0.5 and 5.0. Measured resistance coefficients are less than those obtained by other investigators of smooth bends, probably because tangent losses were not included.
- [5] Allen, C. M., and Winter, I. A., "Comparative Tests on Experimental Draft-Tubes," TRANSACTIONS OF THE AMERICAN SOCIETY OF CIVIL ENGINEERS, Vol. 87, Paper No. 1544, pp. 893-970, 1924, 53 figs., 3 tables. Tests made included some of quarter-turn draft tubes.
- [6] Bailey, F. S., "Diagram Giving Excess Loss of Head in 90 Degree Bends," 1916 ENGINEERING NEWS-RECORD, Vol. 75, pp. 412-413, March 2, 1916, 1 fig. The diagram is based on Fuller's equation  $H_B = KV^{2.25}$  and prepared for bends from 1 in. to 48 in. in diameter and velocities of 2 to 14 ft.

---

\*An abstract of articles so marked appears in the Appendix.

- \* [7] Balch, Leland R., INVESTIGATION OF HYDRAULIC CURVE RESISTANCE EXPERIMENTS WITH THREE-INCH PIPE, Bulletin of the University of Wisconsin No. 578, (Engineering Series, Vol. 7, No. 3), 1913, 52 pp., 18 figs., 18 tables. This is a report of experiments on ten 3-in. 90° bends for R/d up to 20. Head loss and bend coefficient are plotted as functions of R/d.
- [8] Bambach, Richard, "Plötzliche Umlenkung (Stoss) von Wasser in Geschlossenen unter Druck Durchströmten Kanälen (Sudden Deflection of Water Flowing in Closed Pressure Conduits), FORSCHUNGSARBEITEN AUF DEM GEBIETE DES INGENIEURWESENS, No. 327, 1930, 28 pp., 55 figs., 4 tables. This is an investigation of loss of head in pipe bends; many pressure and velocity observations were made.
- [9] Baulin, I., and Idelchik, I., "Experimental Investigation of the Motion of Air Through Elbows," GOSMASHMETIZDAT (GOVERNMENT MACHINE-METAL PUBLICATION), 1934. (Russian article, no known translation.)
- [10] Beck, Cyrus, "Laminar Flow Friction Losses Through Fittings, Bends, and Valves," JOURNAL OF THE AMERICAN SOCIETY OF NAVAL ENGINEERS, Vol. 56, pp. 235-271, May, 1944, 19 figs. This article includes test data for laminar flow through 3 1/2-in. bends for Reynolds numbers from 50 to 1000. The data were analyzed on the basis of theoretical considerations.
- [11] Beck, Cyrus, "Laminar Flow Pressure Losses in 90 Degree Constant Circular Cross-Section Bends," JOURNAL OF THE AMERICAN SOCIETY OF NAVAL ENGINEERS, Vol. 56, pp. 366-388, August, 1944, 9 figs., 5 tables. This is a study of pressure losses in 90° bends covering Reynolds number range of 30 to 1000.
- [12] Beck, Cyrus, and Miller, H. M., "Pressure Losses in Marine Fuel Oil Systems," JOURNAL OF THE AMERICAN SOCIETY OF NAVAL ENGINEERS, Vol. 56, pp. 62-83, February, 1944, 23 figs. Experimental tests to determine head loss in single standard fittings and applicability of results to assemblies of fittings were made.
- \*[13] Beij, K. Hilding, "Pressure Losses for Fluid Flow in 90° Pipe Bends," JOURNAL OF RESEARCH OF THE NATIONAL BUREAU OF STANDARDS, Vol. 21, RP 1110, pp. 1-18, July, 1938, 12 figs., 1 table. Pressure losses were determined for nine 4-ft 90° pipe bends with R/d from one to 20, and compared with those of other investigators. Results are also correlated on the basis of pipe roughness.

- [14] Bellasis, E. S., HYDRAULICS, 2d ed., New York and London, 1911, 303 pp. 1911  
A general discussion of flow in bends of closed conduits and open channels.
- [15] Bossut, Charles, TRAITE THEORETIQUE ET EXPERIMENTAL D'HYDRODYNAMIQUE, 1796  
Paris, 1796.
- \*[16] Bouchayer, A., "Losses of Head in Bends and Branches," ENGINEERING 1925  
(London), Vol. 120, p. 241, August 21, 1925, (summary of "Les Pertes de Charges Dans Les Conduits Coudes et Embranchements," as given at Hydro-Electric Congress, Grenoble, 1925). This paper compares the excess bend resistance for bends of the same curvature ratio but varying deflection angles ( $30^\circ$ ,  $60^\circ$ ,  $90^\circ$ ,  $120^\circ$ ).
- [17] Boussinesq, J. V., "Essai sur la Theorie des Eaux Courantes" (Essay on the Theory of Running Water), MEMOIRES PRESENTES PAR DIVERS SAVANTS A L'ACADEMIE DES SCIENCES DE L'INSTITUT NATIONAL DE FRANCE, Tome 23, pp. 1-666, Supplement 24, 1877.
- [18] Brabbée, K., "Einzelwiderstände in Warmwasserheizungen" (Resistance of Individual Parts of Hot Water Systems), MITTEILUNGEN DER PRÜFUNGSANSTALT FÜR HEIZUNGS-UND LUFTUNG, Vol. 5, Paper No. 15, June, 1913. Reports experiments on miter bends; losses in downstream section are not included. Dimensions of bends are not given.
- \*[19] Brightmore, A. W., "Loss of Pressure in Water Flowing Through Straight and Curved Pipes," MINUTES OF PROCEEDINGS OF THE INSTITUTION OF CIVIL ENGINEERS, Vol. 169, Part 3, Paper No. 3679, pp. 315-336, 1906-07, 10 figs., 6 tables. This paper determined losses in 3-in. and 4-in. rough bends with  $R/d$  from 2 to 14, and analyzes results.
- \*[20] Busey, Frank L., "Loss of Pressure due to Elbows in the Transmission of Air through Pipes and Ducts," TRANSACTIONS, AMERICAN SOCIETY OF HEATING AND VENTILATING ENGINEERS, Vol. 19, pp. 366-376, 1913, 7 figs. Two sets of experiments to determine effects of changing radius of curvature and size of throat upon bend resistance were made. Elbows 12 inches in diameter and elbows with a 12-in. square cross section were used.
- [21] Busquet, R., A MANUAL OF HYDRAULICS, (trans. A. H. Peake), London and New York, 1906, 312 pp. Flow in bends is discussed and a formula for calculating loss of head in bends is presented.

- [22] Clauser, Milton, and Clauser, Francis, "The Effect of Curvature on the Transition from Laminar to Turbulent Boundary Layer," TECHNICAL NOTES, U. S. NATIONAL ADVISORY COMMITTEE FOR AERONAUTICS, No. 613, September, 1937, 37 pp., 41 figs. Turbulence and velocity distribution in boundary layer were measured to establish critical Reynolds numbers for transition to turbulent flow.
- [23] Corp, Charles I., and Hartwell, H. T., EXPERIMENTS ON LOSS OF HEAD IN U, S, AND TWISTED S PIPE BENDS, Bulletin of the University of Wisconsin, (Engineering Series No. 66), 1927, 181 pp., 40 figs., 39 tables. This bulletin tells of measurements of head loss in numerous standard pipe fittings in many combinations.
- [24] Daley, D. H., Schoder, E. W., Bain, P., Jr., and Davis, G. J., "Loss of Head in Screw Pipe Elbows and Tees," THE CORNELL CIVIL ENGINEER, Vol. 20, pp. 107-113, December, 1911, 3 figs. This is a collection on a comparable basis of the results of the several investigators.
- [25] D'Aubuisson, J. F., A TREATISE ON HYDRAULICS, (trans. Joseph Bennett), 1852, Boston, 1852, 532 pp. This work contains a discussion of head loss in pipe bends, based upon experiments of Bossut [15], Rennie [91], and Dubuat [33].
- [26] Davey, T. F., "Velocity at Tangent of Curves of 36-in. Pipe," ENGINEERING NEWS-RECORD, Vol. 97, p. 905, December 2, 1926, 2 figs. Results are given of tests on 36-in. reservoir discharge pipe under a head of 80 ft at the point of tangency of two curves, one the reverse of the other. The tests show that loss in a reverse curve is equal to that of the two separate curves.
- \*[27] Davies, Powys, and Puranik, Shivram, "The Flow of Water Through Rectangular Pipe-Bends," JOURNAL OF THE INSTITUTION OF CIVIL ENGINEERS, Vol. 2, Paper No. 5035, pp. 83-134, 1935-36, 15 figs., 26 tables. Report is made of experiments on teakwood bends of square cross sections. Results are presented for 90° bends with R/d from 0.875 to 2.5, and also for deflection angles from 30° to 180°.
- \*[28] Davis, G. J., INVESTIGATION OF HYDRAULIC CURVE RESISTANCE, Experiments with Two-Inch Pipe, Bulletin of the University of Wisconsin No. 403, (Engineering Series, Vol. 6, No. 4), 1910, 60 pp., 20 figs., 10 tables. Experiments were made on a 2-in. standard pipe for a wide range of R/d.

- [29] Dean, W. R., "Note on the Motion of Fluid in a Sinuous Channel," 1927  
PHILOSOPHICAL MAGAZINE AND JOURNAL OF SCIENCE (Seventh Series), Vol. 3, pp. 912-924, April, 1927, 2 figs. A theoretical treatment of slow motion in which the equations of motion are approximately integrated.
- [30] Dean, W. R., "Note on the Motion of Fluid in a Curved Pipe," 1927  
PHILOSOPHICAL MAGAZINE AND JOURNAL OF SCIENCE (Seventh Series), Vol. 4, pp. 208-223, July, 1927, 3 figs. Integration of the equations of motion for streamline flow in a curved pipe indicates the existence of the spiral currents and permits calculation of the streamlines.
- [31] Dean, W. R., "Fluid Motion in a Curved Channel," 1928  
PROCEEDINGS OF THE ROYAL SOCIETY OF LONDON, Series A, Vol. 121, pp. 402-420 1928, 1 fig. A mathematical treatise on the effect of a small disturbance on laminar flow in a curved channel is given. Results were obtained by approximate integration of equations of motion.
- \*[32] Dean, W. R., "The Streamline Motion of Fluid in a Curved Pipe," 1928  
PHILOSOPHICAL MAGAZINE AND JOURNAL OF SCIENCE (Seventh Series,) Vol. 5, pp. 673-695, April, 1928, 3 figs., 4 tables. This article contains a derivation of a criterion by which the resistance to flow in a curved pipe may be compared to that in a corresponding straight pipe.
- [33] Dubuat-Nancay, L. G., PRINCIPES D'HYDRAULIQUE ET DE PYRODYNAMIQUE, 1816  
3 vols., Paris, 1816. (New ed., revised and considerably augmented.) Twenty-five experiments were made on pipes 1 inch in diameter and a formula was derived for the loss.
- [34] Edwards, W. D., "Pressure Losses in Air Ducts," 1928  
HEATING AND VENTILATING MAGAZINE, Vol. 25, pp. 69-72, February, 1928, 3 figs. This article presents charts for calculating losses in air ducts, including bends.
- [35] Engles, Hubert, HANDBUCH DES WATERBAUES, Part 1, Leipzig and Berlin, 1914  
1914. Formulas based on Weisbach's work are presented for loss of head in bends.
- \*[36] Eustice, John, "Flow of Water in Curved Pipes," 1911  
PROCEEDINGS OF THE ROYAL SOCIETY OF LONDON, Series A, Vol. 84, pp. 107-118, 1911, 3 figs., 4 tables. This article reports of experiments on resistance to flow in helices, mostly in laminar ranges, as compared to flow in straight tubes.

- \*[37] Eustice, John, "Experiments on Stream-line Motion in Curved Pipes," 1911  
 PROCEEDINGS OF THE ROYAL SOCIETY OF LONDON, Series A, Vol. 85, pp. 119-131, 1911, 9 figs. Continuation of experiments on flow in coils to establish cause of increased loss in curved tubes. Dye streams used to delineate flow pattern.
- [38] Eustice, John, "Flow of Water in Pipe Bends," WATER AND WATER ENGINEERING, p. 270ff, July-November, 1924. Discussion of flow in bends and coils presenting experimental evidence.
- [39] Eustice, John, "Flow of Fluids in Curved Passages," ENGINEERING (London), Vol. 120, pp. 604-605, November 13, 1925, 4 figs. An attempt to correlate the resistance of the bend with observations of flow patterns in the laminar range, using dye to delineate the streamlines.
- [40] Fidler, T. Claxton, CALCULATIONS IN HYDRAULIC ENGINEERING, Part 2, 1902  
 London, 1902, 203 pp.
- [41] FLOW OF FLUIDS THROUGH VALVES, FITTINGS, AND PIPE, Technical Paper No. 409, Engineering and Research Division, Crane Co., 92 pp., Chicago, 1942, 51 figs., 7 tables. This is a design manual, including measurements of head loss in pipe bends and data taken from reports of other investigators.
- [42] "Flow of Water in Bends," ENGINEERING RECORD, Vol. 68, pp. 727-728, 1913  
 December 27, 1913, 2 figs. This article discusses various tests made on pipe bends and presents the formula of Jacobs and Sooy for the discharge.
- [43] "Flow of Water Through Pipe Bends," ENGINEERING NEWS-RECORD, Vol. 120, 1938  
 pp. 777-778, June 2, 1938, 2 figs. An abstract of Technical Bulletin No. 577, U. S. Department of Agriculture, presenting results of Yarnell's [120] experiments on 6-in. pipe bends.
- \*[44] Flügel, G., "Strömungsverluste und Krimmerproblem," HYDRAULISCHE PROBLEME (Flow Losses and Bend Problems, Hydraulic Problems), pp. 133-157, Berlin, 1926. The author presents a general discussion of the components of the losses occurring in bends.

- [45] Flügel, G., "Ergebnisse aus dem Strömungsinstitut der Technischen Hochschule Danzig" (Some Recent Experiments Made in the Hydrodynamical Laboratory of the Danzig Technical University), JAHREBUCH DER SCHIFFBAUTECHNISCHEN GESELLSCHAFT, Vol. 31, pp. 87-113, 1930, 30 figs. Includes a discussion of bends based on experiments of Nippert. (See [83].)
- [46] Fosdick, E. R., DIVERSION LOSSES IN PIPE BENDS, Engineering Bulletin No. 51, State College of Washington, 1937, 23 pp., 3 figs., 1 table, 11 photos. Experiments were made on bends of semi-circular cross section but of the same area as the approach tangent.
- [47] Foster, Dean E., "Effect of Fittings on Flow of Fluids through Pipe Lines," TRANSACTIONS, AMERICAN SOCIETY OF MECHANICAL ENGINEERS, Vol. 42, Paper No. 1766, pp. 647-669, 1920, 5 figs., 4 tables. Resistance of elbows and fittings are discussed.
- [48] Freeman, John R., "Experiments Relating to Hydraulics of Fire Streams," TRANSACTIONS OF THE AMERICAN SOCIETY OF CIVIL ENGINEERS, Vol. 21, Paper No. 426, pp. 303-482, November, 1889, 64 figs., 13 tables. This article presents results of experiments on resistance caused by bends in fire hose.
- \*[49] Freeman, John R., FLOW OF WATER IN PIPES AND PIPE FITTINGS, New York, 1941, 349 pp., 196 figs. An exhaustive series of tests on standard pipe fittings and assemblies made in 1892 have been compiled on the basis of present-day concepts of fluid mechanics. Resistances for specific arrangements of fittings are plotted against Reynolds number.
- [50] Fuller, W. E., "Loss of Head in Bends," JOURNAL OF THE NEW ENGLAND WATERWORKS ASSOCIATION, Vol. 27, pp. 509-521, 1913, 4 figs., 1 table. This is a general discussion of loss of head in bends.
- [51] Giesecke, F. E., "The Friction of Water in Iron Pipes and Elbows," JOURNAL OF THE AMERICAN SOCIETY OF HEATING AND VENTILATING ENGINEERS, Vol. 23, pp. 587-594, July, 1917, 6 figs. Measurement of resistance caused by standard elbows of different sizes is given.

- [52] Giesecke, F. E., and Badgett, W. H., "Supplementary Friction Heads in One-Inch Cast-Iron Tees," TRANSACTIONS, AMERICAN SOCIETY OF HEATING AND VENTILATING ENGINEERS, Vol. 38, pp. 111-120, 1932, 9 figs. Photograph of streamlines at a tee when fluid is being diverted is included.
- [53] Giesecke, F. W., and Badgett, W. H., "Loss of Head in Copper Pipe and Fittings," TRANSACTIONS, AMERICAN SOCIETY OF HEATING AND VENTILATING ENGINEERS, Vol. 38, pp. 529-542, 1932, 13 figs. Total head loss was measured in standard 3/4-in., 1-in., 1 1/4-in., and 1 1/2-in. copper elbows.
- [54] Giesecke, F. E., and Hopper, J. S., "A Comparative Study of Friction Heads in Screwed and Welded Elbows," TRANSACTIONS, AMERICAN SOCIETY OF HEATING AND VENTILATING ENGINEERS, Vol. 48, pp. 201-214, 1942, 8 figs., 4 tables. Experiments show lower resistance for standard 1 1/2-in. and 2 1/2-in. elbows with welded connections, as compared to screwed connections.
- [55] Giesecke, F. E., Reming, C. P., Knudson, J. W., Jr., THE FRICTION OF WATER IN ELBOWS, University of Texas Bulletin No. 2712 (Engineering Research Series No. 22), 1927, 36 pp., 15 figs., 8 tables. Measurement of total head loss in standard 90° elbows is given.
- [56] Gregory, W. B., and Schoder, E. W., "Some Pitot Tube Studies," TRANSACTIONS, AMERICAN SOCIETY OF MECHANICAL ENGINEERS, Vol. 30, Paper No. 1199, pp. 351-372, 1908, 9 figs., 4 tables. Velocity traverses by Pitot tube at various sections of bend are presented.
- [57] Grether, Hans, ÜBER POTENTIALBEWEGUNG TROPFBARER FLÜSSIGKEITEN IN GEKRÜMMTEN KANÄLEN (On Potential Flow in Liquids in Curved Channels), Berlin, 1909, 119 pp., 19 figs., 41 tables. The author designed bends on the basis of potential flow and compared the resistances to flow with those in bends consisting of simple arcs.
- [58] Grindley, John H., and Gibson, A. H., "On the Frictional Resistances to the Flow of Air through a Pipe," PROCEEDINGS OF THE ROYAL SOCIETY OF LONDON, Series A., Vol. 80, pp. 114-139, 1908, 8 figs., 6 tables. In connection with the determination of viscosity the resistance to flow in a 1/8-in. tube wound as a helix. Flow was in the laminar range. Data used by White in correlation of resistance according to Dean's criterion.

- [59] HEAD LOSSES IN VARIOUS TYPES OF PIPE BENDS, U. S. Waterways Experiment Station, Limited Edition Series, Paper HS, July, 1933, (Prepared by H. D. Vogel). Data are given on head loss of 6-in., 8-in., and 10-in. pipe bends of  $45^\circ$ ,  $90^\circ$ , and  $180^\circ$  deflection angles.  $R/d$  ranged from 0 to 3.0.
- [60] Hickox, G. H., Peterka, A. J., and Elder, R. A., "Friction Coefficients in a Large Tunnel," PROCEEDINGS OF THE AMERICAN SOCIETY OF CIVIL ENGINEERS, Vol. 73, pp. 451-470, April, 1947, 12 figs., 9 tables. This article includes measurements of losses caused by bends in a large tunnel.
- [61] Hinderks, A., "Nebenströmungen in Gekrümmten Kanälen" (Secondary Currents in Curved Channels), ZEITSCHRIFT DES VEREINES DEUTSCHER INGENIEURE, Vol. 71, Part 2, pp. 1779-1783, December 17, 1927, 18 figs. Photographs and diagrams are given showing secondary currents in the boundary layer.
- \*[62] Hofmann, Albert, "Loss in 90-Degree Pipe Bends of Constant Circular Cross-Section," TRANSACTIONS OF THE HYDRAULIC INSTITUTE OF THE MUNICH TECHNICAL UNIVERSITY, Bulletin 3, 1929, trans. and pub. by American Society of Mechanical Engineers, pp. 29-41, 1935, 18 figs., 14 tables. Very careful experiments were made to determine resistance coefficients in smooth and rough bends for  $R/d$  from one to ten.
- [63] Jacobs, G. S., and Sooy, F. A., "New Method of Water Measurement by Use of Elbows in Pipe Line," JOURNAL OF ELECTRICITY, POWER AND GAS, Vol. 27, pp. 72-78, July 22, 1911, 6 figs. 4 tables. This is a report of tests to establish relationship of pressure difference between inside and outside walls of bend to discharge.
- [64] Kaplan, Viktor, "The Development of Bent Draft Tubes," TRANSACTIONS, WORLD POWER CONFERENCE, Barcelona, Sectional Meeting, Vol. 2, pp. 41-61, 1929. From the results of tests on bent draft tubes the author was led to a design in which the velocity along the inner wall remained greater than a certain minimum to prevent separation.
- [65] Kawada, "On the Measurement of Pressure and Velocity of Water Stream in a Curved Pipe," SOCIETY OF MECHANICAL ENGINEERS, Tokyo, Vol. 32, pp. 454-466, 1929, (in Japanese). This gives results of measurements of pressures and velocities of flow in curved pipe bends.

- \*[66] Keulegan, G. H., and Beij, K. H., "Pressure Losses for Fluid Flow in Curved Pipes," JOURNAL OF RESEARCH OF THE NATIONAL BUREAU OF STANDARDS, Vol. 18, RP 965, pp. 89-114, January, 1937, 15 figs., 5 tables. Experimental and theoretical study was made of the flow in long radius curved pipes in the laminar and turbulent range. Relationships for resistance of established curved flow were obtained.
- \*[67] Keutner, Chr., "Strömungsverhältnisse in einem Senkrechten Krümmer" (Flow Conditions in a Vertical Bend), ZEITSCHRIFT DES VEREINES DEUTSCHER INGENIEURE, Vol. 77, pp. 1205-1209, November 11, 1933, 7 figs. Experiments on the flow in vertical bends, including measurements of pressure and velocity at various cross sections, were made. Formulas presented permit pressure losses to be calculated from the approach velocity.
- \*[68] Kirchbach, Hans, "Loss of Energy in Miter Bends," TRANSACTIONS OF THE HYDRAULIC INSTITUTE OF THE MUNICH TECHNICAL UNIVERSITY, BULLETIN 3, 1929, trans. and pub. by American Society of Mechanical Engineers, pp. 43-64, 1935, 47 figs. This article presents pressure measurements for flow through miter bends of  $30^\circ$ ,  $45^\circ$ ,  $60^\circ$ , and  $90^\circ$  deflections and various combinations of these bends. Curves are presented to show relationship of loss to Reynolds number and to deflection angle for smooth walls.
- [69] Kumabe, K., "An Experiment on the Flow of Water Through a Circular Bend of Rectangular Section," JOURNAL, SOCIETY OF MECHANICAL ENGINEERS, Tokyo, Vol. 26, pp. 49-67, 1923, 4 figs. 9 tables, 18 plates. This paper presents a theoretical treatment for the pressure distribution normal to the bend axis and includes a large number of pressure measurements at numerous points in a  $90^\circ$  bend of square cross section.
- [70] Lansford, W. M., THE USE OF AN ELBOW IN A PIPE LINE FOR DETERMINING THE RATE OF FLOW IN A PIPE, University of Illinois Engineering Experiment Station, Bulletin No. 289, 1936, 33 pp., 22 figs., 2 tables. This bulletin reports on the development of an equation for the relationship of mean velocity to the transverse pressure drop in a bend and presents the results of experiments to establish coefficients of discharge for such a metering device.
- [71] Lea, F. C., HYDRAULICS, New York, 1908, 536 pp. A general discussion of head loss in bends. Work of Weisbach and St. Venant is included.

- \*[72] Lell, Jacob, "Beitrag zur Kenntnis der Sekundärströmung in Gekrümmten Kanälen" (Secondary Flow of Liquids in Curved Channels), ZEITSCHRIFT FÜR DAS GESAMTE TURBINENWESEN, Vol. 11, pp. 129-135, 293-298, 313-317, 1914, 12 figs., 9 tables. This is an early work on the distribution of pressure around a bend and presents photographic evidence of the existence of secondary spiral flow in the bend.
- [73] Löliger, "Untersuchung des Druck-und Strömungsverlaufs in Schaufeln" (Investigation of Pressure Distribution and Flow Pattern around Vanes), dissertation, Zurich, 1913. Spiral flow in bends is discussed.
- \*[74] Lorenz, H., "Der Widerstand von Rohrkrümmern" (The Resistance of Curved Pipes), PHYSIKALISCHE ZEITSCHRIFT, Vol. 30, pp. 228-230, 1929, 1 fig., 1 table. A theoretical treatment is given of the flow through bends to determine the form of the resistance coefficient, based on the pressure gradient normal to the bend.
- \*[75] Madison, R. D., and Parker, J. R., "Pressure Losses in Rectangular Elbows," TRANSACTIONS, AMERICAN SOCIETY OF MECHANICAL ENGINEERS, Vol. 58, AER-58-2, pp. 167-176, 1936, 16 figs. This paper presents data on pressure losses in rectangular elbows as affected by (1) radius ratio of the elbow, (2) aspect ratio, (3) deflection angle, (4) velocity of flow, (5) splitters in elbows, and (6) compound elbows.
- [76] Marks, L. S., Lomax, J., and Ashton, R., "Influence of Bends in Inlet Ducts on the Performance of Induced-Draft Fans," TRANSACTIONS, AMERICAN SOCIETY OF MECHANICAL ENGINEERS, Vol. 55, FSP-55-9, pp. 133-143, 1933, 37 figs., 5 tables. The influence of elbows close to the inlet section of induced-draft fans on the efficiency of the fans and method of improving the efficiency by the use of splitters in the elbow is discussed. The work contains test data on various elbow arrangements.
- [77] Melovich, A., "A Rational Form of Draft Tube for Water Turbines," ENGINEERING (London), Vol. 118, p. 153, August 1, 1924, 2 figs. The author recommends the use of a slightly modified form of a quarter-turn tube having a correct theoretical form such that the dead water space is eliminated.

- [78] Merriman, Mansfield, TREATISE ON HYDRAULICS, New York, 1913, 565 pp. 1913  
A short discussion of the loss of head in bends is included.
- [79] Miyagi, Otogoro, "Flow in Curved Pipes and Its Stability," THE TECHNOLOGY REPORTS OF THE TOHOKU IMPERIAL UNIVERSITY, Sendai, Japan, Vol. 11, pp. 1-15, 1933, 4 figs. This is a theoretical evaluation of the factors involved in curved flow compared to flow in a straight pipe, concluding that for the same velocity the pressure drop in a curved pipe is  $(1 + am)$  times that in a straight pipe, where  $m = d/2R$ , and  $a = \text{constant}$ , independent of dimensions.
- [80] Mockmore, C. A., "Flow Characteristics in Elbow Draft Tubes," TRANSACTIONS OF THE AMERICAN SOCIETY OF CIVIL ENGINEERS, Vol. 103, Paper No. 1990, pp. 402-464, 1938, 32 figs., 8 tables. Experiments were performed of flow in quarter-turn bends designed on the basis of potential flow to measure velocity distribution.
- [81] Moreell, Ben, "Lost-Head Diagrams for Bends in Water Pipe," ENGINEERING NEWS, Vol. 75, pp. 302-304, February 17, 1916, 11 figs. Diagrams are presented for computation of the loss of head in pipe bends.
- [82] Neville, John, HYDRAULIC TABLES, COEFFICIENTS AND FORMULAE, London, 1875. A general discussion is given of the research on flow in bends to that time (1875).
- \*[83] Nippert, H., "Über den Strömungsverlust in Gekrümmten Kanälen" (On the Flow Losses in Bends), FORSCHUNGSARBEITEN AUF DEM GEBIETE DES INGENIEURWESENS, Bulletin 320, 1929, 141 figs., 6 plates. This is an experimental study of the effect upon bend resistance of transverse and longitudinal shape of  $90^\circ$  and  $180^\circ$  bends. Tests include measurement of velocity and pressures in and on the bend.
- [84] Nippert, H., "Neuere Versuche Über den Strömungsvorgang in Gekrümmten Kanälen" (New Experiments on the Flow Phenomena in Curved Channels), DER BAUINGENIEUR, Vol. 11, pp. 76-79, January 31, 1930, 9 figs. This is a discussion of experiments on loss of head in  $90^\circ$  and  $180^\circ$  rectangular bends.
- [85] Nippert, H., "Verlustverminderung in Rechtwinkligen Krümmern" (Reduction of Losses in Rectangular Bends), DIE WAERME, Vol. 52, pp. 792-793, October 19, 1929, 4 figs. Numerous and detailed tests on rectangular pipe bends were made. Data are given on velocity distribution, pressure curves, and losses.

- [86] Nordell, C. H., "Curved Flow in Conduits of Constant Cross-Section," 1940  
 THE OIL AND GAS JOURNAL, Vol. 39, pp. 117-124, May 16, 1940. This is a synopsis of recent investigations on the resistance of bends to flow.
- [87] Nordell, C. H., "Improved Conduit Bends Reduce Frictional Loss," 1940  
 THE OIL AND GAS JOURNAL, Vol. 39, pp. 50-55, June 13, 1940, 9 figs. The author suggests various manners of enlargement of the cross section of bends so as to ease the secondary currents and decrease friction loss.
- [88] Parker, O. E., "An Investigation of Pressure Losses in Air Duct Elbows," 1934  
 Unpublished B.S. in M.E. thesis, Library, Northeastern University, 1934, 34 pp., 9 pp. figs. This is a report on measurement of losses in a 12-in. by 12-in. duct elbow as related to the radius ratio varying from 0 to 3.0.
- [89] Perry, Lynn, "Tests of Loss of Head in Standard Elbows and Tees," 1924  
 ENGINEERING NEWS-RECORD, Vol. 92, p. 940, May 29, 1924, 2 figs. This gives measurement of pressure loss in standard 1-in., 1 1/2-in., 2 1/2-in., and 3-in. elbows as a function of velocity.
- [90] Pfarr, A., "Die Turbinen für Wasserkraftbetrieb" (Turbines for Water Power Plants), 1912  
 ZEITSCHRIFT DES VEREINES DEUTSCHER INGENIEURE, Vol. 56, Part 2, pp. 1713-1714, 1912.
- [91] Rennie, George, PHILOSOPHICAL TRANSACTIONS OF THE ROYAL SOCIETY OF LONDON, 1831  
 pp. 438-439, 1831. A series of tests were made on a lead pipe 1/2 inch in diameter and 15 ft long. Curves had radii of 3 1/4 in. and 7 1/2 inches.
- [92] Richter, H., "Der Druckabfall in Gekrümmten Glatten Rohrleitungen" (The Pressure Drop in Smooth Bends), 1930  
 FORSCHUNGSARBEITEN AUF DEM GEBIETE DES INGENIEURWESENS, Bulletin 338, 1930, 30 pp., 34 figs., 28 tables. This article reports experiments on the pressure drop in smooth copper tubes in relation to the Reynolds number and radius ratio.
- \*[93] Robertson, James M., "A Study of the Flow of Water in Bends," 1938  
 Unpublished B.S. in C.E. thesis, Library, University of Illinois, 1938, 40 pp., 20 figs. A report on the velocity distribution in standard long radius 4-ft, 90° pipe bends at the midpoint of the bend with the corresponding pressure difference between the inside and outside walls.

- [94] De Saint-Venant, M., "Memoire sur l'influence Retardatrice de la Courbure dans les Courants d'Eau" (Memoirs of the Retarding Influence of Curves on Running Water), COMPTES RENDUS HEBDOMADAIRES DES SEANCES DE L'ACADEMIE DES SCIENCES, Vol. 54, pp. 38-42, 1862, 1 table. Dubuat's formula is quoted and data are given on several tests with calculated and observed losses.
- [95] Schmidbauer, Hans, "Behavior of Turbulent Boundary Layers on Curved Convex Walls," thesis for Dr. of Eng. degree, Munich Technical University, 1934, trans. and pub. as Technical Memorandum No. 791, U. S. National Advisory Committee for Aeronautics, 1936, 31 pp., 35 figs. This thesis shows analytically and experimentally that the transition of the boundary layer to turbulent flow occurs at higher Reynolds numbers because of the centrifugal force on convex walls.
- \*[96] Schoder, E. W., "Curve Resistance in Water Pipes," TRANSACTIONS OF THE AMERICAN SOCIETY OF CIVIL ENGINEERS, Vol. 62, Paper No. 1093, pp. 67-112, 1909, 23 figs., 15 tables, 3 plates. This paper is a report of experimental investigation to determine head loss as a function of  $R/d$  in 6-in. circular bends with  $R/d$  varying from 1.3 to 2.0.
- \*[97] Schubart, Werner, "Energy Loss in Smooth- and Rough-Surfaced Bends and Curves in Pipe Lines," TRANSACTIONS OF THE HYDRAULIC INSTITUTE OF THE MUNICH TECHNICAL UNIVERSITY, BULLETIN 3, 1929, trans. and pub. by American Society of Mechanical Engineers, pp. 81-99, 1935, 49 figs. A continuation of the experimental work of Kirchbach [68] includes resistance measurements of single miter bends of varying deflection angles and smooth walls. Experiments were also made on compound miter bends with rough walls.
- [98] Scobey, Fred C., "Flow of Water in Tulsa 60-In. and 54-In. Concrete Pipe Line," ENGINEERING NEWS-RECORD, Vol. 94, pp. 894-897, May 28, 1925, 5 figs. Loss of head caused by bends in large concrete pipes is given.
- \*[99] Spalding, W., "Versuche Über den Strömungsverlust in Gekrümmten Leitungen" (Experiments on Flow Loss in Curved Conduits), ZEITSCHRIFT DES VEREINES DEUTSCHER INGENIEURE, Vol. 77, pp. 143-148, 1933, 26 figs. This is a report on the continuation of Nippert's experiments 83 applied to bends of angles of deflection other than  $90^\circ$  and  $180^\circ$ . The effects of the deflection angle and the inner and outer radius of the bend were studied.

- [100] Stuart, M. C., Warner, C. F., and Roberts, W. C., "Pressure Loss Caused by Elbows in 8-Inch Round Ventilating Duct," TRANSACTIONS, AMERICAN SOCIETY OF HEATING AND VENTILATING ENGINEERS, Vol. 48, pp. 335-350, 1942, 14 figs. Curves are presented showing pressure drop compared to velocity for various bends in a ventilating duct.
- [101] Sullivan, M. E., NEW HYDRAULICS, Denver, 1900, pp. 186-194. The author presents a formula for loss of head in bends, and mentions tests of earlier investigators.
- [102] Szczeniowski, Boleslaw, "Design of Elbows in Potential Motion," JOURNAL OF AERONAUTICAL SCIENCES, Vol. 11, pp. 73-75, January, 1944, 5 figs. This article contains theoretical determination of the shape of bends based upon potential flow theory.
- \*[103] Taylor, G. I., "The Criterion for Turbulence in Curved Pipes," PROCEEDINGS OF THE ROYAL SOCIETY OF LONDON, Series A, Vol. 124, pp. 243-249, 1929, 3 figs., 1 table. An experimental determination of the laminar-turbulent critical for flow in curves by means of dye streams is reported, and it is demonstrated that the critical Reynolds number is higher for curved tubes than for straight tubes.
- [104] Tomita, K., "On the Flow of Water in Pipe Coils," JOURNAL OF THE SOCIETY OF MECHANICAL ENGINEERS, Tokyo, Vol. 35, No. 180, 1932. (In Japanese).
- [105] Trautwine, J. C., Jr., "Resistance Due to Bends in Pipes," PROCEEDINGS OF THE AMERICAN WATER WORKS ASSOCIATION, pp. 328-334, 1904, 4 figs. This is a discussion of the Weisbach formula for resistance with reference to a standard 90° bend and a short radius 90° bend.
- [106] Vazsonyi, Andrew, "Pressure Loss in Elbows and Duct Branches," TRANSACTIONS, AMERICAN SOCIETY OF MECHANICAL ENGINEERS, Vol. 66, pp. 177-183, April, 1944, 14 figs. This is a discussion of pressure losses on the basis of results of several investigators.
- [107] Venturi, J. B., "Experimental Researches Concerning the Principle of the lateral Communication of Motion in Fluids, applied to the Explanation of various Hydraulic Phenomena," trans. and pub. by William Nicholson in A JOURNAL OF NATURAL PHILOSOPHY, CHEMISTRY, AND THE ARTS, Vol. II, pp. 172-179, 273-276, 422-426, 487-494, 1799, and Vol. III, pp. 13-22, 59-61, 1800. A report is given of early experiments on flow through bends.

- [108] von Cordier, "Untersuchung der Wasserströmung in einem Rohrkrümmer" (Investigation of Water Flow in a Pipe Bend), ZEITSCHRIFT FÜR DAS GESAMTE TURBINENWESEN, Vol. 11, pp. 396-398, 405-410, 1914, 16 figs., 1 table. Results of experiments on pressure distribution and flow pattern in a rectangular 90° bend.
- \*[109] Wasielewski, Rudolf, "Verluste in Glatten Rohrkrümmern mit Kreisrundem Querschnitt Bei Weniger als 90° Ablenkung" (Loss in Smooth Pipe Bends of Circular Cross Section for Deflections Less than 90°), MITTEILUNGEN DES HYDRAULISCHEN INSTITUTS DER TECHNISCHEN HOCHSCHULE, Vol. 5, pp. 53-67, 1932. Experiments of Hofmann [62] for smooth bends with deflection angles of less than 90° were continued. Data are presented showing the relationship of resistance coefficient to Reynolds number for smooth pipes.
- \*[110] Wattendorf, F. L., "A Study of the Effect of Curvature on Fully Developed Turbulent Flow," PROCEEDINGS OF THE ROYAL SOCIETY OF LONDON, Series A, Vol. 148, pp. 565-598, February, 1935, 24 figs., (also, Guggenheim Aeronautics Laboratory, California Institute of Technology Publication No. 54). This is a discussion of two-dimensional curved flow concerning shear distribution, flow in concentric cylinders, the Prandtl theory of curved flow, exchange coefficient, Taylor's consideration of vorticity transport and velocity distribution in the neighborhood of the wall.
- [111] Wattendorf, Frank L., SOME EXPERIMENTAL INVESTIGATIONS OF FLOW IN CURVED CHANNELS, Guggenheim Aeronautics Laboratory, California Institute of Technology Publication No. 43, 7 pp., 15 figs. The velocity distribution and longitudinal pressure changes in two-dimensional curved flow were studied and results compared with theoretical distributions. (This is a condensation of [110].)
- [112] Wegmann, Edward, CONVEYANCE AND DISTRIBUTION OF WATER FOR WATER SUPPLY, New York, 1918, pp. 40-49. This book contains a general discussion on loss of head caused by bends. The data on many investigators are presented.
- [113] Weisbach, Julius, EXPERIMENTAL-HYDRAULIK, Freiburg, 1855, p. 157. Tests made on bends and pipes of 1-cm diameter included observations of bend resistance. Formula is presented for loss,  $H_b = \zeta V^2/2g$ , where  $\zeta = 0.131 + 1.847(a/r)^{7/2}$ ,  $a$  = radius of pipe, and  $r$  = radius of curvature.

- \*[114] White, C. M., "Streamline Flow Through Curved Pipes," PROCEEDINGS OF THE ROYAL SOCIETY OF LONDON, Series A, Vol. 123, pp. 645-663, 1929, 10 figs., 2 tables. Correlation is given of experimental data on flow through small tubes in form of helix on the basis of Dean's criterion,  $Re (a/r)^{1/2}$ , for laminar flow; it suggests an increase of Reynolds number of the turbulent critical for curved flow.
- [115] Williams, Gardner S., "The Foundation of our Knowledge of Hydraulic Curve Resistance," THE TECHNIC, New Series No. 12, University of Michigan Engineering Society, pp. 48-59, 1899, 5 tables. This article is a brief synopsis of all known experimental investigations on curve resistance prior to 1899. It includes description and results of experiments conducted by Bossut (1777), Dubuat (1786), Rennie (1831), Venturi (1797), and Weisbach (1863).
- \*[116] Williams, G. S., Hubbell, C. W., and Fenkell, G. H., "Experiments at Detroit, Michigan, on the Effect of Curvature upon the Flow of Water in Pipes," TRANSACTIONS OF THE AMERICAN SOCIETY OF CIVIL ENGINEERS, Vol. 47, Paper No. 911, pp. 1-369, 1902, 131 figs., 90 tables. Data on head loss caused by curvature in 12-in., 16-in., and 30-in. pipes as installed are given.
- [117] Williamson, James, "Considerations of Flow in Large Pipes, Conduits, Tunnels, Bends, and Siphons," JOURNAL OF THE INSTITUTION OF CIVIL ENGINEERS, Vol. 11, Paper No. 5189, pp. 451-502, 1938-39, 15 figs., 11 tables. This paper includes a discussion of flow in bends and cites data of Davies and Puranik [27]; it recommends method of evaluating losses approximately.
- \*[118] Wirt, Loring, "New Data for the Design of Elbows in Duct Systems," GENERAL ELECTRIC REVIEW, Vol. 30, pp. 286-296, June, 1927, 19 figs. Reports experimental study of the factors causing head loss in bends in duct systems, including radius ratio and aspect ratio. The flow paths were determined by making casts of the inside of the bend after air had delineated the pattern in a mixture of lamp-black and oil. Tests on splitters in elbows are included.
- [119] Witoszynski, C., "Change of  $180^\circ$  in the Direction of a Uniform Current of Air," extract from PRZEGLADU TECHNICZNEGO, Vol. 63, 1925, contributed by Aerodynamic Laboratory of the Warsaw Polytechnic Institute, trans. and pub. as Technical Memorandum No. 350, U. S. National Advisory Committee for Aeronautics, 1926, 34 pp., 8 figs. This is a mathematical treatise to establish the flow patterns in bends with curved walls.

- \*[120] Yarnell, David L., FLOW OF WATER THROUGH 6-INCH PIPE BENDS, Technical Bulletin No. 577, U. S. Dept. of Agriculture, October, 1937, 117 pp., 103 figs., 2 plates. This bulletin presents a large number of velocity and pressure measurements in 6-in. pipe bends of 90° and 180° deflection and various compound curves. Data show flow patterns and pressure distributions caused by bend.
- [121] Yarnell, D. L., and Nagler, F. A., "Flow of Water Around Bends in Pipes," TRANSACTIONS OF THE AMERICAN SOCIETY OF CIVIL ENGINEERS, Vol. 100, Paper No. 1914, pp. 1018-1043, 1935, 18 figs. (See [120]).
- \*[122] Yarnell, D. L., and Woodward, S. M., FLOW OF WATER AROUND 180-DEGREE BENDS, Technical Bulletin No. 526, U. S. Dept. of Agriculture, October, 1936, 64 pp., 48 figs. This bulletin contains experimental data presenting a large number of velocity and pressure measurements in 180° bends of square and rectangular cross section.
- [123] Young, Thomas, "Hydraulic Investigations, Subservient to an Intended Croonian Lecture on the Motion of the Blood," PHILOSOPHICAL TRANSACTIONS OF THE ROYAL SOCIETY OF LONDON, pp. 164-186, 1808, 4 tables.
- \*[124] Zur Nedden, F., "Induced Currents of Fluids," TRANSACTIONS OF THE AMERICAN SOCIETY OF CIVIL ENGINEERS, Vol. 80, Paper No. 1364, pp. 844-913, 1916, 36 figs. A general discussion of the development of secondary flow in bends is included and the cause of such currents suggested. Some data of Lell on pressure distribution are presented.

## II. Flow through Conduit Bends with Guide Vanes

- [125] Brown, A. I., "Friction of Air in Elbows," POWER PLANT ENGINEERING, 1932 Vol. 36, pp. 630-631, August 15, 1932, 3 figs. Report of tests of the efficiency of guide vanes in sharp bends of a 12-in. by 12-in. duct is given. Vane shapes varied from simple angles to circular arcs of different radii. Losses caused by the different vanes were compared.
- \*[126] Collar, A. R., "Some Experiments with Cascades of Aerofoils," TECHNICAL REPORT OF THE AERONAUTICAL RESEARCH COMMITTEE, R. & M. 1768, Vol. II, pp. 1281-1287, 1937, 5 figs. This article describes experiments on six vane profiles to determine the most suitable type when considering pressure drop, angularity of downstream flow, and uniformity of velocity. Experiments included a test of corner with 20 per cent expansion.
- \*[127] Collar, A. R., "Cascade Theory and the Design of Fan Straighteners," 1940 TECHNICAL REPORT OF THE AERONAUTICAL RESEARCH COMMITTEE, R. & M. 1885, 1940, 16 pp., 7 figs., 1 table. A theoretical determination is made of the shape and setting of vane fan straighteners without regard for the sense of rotation of the slipstream.
- [128] Collar, A. R., "The Flow of a Perfect Fluid Through Cascades of Aerofoils," 1941 JOURNAL OF THE ROYAL AERONAUTICAL SOCIETY, Vol. 45, pp. 183-213, 1941, 24 figs. This paper contains a theoretical analysis of the flow of a perfect fluid through a cascade of airfoils based on the conformal transformation of a cascade of oval bodies. The paper also describes the process for carrying out the transformation.
- [129] Flügel, G., "Ergebnisse aus dem Strömungsinstitut der Technischen Hochschule Danzig" (Some Recent Experiments Made in the Hydrodynamical Laboratory of the Danzig Technical University), JAHRBUCH DER SCHIFFBAUTECHNISCHEN GESELLSCHAFT, Vol. 31, pp. 87-113, 1930, 30 figs. Includes a discussion of experiments with vanes.
- \*[130] Frey, Kurt, "Verminderung des Strömungs Widerstandes von Körpern Durch Leitflächen" (The Reduction of Flow Resistance of Bodies by means of Guide Vanes), FORSCHUNG AUF DEM GEBIETE DES INGENIEURWESENS, Vol. 4, pp. 67-74, March/April, 1933, 21 figs. Data are given showing the decrease in resistance of solid bodies that might be expected by the use of guide vanes at the nose or tail and experiments leading to the use of fewer vanes to effect a deflection of flow with lowered resistance.

- \*[131] Frey, Kurt, 1934 "Verminderung des Strömungsverlustes in Kanälen durch Leitflächen" (The Reduction of Flow Losses in Canals by means of Guide Vanes), FORSCHUNG AUF DEM GEBIETE DES INGENIEURWESENS, Vol. 5, pp. 105-117, May/June, 1934, 26 figs., 24 tables. This article presents experimental data pertaining to the reduction of corner losses by means of irregularly spaced vanes.
- \*[132] Harris, R. G., and Fairthorne, R. A., 1928-29 "Wind Tunnel Experiments with Infinite Cascades of Aerofoils," TECHNICAL REPORT OF THE AERONAUTICAL RESEARCH COMMITTEE, R. & M. 1206, Vol. I, pp. 286-304, 1928-29, 11 pp. figs., 5 tables. Measurements were made of the forces on and the flow behind the central airfoil of a cascade. Deflection, total head, pressure, and velocity were measured at the centerline covering one gap.
- \*[133] Klein, G. J., Tupper, K. F., and Green, J. J., 1930 "The Design of Corners in Fluid Channels," CANADIAN JOURNAL OF RESEARCH, Vol. 3, pp. 272-285, 1930, 24 figs. This report presents results of tests with a discussion pertaining to pressure drop, velocity distribution, and flow pattern of a series of vane types suggested for use in a wind tunnel. The data include measurement of pressure on the profile of one of the vanes.
- \*[134] Kröber, G., 1932 "Guide Vanes for Deflecting Fluid Currents with Small Loss of Energy," INGENIEUR ARCHIV, Vol. III, pp. 516-541, 1932, trans. and pub. as Technical Memorandum No. 722, U.S. National Advisory Committee for Aeronautics, (n.d.), 43 pp., 42 figs. This is an analytical treatment leading to the profile of guide vanes for corners based on the transformation of the characteristics of a tested profile in parallel flow to that of a deflected flow. Results of tests of the derived profiles are presented.
- \*[135] MacPhail, D. C., 1939 "Experiments on Turning Vanes at an Expansion," TECHNICAL REPORT OF THE AERONAUTICAL RESEARCH COMMITTEE, R. & M. 1876, 1939, 11 pp., 15 figs. This report describes experiments and results of tests to improve the flow following a particular set of vanes where an expansion occurred at the corner. Various types of screens were used to effect a more uniform velocity distribution.
- \*[136] Marcinowski, H., 1946 "The Significance of the Measured Lattice Characteristics for Calculation and Design of Axial Flow Turbines and Compressors," trans. from German published by Research and Standards Branch, Bureau of Ships, Navy Dept., May, 1946, 26 pp., 9 figs. This is a theoretical analysis of the flow through cascades to compare calculated characteristics with measured values.

- [137] Marks, L. S., and Flint, Thomas, "The Design and Performance of a High-Pressure Axial-Flow Fan," TRANSACTIONS, AMERICAN SOCIETY OF MECHANICAL ENGINEERS, Vol. 57, AER-57-1, pp. 383-388, 1935, 11 figs. This article includes tests of guide vanes designed on the basis of the measured flow conditions after the fan was built and presents results of the tests.
- \*[138] Merchant, W., "Flow of an Ideal Fluid Past a Cascade of Blades," Part I, TECHNICAL REPORT OF THE AERONAUTICAL RESEARCH COMMITTEE, R. & M. 1890, 1940, 10 pp., 4 figs. A mathematical analysis based on potential flow theory by the process of conformal transformations.
- \*[139] Merchant, W., and Collar, A. R., "Flow of an Ideal Fluid Past a Cascade of Blades," Part II, TECHNICAL REPORT OF THE AERONAUTICAL RESEARCH COMMITTEE, R. & M. 1893, 1941, 6 pp., 2 figs.
- [140] Nelson, D. W., and Smedberg, G. E., "The Performance of Side Outlets on Horizontal Ducts," TRANSACTIONS, AMERICAN SOCIETY OF HEATING AND VENTILATING ENGINEERS, Vol. 49, pp. 58-74, 1943, 16 figs. Reports the experimental development of vanes and devices to improve the performance of side outlets in duct systems.
- [141] Numachi, Fukusaburo, "Aerofoil Theory of Propeller Turbines and Propeller Pumps with Special Reference to the Effects of Blade Interference upon the Lift and the Cavitation," THE TECHNOLOGY REPORTS OF THE TOHOKU IMPERIAL UNIVERSITY, Sendai, Japan, Vol. 8, pp. 411-469, 1929, 19 figs., 2 tables. A theoretical treatment applying airfoil theory to the design of turbines and pumps. The paper includes a treatment of the effect on lift and drag of airfoils arranged in a cascade.
- [142] O'Brien, M. P., and Folsom, R. G., "Propeller Pumps," TRANSACTIONS, AMERICAN SOCIETY OF MECHANICAL ENGINEERS, Vol. 57, HYD-57-3, pp. 197-202, 1935, 7 figs., 2 tables. A simplified method of design for propeller pumps and fans based essentially on the propeller blade element theory of Pfleiderer.
- [143] O'Brien, M. P., and Folsom, R. G., "The Design of Propeller Pumps and Fans," UNIVERSITY OF CALIFORNIA PUBLICATIONS IN ENGINEERING, Vol. 4, No. 1, 1939, pp. 1-18, 13 figs. Presents a method of design based on theoretical flow through an infinite cascade of airfoils.

- \*[144] Patterson, G. N., "Note on the Design of Corners in Duct Systems," 1936  
TECHNICAL REPORT OF THE AERONAUTICAL RESEARCH COMMITTEE, R. & M. 1773, pp. 1288-1303, 1936, 12 figs., 2 tables. A critical resume of the research pertaining to flow around corners and bends with and without guide vanes. The data are taken from the literature.
- [145] Patterson, G. N., "Corner Losses in Ducts," AIRCRAFT ENGINEERING, Vol. 9, pp. 205-208, August, 1937, 7 figs. A resume of literature pertaining to corners. Much of the data presented in [144] is included.
- [146] Patterson, G. N., "The Design of Aeroplane Ducts," AIRCRAFT ENGINEERING, Vol. 11, pp. 263-268, 1939, 15 figs. A discussion of the losses in corners is included and is essentially a synopsis of the discussion in [144].
- [147] Pistolesi, E., "On the Calculation of Flow Past an Infinite Screen of Thin Airfoils," (pub. in Italian) PUBBLICAZIONI DELLA R. SCUOLA D'INGEGNERIA DI PISA, (seventh series) No. 323, September, 1937, trans. and pub. as Technical Memorandum No. 968, U. S. National Advisory Committee for Aeronautics, 1941, 35 pp., 7 figs. This report deals with the flow past an infinite screen of thin airfoils (two-dimensional problem). The vortex distribution across the profile is established with appropriate expansion in series and the velocity distribution, lift, moment, and profile shape deduced. Inversely, the distribution is deduced from the vorticity.
- [148] Quick, Ray S., "Problems Encountered in the Design and Operation of Impulse Turbines," TRANSACTIONS, AMERICAN SOCIETY OF MECHANICAL ENGINEERS, Vol. 62, pp. 15-27, 1940, 20 figs. The effect of vanes attached to the nozzle of an impulse turbine and their effect on nozzle shape and turbine efficiency are described.
- [149] Ruden, P., "Investigation of Single Stage Axial Fans," Technical Memorandum No. 1062, U. S. National Advisory Committee for Aeronautics, 1944, 115 pp., 41 figs., 3 tables. The article includes a theoretical investigation of the section characteristics of stationary guide vanes and of calculating the energy losses in stationary guide vanes.
- [150] Shimoyama, Yoshinori, "A Contribution to the Design of Axial-Flow Propeller-Type Machines with their Housing," MEMOIRS OF THE FACULTY OF ENGINEERING, KYUSHU IMPERIAL UNIVERSITY, Fukuoka, Japan, Vol. 8, pp. 91-201, 1936-40, 102 figs., 23 tables. Loss of head in cascades of vanes is calculated from airfoil theory.

- \*[151] Shimoyama, Yoshinori, "Experiments on Rows of Aerofoils for Retarded Flow," MEMOIRS OF THE FACULTY OF ENGINEERING, KYUSHU IMPERIAL UNIVERSITY, Fukuoka, Japan, Vol. 8, pp. 281-329, 1936-40, 51 figs. The purpose of the experiments was to study the effect of mutual interference of cascaded airfoils. Drag and lift were determined from pressure measurements on one airfoil.
- \*[152] Stuart, M. C., Warner, C. F., and Roberts, W. C., "Effect of Vanes in Reducing Pressure Loss in Elbows in 7-Inch Square Ventilating Duct," TRANSACTIONS, AMERICAN SOCIETY OF HEATING AND VENTILATING ENGINEERS, Vol. 48, pp. 409-424, 1942, 46 figs. This article tells of experiments with vanes and splitters of various types, including commercial vanes. Tests indicate similar results for all types of vanes. Good photographs of flow patterns are included.
- [153] Tarpely, C. E., "Effect of Vanes on the Flow of Water Through a 24-Inch Pipe," Unpublished M. S. thesis, Library, University of Illinois, 1940. Effect of vanes in elbows was determined by measurement of velocity distribution at points downstream of the vanes.
- \*[154] Weinig, F., "The Flow around Turbine and Compressor Blades," trans. from German pub. by Research and Standards Branch, Bureau of Ships, Navy Dept., May, 1946, 173 pp., 120 figs. A theoretical analysis is presented in great detail.

## III. Flow in Open Channel Bends

- [155] Beyerhaus, E., "Die Wirkungen einer Krümmung in offenen Wasserläufen auf Bewegungsvorgang und Bettgestaltung" (The Effects of a Curve in Open Channels upon Sediment Transportation and Bed Formation), ZEITSCHRIFT FÜR BAUWESEN, Vol. 72, pp. 156-163, 1922. This article describes the action of a bend in an open channel on the sediment movement and bed form.
- [156] Blue, F. L., Jr., Herbert, J. K., and Lancefield, R. L., "Flow Around a River Bend Investigated," CIVIL ENGINEERING, Vol. 4, pp. 258-260, May, 1934, 3 figs., 1 photo. Measurements of the flow around a bend of the Iowa River were made to verify theoretical considerations and establish the fact of spiral flow.
- [157] Chatley, Herbert, "Curvature Effect in Alluvial Channels," ENGINEERING (London), Vol. 131, pp. 196-197, February 13, 1931, and pp. 260-261, February 20, 1931. This article contains a discussion of the mechanics of flow around open channel curves and gives a formula showing relation between depth, radius of curvature, and angle of curvature.
- [158] Eakin, Henry M., "Diversity of Current-Direction and Load-Distribution on Stream-Bends," TRANSACTIONS OF THE AMERICAN GEOPHYSICAL UNION, Part II, pp. 467-472, 1935, 5 figs, 2 plates. This work presents observations of velocity and sediment movement in a river bend which indicate existence of helicoidal flow and magnitude of transverse slope.
- [159] Eddy, H. P., "Effect of Curvature upon Flow in Open Channels," ENGINEERING NEWS-RECORD, Vol. 87, pp. 516-517, September, 1921, 1 table.
- [160] Gangadharan, G., "Spiral Flow in Curved Channels," Unpublished M.S. thesis, Library, University of Iowa, 1927. An explanation is given of the development of spiral flow in curved open channels.
- [161] Gockinga, R. H., "La Pente Transversale et son Influence sur l'etat des Rivieres" (The Transverse Slope and its Influence on the State of Rivers), ANNALES DES PONTS ET CHAUSSEES, Paper No. 4, pp. 112-133, 1913, 9 figs. This paper is an analytical discussion of the transition from straight to curved portions of open channels.

- \*[162] Hegly, V. M., "Flow in Earthen Canals of Compound Cross-Section," abridged trans. from ANNALES DES PONTS ET CHAUSSEES, Vol. 106, pp. 445-528, 1936, appearing in Proceedings, American Society of Civil Engineers, Vol. 63, pp. 36-48, November, 1937, 4 figs. Experiments include tests of curved channels. Velocity distribution, head loss caused by curvature, and surface profiles were measured.
- [163] Hopson, E. G., "Gaugings in the Concrete Conduit of the Umatilla Project," ENGINEERING RECORD, Vol. 64, pp. 480-481, October, 1911. Losses caused by friction and curvature in concrete lined channel were measured.
- [164] Humphreys, A. A., and Abbott, H. L., "Report upon the Physics and Hydraulics of the Mississippi River," Professional Papers of the Corps of Topographical Engineers, United States Army, No. 4, pp. 313-315, 1861. Observations of the Mississippi River, including flow around bends, were made.
- [165] Ippen, A. T., "An Analytical and Experimental Study of High Velocity Flow in Curved Sections of Open Channels," Unpublished Ph.D. thesis, Library, California Institute of Technology, 1936. (See [166].)
- [166] Ippen, A. T., and Knapp, R. T., "A Study of High Velocity Flow in Curved Channels of Rectangular Cross-Section," TRANSACTIONS OF THE AMERICAN GEOPHYSICAL UNION, Part II, 1936, pp. 516-521, 5 figs. An analysis of the depth and surface profiles for supercritical flow is given and verified by experiment.
- [167] Knapp, Robert T., and Ippen, Arthur T., "Curvilinear Flow of Liquids with Free Surfaces at Velocities Above that of Wave Propagation," PROCEEDINGS OF THE FIFTH INTERNATIONAL CONGRESS FOR APPLIED MECHANICS, pp. 531-536, 1938, 5 figs. (See [166].)
- [168] Leliavsky, M., "Des Courants Fluviaux et de la Formation du Lit Fluvial" (Fluvial Streams and the Formation of Fluvial Deposits), 6th International Congress Interieure Navigation, The Hague, 6th question, No. 4, 1894, 46 pp. Observations of secondary currents in open channel bends are included.

- [169] MacMeeken, J. W., "Turbulence in Centrifugal Pumps," TRANSACTIONS, AMERICAN SOCIETY OF MECHANICAL ENGINEERS, Vol. 54, HYD-54-4, pp. 47-63, 1932, 23 figs. The method of computing head losses in river bends when velocities and radii are known is given.
- [170] Macphail, Jeffrey B., "Flow at High Velocity in a Curved Rectangular Flume," CIVIL ENGINEERING, Vol. 12, pp. 158-159, March, 1942, 2 figs. Calculations for the design and analysis of the curvature are given (design aspects of flume at LaTugne Plant of St. Maurice Power Corporation for sliding logs).
- \*[171] Mockmore, C. A., "Flow Around Bends in Stable Channels," TRANSACTIONS OF THE AMERICAN SOCIETY OF CIVIL ENGINEERS, Vol. 109, Paper No. 2217, pp. 593-628, 1944, 21 figs., 4 tables. This paper gives a mathematical analysis of the flow around open channel bends based upon the theories of hydrodynamics.
- \*[172] Raju, Sanjiva P., "Resistance to Flow in Curved Open Channels," abridged trans. from MITTEILUNGEN DES HYDRAULISCHEN INSTITUTS DER TECHNISCHEN HOCHSCHULE, MUNCHEN, Vol. 6, pp. 45-60, 1933, appearing in Proceedings, American Society of Civil Engineers, Vol. 63, pp. 49-55, November, 1937, 5 figs. The author compares the resistance of open channel bends to that of conduits by experiments in two bends of rectangular cross section.
- [173] "Recent Russian Studies of Flow in Rivers," ENGINEERING NEWS, Vol. 1904, pp. 183-186, September 1, 1904, 5 figs., 3 tables. A discussion of experiments of Leliavsky on helical motion of water in streams.
- \*[174] Ripley, H. C., "Relation of Depth to Curvature of Channels," TRANSACTIONS OF THE AMERICAN SOCIETY OF CIVIL ENGINEERS, Vol. 90, Paper No. 1599, pp. 207-265, 1927, 16 figs., 35 tables. The author devised several formulas for the shape of the cross section as a function of radius of curvature width and mean depth for bends in natural streams with movable beds.
- \*[175] Schwarz, A. I., "Flow of Water in Channels Curved in Vertical Plane to an Arc of a Circle," (In Russian), TRANSACTIONS OF THE SCIENTIFIC RESEARCH INSTITUTE OF HYDROTECHNICS, Leningrad, Vol. 16, pp. 129-147, 1935. Theoretical analysis resulted in a differential equation for the depth at different points. Only approximate solutions of the equation are as yet possible.

- \*[176] Thomson, J., "Experimental Demonstration in respect to the Origin of Windings of Rivers in Alluvial Plains and to the Mode of Flow of Water round Bends of Pipes," PROCEEDINGS OF THE ROYAL SOCIETY OF LONDON, Vol. 26, pp. 356-357, 1877. Early observations were made of secondary currents in bends by use of threads attached to the bed.
- [177] Vogel, H. D., and Thompson, P. W., "Flow in River Bends," CIVIL ENGINEERING, Vol. 3, pp. 266-268, 471, May, 1933, 2 figs., 2 photos. The authors discuss the development of helicoidal flow in river bends.
- [178] Wilson, Warren E., "Effect of Curvature in Supercritical Flow," 1941 CIVIL ENGINEERING, Vol. II, pp. 94-95, February, 1941, 5 figs. Tests indicated subhydrostatic pressures at bends at supercritical flow. An equation for relative depth is developed on this basis.
- [179] Woodward, Sherman M., HYDRAULICS OF THE MIAMI FLOOD CONTROL PROJECT, 1920 Technical Report, Part VII, Ohio Miami Conservancy District, pp. 264, 270, 1920. Formula is presented for transverse slope in open channel bend.
- \*[180] Yen, C. H., and Howe, J. W., "Effects of Channel Shape on Losses in a Canal Bend," CIVIL ENGINEERING, Vol. 12, pp. 28-29, January, 1942, 1 table, 2 photos. This article reports on experimental study of flow through a circular bend of rectangular cross section.

## A P P E N D I X

## INDEX TO ABSTRACTS

	Page
Adler, "Strömung in Gekrümmten Rohren" (Flow in Curved Pipes) . . . . .	64
Alexander, "Resistance Offered to the Flow of Water in Pipes by Bends and Elbows" . . . . .	67
Balch, INVESTIGATION OF HYDRAULIC CURVE RESISTANCE EXPERIMENTS WITH THREE-INCH PIPE . . . . .	68
Beij, "Pressure Losses for Fluid Flow in 90° Pipe Bends" . . . . .	70
Bouchayer, "Losses of Head in Bends and Branches" . . . . .	74
Brightmore, "Loss of Pressure in Water Flowing Through Straight and Curved Pipes" . . . . .	75
Busey, "Loss of Pressure due to Elbows in the Transmission of Air through Pipes and Ducts" . . . . .	78
Collar, "Some Experiments with Cascades of Aerofoils" . . . . .	162
Collar, "Cascade Theory and the Design of Fan Straighteners" . . . . .	165
Davies and Puranik, "The Flow of Water Through Rectangular Pipe Bends" . . . . .	81
Davis, INVESTIGATION OF HYDRAULIC CURVE RESISTANCE . . . . .	83
Dean, "The Streamline Motion of Fluid in a Curved Pipe" . . . . .	86
Eustice, "Flow of Water in Curved Pipes" . . . . .	87
Eustice, "Experiments on Stream-line Motion in Curved Pipes" . . . . .	89
Flügel, "Strömungsverluste und Krümmerproblem" (Flow Losses and Bend Problems) . . . . .	90
Freeman, FLOW OF WATER IN PIPES AND PIPE FITTINGS . . . . .	95
Frey, "Verminderung des Strömungs Widerstandes von Körpern Durch Leitflächen" (The Reduction of Flow Resistance of Bodies by means of Guide Vanes) . . . . .	169
Frey, "Verminderung des Strömungsverlustes in Kanälen durch Leitflächen" (The Reduction of Flow Losses in Canals by means of Guide Vanes) . . . . .	170
Harris and Fairthorne, "Wind Tunnel Experiments with Infinite Cascades of Aerofoils" . . . . .	172
Hegly, "Flow in Earthen Canals of Compound Cross-Section" . . . . .	210
Hofmann, "Loss in 90-Degree Pipe Bends of Constant Circular Cross-Section" . . . . .	98
Keulegan and Beij, "Pressure Losses for Fluid Flow in Curved Pipes" . . . . .	101
Keutner, "Strömungsverhältnisse in einem Senkrechten Krümmer" (Flow Conditions in a Vertical Bend) . . . . .	105
Kirchbach, "Loss of Energy in Miter Bends" . . . . .	106
Klein, Tupper, and Green, "The Design of Corners in Fluid Channels" . . . . .	175
Kröber, "Guide Vanes for Deflecting Fluid Currents with Small Loss of Energy" . . . . .	179
Lell, "Beitrag zur Kenntnis der Sekundärströmung in Gekrümmten Kanälen" (Secondary Flow of Liquids in Curved Channels) . . . . .	110
Lorenz, "Der Widerstand von Rohrkrümmern" (The Resistance of Curved Pipes) . . . . .	113
MacPhail, "Experiments on Turning Vanes at an Expansion" . . . . .	187
Madison and Parker, "Pressure Losses in Rectangular Elbows" . . . . .	115
Marcinowski, "The Significance of the Measured Lattice Characteris- tics for Calculation and Design of Axial Flow Turbines and Compressors" . . . . .	191

Merchant, "Flow of an Ideal Fluid Past a Cascade of Blades" . . . . .	193
Merchant and Collar, "Flow of an Ideal Fluid Past a Cascade of Blades" . . . . .	197
Mockmore, "Flow Around Bends in Stable Channels" . . . . .	213
Nippert, "Über den Strömungsverlust in Gekrümmten Kanälen" (On the Flow Losses in Bends) . . . . .	118
Patterson, "Note on the Design of Corners in Duct Systems" . . . . .	199
Raju, "Resistance to Flow in Curved Open Channels" . . . . .	216
Ripley, "Relation of Depth to Curvature of Channels" . . . . .	220
Robertson, "A Study of the Flow of Water in Bends" . . . . .	122
Schoder, "Curve Resistance in Water Pipes" . . . . .	127
Schubart, "Energy Loss in Smooth- and Rough-Surfaced Bends and Curves in Pipe Lines" . . . . .	128
Schwarz, "Flow of Water in Channels Curved in Vertical Plane to an Arc of a Circle" . . . . .	222
Shimoyama, "Experiments on Rows of Aerofoils for Retarded Flow" . . . . .	201
Spalding, "Versuche Über den Strömungsverlust in Gekrümmten Leitungen" (Experiments on Flow Loss in Curved Conduits) . . . . .	132
Stuart, Warner, and Roberts, "Effect of Vanes in Reducing Pressure Loss in Elbows in 7-Inch Square Ventilating Duct" . . . . .	205
Taylor, "The Criterion for Turbulence in Curved Pipes" . . . . .	134
Thomson, "Experimental Demonstration in Respect to the Origin of Windings of Rivers in Alluvial Plains and to the Mode of Flow of Water round Bends of Pipes" . . . . .	225
Wasielowski, "Verluste in Glatten Rohrkrümmern mit Kreisrundem Querschnitt Bei Weniger als 90° Ablenkung" (Loss in Smooth Pipe Bends of Circular Cross Section for Deflections Less than 90°) . . . . .	135
Wattendorf, "A Study of the Effect of Curvature on Fully Developed Turbulent Flow" . . . . .	137
Weinig, "The Flow around Turbine and Compressor Blades" . . . . .	208
White, "Streamline Flow Through Curved Pipes" . . . . .	142
Williams, Hubbell, and Fenkell, "Experiments at Detroit, Michigan, on the Effect of Curvature upon the Flow of Water in Pipes" . . . . .	145
Wirt, "New Data for the Design of Elbows in Duct Systems" . . . . .	147
Yarnell, FLOW OF WATER THROUGH 6-INCH PIPE BENDS . . . . .	149
Yarnell, and Woodward, FLOW OF WATER AROUND 180-DEGREE BENDS . . . . .	154
Yen and Howe, "Effects of Channel Shape on Losses in a Canal Bend" . . . . .	227
Zur Nedden, "Induced Currents of Fluids" . . . . .	158

## Abstract 1

Adler, M., "Strömung in Gekrümmten Röhren" (Flow in Curved Pipes), ZEITSCHRIFT VON ANGEWANDTE MATHEMATIK UND MECHANIK, Vol. 14, pp. 257-275, October, 1934, 23 figs.

Experiment has shown that the flow in curved pipes is characterized by the development of secondary currents superimposed upon the main flow. The secondary currents take the form of double spirals flowing in a thin layer close to the upper and lower walls toward the inside of the bend and then back to the outer wall along the diameter in the plane of the bend. As a result of the curvature, the resistance to flow in a curved pipe is greater than that of a corresponding flow in a straight pipe. Analytical work by Dean established a resistance formula as a function of the parameter  $G^2 a^7 / \mu^2 \nu^2 r$ , where  $G$  is the pressure drop,  $a$  is the radius of the pipe,  $\mu$  is the absolute viscosity of the fluid,  $\nu$  is the kinematic viscosity of the fluid, and  $r$  is the radius of the bend. White rearranged this parameter into the form  $\frac{\lambda}{\lambda_0} = f \left[ \text{Re} \left( \frac{a}{R} \right)^{1/2} \right]$ , where  $\lambda$  is the resistance coefficient for the curved pipe;  $\lambda_0 = 64/\text{Re}$ , the corresponding resistance coefficient for straight pipes; and  $\text{Re} = vd/\nu$ , the Reynolds number of the flow. The series obtained by Dean [32], however, for expressing the relationship of the resistance to the parameter is valid only for small values of Reynolds number in the laminar range.

The purpose of this report is to establish a resistance relationship which is valid for high Reynolds numbers in the laminar range. The analysis is based upon Prandtl's boundary layer theory that a substantial friction effect exists only in a very thin layer at the boundary of the fluid where the velocity decreases to zero from that in the main flow body. Outside of the boundary the fluid can be treated as frictionless. In accordance with the boundary layer theory for flow in curved pipes, it is assumed that the secondary flow from the outside wall toward the inside wall takes place within the boundary layer; and from the middle of the inside wall, where the two streams unite, the combined current flows across the center of the bend to the outside. •

At the edge of the boundary layer near the outer wall, the return current is continuously flowing into the boundary layer at a velocity that is relatively small because of the increased flow area across the main stream. If an element of the boundary layer is cut out from the rest by two planes

forming an angle,  $d\phi$ , at the center of curvature and two planes forming an angle,  $d\psi$ , at the center of the cross section, the change in momentum of the flow through the element can be calculated. Considering steady flow, the change in momentum of the flow through the elemental volume is equal to the external forces acting on it.

The author carried out the indicated calculations and obtained the following equation for the resistance coefficient for the flow:

$$\lambda = 5.12 a^{-1} \left(\frac{a}{R}\right)^{1/3} \left(\frac{\partial p}{R \partial \phi}\right)^{-1/3} \rho^{1/3} \nu^{2/3} \quad (1)$$

Introducing Reynolds number, equation (1) becomes

$$\lambda = 6.81 \left(\frac{a}{R}\right)^{1/4} Re^{-1/2}$$

Since  $\lambda_0 = 64/Re$  is the resistance coefficient for straight pipe for laminar flow,

$$\frac{\lambda}{\lambda_0} = 0.1064 \left[ Re \left(\frac{a}{R}\right)^{1/2} \right]^{1/2} \quad (2)$$

Experiments were made to verify this expression for the resistance in curved pipes on three 1-cm diameter,  $90^\circ$  bends with curvature ratios,  $a/R = 1/50, 1/100, 1/200$ . The pressure gradient along the pipe and the velocity distribution near the discharge end were measured. The results were plotted in the form  $\lambda/\lambda_0$  in terms of the parameter  $Re\left(\frac{a}{R}\right)^{1/2}$  in Fig. 1. The points for all three bends fall on a single curve and agree very well with the results of White's experiments. The analytical curve, equation (2), is also plotted to show the agreement with the experimental points for larger values of Reynolds number. The points all deviate from the single curve when the flow becomes turbulent. Figure 1 also shows Prandtl's approximation formula for the resistance curve

$$\frac{\lambda}{\lambda_0} = 0.37 \left[ Re \left(\frac{a}{R}\right)^{1/2} \right]^{0.36} \quad (3)$$

Figures 2 and 3 show the velocity curves for laminar and turbulent flow for the bend with  $\left(\frac{a}{R}\right) = 1/100$ .

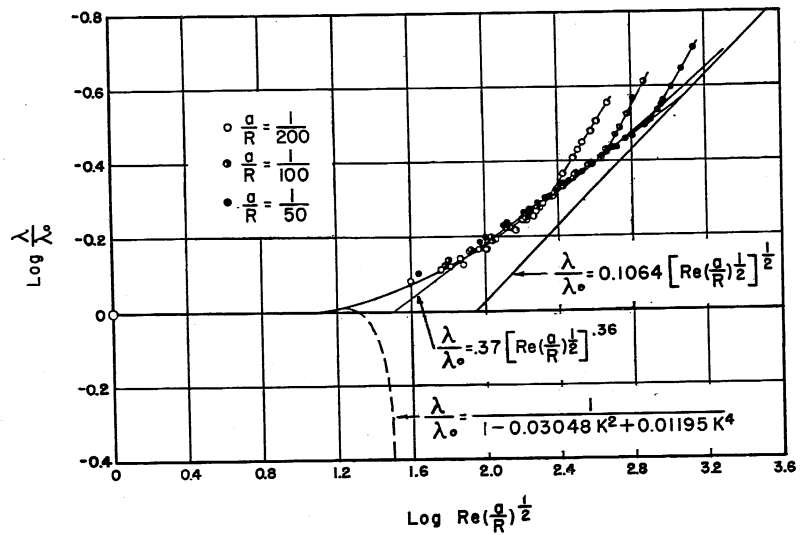


Fig.1—Dimensionless Plot of Resistance in Bends to Laminar Flow

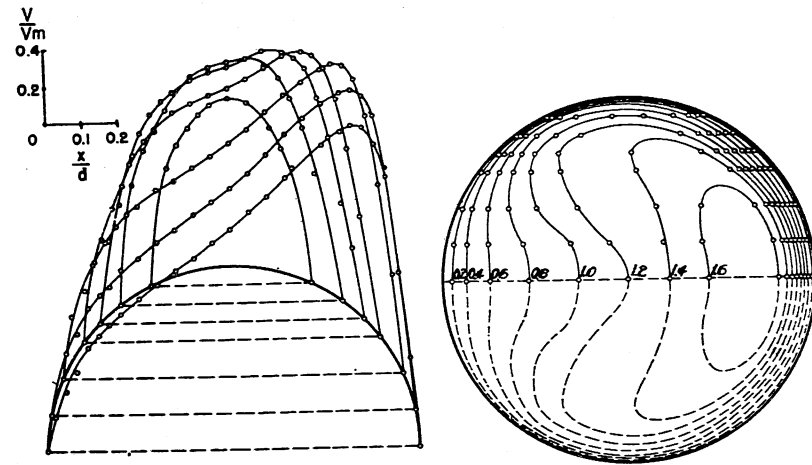


Fig.2—Velocity Distribution in Bend for Laminar Flow,  
 $\frac{a}{R} = \frac{1}{100}$   $\text{Re} = 2050$

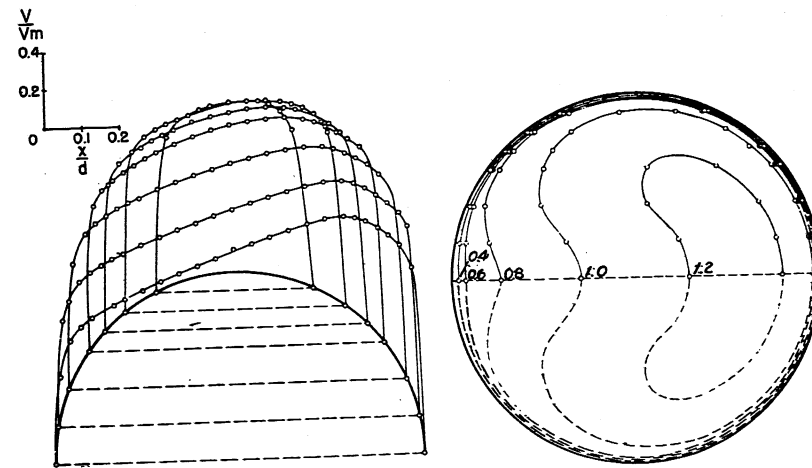


Fig.3—Velocity Distribution in Bends for Turbulent  
Flow,  $\frac{a}{R} = \frac{1}{100}$   $\text{Re} = 11770$

## Abstract 2

Alexander, C. W. L., "Resistance Offered to the Flow of Water in Pipes by Bends and Elbows," PROCEEDINGS OF THE INSTITUTION OF CIVIL ENGINEERS, Vol. 159, Paper No. 526, pp. 341-364, 1905, 14 figs., 3 tables.

This article describes experiments made to measure the pressure loss in bends in order to establish the influence of the radius ratio, (the ratio of the mean radius of curvature to the diameter of the pipe), upon the resistance as propounded by Weisbach. The experiments were performed on ten bends of varying radii of curvature. The values of  $R/d$  ranged from  $1/2$  to 5. Additional tests on a straight pipe of the same size were made to determine the loss caused by friction alone. The bends were constructed of wood in two parts and joined together with dowel pins. The inside diameter was  $1\ 1/4$  inch. Four coats of clear shellac varnish were applied to the interior to provide a smooth surface. Metal pipes were fitted to the two ends of the bends to provide exit and entrance segments. Piezometer taps were installed 2 in. from each end of the bends for the purpose of measuring the pressure drop. The pressure drop was measured in each bend for various velocities. The results were expressed by equations for the excess loss caused by the bend in the form,  $h_b = KV^{1.777}$ , where  $K$  is a constant for each bend. The results are plotted in Fig. 2, p. 16, in the form of bend coefficient,  $\eta = \frac{h_b}{v^2/2g}$ , in terms of radius ratio  $R/d$  for a velocity of 10 ft per sec.

The experiments indicated a bend coefficient of very low value compared to the results obtained by other investigators of smooth bends. Probably this was because the tangent losses downstream of the bend were not measured. Although it is not sharply defined, the results did suggest a minimum value of the bend coefficient in the neighborhood of  $R/d = 3$ .

## Abstract 3

Balch, Leland R., INVESTIGATION OF HYDRAULIC CURVE RESISTANCE EXPERIMENTS WITH THREE-INCH PIPE, Bulletin of the University of Wisconsin No. 578, (Engineering Series, Vol. 7, No. 3), 1913, 52 pp., 18 figs., 18 tables.

This bulletin presents the results of experiments on loss of head in 3-in. 90° pipe bends having radii of curvature such that the radius ratio,  $R/d$ , varied from 0.725 to 19.93. The purpose of the experiments was to investigate the relation of the loss of head to the radius of the bend. The bends were of several types. The long radius bends were bent to the proper curvature from 3-in., lap-welded wrought iron pipe; the remainder were standard elbows of different radii of curvature.

The piezometers for measuring the pressure loss were located about one foot upstream of the bend and 9 ft or 36 diameters downstream of the bend. As each bend was tested, a simultaneous comparative set of readings was taken on a straight length of pipe in the line containing the bend. The various other straight pipes in the assembly had been previously tested to determine their losses.

The net loss of head caused by the bend was determined from logarithmic plots of the head loss per foot in the bend and the head loss per foot in the straight pipe. The difference between the corresponding curves represents the net loss per foot caused by the bend only. The total loss,  $h_b$ , through the bend was simply the product of the loss per foot and the length of bend. In Fig. 1 the net loss of head per unit length equal to one pipe diameter is plotted in terms of  $R/d$  for a velocity of 10 ft per sec.

The bend coefficient  $\beta = \frac{h_b}{v^2/2g}$  is shown in Fig. 2 in terms of  $R/d$ . Results of other experiments are also included. The differences in loss of head in the results of various investigators are greater for large values of  $R/d$ , but good agreement is shown for small values of  $R/d$ .

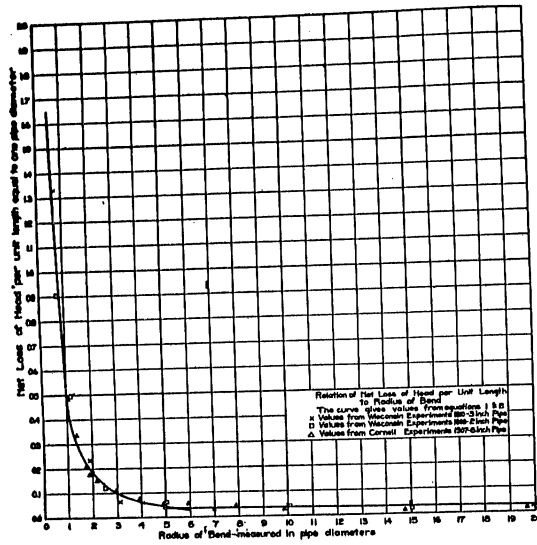


Fig. 1—Relation of Net Loss of Head Per Unit Length to Radius of Bend

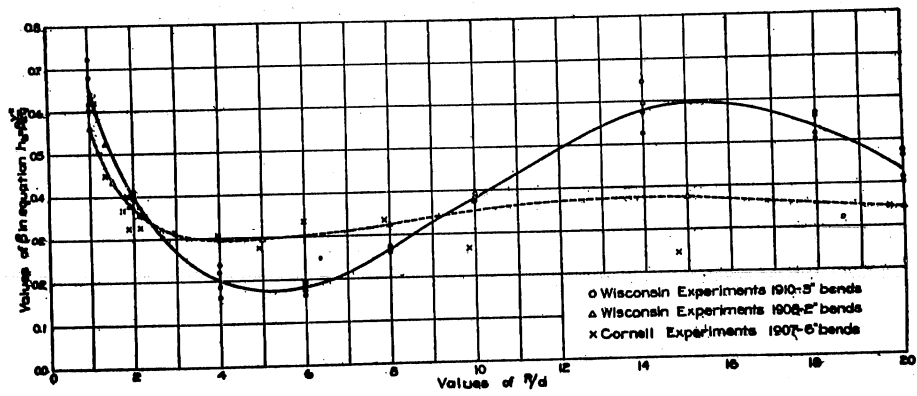


Fig. 2—Relation of Bend Coefficient  $\beta$  to Radius Ratio  $\frac{R}{d}$

## Abstract 4

Beij, K. Hilding, "Pressure Losses for Fluid Flow in 90° Pipe Bends," JOURNAL OF RESEARCH OF THE NATIONAL BUREAU OF STANDARDS, Vol. 21, RP 1110, pp. 1-18, July, 1938, 12 figs., 1 table.

The total pressure loss resulting from fluid flow in a bend consists of the loss occurring in the bend itself, the loss in the downstream tangent caused by the abnormal velocity distribution, and the normal friction loss that would occur in a similar straight pipe of equal length. The total pressure loss may be expressed as

$$\frac{P}{\gamma} = H = \lambda_s \frac{\ell}{d} \frac{V^2}{2g} + \zeta \frac{V^2}{2g} + \theta \frac{V^2}{2g} \quad (1)$$

where P = the total pressure loss,

$\gamma$  = the specific weight of the fluid,

H = total head loss (measured as a column of the same fluid as that flowing),

V = the mean velocity,

g = acceleration of gravity,

$\ell$  = the length of pipe over which the loss is to be measured,

d = diameter of the pipe,

$\lambda_s$  = coefficient of resistance for a straight pipe,

$\zeta$  = the deflection coefficient, and

$\theta$  = the tangent coefficient.

The deflection loss and the tangent loss may be combined into a single bend loss described by the bend coefficient,  $\eta$ , where  $\eta = \zeta + \theta$ . The bend coefficient is, in general, a function of the dimensions and roughness of the pipe and bend and the Reynolds number.

The bends tested were constructed from steel tubing of nominal 4-in. internal diameter. The measured internal diameter averaged 10.23 cm. A diagram of the pipe line and the manometer connections and a table of the relative radius, R/d, is given in Fig. 1. The flow was held constant to one part in 1000, and the temperature was read to the nearest tenth of a degree from a calibrated thermometer set into the pipe. Because of the progressive rusting of the pipe and bends, observations were continued until the pressure differences measured between piezometer stations became constant. The friction coefficient,  $\lambda_s$ , was measured for each bend from the pressure differences

along the downstream tangent sufficiently far from the bend so that the velocity distribution characteristic of a straight pipe existed.

For these experiments the bend coefficient,  $\eta$ , was found in general to be independent of the Reynolds number, and an average value of  $\eta$  could be assumed for the entire range of Reynolds number. The average values of the bend coefficient for each bend are plotted in Fig. 2 in terms of the relative radius,  $R/d$ . They are replotted in Fig. 3 together with the results of other investigators. Qualitatively, there is some agreement among the several curves in that they indicate two regions of flow. For the lowest relative radii the coefficient decreases to a minimum in the neighborhood of  $R/d = 5$ . Then there is a gradual rise to an apparent maximum somewhere near the value  $R/d = 15$ . Finally, as  $R/d$  becomes very large, there is probably a third region in which the coefficient decreases--presumably approaching zero as the relative radius approaches infinity.

In the discussion of the results, the effect of rusting of the pipes was mentioned as a factor causing continuous change of roughness of the wall and as an indeterminate factor which has possible effects upon the pressure readings.

A relationship is established for the relative roughness of pipes on the basis of the value of  $\lambda_s$ . For rough pipes the following relations may be applied:

$$\frac{V}{V_*} = 8.12 \left[ \frac{r}{2k} \right]^{1/6} \quad \text{and} \quad \frac{V}{V_*} = \sqrt{\frac{8}{\lambda_s}}$$

where  $V_*$  = the shear velocity,  $k$  = the absolute roughness, and  $r$  = the radius of the pipe. Combination of these relations results in

$$\frac{k}{r} = 280 \lambda_s^3$$

From this equation and the published results the relative roughness of the various bends was computed or estimated. The bend coefficient, as obtained by several investigators, is plotted in Fig. 4 in terms of the relative roughness for several values of  $R/d$ . Roughness may affect the velocity distribution at the entrance to the bend, the shear on the wall of the bend itself, and the excess loss downstream, and therefore it may influence the bend coefficient.

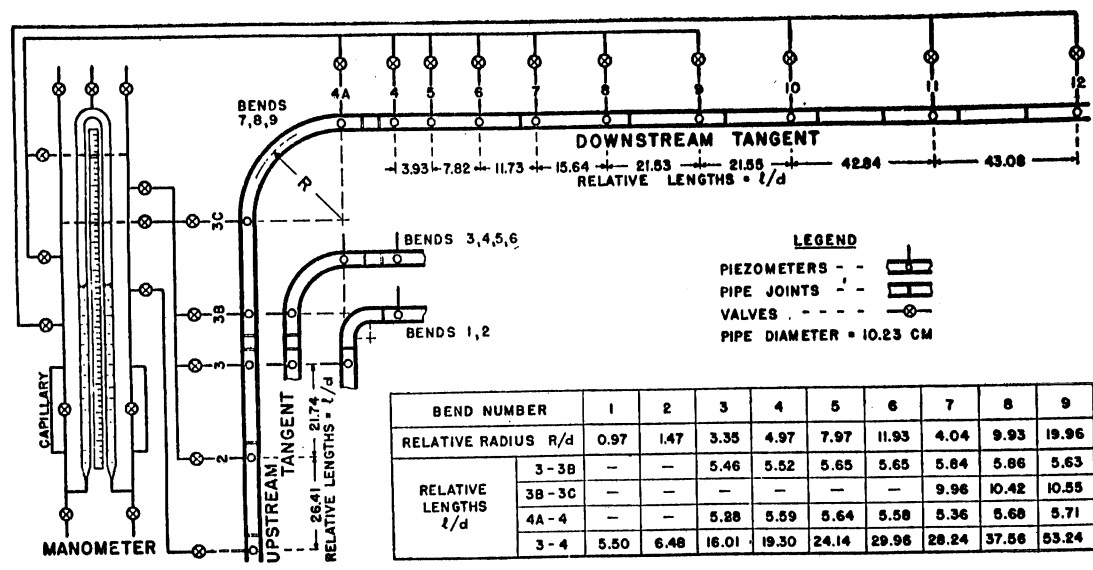


Fig. 1—Diagram of Pipe and Bend, Showing Location of Pipe Joints, Piezometers, and Arrangement of Pressure Connections to Manometer

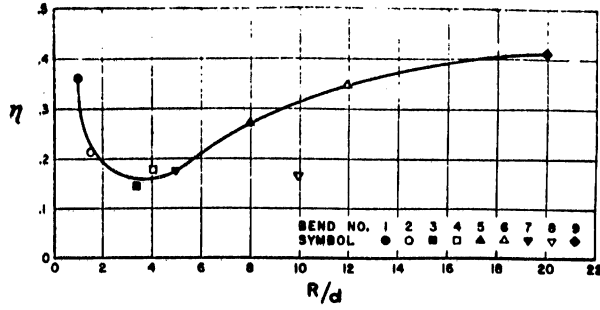


Fig. 2—Bend Coefficients as Function of the Relative Radius

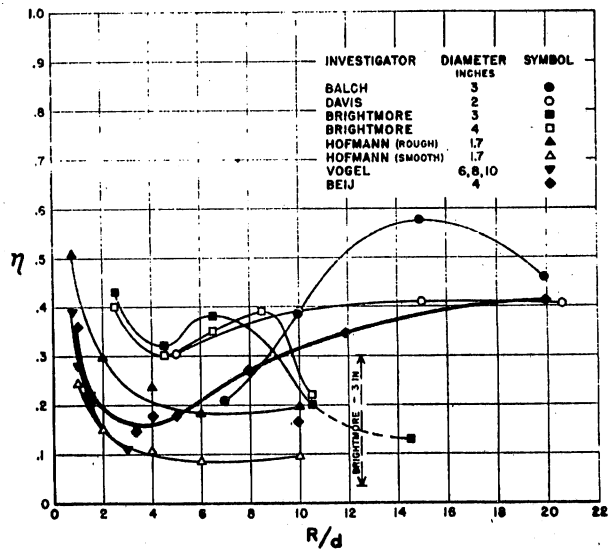


Fig. 3—Bend Coefficients Found by Various Investigators

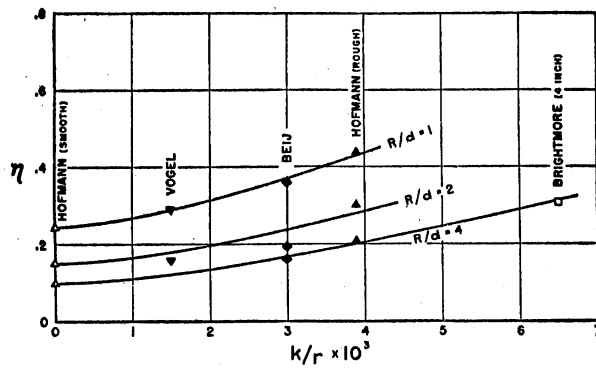


Fig. 4—Bend Coefficients for Bends of Small Relative Radii as Function of the Relative Roughness

## Abstract 5

Bouchayer, A., "Losses of Head in Bends and Branches," ENGINEERING (London), Vol. 120, p. 241, August 21, 1925, (summary of "Les Pertes de Charges Dans Les Conduits Coudees et Embranchements," as given at Hydro-Electric Congress, Grenoble, 1925).

The experiments to determine the loss of head in bends were carried out on a pipe 300 mm in diameter and 77.25 meters in total length. Four bends were inserted along the pipe line so that each was preceded and followed by a length of straight pipe. Beginning at the inlet, the arrangement of bends consisted of 18.87 meters of straight pipe, a 30° bend, 12 meters of straight pipe, a 90° bend, 18 meters of pipe, a 120° bend, 12 in. of pipe, a 60° bend, and a final length of straight pipe 12 meters long. Succeeding bends were placed to deflect the flow in opposite directions. The mean radius of each bend was 900 mm. The resistance of the straight pipe had been accurately determined in previous research. The observations were made at four discharges, 138.1, 107.8, 82.5, and 70.3 liters per sec, so that the corresponding velocities were 1.955, 1.525, 1.165, and 0.995 meters per sec respectively.

By subtracting the head loss caused by friction in an equivalent length of straight pipe from the measured total head loss, the loss of head resulting from each bend was determined. The results are tabulated in Table I.

TABLE I  
Head Loss caused by Bends for Various  
Velocities and Deflection Angles

Deflection Angle	Velocity - meters per sec			
	0.995	1.165	1.525	1.955
	mm	mm	mm	mm
30°	9.5	12.75	18.75	30.75
60°	3.25	4.75	5.5	9.25
90°	10.25	14.5	24.0	39.75
120°	15.25	21.75	37.5	60.75

The large head loss for the 30° bend, as compared to the 60°, 90°, and 120° bends, was not explained.

## Abstract 6

Brightmore, A. W. "Loss of Pressure in Water Flowing Through Straight and Curved Pipes," MINUTES OF PROCEEDINGS OF THE INSTITUTION OF CIVIL ENGINEERS, Vol. 169, Part 3, Paper No. 3679, pp. 315-336, 1906-07, 10 figs., 6 tables.

The experiments described in this paper include some on the excess loss of head caused by pipe bends over that caused by an equivalent straight pipe. The bends experimented with consisted of one 3-in. right-angled elbow and seven 3-in.  $90^\circ$  bends with radii equal to 2, 4, 6, 8, 10, 12, and 14 diameters, and one 4-in. right-angled elbow and five 4-in.  $90^\circ$  bends of radii equal to 2, 4, 6, 8, and 10 diameters. The bends were uncoated and the interior surface was allowed to rust. For the 3-in. bends piezometers were connected at points 4 in. upstream of the bend and 6 ft 8 in. and 16 ft 8 in. downstream of the bend, and for the 4-in. bends the piezometers were connected at points 7 in. upstream and 5.0 ft and 12.0 ft downstream of the bend. In some of the experiments on 4-in. bends the first downstream piezometer was connected 6 ft 7  $\frac{1}{4}$  in. from the bend. The discharge was measured volumetrically, the pressures by means of a differential gauge.

The downstream pipes connected to the 3-in. bends were galvanized, so the resistance coefficients of these pipes were determined separately. For the 4-in. bends the downstream tangent was of cast iron, as were the bends, and had the same coefficients as the cast iron pipe previously tested.

The results of the experiments are plotted in Figs. 1 and 2 for the 3-in. bends and 4-in. bends, respectively, with the velocity in ft per sec as abscissas and loss of head caused by curvature in inches of water as ordinates. It will be noticed that the curves for bends of radii 6 and 8 diameters are steeper than those for bends of either the next smaller or the next larger radius. For the 3-in. bend of radius equal to 12 diameters, the flow becomes unstable for velocities greater than 3 ft per sec, the loss of head sometimes being much smaller than would be inferred from the losses in the bends of greater or less radius. In Fig. 3 the loss of head caused by the 3-in. and 4-in. bends is plotted against the radius of the bend in diameters for velocities of 5, 7.5, and 10 ft per sec. The curves indicate that the loss of head attains a minimum for a radius of from 3 to 4 diameters, then increases to a maximum for a radius of 6 to 7 diameters, and then finally decreases as the radius increases beyond 7 diameters.

From the experiments the author concluded in part:

1. That the flow of water in rusted but not tubercled cast iron pipes of 3 in. diameter or larger may be expressed by the formula  $v = \frac{56}{1 + 1/40 d^2} \sqrt{di}$ , where  $d$  is the diameter of the pipe in feet, and  $i$  is the loss of head per unit length of pipe.

2. That the actual loss of head at contractions and enlargements shows close agreement with the theoretical values, particularly for a ratio of the areas as great as 4 to 1.

3. That the additional loss of head in right-angled elbows on pipes of 3-in. or 4-in. diameter, caused by the deflection of the current through a right angle, is the same at identical velocities.

4. That the additional loss of head in right-angled pipe bends of these diameters has a minimum value for bends of a radius equal to 4 diameters, irrespective of the velocity of flow.

5. That the additional loss of head in pipes of these diameters attains a maximum for a bend radius of 6 or 7 diameters and falls again for larger bend radii.

6. That the loss of head in right-angled bends of a radius giving this minimum loss is independent of the size of the pipe, and depends only on the velocity of flow and the condition of the internal surface of the pipes.

7. That the additional loss of head in the case of short bends occurs in the length of pipe following the bend, owing to the intensified eddying motion there, caused by the rearrangement of velocities.

8. That in the bends experimented upon, the flow tends to approximate to a "free" vortex, the pressure being greatest at the outside and least at the inside of the bend.

The last conclusion is confirmed by the fact that the velocity was found to be a maximum at the inside of the bend and a minimum at the outside, their relative values being approximately inversely proportional to the radii.

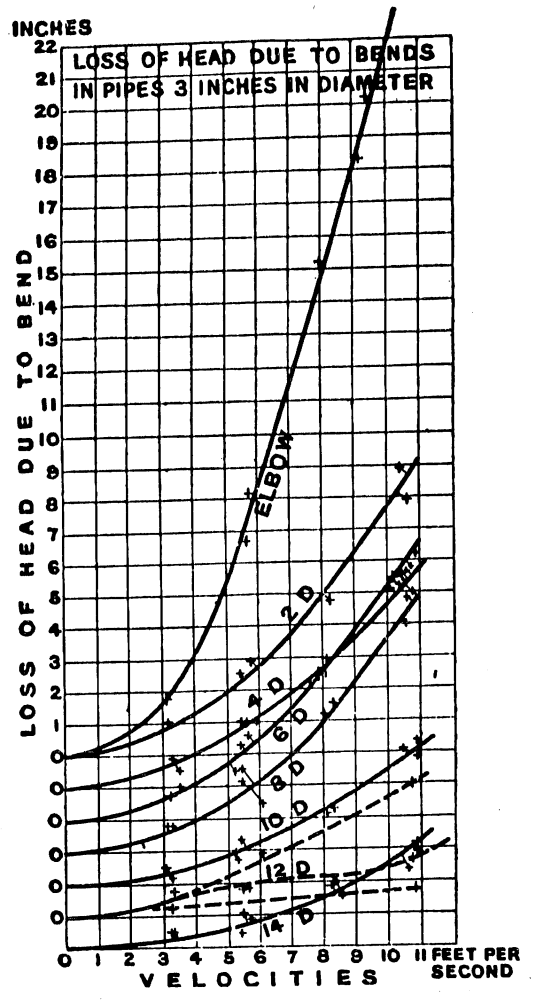


Fig. 1—Loss of Head due to Bend in 3 Inch Pipe

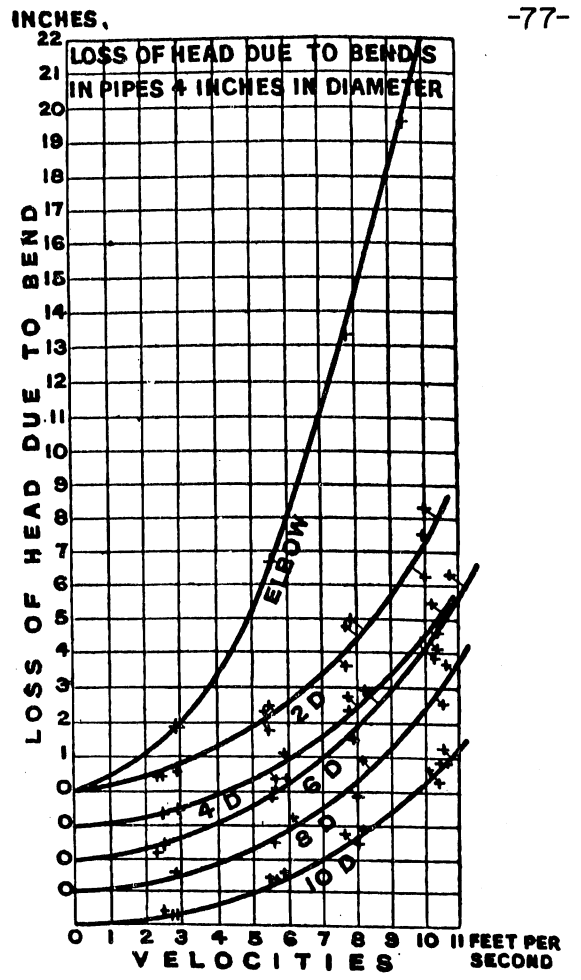


Fig. 2—Loss of Head due to Bend in 4 Inch Pipe

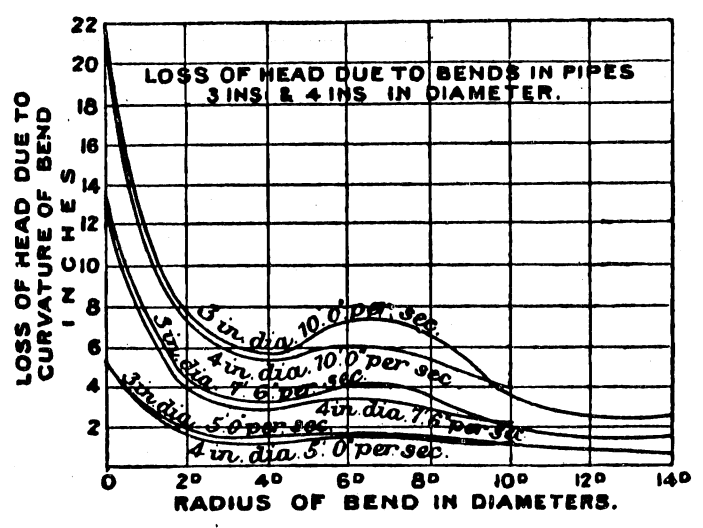


Fig. 3—Relation of Bend Loss of Head to Radius Ratio

## Abstract 7

Busey, Frank L., "Loss of Pressure Due to Elbows in the Transmission of Air Through Pipes and Ducts," TRANSACTIONS, AMERICAN SOCIETY OF HEATING AND VENTILATING ENGINEERS, Vol. 19, pp. 366-376, 1913, 7 figs.

Two sets of experiments were conducted--the first to determine the effect of changing the radius of curvature of the elbow, and the second to study the effect of reducing the throat area.

The apparatus consisted of a blower discharging into an airtight box to which a piece of pipe 3 diameters long was attached. The test bends were attached to this pipe and were followed by another short length 3 diameters long. A Pitot tube in the outlet length of pipe was used for determining the velocity head. The static head in the airtight box was adjusted for each elbow tested so that the velocity through the outlet pipe remained constant. The increase in static head caused by the test bend was a direct measure of the pressure loss caused by the elbow.

The bends tested are shown in Fig. 1 and listed in Table I. The pipe sizes were 12 inches in diameter or 12-in. by 12-in. square section.

TABLE I  
Dimensions of Experimental Bends

R = Centerline Radius    r = Inner Radius		
Diameters	Inches	Inches
Square turn	-----	-----
0.50	6	0
0.75	9	3
1.00	12	6
1.25	15	9
1.50	18	12
2.00	24	18
2.50	30	24
3.00	36	30

The results of the tests are shown in Figs. 2 and 3 for the round and square pipes respectively. The losses are given as a percentage of the velocity head in terms of the curvature ratio  $R/d$ . The results indicate that for minimum loss the  $R/d$  for the bend should be at least 1.5 diameters.

## Abstract 7, Busey

Tests of the special elbow with the reduced throat and the expanding downstream outlet reduced the loss of a short bend of  $R/d = 0.5$  from 94 to 37 per cent of the velocity head.

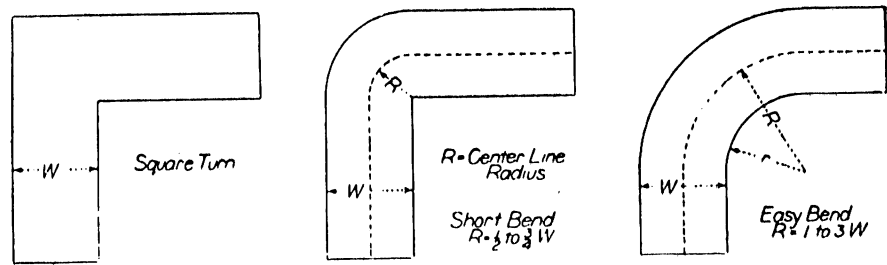


Fig.1—Type of Elbows Used in Tests

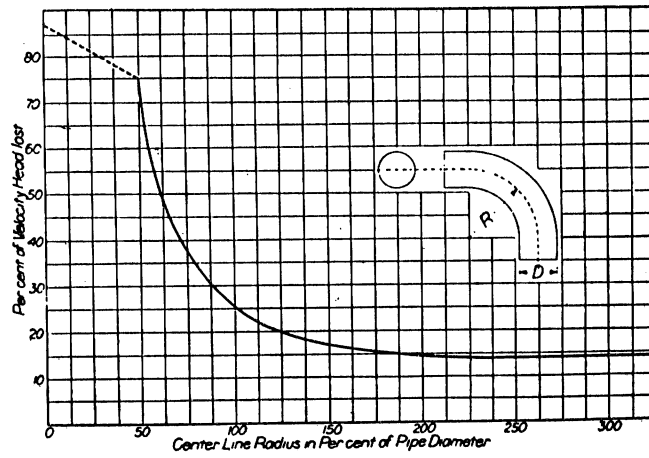


Fig.2—Diagram Showing Pressure Loss in Round Elbows

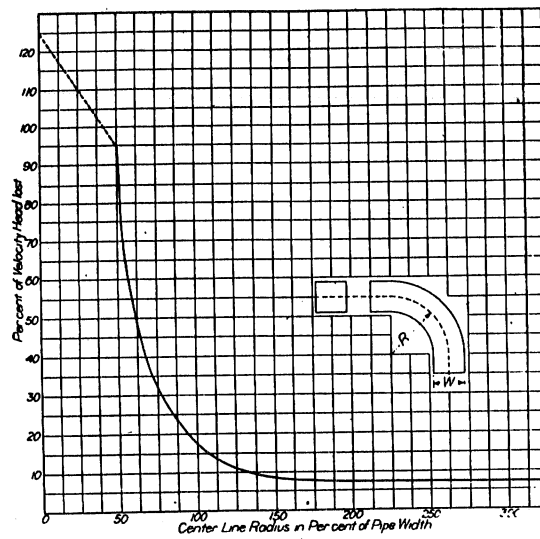


Fig.3—Diagram Showing Pressure Loss in Square Elbows

## Abstract 8

Davies, Powys, and Puranik, Shivram, "The Flow of Water Through Rectangular Pipe-Bends," JOURNAL OF THE INSTITUTION OF CIVIL ENGINEERS, Vol. 2, Paper No. 5035, pp. 83-134, 1935-36, 15 figs., 26 tables.

This paper presents the results of experiments to determine the resistance for various 4-in. by 4-in. bends constructed of teakwood. The bend coefficient,  $\zeta = \frac{h_b}{v^2/2g}$ , is defined as the ratio of the head loss caused by the bend to the velocity head of the flow through the bend. The bends used in the experiments had radius ratios (the ratio of the radius of curvature of the centerline of the bend to the width in the plane of the bend) varying from 0.875 to 2.5 and deflection angles from  $30^\circ$  to  $180^\circ$ . The pressure loss was determined by the difference in pressure between points upstream and downstream of the bend. The piezometers were placed at points one diameter upstream and 2 diameters downstream of the bend. In certain cases these distances were different, so the pressure loss was corrected by using the loss in a straight pipe of length equal to the variation from the standard points. For the sharp bends an additional piezometer station was established near the outlet, since additional losses occurred further downstream than the piezometric station immediately below the bend. For these cases the friction loss in a straight pipe equal in length to the distance between the downstream piezometers was subtracted from the total pressure loss to reduce the loss to the standard. Apparently the head losses reported include the normal friction along the wall in the bend between the stations immediately upstream and downstream of the bend, as well as the excess loss caused by the presence of the bend. The results of the experiments are given in Table I.

TABLE I  
Results of Experiments on Bends

Radius Ratio	Angle of Deflection					
	180°	123°-30'	114°-15'	90°	60°	30°
Sharp Bends						
0.875	0.84	---	0.59	0.43	0.28	0.13
1.06	---	---	0.39	0.31	---	---
Easy Bends						
1.5	---	---	0.27	0.20	0.19	0.11
1.75	0.33	---	0.30	0.21	---	---
2.00	---	---	0.25	0.23	---	---
2.25	---	---	0.27	0.20	---	---
2.5	0.36	0.30	---	0.18	0.18	0.09

## Abstract 9

Davis, G. J., INVESTIGATION OF HYDRAULIC CURVE RESISTANCE, Experiments with Two-Inch Pipe, Bulletin of the University of Wisconsin No. 403, (Engineering Series, Vol. 6, No. 4), 1910, 60 pp., 20 figs., 10 tables.

This bulletin reports the results of experiments on the loss of head caused by 90° bends in a 2-in. pipe line. The dimensions of the test bends are given in Table I. Each test bend was installed in the pipe line and pressure measurements were obtained at piezometer taps located 1.0 ft and 11.0 ft upstream of the bend and 1.0 ft, 7.0 ft, and 17.0 ft downstream of the bend. The 2-in. pipe line was connected to an 8-in. drum fitted with baffles to insure good entry flow. The tests were made at velocities ranging from 1.5 to 15 ft per sec. The head loss was determined from the total difference of head observed between the piezometer connections. The loss caused by the bends was determined by subtracting the loss due to an equivalent length of straight pipe from the total loss as measured. The head loss caused by the straight pipe had been previously determined.

The results of these experiments are plotted in Fig. 1 as loss of head in feet in terms of the radius ratio (the ratio of the mean radius of curvature to the diameter of the pipe). The upper curve (Case 2) includes the straight pipe friction indicated by the straight line and thus corresponds to the total head loss. The lower curve (Case 1) indicates net loss caused by the bends alone. The experimental values determined by Schoder are also plotted in Fig. 1 for Case 1.

In Fig. 2 the data of Fig. 1 are presented as the bend coefficient in terms of the radius ratio for a velocity of 8 ft per sec. The bend coefficient is the ratio of the net loss of head in the bend to the velocity head

of the fluid flowing, or  $\eta = \frac{h_b}{V^2/2g}$ . The curve is similar to that in Fig.

1 and shows a rapid decrease for small values of the radius ratio to a minimum at  $R/d \approx 5$ . The bend coefficient then increases again to a second maximum at  $R/d \approx 15$ , at which point it begins to decrease again throughout the remainder of the range.

TABLE 1  
DESCRIPTION OF CURVES

1.	2.	3.	4.	5.	6.	7.	8.
No. of curve	Internal diameter in inches	Radius in inches, R.	Radius in feet.	$\frac{R}{d_p}$	Length, in feet.	Material.	Description.
1	2½	1½	.135	.788	.21	Malleable iron ....	Elbow.
2	2½	2½	.108	1.15	.31	Cast iron .....	Long turn, drainage elbow.
3	2½	1½	.125	.728	.20	Cast iron .....	Drainage elbow.
4	2½	1½	.125	.728	.20	Cast iron .....	Short turn.
5	2½	3½	.200	1.52	.41	Cast iron .....	Long sweep.
6	.....	0	0	0	0	Cast iron .....	Tee.
7	2½	5½	.490	2.5	.68	Cast iron .....	Special casting.
8	2½	10½	.861	5.0	1.35	Wrought iron or steel .....	Bent pipe.
9	2½	20½	1.720	10.0	2.71	Wrought iron or steel .....	Bent pipe.
10	2.00	31	2.580	15.0	4.06	Wrought iron or steel .....	Bent pipe.
11	2.00	42½	3.540	20.6	5.56	Wrought iron or steel .....	Bent pipe.
12	2.01	85	7.060	41.2	11.12	Wrought iron or steel .....	Bent pipe.

$\frac{R}{d_p}$  = Ratio of radius of curve to diameter of straight pipe.  $d_p = 2½$  inches.

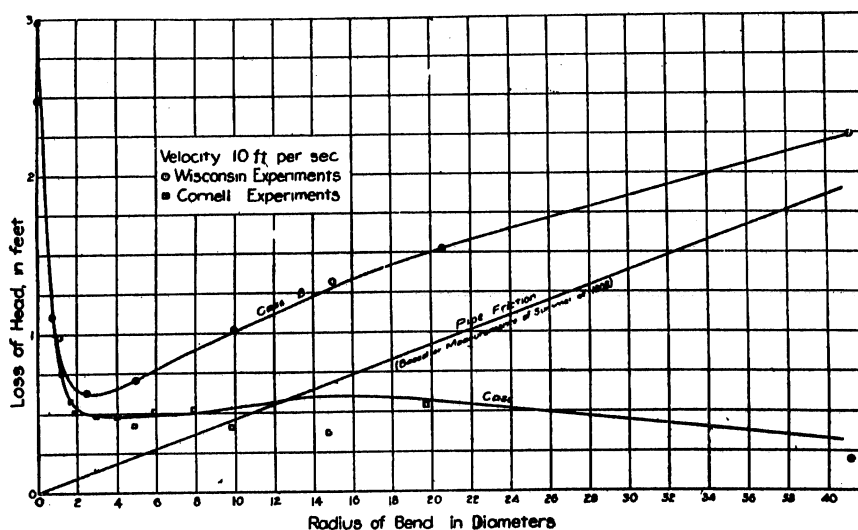


Fig. 1—Relation of Loss of Head and Radius of Bend

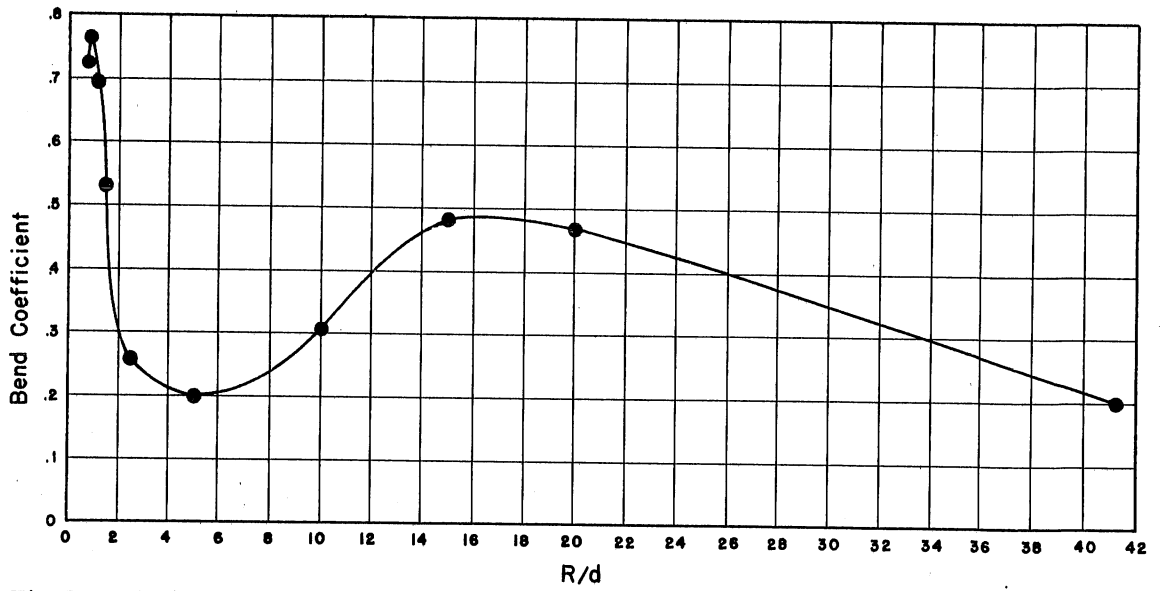


Fig.2-Relation of Bend Coefficient and Radius of Bends in Diameters

## Abstract 10

Dean, W. R., "The Streamline Motion of Fluid in a Curved Pipe," PHILOSOPHICAL MAGAZINE AND JOURNAL OF SCIENCE, (Seventh Series), Vol. 5, pp. 673-695, April, 1928, 3 figs., 4 tables.

An approximate solution of the differential equations of motion for streamline flow in a bend resulted in an equation relating the discharge and the pressure drop to the curvature of the bend when the radius of the pipe is small in comparison with the radius of curvature. The approximate equation derived for the relationship of the discharges in curved and straight pipes for a given pressure drop is

$$\frac{Q_c}{Q_s} = 1 - 0.03058 \left(\frac{K}{576}\right)^2 + 0.01195 \left(\frac{K}{576}\right)^4 \dots \quad (1)$$

where  $Q_c$  and  $Q_s$  are the discharges through curved and straight pipes respectively and

$$K = G^2 a^7 / 8 \mu^2 \nu^2 R \quad (2)$$

where  $G$  = the pressure gradient,

$a$  = radius of the pipe,

$R$  = radius of the bend,

$\mu$  = absolute viscosity of the fluid, and

$\nu$  = kinematic viscosity of the fluid.

The calculation of additional terms of equation (1) becomes increasingly difficult so the upper limit of validity of equation (1) is for values of  $K$  of 650 or less, which correspond to low Reynolds numbers for sharper bends.

A significant result of the analysis is that it provides a criterion by which the results of experiments on streamline flow in bends may be correlated. Equation (1) may be written in the form

$$\frac{Q_c}{Q_s} = f(K) = f\left(G^2 a^7 / 8 \mu^2 \nu^2 R\right) \quad (3)$$

which states that for a given pressure drop the ratio of the discharge through a curved pipe to that in a corresponding straight pipe depends upon the criterion  $G^2 a^7 / 8 \mu^2 \nu^2 R$ .

## Abstract 11

Eustice, John, "Flow of Water in Curved Pipes," PROCEEDINGS OF THE ROYAL SOCIETY OF LONDON, Series A, Vol. 84, pp. 107-118, 3 figs., 1911, 4 tables.

For the purpose of these experiments, Eustice used a flexible pressure tubing (approximately 0.37 cm I.D.) with thick walls, the material being a composite of rubber and canvas. By the use of this tubing, the author hoped to overcome the effect of variation of roughness between apparently similar metal tubes, but with the tubing other difficulties were encountered in the variations of shape and areas of cross sections, with bending and a slow recovery from a strain caused by distortion.

In the preliminary experiments water was introduced at one end of the tube under a fairly constant pressure, first when the tube was laid out straight, and then as it was coiled around a cylinder. A sizable diminution of flow was evident in the coiled tube.

In an extension of the experimentation, the water supply was taken from a tank where a 36-ft head was available so that velocities both above and below the laminar-turbulent critical could be investigated. A series of experiments was conducted on the tube when it was extended out straight, with "squeezing blocks" installed to alter the area and the cross section to compare with the areas and cross sections encountered when the tube was wound about the cylinders.

The cylinders were turned down to diameters that would allow five-sixths of the length of the tube to form an integral number of turns. Experiments were conducted on coils of from 1 to 10 turns, all having the same pitch. Tests were also conducted on a coil of a half turn and in the same tube when it was laid out straight but not drawn taut so that it was sinuous in form. For each coil the tests were run over a range of pressure values and the quantity discharged in a given time then became the basis for comparison between the various windings. These results, along with the geometrical dimensions of the cross section of each coil, are tabulated in the two tables included in the paper.

In the author's plot of the results, it is evident that the value of critical velocity at which the flow becomes turbulent increases in proportion to the degree of curvature and the number of turns. With the pressure

## Abstract 11, Eustice

available and with the given diameter of the tube, the critical velocity was not attained in the coils of greatest curvature or number of turns.

Although the uncertainties caused by the elastic walls and by the change of cross section because of bending make comparisons difficult, the experiments adequately illustrate:

1. The resistance to flow is greater in a curved or coiled tube than in a comparable straight tube.
2. The critical velocity in a tube increases in some proportion to the degree of curvature.
3. Flow in flexible straight tubes obeys the laws of flow in metal tubes as investigated by Reynolds.

## Abstract 12

Eustice, John, "Experiments on Stream-line Motion in Curved Pipes," PROCEEDINGS OF THE ROYAL SOCIETY OF LONDON, Series A, Vol. 85, pp. 119-131, 1911, 9 figs.

The experiments described in this paper were conducted as a supplement to the previous experiments conducted by the author on the flow of water in curved pipes. The flow investigated was in the laminar range and the comparison was made by observing the paths of dye streams in relation to one another as they proceeded around the bends.

The bends under observation included U-tubes, right-angled bends, miter bends, and long radius bends. The tubes were all 1 cm in diameter except for a U-tube, which had an internal diameter of 1.7 cm. The supply of water from a tank flowed through a conical converging section before it reached the bend under observation. Inside of this conical section were six equally spaced nozzles, each of which was connected to an exterior connection. If dye was introduced into any combination of the nozzles, the parallel flow of the water past the nozzles would carry the dye stream along through the convergence and into the bend.

The path lines of the dye streams that were observed in the several bends of each type for velocities up to 0.6 ft per sec are described in detail. This description is qualitative throughout and is accompanied by diagrams showing the dye lines in each one of the 17 bends tested.

The experiments showed that, when water is flowing at low velocities in a straight tube of uniform bore, filaments of color maintain their form and relative positions but, upon entering a curved portion of the tube, some of the filaments spread out into bands of color and cross to the inner part of the tube, traveling round its section close to the walls. If the curvature is sufficiently large or the curve sufficiently long, all the filaments are affected.

These results were compared with the indicated results of the author's earlier experiments and they were found to agree.

## Abstract 13

Flügel, G., "Strömungsverluste und Krimmerproblem," HYDRAULISCHE PROBLEME (Flow Losses and Bend Problems, Hydraulic Problems), pp. 133-157, Berlin, 1926.

The author defines two types of flow losses: (1) useful energy is destroyed by conversion into heat; (2) unusable kinetic energy is produced in the form of cross currents. These are designated respectively as friction losses and cross flow losses. The author restricted himself to the analysis of the former. The friction losses were divided into three distinct classes: (a) wall friction, represented by the equation for turbulent flow conditions, (b) separation, (c) cavitation. The friction loss was represented by an equation,  $dW = K dA q$ , where  $dA$  is the friction surface,  $q$  is equal to  $\gamma v^2/2g$  or the dynamic pressure at the point, and  $K$  is the friction coefficient, which in first approximation may be considered constant. An equation valid for diffusers was given for the separation loss. Further classification was made in accordance with various types of "combined" losses. The bend loss was considered as consisting of wall and separation losses to which cavitation, wave, and cross flow losses must be added for certain conditions.

The author analyzed the friction coefficient  $K$  with reference to three possible types of flow--uniform, accelerated, and retarded. Values of  $K$  for uniform flow are sufficiently well established. There are empirically verified expressions also for accelerated flow. There is little substantiating information regarding  $K$  for retarded flow. The separation losses were analyzed and evaluated in the form of equations on the bases of von Kármán's and Foppl's theories. The formation of eddy fields around immersed bodies, their type and influence, were evaluated theoretically. The writer concluded that the separation losses might be regarded as wall friction losses on a body enlarged by the eddy field, provided the fact was considered that lengthwise the eddy field  $K_D$  was greater than  $K$  ( $K_D$  is the friction coefficient between the main flow and eddy field). The friction of the eddy field can be designated as "diffuser friction" to distinguish it from the pure wall friction.

On the basis of the division of bend losses into wall friction and diffuser losses, it was possible to calculate each of these two losses separately. Although the flow through the bend was three dimensional, an expression similar to one for laminar flow was applied for the evaluation of the diffuser loss caused by limited discharge, in which the energy loss per unit

## Abstract 13, Flügel

weight of discharge at the outer side was  $E_a = \zeta \Delta p_a / \gamma$  and at the inner side was  $E_i = \zeta \Delta p_i / \gamma$  ( $\Delta p_a$  is the pressure rise along the outer wall and  $\Delta p_i$  is the pressure rise on the inner side). Accordingly, the total diffuser loss in bends was  $E_v = \zeta / \gamma (\Delta p_a + \Delta p_i)$ . This simple expression was, of course, valid primarily only for bends of rectangular cross section and constant depth. For any other cross-sectional shape, reductions should be applied. According to present investigations, the loss coefficient should be taken, as in the most favorable case of Venturi nozzles, as  $\zeta \cong 0.1$ . Under the assumption of ideal flow, the pressure changes  $\Delta p$  could be determined with sufficient precision by means of known methods, as long as the deflection was not too steep. This constituted a means for the determination of the most favorable shape of a bend corresponding to the ratios at which the losses were a minimum.

To date the knowledge of bend losses has been based mainly upon the old tests of Weisbach. A series of newer experiments has determined solely the pressure and velocity distributions in bends, but not the important energy loss. In all of these investigations the double spiral generated in the bend and superimposed upon the main flow was especially emphasized. Bend experiments were performed to establish not only the influence of the sharpness of the deflection upon the energy loss but also the influence of the cross section of the bend. The tests were carried out on channels of rectangular cross section having constant height and deflection angles of  $90^\circ$  and  $180^\circ$ . Figure 1 shows the  $90^\circ$  test bend into which the roundings at the inner and outer walls were introduced and combined with each other in various manners. The results of the measurements when the inflow width is equal to the outflow width are given in Fig. 2. Figures 3, 4, and 5 represent the measurements for expanded bends. In Figs. 2 and 5 the energy loss per unit weight is expressed as  $E_v = \zeta v_1^2 / 2g$ , while the diffuser loss per unit weight (Figs. 3 and 4) is  $E_v = \zeta D (v_1^2 - v_2^2) / 2g$ .

Previous reports referred to "deep" bends whose dimension normal to the plane of flow was large compared to the width. Additional experiments should be conducted also on "flat" bends, in which the flow pattern differs considerably from that of deep bends because the above-mentioned double spiral plays a much greater role as far as loss is concerned than in the deep bends in which the main losses result from separation. Of course, as long

## Abstract 13, Flügel

as the dead-water area is not especially large, the separation at the outer side does not seem to set in. Introduction of color solution at mid-depth of an  $180^\circ$  bend has shown that no definite separation could be observed in a normal bend shape as shown in Fig. 6(a), whereas in a channel shape as shown in Fig. 6(b) a very strong outer as well as inner separation occurred as per curves A and B, and at the outer side the color solution even worked its way upward.

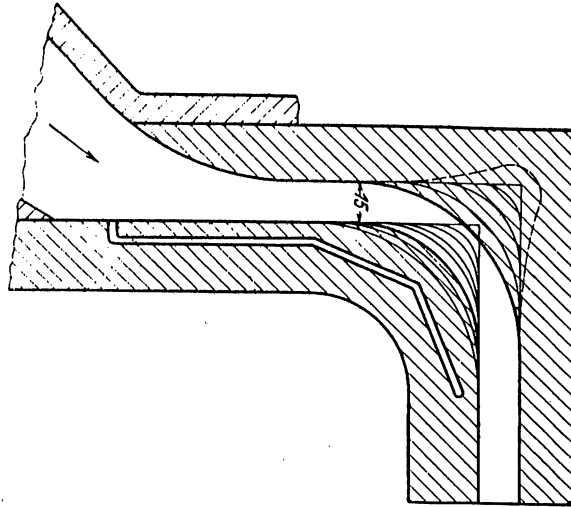


Fig.1-90° Experimental Bend

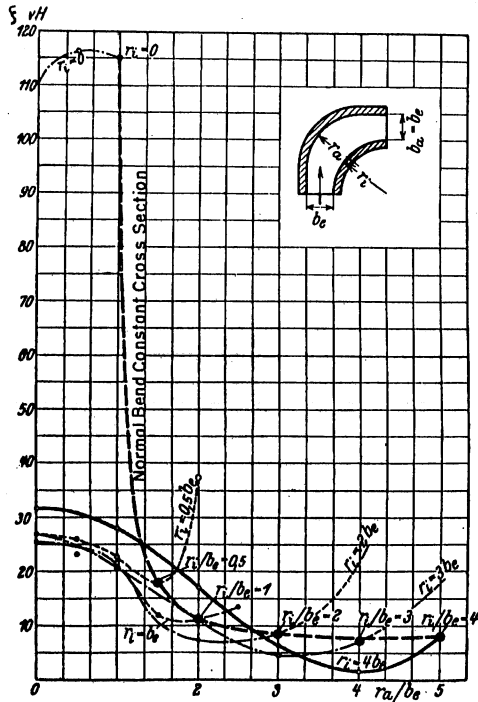


Fig.2-Loss Coefficient,  $\zeta$ , for 90° Bends with Equal Entrance and Exit Cross section

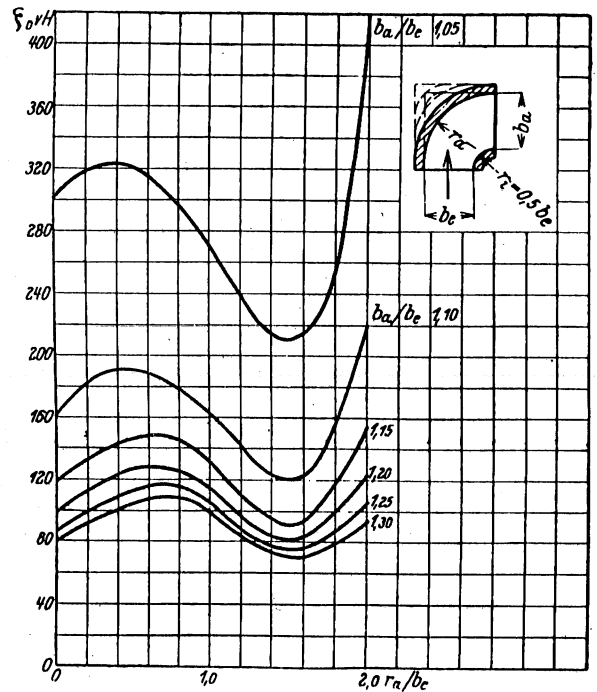


Fig.3-Loss Coefficient,  $\zeta$ , for Expanding 90° Bend;  $r_i = 0.5 b_e$

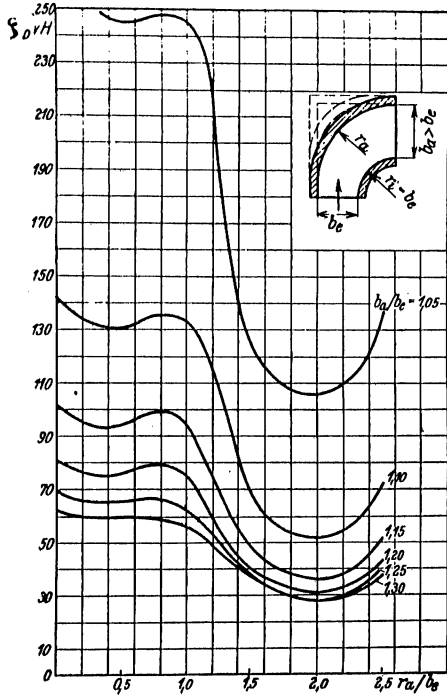


Fig.4—Loss Coefficient,  $\zeta$ , for Expanding 90° Bend  $r_i = b_e$

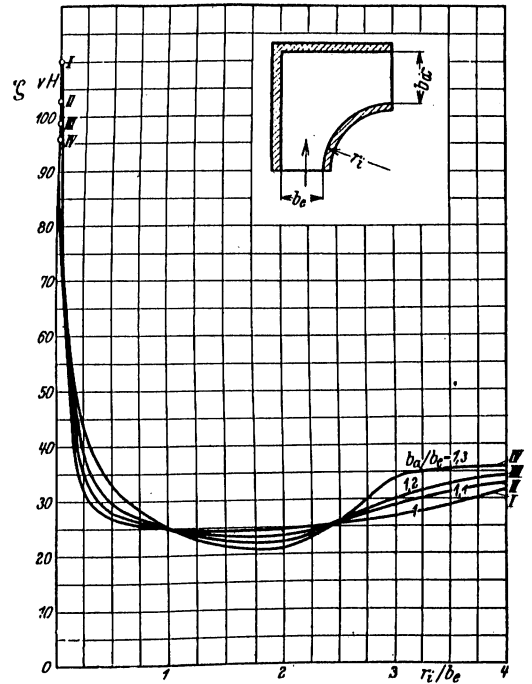


Fig.5—Loss Coefficient for Expanding 90° Bend with Square Outside Corner

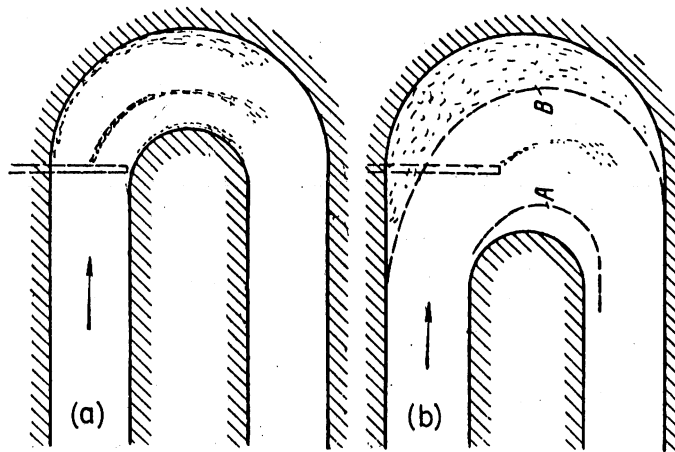


Fig.6—Investigation of Flow in 180° Bend by Use of Dye

## Abstract 14

Freeman, John R., FLOW OF WATER IN PIPES AND PIPE FITTINGS, New York, 1941, 349 pp., 196 figs.

The experiments on pipes and pipe fittings made in 1892 have been recomputed on the basis of Reynolds numbers and published in the above form. The section on pipe fittings includes experiments on the losses of standard fittings, including elbows, and on numerous combinations of fittings. Standard elbows of short, long, and extra long radius were tested in sizes varying from 8-in. to 2 1/2-in. diameter. In general the test arrangement contained four elbows separated by pipes of various lengths and arranged in the shape of a U. The head loss of the entire assembly was measured. After subtracting the head loss caused by friction in an equivalent length of straight pipe from the total measured loss, the result was divided by the number of elbows in the assembly to determine the net head loss caused by a single elbow. The bend coefficient was then computed in the usual way as the ratio of the head loss of a single bend to the velocity head of the fluid flowing. The Reynolds number of the tests ranged from about 20,000 to 900,000.

The loss caused by a bend may be expressed in terms of a length of straight pipe of identical characteristics which causes an equal head loss. The results of the experiments are shown graphically as the equivalent length of pipe in terms of the Reynolds number for the test. In Fig. 1 the equivalent lengths in diameters for all screw-type elbows are plotted against the Reynolds number. Similar data are shown in Figs. 2 and 3 for all of the drainage-type and flange-type elbows respectively. The effect of spacing of the elbows is shown by the difference in the equivalent length required for the same elbows spaced a greater or lesser distance apart. The data presented in Figs. 1, 2, and 3 supply considerable information useful for design of layouts of standard fittings.

In general, the influence of Reynolds number on the bend coefficient was negligible for Reynolds numbers over 100,000. The results of the experiments may therefore be represented by a single point which is the value of the bend coefficient for high Reynolds numbers. The influence of the relative radius,  $R/d$ , as well as the magnitude of the bend coefficient, is shown in Fig. 4.

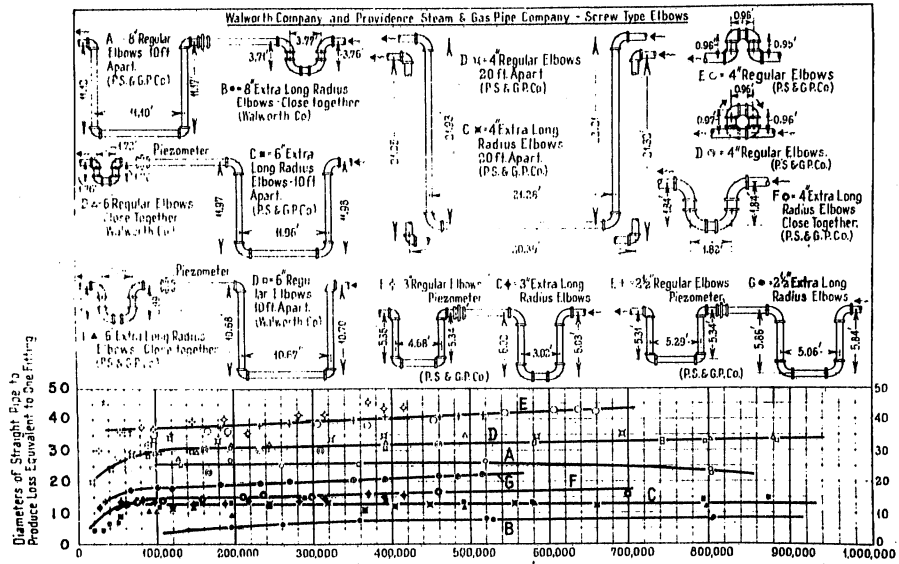


Fig. 1 - Relation of Resistance to Reynolds Number for Screw-Type Elbows

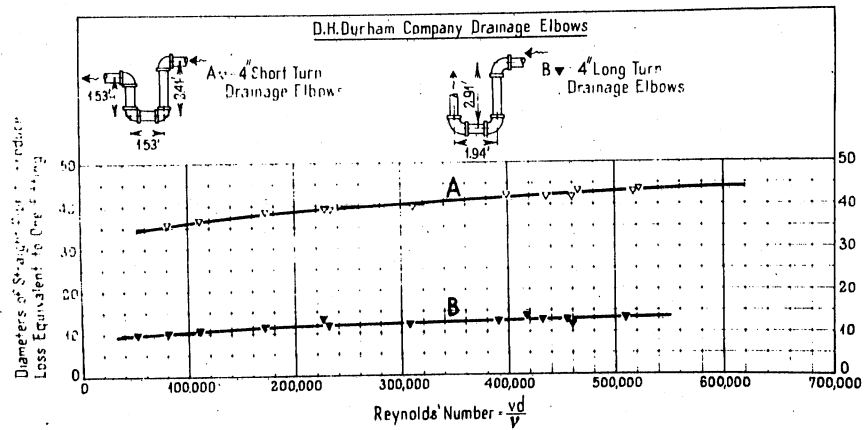


Fig. 2 - Relation of Resistance to Reynolds Number for Drainage Elbows

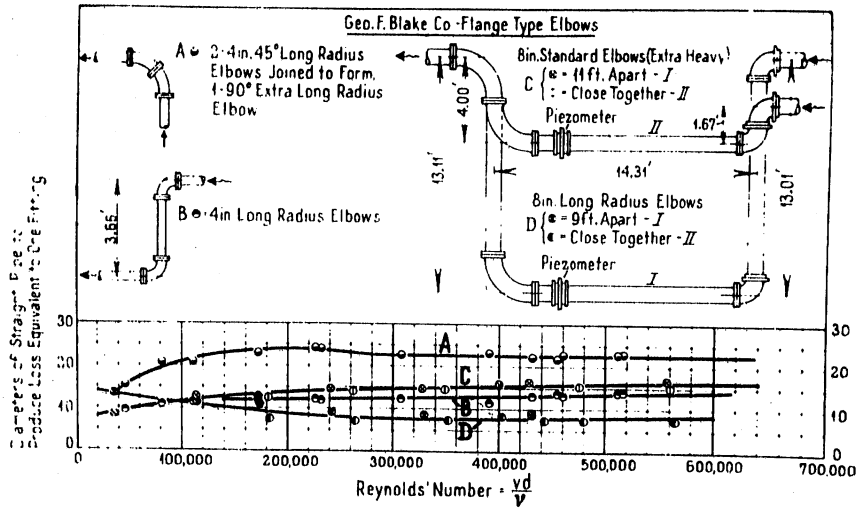


Fig.3 - Relation of Resistance to Reynolds Number for Flange-Type Elbows

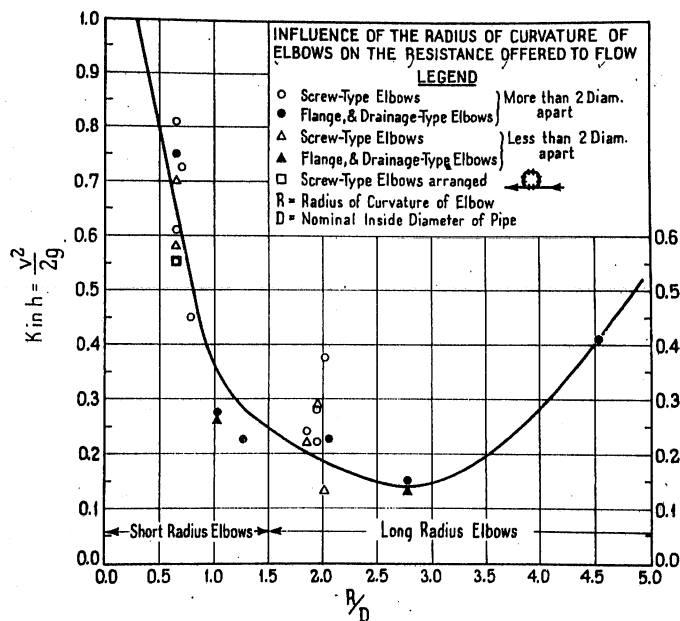


Fig.4 - Influence of the Radius of Curvature of Elbows on the Resistance Offered to Flow

## Abstract 15

Hofmann, Albert, "Loss in 90-Degree Pipe Bends of Constant Circular Cross Section," TRANSACTIONS OF THE HYDRAULIC INSTITUTE OF THE MUNICH TECHNICAL UNIVERSITY, BULLETIN 3, 1929, trans. and pub. by American Society of Mechanical Engineers, pp. 29-41, 1935, 18 figs., 14 tables.

The experiments reported in this article were made on five circular 90° bends. All were 43 mm in diameter and differed only in the radius of curvature. The ratios of radius of curvature,  $R$ , of the circular centerline to the inside diameter,  $d$ , of the circular cross section were 1, 2, 4, 6, and 10. The bends were made in split halves and great care was taken in machining the bends to have the interior of correct size and very smooth. Two series of experiments were conducted--the first on the smooth bends and the second on rough bends. After the experiments on the smooth bends were complete, the bends were made rough by coating the interior of the bends and the tangents with a mixture of sand and oil paint. The sand used passed a sieve whose mesh was 120 per sq cm. The mixture was made up in the proportion of 1 kg of paint to 0.365 kg of sand. Microscopic examination of the roughened pipe showed that the maximum elevation of the individual grain was about 1/4 mm. The average diameter of each pipe section was determined by weighing the quantity of water required to fill the unit. The average diameter used in computations of the velocity was the average of diameters of each pipe length weighted in proportion to its length.

For the smooth bends, by substituting a length of straight pipe of the same length and diameter as the bend, the wall friction of a straight pipe was determined for each bend. The pressure loss for each bend was then determined by subtracting the measured pressure for the straight pipe from that measured at each corresponding piezometer hole for the bend. The bend coefficient,  $\zeta = \frac{h_b}{V^2/2g}$ , is plotted in Fig. 1 as a function of Reynolds number for each bend tested ( $h_b$  is the head loss caused by bend only,  $V$  is the mean velocity,  $Re$  is equal to  $Vd/\nu$ ).

Similar experiments were carried out for the rough bends. The results are plotted in Fig. 2 for  $\zeta = \frac{h_b}{V^2/2g}$  as a function of Reynolds number for each bend.

## Abstract 15, Hofmann

The variation of  $\zeta$  with  $R/d$  for a Reynolds number of 146,000 is plotted in Fig. 3. It is evident from Figs. 1 and 2 that the value of  $\zeta$  decreases as the Reynolds number increases, but in the case of rough pipes it quickly approaches a constant value. The values for  $\zeta$  for rough bends for all curvature ratios were found to be 2.0 to 2.1 times those for smooth bends, while values for  $\lambda$ , the resistance coefficient, for straight rough pipes were only about 1.5 times those for smooth pipes at the same Reynolds number. The data indicate a minimum value of  $\zeta$  at  $R/d = 7$  to 8 for rough as well as smooth bends. The effect of the bends was noticeable for distances of 50 to 70 diameters downstream of the bends.

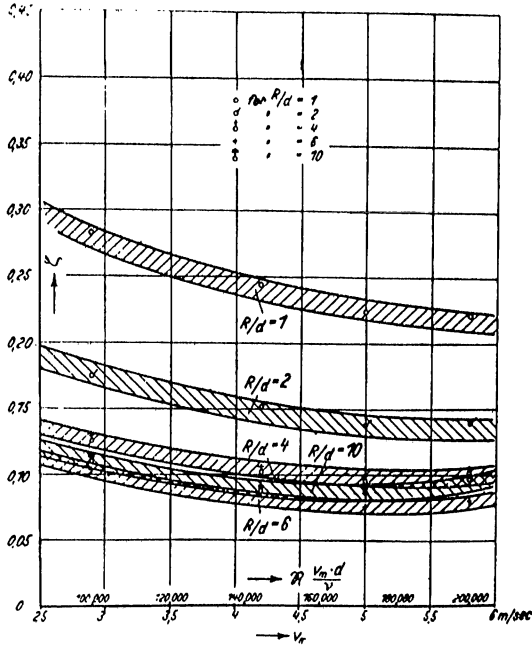


Fig 1-Bend Coefficient,  $\zeta$ , for Smooth Bends as a Function of the Water Velocity  $V_m$  and Reynolds Number  $R = \frac{V_m \cdot d}{\gamma}$

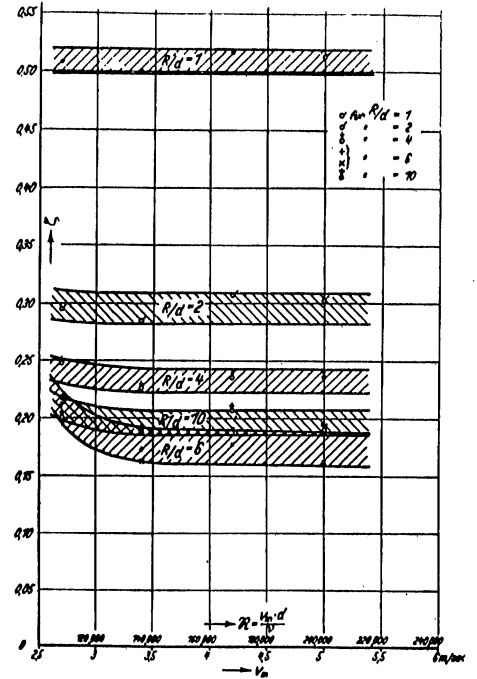


Fig.2-Bend Coefficient,  $\zeta$ , for Rough Bends as a Function of the Water Velocity and the Reynolds Number  $R = \frac{V_m \cdot d}{\gamma}$

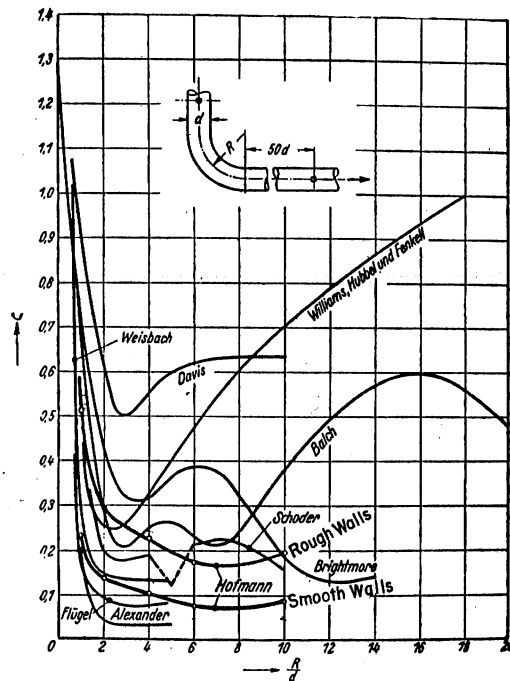


Fig. 3 - Curves Comparing Author's Tests with Those by Previous Investigators

## Abstract 16

Keulegan, G. H., and Beij, K. H., "Pressure Losses for Fluid Flow in Curved Pipes," JOURNAL OF RESEARCH OF THE NATIONAL BUREAU OF STANDARDS, Vol. 18, RP 965, pp. 89-114, January, 1937, 15 figs., 5 tables.

This paper discusses fluid flow through long radius pipe bends, including the flow in the entrance transition and in the downstream tangent, in so far as flow characteristics in them are modified by the presence of the bend. Experiments were made to provide data required for calculating the total loss resulting from a long bend. The greater portion of the paper deals with laminar flow and the transition from laminar to turbulent flow.

The experiments were performed on pipes of smooth-drawn brass of 3/8-in. internal diameter, especially selected for straightness and uniformity of bore. All of the bends were obtained by bending the pipe elastically into a circular arc of the proper degree of curvature.

The resistance in a bend, including the transition section, may be expressed by an equation similar to that for a straight pipe

$$\frac{1}{\gamma} \Delta P = \lambda_x \cdot \frac{x}{d} \frac{U^2}{2g} \quad (1)$$

where  $\Delta P$  = the pressure loss between the entrance of the bend and a point a distance  $x$  downstream,

$d$  = the pipe diameter,

$U$  = the mean velocity, and

$g$  = the acceleration of gravity.

In this equation,  $x_1 < x < \ell$ , where  $x_1$  and  $\ell$  are the lengths of the transition segment and of the bend respectively. In general, it would be expected that

$$\lambda_x = f\left(\frac{x}{d}, \frac{d}{D}, \text{Re}\right) \quad (2)$$

where  $D$  is twice the radius of curvature of the bend.

If  $\lambda_x$  is a function of the length, then

$$\lambda_x \cdot x = \int_0^{x_1} \lambda_a dx + \lambda_c (x - x_1) = k_x (\lambda_c - \lambda_s) x_1 + \lambda_s x_1 + \lambda_c (x - x_1) \quad (3)$$

where  $\lambda_a$  is the resistance coefficient applicable to a given point,  $a$ ,

where  $0 < a < x_1$ ;  $\lambda_c$  is the resistance coefficient applicable to the bend downstream of the transition segment, and  $\lambda_s$  is the resistance coefficient applicable to a straight pipe which has characteristics similar to those of the bend. Equation (3) may be rearranged to give

$$\frac{\frac{\lambda_c}{\lambda_s} - \frac{\lambda_x}{\lambda_s}}{\frac{\lambda_c}{\lambda_s} - 1} \cdot \frac{x}{d} = \beta \quad (4)$$

Assuming  $\beta$  to be independent of Reynolds number, an experimental expression for  $\beta$  in terms of  $(d/D)$  was found from experimental data in the form

$$\frac{1}{\beta} = 0.0059 + 0.844 \left(\frac{d}{D}\right)^{1/2} \quad (5)$$

Substitution of equation (5) in equation (4) results in

$$\lambda_x = \lambda_c - \frac{d}{x} \frac{(\lambda_c - \lambda_s)}{[0.0059 + 0.844 (d/D)^{1/2}]} \quad (6)$$

as the effective coefficient of resistance from the beginning of the bend to any point  $x$  greater than the transition length  $x_1$ .

An expression satisfying the boundary conditions for  $\lambda_a$ , the resistance coefficient at any point  $0 < a < x_1$ , was set up as a first approximation, resulting in an equation for the length of the transition segment,  $x_1$ .

$$\frac{x_1}{d} = \frac{3\pi}{3\pi - 4} \cdot \beta = \frac{1.74}{0.0059 + 0.844 \left(\frac{d}{D}\right)^{1/2}} \quad (7)$$

The experimental results suggest that an equation of this form is not greatly in error.

In the tangent downstream of the bend, a certain transition length is necessary for the velocity distribution characteristic of a bend to change

to that characteristic of the straight pipe. In a manner similar to that for the entrance transition, an equation for the effective resistance coefficient downstream of the bend was established in the form

$$\lambda_z = \lambda_s + \frac{d}{z} [0.141(\frac{d}{D})^{-1/2} + 4.50]^2 \frac{(\lambda_c - \lambda_s)^2}{\lambda_s} \quad (8)$$

where  $\lambda_z$  is the effective resistance coefficient applicable from the end of the bend to a point  $z > z_1$ . The length of the transition segment is  $z_1$ .

When the flow in the bend is turbulent, the relative increase in resistance may be defined by the ratio  $(\lambda_c - \lambda_s)/\lambda_s$ , which the experiments indicated was small and was approximately proportional to the curvature. No increase in resistance resulting from the presence of the bends could be detected in the straight pipes downstream of the bends.

The transition from laminar flow to turbulent flow in bends appears to be a function of the curvature of the bend. As the ratio  $d/D$  increases, the critical Reynolds number also increases above 2,200, the critical for a straight pipe. By using a well-rounded entrance and considerable care, the authors were able to raise the critical Reynolds number for the straight pipe to 9,200. The critical Reynolds number for the bend following the straight entrance then gradually decreased with increasing values of  $d/D$  until the curve approached that obtained by other investigators, whose results were based upon initially disturbed entrance flow. In Fig. 1, the results of the authors and other investigators are plotted to show the increase in the critical Reynolds number with increase in curvature.

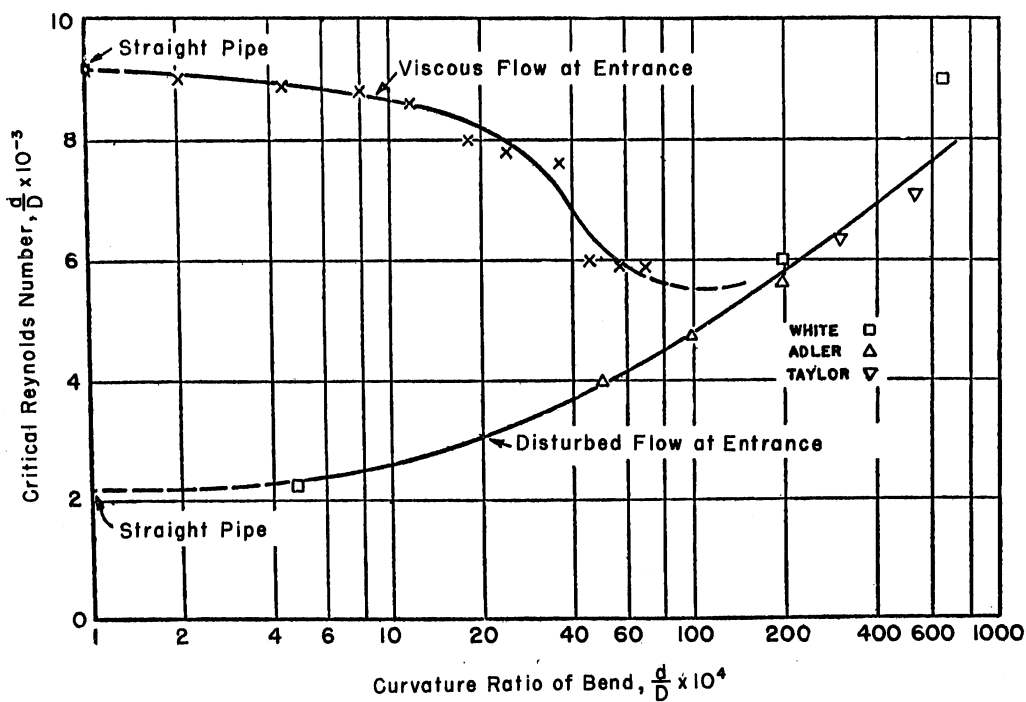


Fig.1-Relation of Critical Reynolds Number to Curvature Ratio

## Abstract 17

Keutner, Chr., "Strömungsverhältnisse in einem Senkrechten Krümmer" (Flow Conditions in a Vertical Bend), ZEITSCHRIFT DES VEREINES DEUTSCHER INGENIEURE, Vol. 77, pp. 1205-1209, November 11, 1933, 7 figs.

The investigations of the vertical bend described in this report have been evaluated in terms of pressure and velocity distribution, the purpose being to establish a basic means for comparison with the experiments which have been carried out on horizontal bends. An evaluation of the effect of gravity and the restraining influence of the bend walls was made and a theoretical analysis of their effect on the flow is presented.

A vertical bend of circular cross section with a deflection angle of  $90^\circ$  and a  $R/d$  ratio of 1.5 was used for the experiments. The bend was located in a longer conduit, midway between two pieces of straight pipe each 12 diameters long. The bend was drilled at 29 points for pressure measurements and the horizontal supply pipe and the vertical discharge pipe were drilled at four places each. The 37 pressure gauging points were led to one bank of piezometer tubes where they could be simultaneously recorded photographically.

The bulk flow during an experiment was accurately measured and the velocity at various points was obtained by means of a Pitot tube. All of the mean velocities used in the analysis were well above the critical value for turbulent flow. The piezometer taps were arranged along the bend in rows, so that the increment of pressure between any two points in a line had to be corrected for the difference in geodetic head. This pressure distribution showed many apparent inconsistencies that had to be explained by a measurement and an analysis of the velocity distribution. A series of velocity traverses were taken at sections all the way around the bend as well as in the horizontal upstream tangent. The distribution in the upstream tangent indicated that the effect of the bend was a dominant factor upstream since the highest velocities were along the inside wall. The velocity profiles around the bend were similar to those found in horizontal bends. No separation was observed along the outer bend wall but it was apparent at the downstream end of the bend along the inner wall.

Diagrams of the velocity profiles are included in the report, along with a plot of the differences in pressure from point to point around the bend.

## Abstract 18

Kirchbach, Hans, "Loss of Energy in Miter Bends," TRANSACTIONS OF THE HYDRAULIC INSTITUTE OF THE MUNICH TECHNICAL UNIVERSITY, BULLETIN 3, 1929, trans. and pub. by American Society of Mechanical Engineers, 1935, pp. 43-64, 47 figs.

The loss of energy ascribed to the miter bend is the total loss of head between the measuring points less the loss of head caused by normal pipe friction. The normal pipe friction was determined by substituting a length of straight pipe equal in length to that of the bend. The bend coefficient was  $\zeta = \frac{h_b}{V^2/2g}$  ( $h_b$  is the total loss minus friction loss;  $V$  is the mean velocity).

Five series of experiments were undertaken as follows:

- Series A. Bends containing a single miter joint with deflection angles,  $\delta = 22.5^\circ, 30^\circ, 45^\circ, 60^\circ, 90^\circ$ .
- Series B. (a) Bends containing two equal deflections in the same direction,  $\delta_1 = \delta_2 = 22.5^\circ, 30^\circ, 45^\circ$ , with various lengths between joints.
- (b) Bends containing three or four equal deflections of  $22.5^\circ$  and  $30^\circ$  in the same direction, with equal spacing between joints.
- (c) Bends containing three equal deflections in the same direction, with unequal spacing between joints.
- Series C. Bends containing two unequal changes in the same direction, with equal spacing between joints.
- Series D. Bends containing two equal changes in opposite directions, with varying spacing between joints.

The results of the experiments are shown in a series of curves for the various experimental arrangements. Figure 1 shows the increase in  $\zeta$  with increasing deflection angle,  $\delta$ , and includes a curve as proposed by Weisbach. The effect on the bend coefficient of increasing the spacing between joints in bends consisting of two equal miter bends of  $45^\circ$ , the velocity being constant, is shown in Fig. 2. The Reynolds numbers corresponding to 2, 4, and 6 m per sec are 74,000, 148,000, and 222,000 respectively. The curves indicate that the optimum spacing between joints is approximately 1.5 diameters. As the distance between joints increases, the total loss approaches that of

## Abstract 18, Kirchbach

two separate  $45^\circ$  bends. The relationship of the bend coefficient to the length between joints for two equal bends in opposite directions and separated by various lengths of straight pipe are shown in Fig. 3.

The experiments show that, for a Reynolds number greater than 74,000, the bend coefficient for all arrangements of bends is nearly independent of the Reynolds number. Figure 4 shows the bend coefficient in relation to the Reynolds number for a multiple bend made up of three miter joints. The results of Bouchayer for a similar bend for larger values of Reynolds number are also plotted in Fig. 4. There is good agreement between these results.

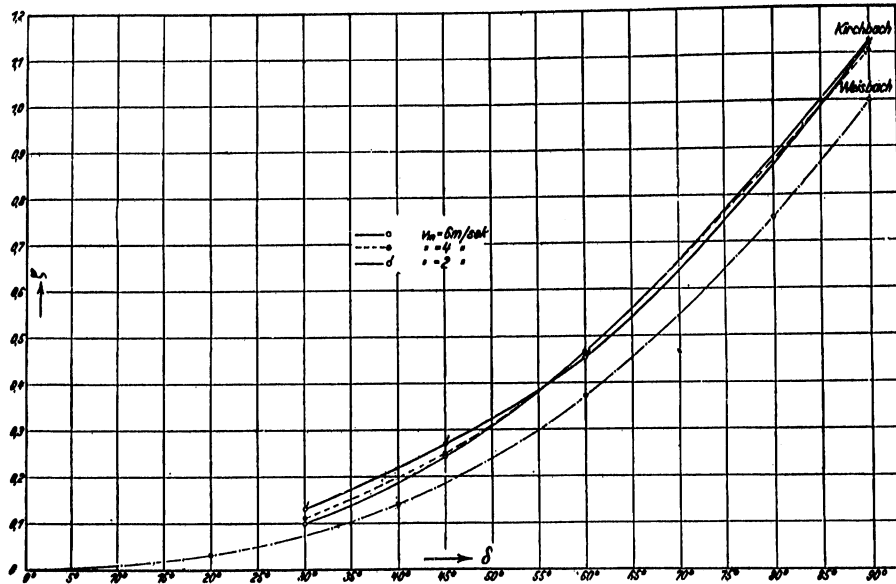


Fig.1-Influence of Deflection Angle  $\delta$  on Bend Coefficient  $\zeta$

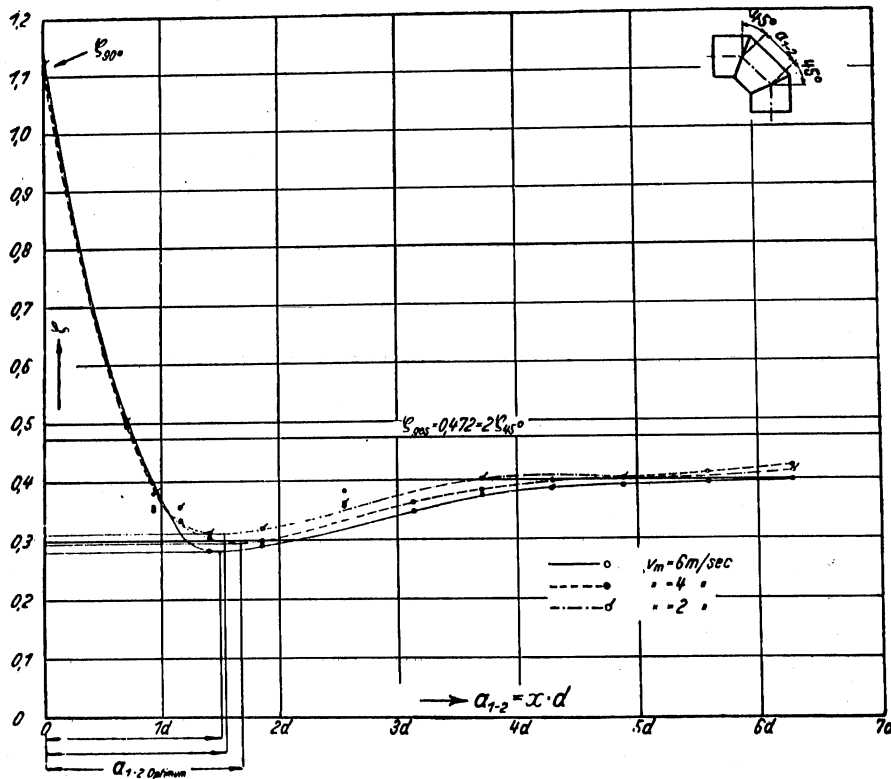


Fig.2-Effect of Spacing of Two Miter Bends Turned in Same Direction on the Bend Coefficient  $\zeta$

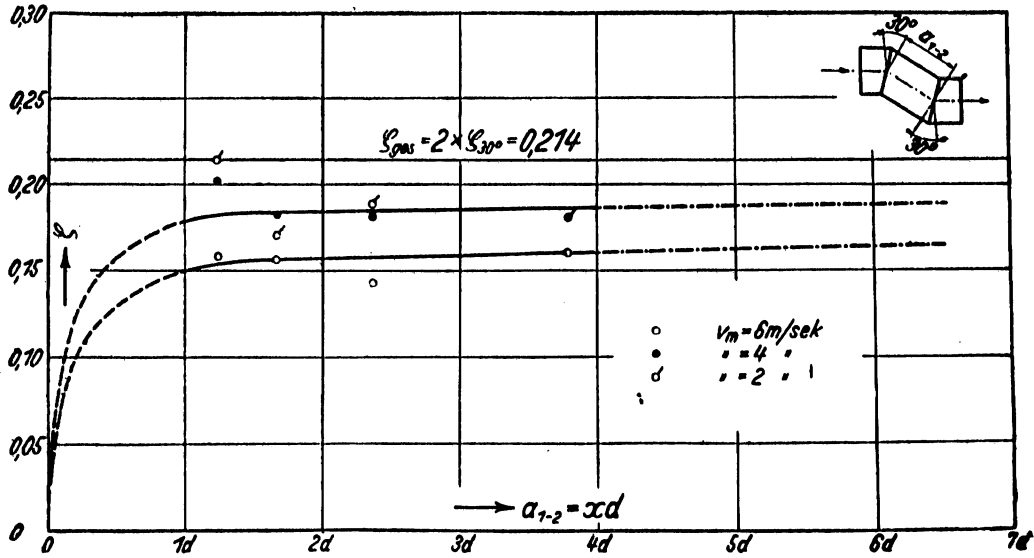


Fig.3-Effect of Spacing of Two Miter Bends Turned in Opposite Directions on the Bend Coefficient,  $\zeta$

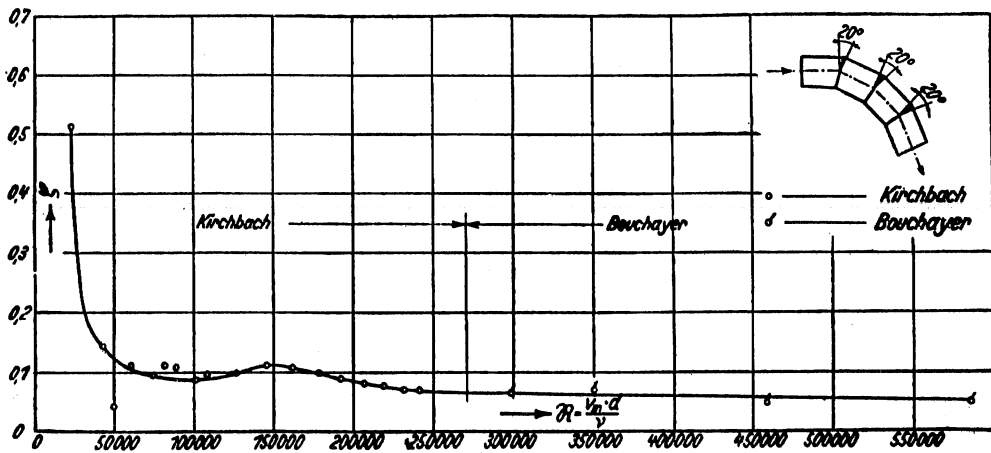


Fig.4-Relation of Reynolds Number to Bend Coefficient  $\zeta$  for a Multiple Miter Bend

## Abstract 19

Lell, Jacob, "Beitrag zur Kenntnis der Sekundärströmung in Gekrümmten Kanälen" (Secondary Flow of Liquids in Curved Channels), ZEITSCHRIFT FÜR DAS GESAMTE TURBINENWESEN, Vol. 11, pp. 129-135, 293-298, 313-317, 1914, 12 figs., 9 tables.

The author conducted a series of experiments to determine:

1. The influence of secondary currents upon the main flow and upon the pressure distribution on the walls of a bend and in its approach and discharge tangents.
2. The influence of various degrees of wall roughness upon the formation of secondary currents.
3. The influence of piezometer holes upon the wall roughness.

A closed, horizontal, rectangular channel 100 mm by 200 mm in cross section was used. An approach tangent, 3130 mm long, was made of cast iron which had been smoothed by a file for 1000 mm from the bend. The discharge tangent was 2000 mm long, made of cast iron with planed walls. The bend was 180°, made with cast iron base, forged iron walls, and tested with glass and cast iron top, both bored and unbored.

Test velocities ranged from 0.1 to 9 m per sec, but results are given only for velocities of 3, 6, and 9 m per sec. Four tests were made with each velocity; special attention was paid to phenomena at the inner wall and its vicinity.

The installation and procedure are described in great detail and various methods for determination of direction of flow are discussed. The pressure observations were made by means of instantaneous photographs of manometers. The author introduced compressed air bubbles into the flow at various levels to delineate the flow pattern.

The results of the investigations are presented in a series of tables and pressure distribution graphs. The phenomena are analyzed theoretically and the results are evaluated in detail.

The following results were obtained:

1. Friction losses in the boundary layers are higher than in the main flow; this results in a pressure drop in the boundary layers which causes currents to flow from the outer wall toward the inner wall, or secondary flow.

2. Change in velocity does not affect the direction of the stream paths.

3. Compared to loss in an equivalent straight length, the increase in friction loss in the bend caused by the velocity distribution is negligible, as long as the relationship  $h_r = \gamma v^2$  is valid ( $h_r$  is the head loss,  $\gamma$  is the constant depending upon channel dimensions, roughness, and temperature).

4. The large loss of energy in the bend is caused by:

- (a) Constant changing of the vortex state, resulting from the large differences in velocities of adjacent layers (in  $h_r = \gamma v^2$ ,  $\gamma$  becomes a function of  $v$ ).
- (b) The repeated transformations of velocity into pressure and of pressure into velocity.
- (c) The secondary currents as manifested by pressure head needed for forming of the currents, and contraction of the flow cross section resulting in higher velocity of the main flow and, therefore, in further expenditure of energy.

5. The intensity of the secondary currents increases from cross section to cross section.

6. The influence of the secondary flows upon the pressure distribution increases at the inner wall and in its vicinity.

7. Greatest pressure differences between inner and outer walls of the bend occur at some distance before the crown of the bend. From that point on, the pressure increases both at the outer and inner walls, the increase at the inner wall being more rapid and extending well into the discharge tangent.

8. The loss in the bend is at least 5.5 times, in one case even 6.25 times, the loss in an equivalent length of straight channel.

9. Introduction of guide vanes (vertical partition walls) which extend from the beginning to the end of the bend improve the velocity distribution and decrease the head loss.

10. The required head in the bend, which increases slightly with increasing roughness, indicates that the secondary currents

## Abstract 19, Lell

are dependent to some extent upon roughness; this is not obvious as far as direction of flow is concerned.

11. The influence of the piezometer holes upon the roughness is negligible.

## Abstract 20

Lorenz, H., "Der Widerstand von Rohrkrümmern" (The Resistance of Curved Pipes), PHYSIKALISCHE ZEITSCHRIFT, Vol. 30, pp. 228-230, 1929, 1 fig., 1 table.

There is such a wide difference in the results of experiments on the pressure drop of fluids flowing through pipe bends that it is difficult to fit them into a curve that can be represented by an empirical formula. The only fact that is established is that, for a deflection of  $90^\circ$ , the minimum value of the resistance occurs between 1:7 and 1:8 for the ratio of pipe radius to the mean bend radius.

An equation for the pressure drop for a given deflection was established on the basis of the transverse pressure distribution, the separation at the outside and inside walls, and the friction along the wall. Assuming potential vortex flow through a  $360^\circ$  annular ring, the transverse pressure gradient  $\frac{\delta p}{\delta r} = \frac{\gamma}{g} \cdot \frac{u^2}{r}$  ( $u$  is the tangential velocity at radius  $r$ ,  $p$  is the pressure,  $\gamma$  is the unit weight of the fluid, and  $g$  is the acceleration of gravity). Integration of the pressure gradient between the inside and the outside walls,  $r_1$  and  $r_2$ , results in

$$P_2 - P_1 = \frac{\gamma}{2g} U_0^2 r_0^2 \left( \frac{1}{r_1^2} - \frac{1}{r_2^2} \right) \quad (1)$$

( $U_0$  is the mean velocity and  $r_0$  is the radius corresponding to the mean velocity). For small values of  $a/r$ , where  $a$  is the radius of the pipe, equation (1) may be written with the approximation

$$2r_1^2 r_2^2 \approx (r_1 + r_2) r_0^3 \quad \text{as} \quad P_2 - P_1 = \frac{\gamma}{g} \frac{U_0^2}{r_0} (r_2 - r_1) \quad (2)$$

As a consequence of this pressure drop toward the inner wall, the often-observed spiral currents develop. The right side of equation (2) thus represents the spiral energy of the fluid mass which must be maintained by a pressure drop in the direction of the flow. With sufficient approximation  $U_0$  may be considered to be the mean velocity and  $r_0$  the mean radius. If the bend includes an angle  $\phi$ , the formation of the double spiral will not be complete because of the transition to straight flow at the entrance and

exit. Therefore, the pressure drop in the direction of the flow will be proportional to the deflection angle, or

$$\Delta P' = \frac{\phi}{2\pi} (P_2 - P_1) = \frac{\gamma}{g} \frac{U_o^2 a}{r_o} \frac{\phi}{\pi} \quad (3)$$

where  $(r_2 - r_1) = 2a$ .

The author analyzed the effect of separation on the basis of a flow expansion and deduced that the loss in pressure caused by the expansion in the direction of flow is negligible, being of the second order compared to the pressure drop caused by the spiral currents. The expression for the loss in pressure caused by separation is

$$\Delta P'' = \frac{U_o^2 \gamma}{g} \cdot \frac{8\Delta r \tan \zeta}{3\pi a} = \frac{16 U_o^2 \gamma \Delta r^2}{3g\pi\phi a r_o} \quad (4)$$

( $\Delta r$  is the displacement of mean velocity from the centerline of the bend).

The additional pressure loss caused by friction on the walls is expressed in the usual form

$$\Delta P''' = \frac{\phi r_o}{a} \lambda \frac{U_o^2 \gamma}{2g} \quad (5)$$

( $\lambda$  is the friction coefficient).

The total pressure drop along the bend is the sum of the partial pressure drops, so

$$\Delta P = \frac{\phi}{\pi} \cdot \frac{U_o^2}{2g} \gamma \left( \frac{2a}{r_o} + \pi\lambda \frac{r_o}{a} \right) \quad (6)$$

In the usual notation for the bend coefficient,  $\zeta = \frac{2a}{r_o} \frac{\phi}{\pi}$ .

The minimum value of the pressure drop is

$$\Delta P_o = \frac{\phi}{\pi} \frac{U_o^2 \gamma}{2g} \sqrt{2\pi\lambda} \quad (7)$$

when  $\frac{a}{r_o} = \sqrt{\frac{\pi\lambda}{2}}$ . If  $\lambda$  is taken as 0.01 for cast iron,  $\frac{a}{r_o} = 0.125 = 1/8$ , which agrees with the results of other investigators.

## Abstract 21

Madison, R. D., and Parker, J. R., "Pressure Losses in Rectangular Elbows," TRANSACTIONS, AMERICAN SOCIETY OF MECHANICAL ENGINEERS, Vol. 58, pp. 167-176, 1936, 16 figs.

Data are given on pressure losses in rectangular elbows as affected by the radius ratio, the aspect ratio, the deflection angle, and the size and the velocity of flow. Tests were also made using splitters in single elbows and on compound elbows.

The elbow being tested was installed in a calibrated duct in which the velocity was measured by a Pitot tube. The difference between the static pressure in the straight duct without the elbow and the static pressure with the elbow, the velocity being constant, was taken as the pressure loss. The ratio, in per cent, of the pressure loss to the velocity head existing during the test was taken as a measure of the efficiency of the elbow. The effect of the radius ratio (the radius of the centerline divided by the width of the duct in the plane of the bend) on the loss as a per cent of velocity head for an aspect ratio of 1.0 is shown in Fig. 1 for radius ratios up to 3.0. The results of other investigators are also shown.

The aspect ratio is the ratio of the depth of the duct normal to the plane of the bend to the width in the plane of the bend. For aspect ratios less than one the loss is increased, and for aspect ratios greater than one the loss is decreased, as shown in Fig. 2. The pressure loss appears to be proportional to the deflection angle for angles of  $45^\circ$  and  $90^\circ$ , but for an angle of  $180^\circ$  the loss is less than twice the loss in a  $90^\circ$  elbow. Figure 3 shows the effect of the deflection angle upon the loss.

The loss resulting from an elbow that discharges directly into the atmosphere is increased considerably because there is no pressure regained as there is when the elbow is followed by a duct. The losses resulting from free discharge are shown in Fig. 4 for various aspect ratios and radius ratios.

When several elbows were placed in tandem, the loss of the assembly was usually not equal to the sum of the individual losses because the loss in the second elbow was affected by the presence of the first, so that the velocity distribution entering the second elbow was not normal. It is necessary to test the various combinations of elbows to determine the loss. Results of tests of simple combinations are shown in Figs. 5 and 6, where the actual loss and the estimated loss are shown for comparison.

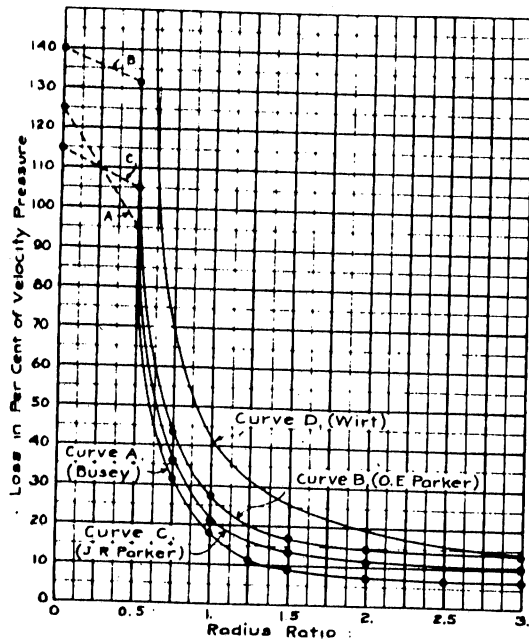


Fig. 1—Pressure Loss in 90° Elbows Followed by Ducts, for Increasing Radius Ratio

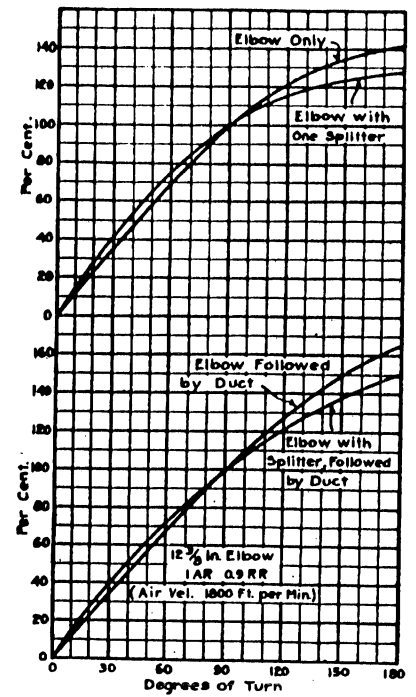


Fig. 3—Effect of Deflection Angle on Pressure Loss as Percent of Loss in 90° Elbows

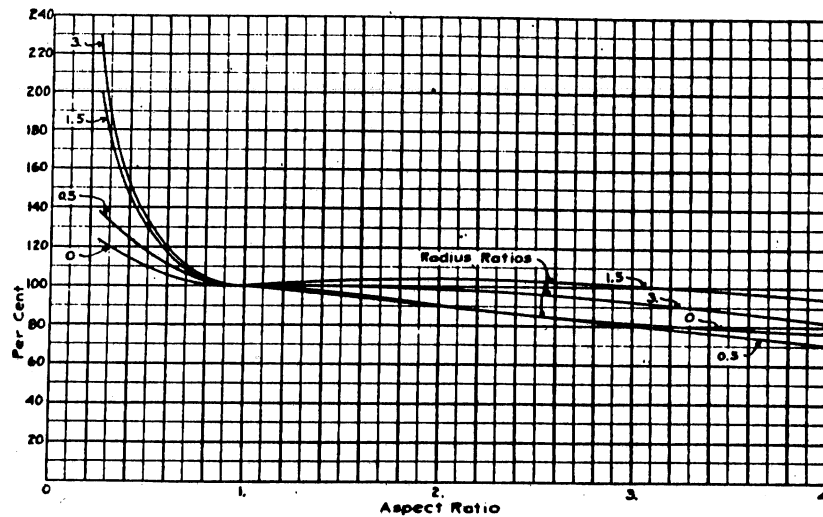


Fig. 2—Effect of Aspect Ratio on Pressure Loss as Percent of Loss for Aspect Ratio of Unity for Various Radius Ratios

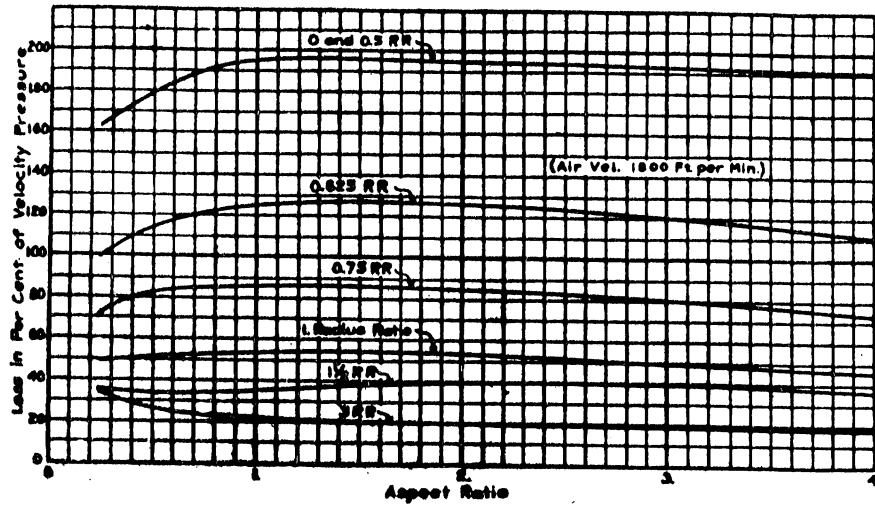


Fig. 4—Pressure Losses in Rectangular 90° Elbows Discharging Directly Into the Air

Case No.	First Elbow		Second Elbow		Elbows Only			Elbows followed by Duct		
	RR	AR	RR	AR	Act.	Est. % of Sum	% of Est.	Act.	Est. % of Sum	% of Est.
(1)	3.	4	1.5	4	57.2	48.5	77.	27.6	21.5	128.
(2)	1.5	4	3.	4	24.2	30.	91	26.4	21.5	123.
(3)	1.5	4	0.5	4	248	202	121.	115	82.	153.
(4)	0.5	4	1.5	4	162	112	69.	103	85	121.
(5)	1.5	4	1.5	0.25	45.5	48.	95.	34.6	30.	91
(6)	1.5	0.25	1.5	4	55.	6.5	85.	38.5	30.	101.

Fig. 5—Results of Tests on 3-In. X 12-In. Compound Elbows

Case No.	Plain Elbows			1.5 Radius Elbows			Splitter in Each Elbow		
	Act.	Est. % of Sum	% of Est.	Act.	Est. % of Sum	% of Est.	Act.	Est. % of Sum	% of Est.
(1)	104.2	100.	104.	94.5	100.	55.	26.	30	62
(2)	83.7	100.	94.	105.	100.	100.	25.	30	73.
(3)	68.5	100.	64.	75.1	100.	75.	27.4	30	94
(4)	43.	92	83.	34.4	98.	68.	15.	30	73.
(5)	62.2	92.	120.	68.3	92.	131.	16.0	30	94
(6)	41.0	92.	91.	48.7	92.	86.	38.5	30	102.

Fig. 6—Results of Tests on 12 3/8-In. X 12 3/8-In. Compound Elbows

## Abstract 22

Nippert, H., "Über den Strömungsverlust in Gekrümmten Kanälen" (On the Flow Losses in Bends), FORSCHUNGSARBEITEN AUF DEM GEBIETE DES INGENIEURWESENS, Bulletin 320, 1929, 141 figs., 6 plates.

This paper presents the results of an extensive series of experiments on  $90^\circ$  and  $180^\circ$  bends of rectangular cross section to determine the influence of radius ratio and form and sequence of cross sections on the bend coefficient for various velocities.

Each one of the basic rectangular bends was constructed so that the use of various inserts could vary the section along its length as to the ratio of radii of inner and outer wall, the ratio of inlet to outlet, the sequence of sections, or the  $R/d$  ratio. Since this method made construction difficult in a bend of circular cross section, this type was limited to one series.

The apparatus consisted of a test stand, arranged so that any bend could be inserted. The supply of water came from a tank that fed the system by gravity. The volume of the tank between two levels was carefully calibrated, and the time necessary for this volume to flow through the conduit and bends was the basis for comparison between the bends. The pressure drop through the bends was taken at a point between the upstream point of tangency and a point about 10 diameters below the downstream point of tangency. An  $R/d$  ratio of 6 was the highest used in the tests. The large number of runs that resulted from the use of all the combinations of inserts were checked by the orderly progression of the curves and were run over if this progression indicated a discontinuity. Static pressure readings were obtained by the use of mercury and water manometer gages.

Pitot traverses were made at a cross section between the end of the bend and the exit section of the apparatus. Pressure readings for each combination were also made. In order to keep the head constant during the time that the velocity traverse was made, a pump kept the tank at a constant level.

The discharge from the apparatus was in the form of a jet. This jet was smooth and uniform in most instances and particularly when the sequence of sections in the bend produced a contraction. In the bends where the sequence of sections formed an expansion, the jet was milky in appearance and was relatively unstable. If the fluid jet did not take up the full cross section of the exit section, the run was rejected. When miter sections were

## Abstract 22, Nippert

tested, cavitation was often detected by a rattling sound in the bend, by extreme milkiness of the jet, and by apparent oscillations along its length.

In order to compute the loss coefficient that defines the pressure drop in terms of the velocity head, it was necessary to define the variable velocity resulting from the lowering of the water level in the tank. Since the pressure readings were not recorded until acceleration of the water was constant after the valve was opened, the retardation of velocity resulting from the lowering of head could be evaluated by Bernoulli's equation, and the loss could be represented as a constant times the loss for uniform flow.

The results were not recorded in tabular form because of the large number of separate runs made and the difficulty in isolating the effect of any one variable in a study of tables. In an analysis of the effect of any given variable, the pertinent runs were grouped into similar sets and the average of the results of each of these sets defined points along the curves pertaining to that variable. These graphs are included in the paper along with the corresponding plots of the velocity profiles at the exit section.

With the experimental data as a basis, a qualitative discussion is given of the influence on the flow of each of the variables investigated. The 90° bends were subdivided into upright, flat, and circular bends, and the upright bends were further subdivided into bends of the same entrance and exit sections, nozzles, and diffusers. An analysis was made of the velocity and energy distribution in each of the divisions. A general analysis of the effect of the temporal variability, velocity distribution, the influence of variable height, and the influence of temperature variation was also made. The last study was made with a separate series of runs having temperature, and hence viscosity, of the water as the only variable.

The general conclusions drawn from the experiments are as follows:

1. The distortion of the velocity profile increases as the bend becomes sharper. In all cases the point of maximum velocity migrates toward the outside wall as it proceeds around the bend.
2. A crosswise flow is superimposed over the main flow as a result of the unequal energy content of the particles in a cross section of the bend. This flow forms two spirals that rotate around axes parallel to the bend axis.

## Abstract 22, Nippert

3. The rearrangement of this distortion can take place only through friction in the connecting straight lengths, necessitating long tangents to give a quantitative measure of the loss.

4. The measured pressures around a miter bend agree with the pressures expected in the flow of an ideal fluid.

5. The increase of pressure around bends indicates according to the laws governing the boundary layer, that separation is taking place on the outside as well as the inside wall. The magnitude of the separation and the spirals are dependent on the magnitude of the flow velocity.

6. The bend loss can be divided into three separate parts; namely, wall friction, separation from the walls of the conduit, and the cross current. The wall friction loss in the bend can be approximated by comparison to straight conduits. The loss caused by separation in a bend decreases very rapidly as the bend radius increases, reaching a minimum at an  $R/d$  of 3.5. The separation loss increases considerably in diffuser bends but decreases rapidly for contracting bends. In all of the bends the loss caused by transverse flow is negligible.

7. The bend loss decreases rapidly with increasing bend radius and then increases slowly in an approximately linear manner after reaching a certain minimum (within the range investigated).

8. For small values of the radius of the inner wall divided by the breadth of the entrance section, ( $r_i/b_e = 0.0$  to  $0.75$ ), large values of the bend coefficient occur. The loss decreases rapidly with increasing values of  $r_i/b_e$ ; however, for  $r_i/b_e$  greater than 4.0 the decrease in loss is insignificant.

9. The outer radius  $r_a$  has in the range,  $0.0 \leq r_a/b_e \leq 1.5$ , no appreciable influence on the bend coefficients as long as no contracted section is formed.

10. The most favorable bend form is achieved through a moderate enlargement in the midpoint of the bend.

11. For  $90^\circ$  bends with a contracting section (nozzles) the outer radius has little significance, but a smaller loss is to be expected for increasing inner radius. The influence of the combination

of the outer and inner radii disappears with increasing nozzle-like contraction.

12. For  $90^\circ$  bends with an expanding section any increase in difference between the outer and inner radii increases the loss. The largest possible inner radius within the experimental range yields the smallest loss.

13. For  $180^\circ$  bends in addition to the conformation of the principles listed for  $90^\circ$  bends, a ratio of height of conduit to breadth of conduit ( $h/b$ ) of 2.0 indicates the smallest loss.

14. For a  $90^\circ$  bend of constant cross section, the bend coefficient is independent of the depth-width ratio within the range of experiment.

15. The bend loss is dependent upon the velocity according to a power law. At velocities above 23 ft per sec the quadratic form is sufficiently accurate.

16. The bend loss is also dependent upon the viscosity according to a power law where the exponent varies with the bend form. The change in exponent was not investigated closely.

17. The influence of velocity and viscosity upon the bend loss as shown in 15 and 16 suggest a relationship of bend loss to Reynolds number, a contradiction that could not be clarified by the experiments.

18. The velocity profile existing at the entrance to the bend affects the losses in the bend.

19. A relationship between the losses and the wall friction at the midpoint seems to exist, but could not be proved in a straightforward manner.

## Abstract 23

Robertson, James M., A STUDY OF THE FLOW OF WATER IN BENDS, Unpublished B. S. in C. E. Thesis, Library, University of Illinois, 1938, 40 pp., 20 figs.

During the investigation velocity measurements at the midpoint of the bend were made on several 90° bends with different radii. The bends tested were 4-in. 90° flanged, cast iron pipe elbows. The dimensions and R/d ratio for each bend are given in Table I. By using a special Pitot tube, the velocity was measured at 45° along the radius of curvature of the bend in a cross section normal to the direction of flow. The Pitot tube was calibrated by comparing the measured average velocity in a pipe with that determined from the discharge and cross-sectional area.

The results of the velocity traverses are shown in Figs. 1, 2, 3, and 4. These curves show a close similarity between the velocity distribution obtained for different mean velocities. In Figs. 5 and 6 the velocity distributions for different R/d values and for a constant mean velocity show the effect of R/d on the velocity distribution at the midpoint. The maximum value occurred at 1/4, 1/2, 3/4, and 1 1/4 in. from the inner wall for an R/d of 0.8, 1.0, 1.5, and 2.0 respectively. The potential velocity distribution,  $V_r = \text{constant}$ , is plotted upon the measured distribution for several conditions in Fig. 7 where the constant was taken as the product of the average velocity and the mean radius of the bend.

The effect of the R/d ratio upon the difference in pressure on the inner and outer walls at the 45° point is shown in Fig. 8 where

$$\frac{P_o}{w} - \frac{P_i}{w} = C_k \frac{V^2}{2g}$$

and  $P_o$  and  $P_i$  are the pressures on the outer and inner walls respectively. The equations of the curves are given on the figure.

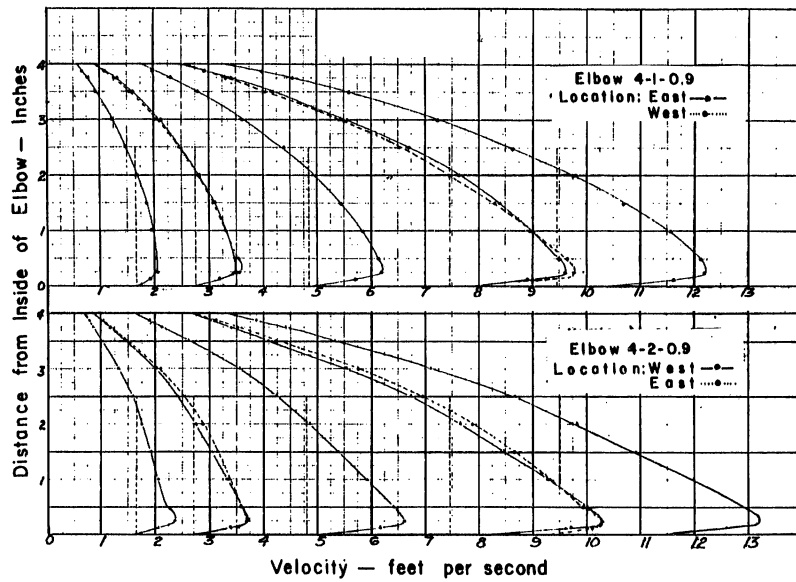


Fig. 1—Velocity Distribution at Midpoint of 90° Bend,  
 $\frac{R}{d} = 0.8$

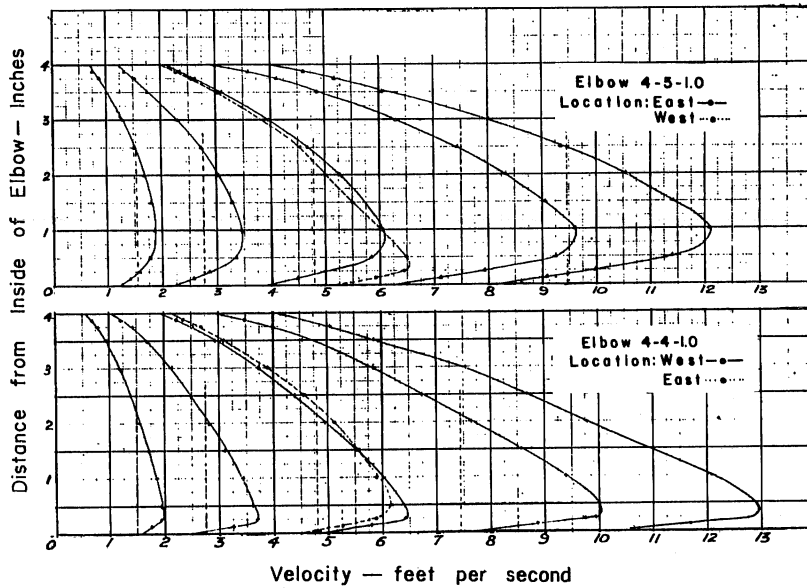


Fig. 2—Velocity Distribution at Midpoint of 90° Bend,  
 $\frac{R}{d} = 1.0$

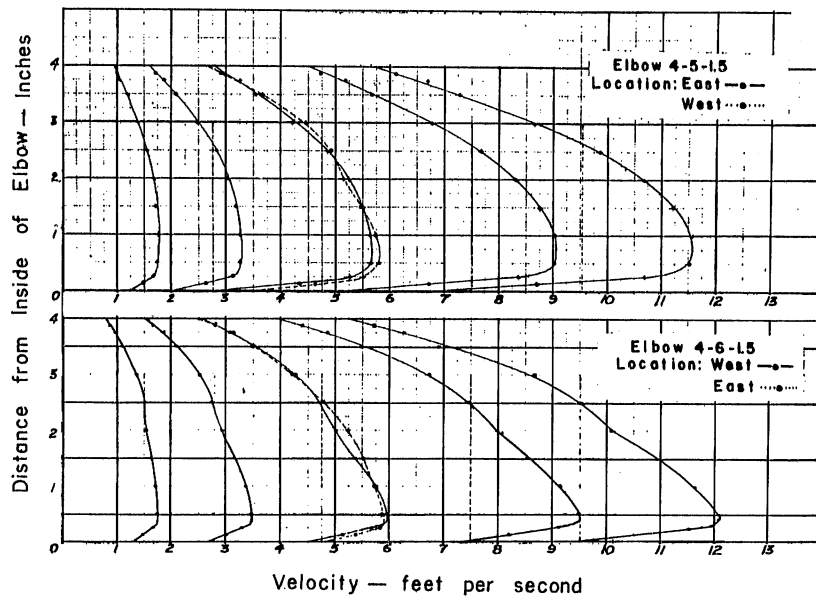


Fig.3-Velocity Distribution at Midpoint of 90° Bend,  
 $\frac{R}{d}=1.5$

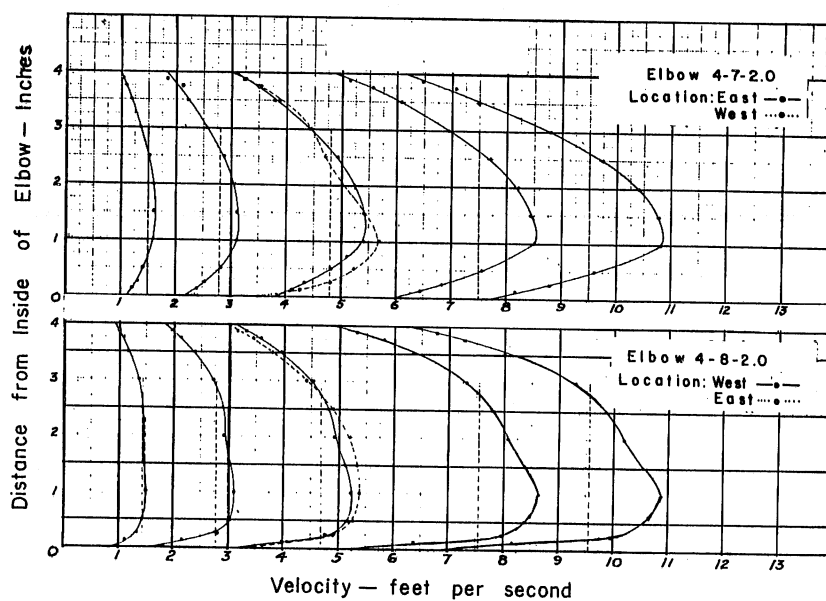


Fig.4-Velocity Distribution at Midpoint of 90° Bend,  
 $\frac{R}{d}=2.0$

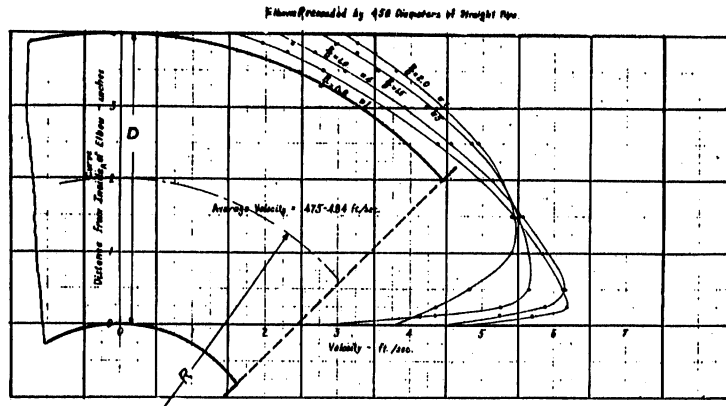


Fig.5 — Influence of Radius Ratio on Velocity Distribution at Midpoint of 90° Bend

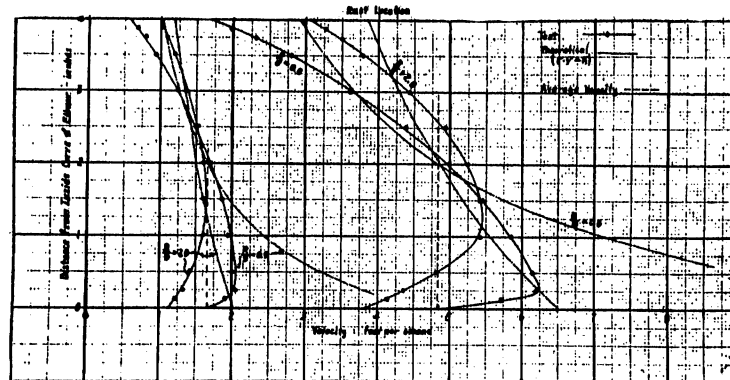


Fig.6—Comparison of Potential Velocity Distribution with the Actual Distribution for Several Values of  $\frac{R}{d}$

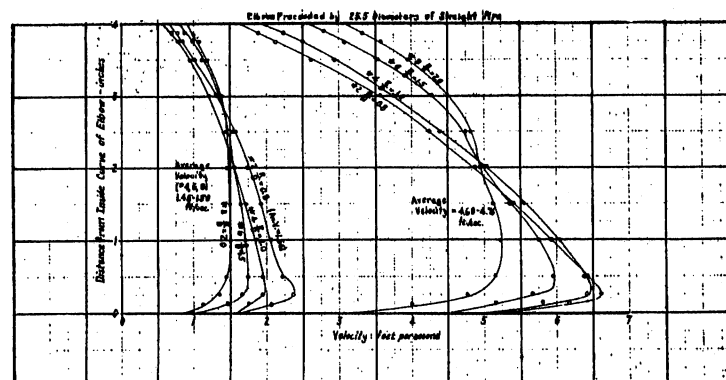


Fig.7—Influence of Radius Ratio on Velocity Distribution at Midpoint of 90° Bend

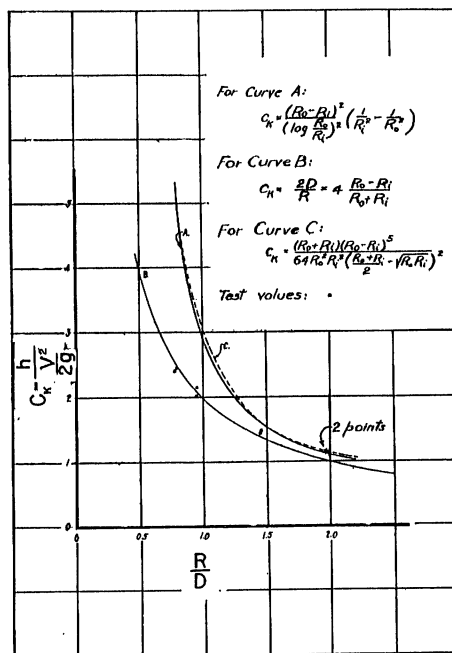


Fig.8-Relation between Elbow Constant and Curvature of Elbows

TABLE I.  
 ELBOW DIMENSIONS

Elbow	Diameter in.	Outside Radius in.	Inside Radius in.	R in.	R/D
4-1-0.8	4.01	5.10	1.10	3.10	0.78
4-2-0.8	4.03	5.20	1.20	3.20	0.80
4-3-1.0	4.01	5.90	1.90	3.90	0.97
4-4-1.0	4.02	5.85	1.85	3.85	0.96
4-5-1.5	4.01	7.90	3.90	5.90	1.47
4-6-1.5	3.99	7.90	3.90	5.90	1.48
4-7-2.0	4.01	9.80	5.80	7.80	1.95
4-8-2.0	4.01	9.80	5.80	7.80	1.95

## Abstract 24

Schoder, E. W., "Curve Resistance in Water Pipes," TRANSACTIONS OF THE AMERICAN SOCIETY OF CIVIL ENGINEERS, Vol. 62, Paper No. 1093, pp. 67-112, 1909, 23 figs., 15 tables, 3 plates.

This article reports the results of a series of experiments on the loss of head caused by 90° bends in a 6-in. pipe line. Twelve curves were tested. Six were of wrought iron with radii such that the R/d values of the bends were 5, 6, 8, 10, 15, and 20. The other six bends were of cast iron, made to order for the experiments. The values of R/d for the cast iron bends were 1.34, 1.76, 1.90, 2.16, 3, and 4.

The head loss caused by the straight pipe used in the line was determined separately at two different times with somewhat different results, probably because of progressive rusting of the interior. The total loss in the bend and the adjacent downstream tangent was determined from piezometers located 1.1 ft upstream and 20.6 ft downstream of the bend. The excess loss of head caused by the bend was determined as the difference between the total head loss and the loss in the straight pipe of corresponding length. The results of the experiments were given as the excess loss of head over that of a straight pipe alone for various velocities. Figure 2, p. 16, is a plot of the results in terms of the bend coefficient,  $\frac{h_b}{V^2/2g}$ , where  $h_b$  is the net loss of head in feet of water caused by the bend alone, and  $V^2/2g$  is the velocity head.

## Abstract 25

Schubart, Werner, "Energy Loss in Smooth- and Rough-Surfaced Bends and Curves in Pipe Lines," TRANSACTIONS OF THE HYDRAULIC INSTITUTE OF THE MUNICH TECHNICAL UNIVERSITY, BULLETIN 3, 1929, trans. and pub. by American Society of Mechanical Engineers, pp. 81-99, 1935, 49 figs.

The experiments and results described in this report are a continuation of the experiments of Kirchbach (p. 106), and include experiments on single and multiple miter bends with smooth and rough walls. The bends tested are shown in Fig. 8. They were constructed of bronze so that corrosion would not affect the experimental results. They were made smooth by careful machining. For the second series of tests the walls were roughened by coating with a mixture of sand and varnish after the method of Hofmann (p. 98).

The bend coefficient was computed in the usual manner as the ratio of the loss caused by the bend to the velocity head  $\zeta = \frac{h_b}{v^2/2g}$ . The loss caused by the bend is equal to the difference between the total head loss including the bend and the head loss occurring in an equivalent length of straight pipe. The tests were performed for Reynolds numbers ranging from 25,000 to about 300,000. The resistance factor,  $\lambda$ , for the straight pipe with smooth and rough walls is shown in Fig. 1. In Fig. 2 the bend coefficient for smooth walls as a function of Reynolds numbers is given for deflection angles of  $5^\circ$ ,  $10^\circ$ ,  $15^\circ$ ,  $22.5^\circ$ , and  $30^\circ$ . In Fig. 3 are corresponding curves for rough-walled bends. Figures 4 to 7 show the bend coefficient for several multi-joint bends in terms of Reynolds number. Figure 8 shows the bend coefficients for the various combinations of miter bends corresponding to a Reynolds number of approximately 225,000.

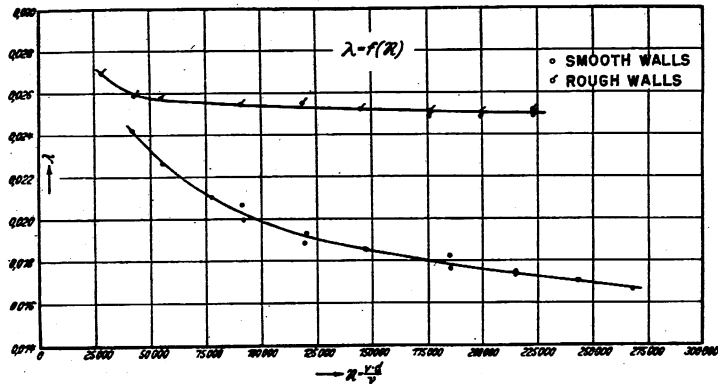


Fig.1-Relation of the Friction Factor,  $\lambda_s$ , for a Straight Pipe to Reynolds Number

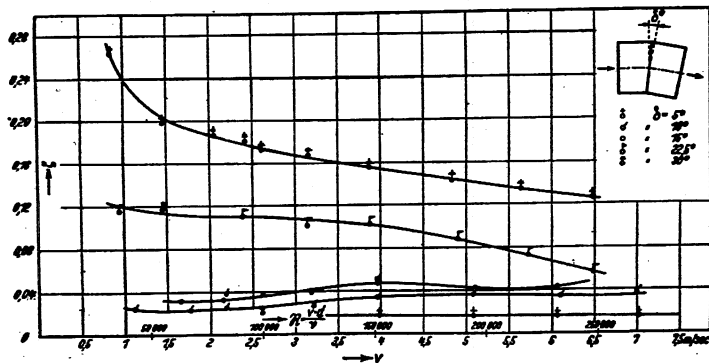


Fig.2-Relation of Bend Coefficient,  $\zeta$ , to Reynolds Number for Miter Bends with Smooth Walls

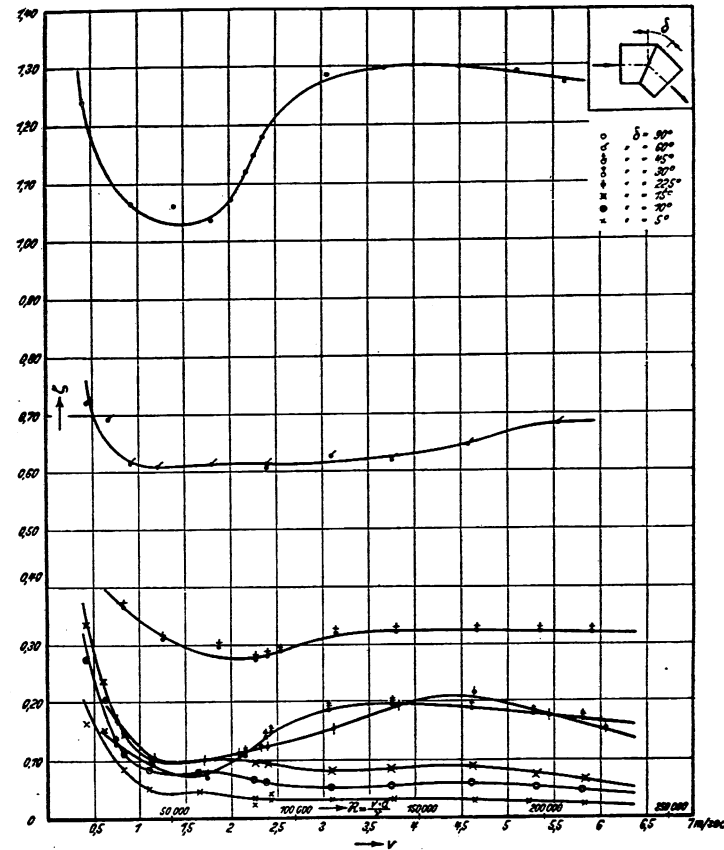


Fig.3-Relation of Bend Coefficient,  $\zeta$ , to Reynolds Number for Miter Bends with Rough Walls

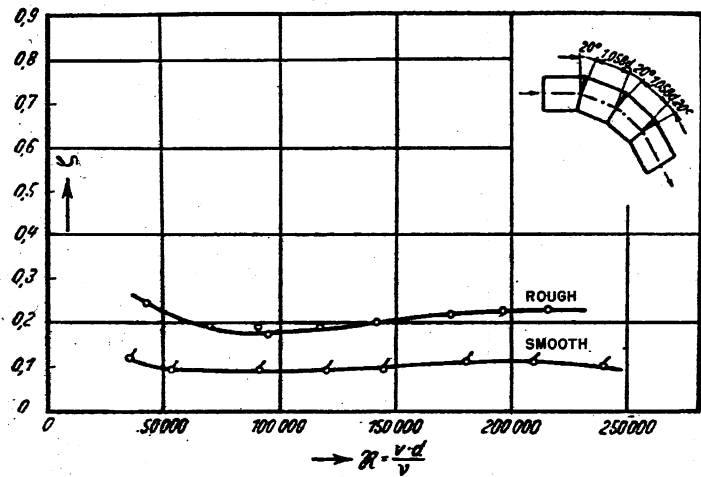


Fig. 4

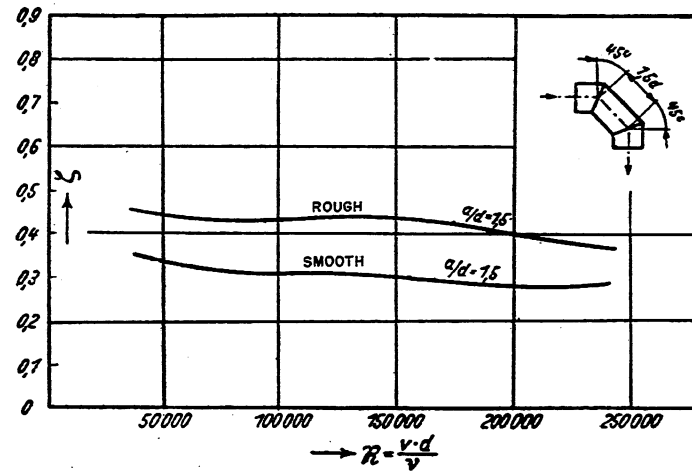


Fig. 5

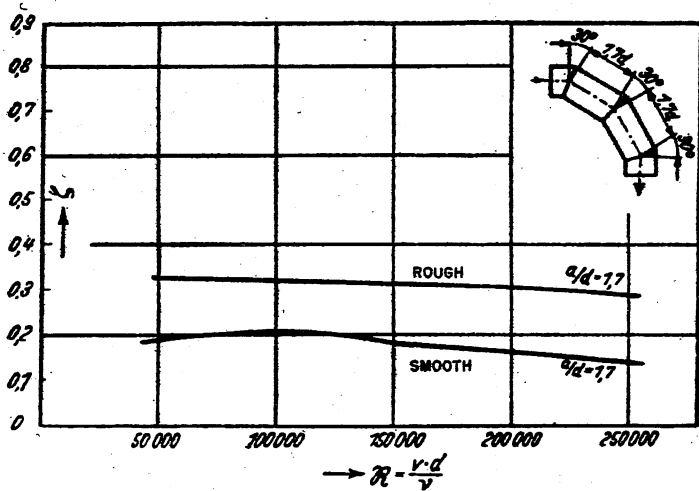


Fig. 6

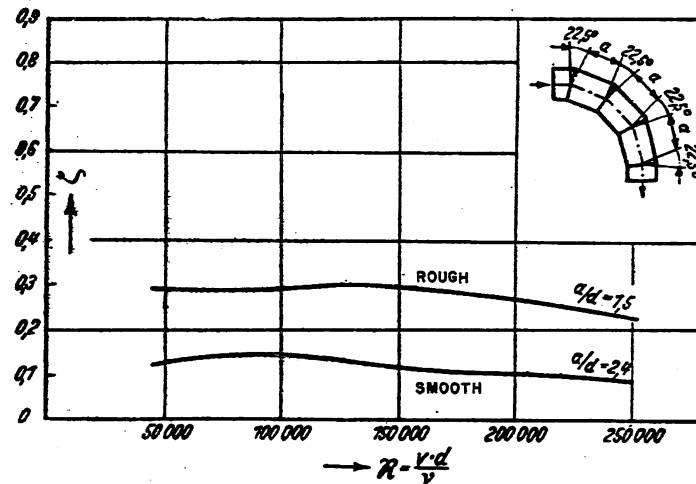


Fig. 7

Figs. 4-7 Relation of Bend Coefficient,  $\zeta$ , to Reynolds Number for Multi-Joint Miter Bends

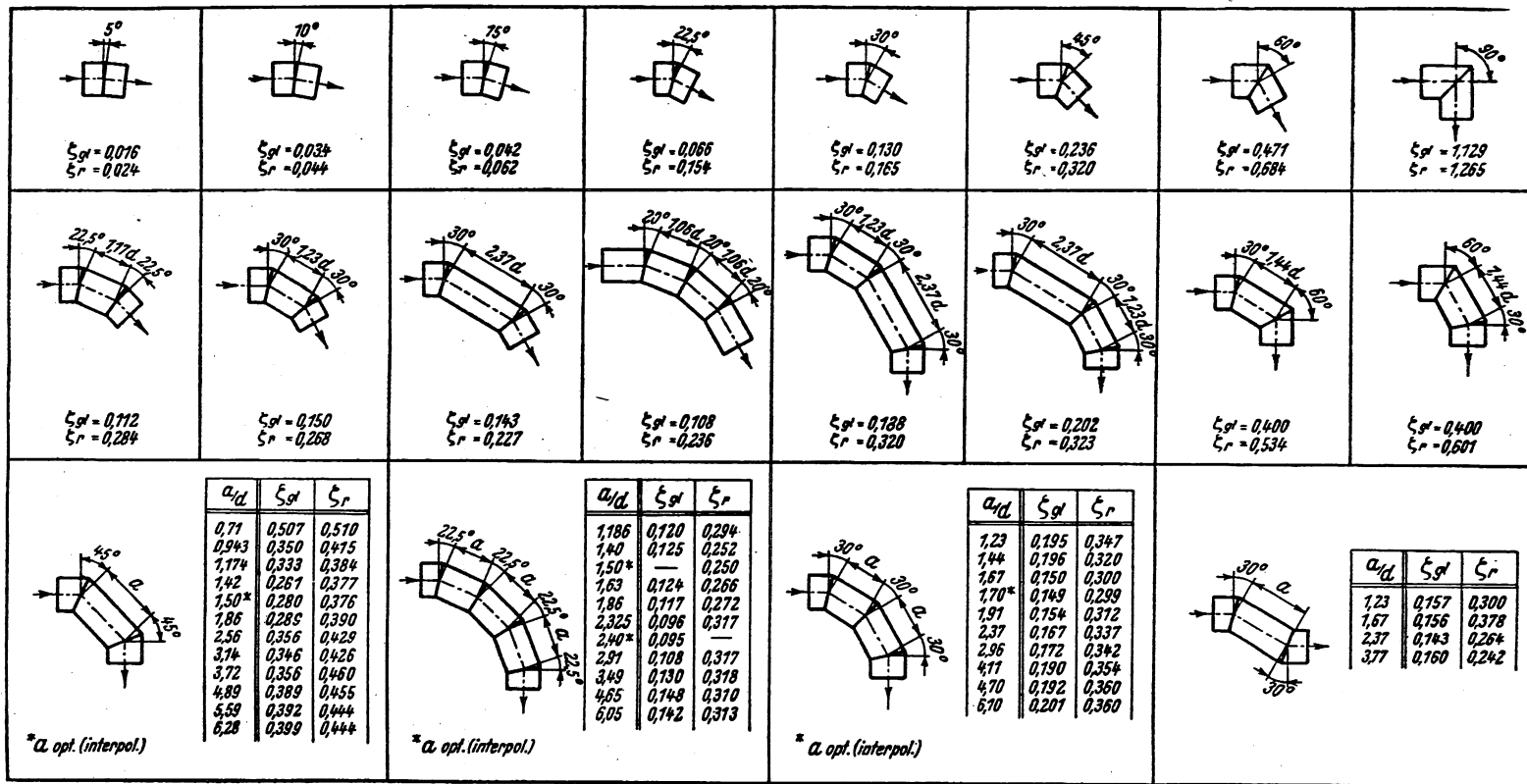


Fig.8-Bend Coefficients,  $\xi$ , Corresponding to a Reynolds Number of 225,000 (approx.)

## Abstract 26

Spalding, W., "Versuche Über den Strömungsverlust in Gekrümmten Leitungen" (Experiments on Flow Loss in Curved Conduits), ZEITSCHRIFT DES VEREINES DEUTSCHER INGENIEURE, Vol. 77, pp. 143-148, 1933, 26 figs.

In these experiments, the investigations of Nippert were extended to include a study of the effect of deflection angle on the losses in curved conduits. Guided by the results submitted in Nippert's report, an evaluation was made of the losses caused by various inner and outer radii and by constant contracting and expanding cross section in bends with deflection angles of  $45^\circ$ ,  $67^\circ$ ,  $112.5^\circ$ , and  $135^\circ$ .

These experiments were intended for use both in the relatively narrow field of pipe flow and in the broader applications relative to hydraulic machinery. In these applications the uniform distribution of the long inlet course can no longer be used as a valid simplifying assumption.

Spalding used Nippert's experimental apparatus, which consisted of a test stand fitted so that inserts could be added to give the desired inner or outer radius and the desired  $R/d$  value. The supply of water came from a small diameter tank, so that variable head was a factor in the computations. The comparison between different bends was based on the stop-watch time necessary for the water level in the tank to descend from one fixed level to another. The various deflection angles were obtained by replacing the inner radius used by Nippert with a rigid angle that could be fitted with inserts to give the desired deflection angle. The exit section was fitted so that a velocity traverse could be made with a Pitot tube. Pressure measurements around the bend were obtained by the use of wall taps in the apparatus.

The bends tested by Spalding had a constant height (60 mm) and a constant width (15 mm) at the inflow section. The shape was varied from nozzles with a minimum exit width of 0.5 of the width at the inflow section to diffusers with a maximum exit width of 1.5 times the width at the inflow section.

Since experimental results comparable with those of Nippert were obtained, Spalding established the agreement of the measuring technique so that his experiments would be a valid quantitative extension.

The derivation of the bend coefficient is the same as that of Nippert's. The bend coefficient for each bend of each deflection angle under

## Abstract 26, Spalding

consideration is shown in a graph of the curvature of the inner radius divided by the breadth of the entrance section against the bend coefficient expressed in per cent of the velocity head. A plot of the ratio of the breadths of exit to the entrance section against the bend coefficient for each deflection angle is also shown. Diagrams of the velocity profiles are made for four representative bends. The text includes a brief description and interpretation of the results presented in the graphs and diagrams for each one of the four deflection angles considered.

In these experiments it was found that, for bends with an equal inlet and outlet cross section and with not too sharp a deflection, a certain addition to the cross section of the channel at the crest of the bend resulted in a reduction in the bend loss when compared with the bend loss when the cross section was not changed. From the measurements for each deflection angle, one can deduce the most favorable form of the bend in relation to the flow resistance.

## Abstract 27

Taylor, G. I., "The Criterion for Turbulence in Curved Pipes," PROCEEDINGS OF THE ROYAL SOCIETY OF LONDON, Series A, Vol. 124, pp. 243-249, 1929, 3 figs., 1 table.

The purpose of the experiments described was to observe visually the transition from laminar flow to turbulent flow in curved pipes. The observations were on two glass helices of 11.4-cm and 18.1-cm mean diameter which were formed from glass tubes of 0.610-cm and 0.568-cm inside diameter respectively. The flow patterns were observed by introducing a concentrated solution of fluorescein through 0.5-mm holes bored into the side of the tube at a distance of 1 coil and 2 1/2 coils from the entrance. Flow at these points was considered fully established.

For low velocities the circulation pattern was in the form of a spiral. The colored fluid flowed along the wall to the inside of the curve. At the innermost point it left the wall and flowed across the section to the outermost point of the curve, at which point it then again moved along the wall toward the inside of the bend. Sometimes, at the outer boundary, all of the colored fluid turned back along the wall on the same side at which it started, but occasionally some of it flowed in the opposite direction.

The first sign of instability of flow with increasing velocities was an irregular vibration, but the colored fluid still maintained its course. Further increase in speed resulted in increased vibrations, until the stream became so turbulent that the identity of the color band was lost within a few millimeters of its source. Table I gives the results of the experiments.

TABLE I  
Influence of Curvature on Critical Reynolds Number

Helix	Diam of Tube d-cm	Diam of Helix D-cm	$(\frac{d}{D})^{1/2}$	Highest Reynolds number at which the flow was steady	Lowest Reynolds number at which the flow was completely turbulent
I	0.610	11.4	0.232	5830	7100
II	0.568	18.1	0.177	5010	6350

These results, as well as the data of White and the line indicating the Reynolds number for turbulent flow in a straight pipe, are included in Fig. 1, p. 104.

## Abstract 28

Wasielowski, Rudolf, "Verluste in Glatten Rohrkrümmern mit Kreisrundem Querschnitt Bei Weniger Als  $90^\circ$  Ablenkung" (Loss in Smooth Pipe Bends of Circular Cross Section for Deflections Less than  $90^\circ$ ), MITTEILUNGEN DES HYDRAULISCHEN INSTITUTS DER TECHNISCHEN HOCHSCHULE, Vol. 5, pp. 53-67, 1932.

This paper presents the results of experiments made to determine the loss caused by bends of less than  $90^\circ$  deflection. The bends were made of smooth machined brass with 43-mm internal diameter and were constructed to have radius ratios,  $R/d$ , of 1, 2, 4, 6, and 10 (where  $R$  is the radius of curvature and  $d$  is the bend diameter) and deflection angles,  $\delta$ , of  $15^\circ$ ,  $22\ 1/2^\circ$ ,  $30^\circ$ ,  $45^\circ$ ,  $60^\circ$ , and  $75^\circ$ . The  $75^\circ$  bend was composed of the  $30^\circ$  and  $45^\circ$  bends, and was tested at  $R/d$  values of 2, 4, 6, and 10. Each bend was tested at 23 different velocities ranging from 1 to 6 meters per sec, which corresponds to Reynolds numbers ranging from about 35,000 to 225,000.

The test section consisted of three parts, an upstream tangent 9 diameters long, the bend, and a downstream tangent 50 diameters long. The head loss in the bend,  $h_b$ , was obtained by subtracting the head loss in an equivalent length of straight pipe from the observed pressure difference with the bend in place, that is,

$$h_b = h_{\text{total}} - h_{\text{friction}}$$

The resistance coefficient of the bend,  $\zeta$ , was evaluated from the expression

$$\zeta = \frac{h_b}{v^2/2g}$$

where  $v$  is the mean flow velocity.

The influence of Reynolds number on the bend coefficient for each radius ratio and each deflection angle is shown in Fig. 1. The curves indicate that for Reynolds numbers beyond about 120,000, the bend coefficient is practically independent of the Reynolds number, but that the bend coefficient increases as the Reynolds number decreases below 120,000.

Figure 2 shows that, for small deflection angles to about  $\delta = 22\ 1/2^\circ$ , the resistance coefficient is proportional to the deflection angle and is practically independent of the curvature ratio,  $R/d$ , although it is considerably smaller than the resistance coefficient for a miter bend of the same deflection angle. At deflection angles larger than  $22\ 1/2^\circ$ , the influence of the curvature ratio upon the resistance coefficient is apparent.

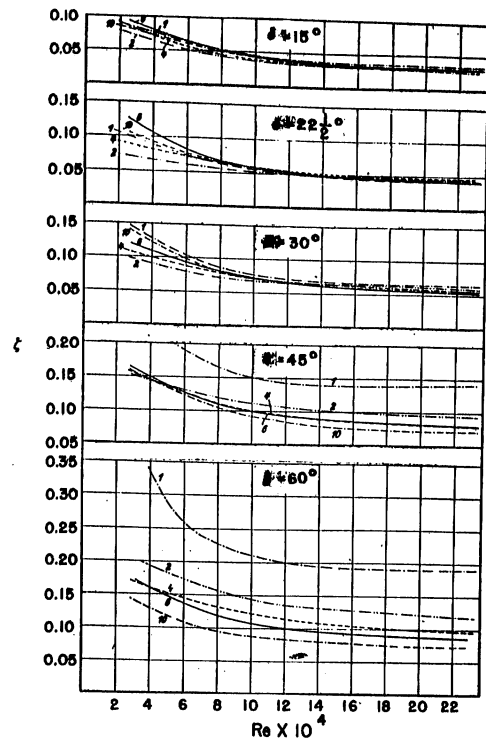


Fig.1—Influence of Reynolds Number on the Bend Coefficient,  $\zeta$ , for Various Values of  $\frac{R}{d}$  and Deflection Angle

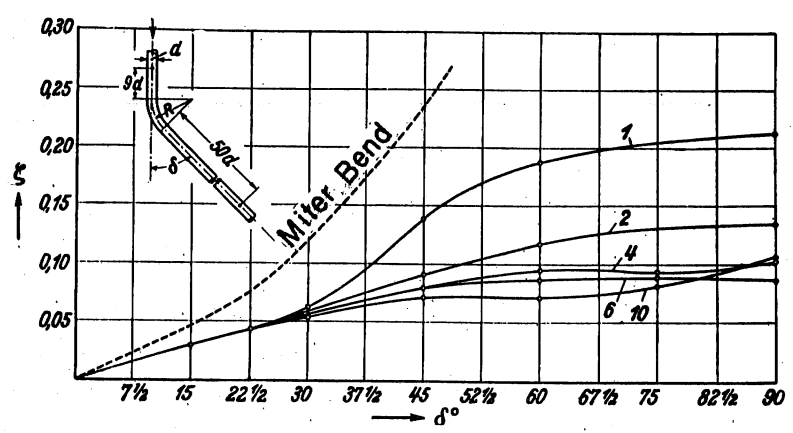


Fig.2—Influence of the Deflection Angle on the Bend Coefficient,  $\zeta$ , for a Reynolds Number of 225,000 and for Different Radius Ratios

## Abstract 29

Wattendorf, F. L., "A Study of the Effect of Curvature on Fully Developed Turbulent Flow," PROCEEDINGS OF THE ROYAL SOCIETY OF LONDON, Series A, Vol. 148, pp. 565-598, February, 1945, 24 figs., (also, Guggenheim Aeronautics Laboratory, California Institute of Technology Publication No. 54).

This investigation deals with two-dimensional flow in curved channels. By making the test channel very deep, compared with the width, the influence of the upper and lower boundaries was negligible, and the effect of curvature on turbulent flow could thereby be isolated. The experiments were conducted in two channels whose walls at the curved section were bent in concentric circular arcs 5 cm apart, the radius of the inner walls being 20 cm (Channel II) and 45 cm (Channel I). The depth of the conduit normal to the plane of the bend was 90 cm. A straight section 305 cm long preceded the curved portion, which extended through about  $300^\circ$  of arc in order to obtain fully developed curved flow.

Measurement of the pressure drop along the straight and curved portions of the channel indicated that the resistance coefficient,  $\lambda$ , for the curved portion was only slightly higher than for the straight section (see Fig. 1). The computation of  $\lambda$  was based on the pressure drop along the centerline of the curved channel which was expressed as

$$\frac{dp}{r_c d\theta} = \frac{\lambda}{b} \cdot \frac{1}{2} \rho \bar{U}^2$$

where  $r_c$  is the radius of the centerline of the curved portion,  $b$  is the width of the channel in the plane of the curve,  $\rho \bar{U}^2 / 2$  is the dynamic pressure of the flow, and  $dp/r_c d\theta$  is the pressure drop along the centerline.

The velocity distribution was measured at a series of stations around the curve for one Reynolds number. The velocity curves for successive sections around the curve are shown in Fig. 2, which also shows the transition in velocity distribution from that characteristic of straight flow to a distorted distribution as a result of curvature. Figures 3 and 4 show the dimensionless plot of the velocity distribution at  $210^\circ$  for both channels at various velocities. Superposed upon the velocity curve is the potential distribution,  $U_r = \text{constant}$ .

Application of von Kármán's expression for velocity distribution for the region outside of the wall neighborhood in the form

$$\frac{U_p - U}{\sqrt{\frac{1}{\rho} \frac{dp}{r_p d\theta}} b_e}$$

in terms of the function  $y/b_e$ , resulted in a single curve for the velocity distribution near both the inside and outside walls for both test channels.  $U_p$  is the potential velocity at the point  $b_e$  where the potential distribution is tangent to the actual velocity distribution. The radius of this point is  $r_p$ . The relationship is plotted in Fig. 5. It will be noted that the distribution curves for the curved portion of the flow all fall on a single line which is different from that for straight flow on a similar basis. Before definite conclusions are drawn regarding the similarity of the curves, the author feels that more experiments with less curvature should be performed.

The velocity distribution in the neighborhood of the wall, represented by  $\frac{U}{\sqrt{\frac{\tau_0}{\rho}}}$  in terms of  $\sqrt{\frac{\tau_0}{\rho}} \frac{y}{\nu}$ , is plotted in Fig. 6, which shows that the

deviation from the straight flow curve is in opposite directions for convex and concave curvature, and that the magnitude of the deviation increases with the curvature.

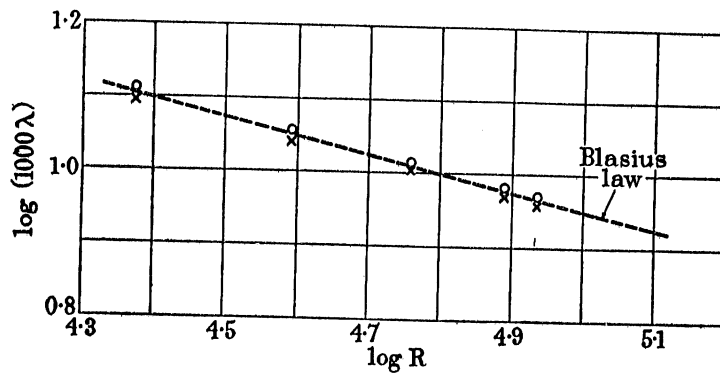


Fig. 1-Resistance Law for Curved Channel II. x, Straight Sections; o, Curved Section

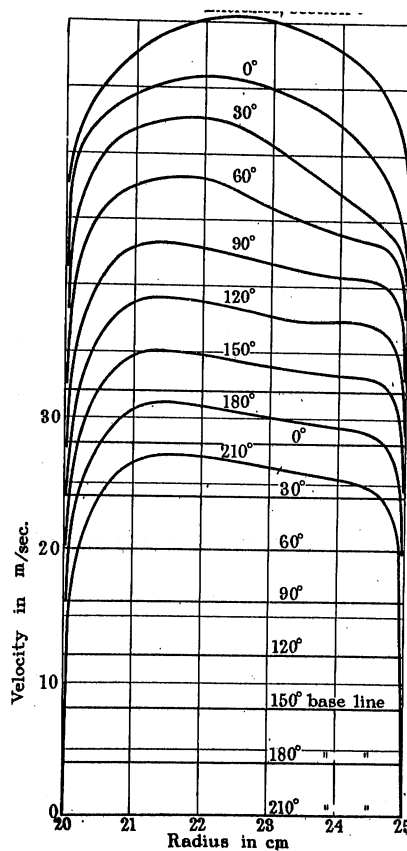


Fig. 2-Velocity Distribution in Curved Channel II

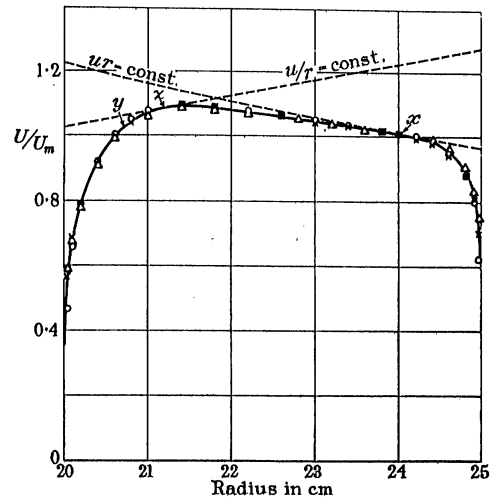


Fig.3—Dimensionless Velocity Distribution in Curved Channel II.  $\circ$ ,  $U_m = 8.44$  m/sec;  $\times$ ,  $U_m = 17.65$  m/sec;  $\Delta$ ,  $U_m = 25.00$  m/sec

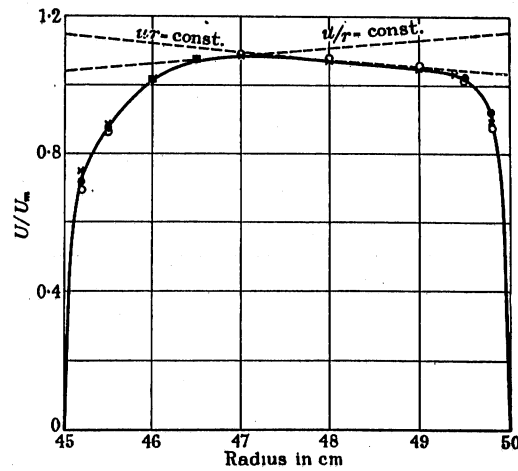


Fig.4—Dimensionless Velocity Distribution in Curved Channel I.  $\bullet$ ,  $U_m = 31.0$  m/sec;  $\times$ ,  $U_m = 25.0$  m/sec;  $\circ$ ,  $U_m = 10.0$  m/sec

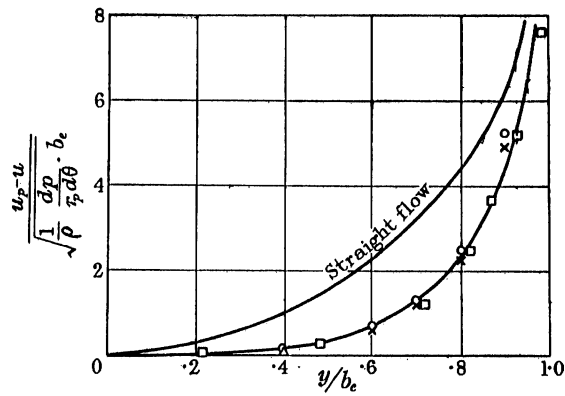


Fig.5-Dimensionless Velocity Distributions in Curved Channels I and II.  $\square$ , Channel I Inner;  $\Delta$ , Channel II Inner;  $\circ$ , Channel I Outer;  $\times$ , Channel II Outer

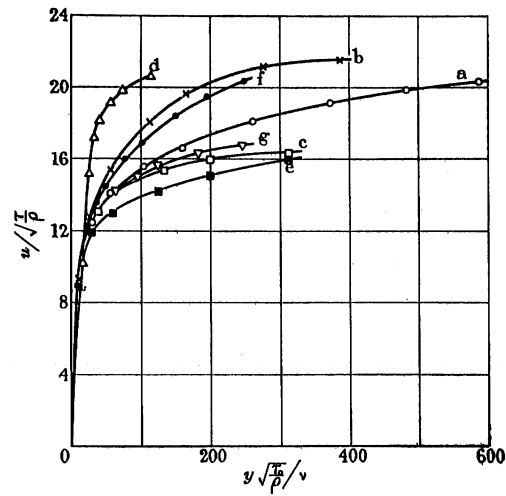


Fig.6-Dimensionless Velocity Distribution Near Wall for Curved Channel II and Concentric Cylinder. a,  $\circ$  Straight; b,  $\times$  Curved Channel II Inner; c,  $\square$  Curved Channel II Outer; d,  $\Delta$  Inner Rotating Cylinder; e,  $\blacksquare$  Outer Stationary Cylinder; f,  $\bullet$  Curved Channel I Inner; g,  $\nabla$  Curved Channel I Outer

## Abstract 30

White, C. M., "Streamline Flow Through Curved Pipes," PROCEEDINGS OF THE ROYAL SOCIETY OF LONDON, Series A, Vol. 123, pp. 645-663, 1929, 10 figs., 2 tables.

This article reports the results of experiments on the pressure loss through coiled pipes compared to that for straight pipes. The results were correlated on the basis of Dean's criterion (p. 86) for the pressure loss. The results for the various coils examined were found to agree very satisfactorily.

Coils with three degrees of curvature were tested. The data pertaining to the test pipes are given in Table I.

TABLE I  
Test Bends and Range of Experiments

Pipe No.	Diam of Pipe - d cm	Diam of Coil - D cm	Curvature Ratio - d/D	Range of Re	Fluid
II	0.630	31.7	1/50	16-13000	Water
I	1.032	15.62	1/15.15	0.058-41000	Oil and Water
III	0.298	610.5	1/2050	220-4000	Water
Grindley & Gibon	0.317	36.6	1/112	25-1400	Air

The pressure loss was measured over a given length of coil following a length sufficient to establish curvilinear flow. The friction factor for the flow in the coils was plotted in terms of Reynolds number for each coil and compared with that for straight pipe as defined by the equation  $\lambda = 64/Re$ . Dean's criterion was rewritten to state that, for the same velocity, the ratio of the resistance coefficient for straight pipes to that for curved pipes is a function of the parameter  $Re (d/D)^{1/2}$ , that is

$$\frac{\lambda}{\lambda_0} = F [Re (d/D)^{1/2}]$$

The results of the tests on the three coils, as well as those of Grindley and Gibson, define a single curve (Fig. 1). The fact that the points fall on a single curve substantiates the criterion. It is observed in Fig. 1

Abstract 30, White

that each set of data departs from the main curve at points which appear to coincide with the change in the type of motion. The results of these experiments are apparently applicable to flow in coils where curvilinear laminar flow is fully established.

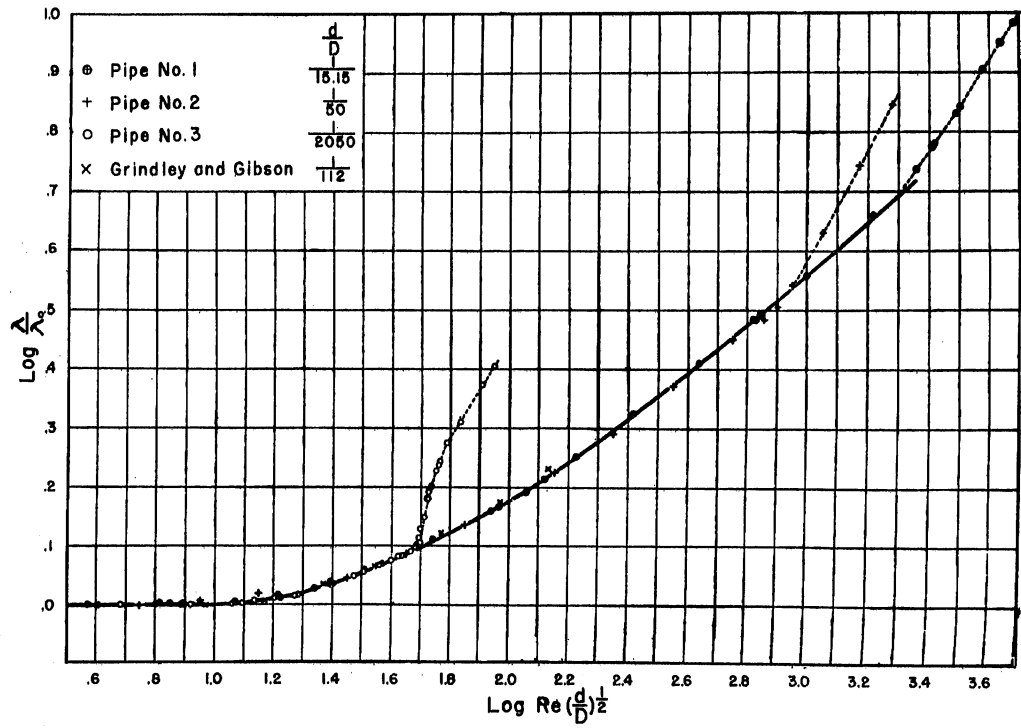


Fig.1 - Relation of Flow Resistance to Curvature and Reynolds Number

## Abstract 31

Williams, G. S., Hubbell, C. W., and Fenkell, G. H., "Experiments at Detroit, Mich., on the Effect of Curvature upon the Flow of Water in Pipes," TRANSACTIONS OF THE AMERICAN SOCIETY OF CIVIL ENGINEERS, Vol. 47, Paper No. 911, pp. 1-369, 1902, 131 figs., 90 tables.

A study of the effect of curvature upon the resistance to flow was included in an extensive series of measurements of the flow in 30-in., 16-in., and 12-in. water mains. During the construction of the mains, provision was made for measuring pressures and velocities at certain specified points, which made it possible to measure the loss incurred because of the bends. The pipes were standard cast iron pipes with bell and spigot joints. The tangent sections were coated with coal tar, and the bends were painted with graphite paint. The bends were not as smooth as the tangent sections.

The results of curvature studies are shown in Fig. 1. The percentage of excess loss in a curved section 80 diameters long over the loss in a straight pipe 80 diameters long is plotted in terms of the radius of the bend in diameters and the length of curve in diameters. The results showed a minimum excess loss for an  $R/d$  of about 2.5. After passing the minimum, the loss increased continually as the  $R/d$  increased up to the maximum  $R/d$  tested.

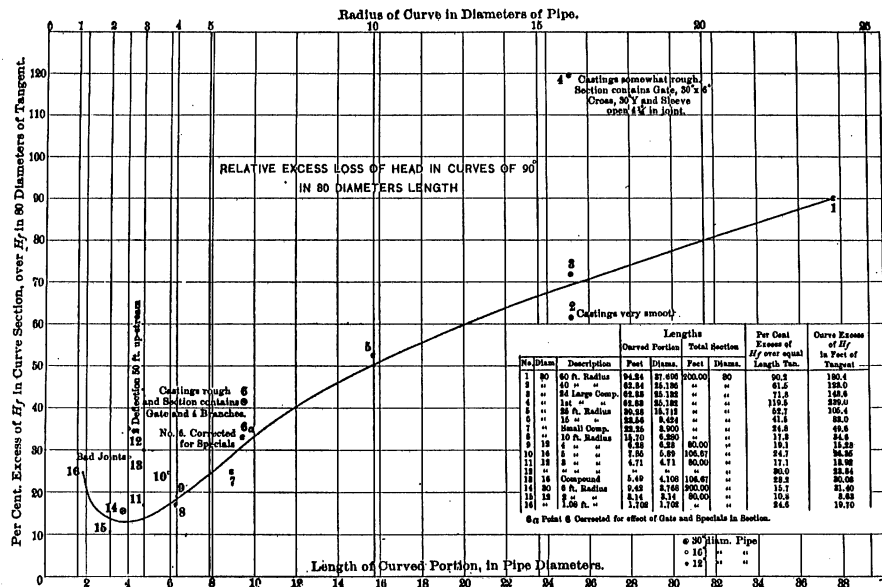


Fig. 1—Relation Excess Loss of Head in Curves of 90° in 80 Diameters Length

## Abstract 32

Wirt, Loring, "New Data for the Design of Elbows in Duct Systems," GENERAL ELECTRIC REVIEW, Vol. 30, pp. 286-296, June, 1927, 19 figs.

Data pertaining to experiments on the pressure loss of elbows and flow patterns within elbows, and the effect of vanes on the pressure loss and velocity in bends are given in this article. The elbows were installed immediately following a rounded duct entrance and, in some cases, were followed by a length of duct about 4 diameters long. The pressure loss was taken as the difference between the orifice pressure before and after the elbow was installed and was given as a percentage of the velocity head. Using air as the flowing fluid, the measurements included the pressure loss for elbows of square cross section and of various radius ratios. The results are shown in Fig. 1. For elbows of varying aspect ratios, the pressure loss decreased with increasing aspect ratio (the ratio of width normal to the plane of the bend to the width in the plane of the bend), particularly for small radius ratios. The results of the tests of elbows of various aspect ratios are shown in Fig. 2.

In an attempt to delineate the flow pattern within the elbow, flow casts were made as follows: the interior walls were painted with a mixture of lamp black and oil; the air was then allowed to flow through the bend, creating streaks in the mixture in the direction of the streamlines near the boundary; after the air was stopped, the model bend was filled with plaster of Paris which, when it hardened, absorbed the lines. Removal of the cast resulted in a record of the flow pattern for the particular flow. Flow casts for various elbows are shown in Fig. 3, with Fig. 3(a) showing the flow pattern for an elbow with vanes, a square or miter bend, and a circular bend. The development of the spiral flow characteristic of bends is most clearly shown in the circular bend, while the spiral flow in the square bend is obscured by the separation which took place in the corner. The effect of guide vanes on the flow is clearly shown in the photograph to the left in Fig. 3(a). Flow patterns for other types of elbows are shown in Figs. 3(b) and 3(c).

Vanes in the corner greatly improved the flow and reduced individual pressure losses to approximately 20 per cent of the local velocity head. The results of the tests indicated that plate vanes bent as arcs of a circle are not very sensitive to slight variations in shape. Bends with other degrees of curvature gave similar reductions when vanes were installed.

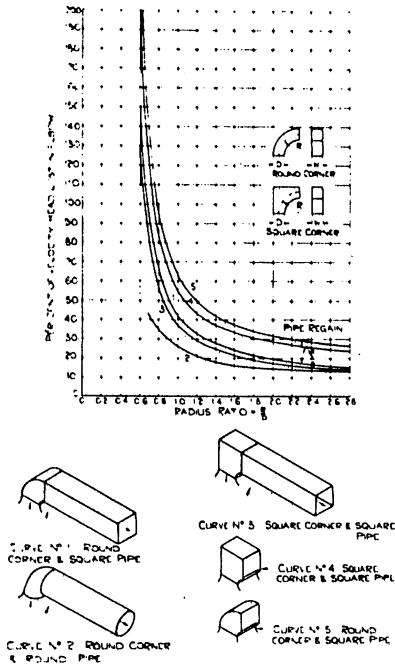


Fig. 1—Effect of Radius Ratio on the Loss

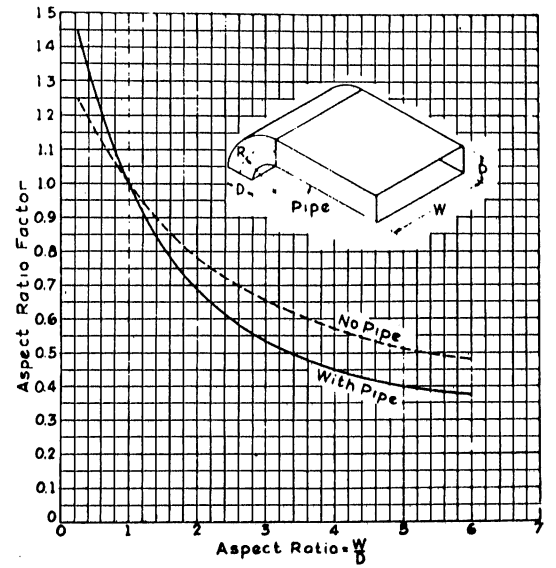


Fig. 2—Aspect Ratio Factor

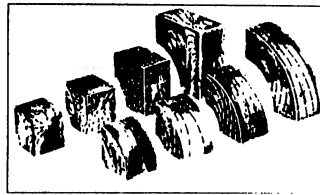
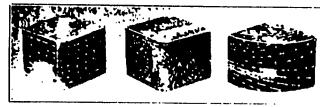


Fig. 3—Flow Casts for Various Elbows

## Abstract 33

Yarnell, David L., FLOW OF WATER THROUGH 6-INCH PIPE BENDS, Technical Bulletin No. 577, U. S. Dept. of Agriculture, October, 1937, 117 pp., 103 figs., 2 plates.

This report presents and discusses the results of measurements of velocity distribution, pressure changes, and the loss of head in 6-in. pipe bends and their approach tangents. The bends tested included bends of  $45^\circ$ ,  $90^\circ$ ,  $180^\circ$  continuous curvature,  $180^\circ$  reverse curve,  $270^\circ$  with two reversals of curvature, three  $90^\circ$  special shape bends, and a  $90^\circ$  miter bend. All bends were constructed of transparent celluloid, 6 inches in diameter and circular in cross section at the ends. The radius of curvature of the standard bend was  $8 \frac{1}{4}$  inches. One of the  $90^\circ$  special shape bends, type M, gradually changed to an oval section at midlength with a major axis of 9.87 in. and a minor axis of 6 inches. In the plane of the bend, the inner and outer boundary curves were hyperbolas. Another, type N, had a constant curvature radius of 15 inches. The cross section gradually changed to elliptical at midlength, with a major axis of 10 in. and a minor axis of 3.60 in., maintaining a constant cross-sectional area. The third, type W, was of circular cross section throughout, but increased to approximately 7 inches in diameter at midlength. The radius of curvature decreased from infinity at the point of tangency to 5 in. at midlength.

Velocity traverses and pressure determinations were made on cross sections at  $22 \frac{1}{2}^\circ$  intervals around the bend and at several cross sections of the upstream and downstream tangents. Head loss determinations were made at velocities from 2 to 14 ft per sec for uniform velocity distributions in the approach tangent. Effect of changes in upstream velocity distribution was studied by means of velocity traverses in each cross section for mean velocities of 5.8 and 12 ft per sec.

Velocity distribution and peripheral pressures in the bends were measured for all bends tested and are shown in a set of 63 figures. Pressures along the inner side and outer side of the bends and loss of head in the bends are given in a set of 17 figures. Figures 1, 2, 3, and 4, reproduced here, show the results for a standard bend and for a  $180^\circ$  continuous curvature bend.

With a uniform velocity distribution in the approach tangent, the loss of head caused by the bend increased for about 5 ft downstream from the

bend. The end of this zone of increase is at the section at which the energy gradient for the bend becomes parallel to the energy gradient for straight pipe.

The loss of head in the pipe bends is expressed by  $H_b = K' \frac{v^2}{2g}$ , where  $H_b$  is the loss of head in the bend, exclusive of friction,  $K'$  is a constant including size of pipe and radius of curvature of the bend, and  $v^2/2g$  is the velocity head in the approach tangent.

The values of  $K'$  as measured and the ratios of the loss of head caused by other round pipe bends to that caused by the standard  $90^\circ$  bend,  $K'/K'(90^\circ)$ , are listed in the following table.

TABLE I  
Results of Experiments

Type of Bend	$K'$	$K'/K'(90^\circ)$
$45^\circ$	0.11	0.75
$90^\circ$ , standard	0.15	
$180^\circ$ , continuous curvature	0.19	1.25
$180^\circ$ , reversed curvature	0.31	2.1
$270^\circ$	0.40	2.7
Type M	0.15	
Type N	0.13	
Type W	0.17	
Miter	1.17	7.8

The following conclusions were reached as a result of the study:

1. All bends act as obstructions to flow, causing greater loss of head than an equal length of straight pipe.
2. The velocities of the filaments along the inner side of the bend are increased and those along the outer side are decreased from their velocities in the tangent approaching the bend.
3. The loss of head increases with increase in length of the bend for pipe of equal size, equal radius of curvature, and like

material and condition, and is greatest in a bend in which the tangents are joined or mitered without an intervening curved section.

4. For a given bend and given quantity of flow, the head loss in the bend is influenced by the velocity distribution in the approach tangent. With velocity in the approach tangent high toward the inner side, the losses of head shown by all the bends ranged from about 1.5 to 4 times that obtained when uniform velocity prevailed in the approach tangent. With the approach velocity high toward the outer side, some bends showed slightly less and some slightly greater losses than obtained with uniform velocity of approach. With high velocity at the top of the approach tangent, the loss for each bend was between 1.25 and 2 times that obtained with uniform approach velocity, and with approach velocity high at the bottom the loss was between 1.3 and 3 times that obtained with uniform velocity. These ratios were obtained with a high velocity along one side of the approach tangent about three times the low velocity along the other side.

5. From the difference between the pressures on the inner and outer sides of a bend at the point of maximum differences, and with the size of pipe and radius of curvature of the bend, it is possible to compute the mean velocity and therefore the quantity of flow. When a pipe bend has been calibrated it may be used as a flow meter with which the discharge can be determined by measuring merely the difference in pressure.

6. The losses in the pipe bends experimented upon appear to vary as the square of the velocity.

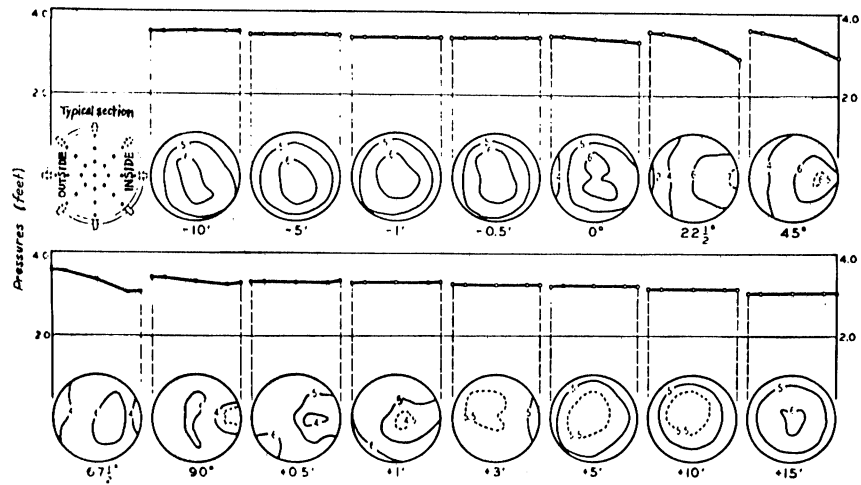


Fig.1-Velocity Distribution and Peripheral Pressures in Standard Bend; Mean Velocity, 5 ft per sec

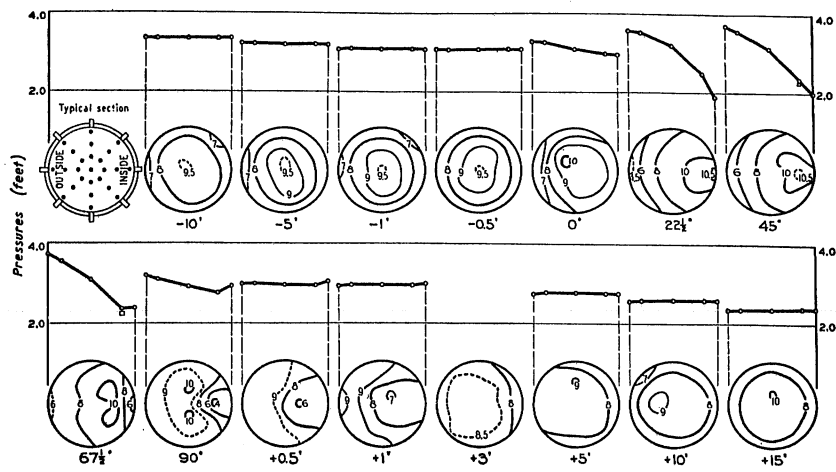


Fig.2-Velocity Distribution and Peripheral Pressures in Standard Bend; Mean Velocity, 8 ft per sec

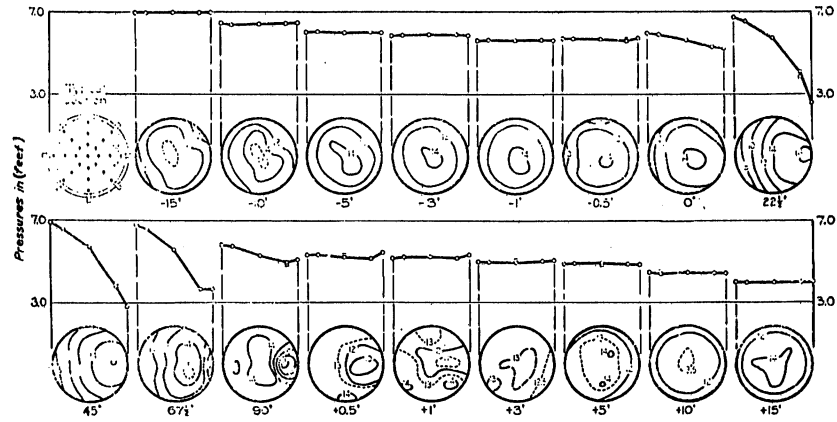


Fig. 3—Velocity Distribution and Peripheral Pressure in Standard Bend; Mean Velocity, 12 ft per sec

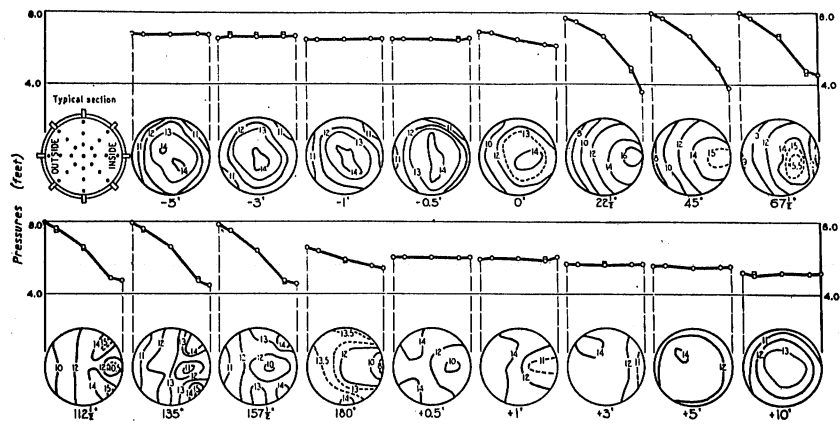


Fig. 4—Velocity Distribution and Peripheral Pressures in 180° Bend of Continuous Curvature; Mean Velocity, 12.1 ft per sec

## Abstract 34

Yarnell, D. L., and Woodward, S. M., FLOW OF WATER AROUND 180-DEGREE BENDS, Technical Bulletin No. 526, U. S. Dept. of Agriculture, October, 1936, 64 pages, 48 figs.

The distribution of pressure and velocity of water flowing through a 180° bend of rectangular cross section were measured for conditions of uniform velocity distribution in the approach conduit. Three 180° bends were studied, one 10 in. square with a 5-in. inner radius, one 10 in. deep and 5 in. wide in the plane of the bend with a 10-in. inner radius, and one 10 in. deep and 5 in. wide with a 5-in. inner radius. The straight approach section was 25 ft long and the discharge section 28 ft long. The pressures were measured piezometrically at numerous points along the bend and on the periphery of the cross section. Velocities were determined by a special Pitot tube that was introduced into the top of the bend through tubes of sufficient height to act also as piezometers.

The pressure and velocity distributions in the 10- by 10-in. bend for a discharge of 2.67 cu ft per sec are shown in Fig. 1. As the bend was approached, the speed of the water at the inner side was increased to a maximum at section 9 (67 1/2°). However, at the outer wall the water speed decreased to a minimum at section 9. After the water passed the halfway point of the bend, the maximum velocity gradually shifted toward the outer wall so that at section 13 (180°) it was substantially uniform. The low velocity at the center of the inner wall at sections 12, 13, 14, and 15 suggested a point of separation. Similar results were obtained for the other two conduits as shown in Figs. 2 and 3. The pressure distribution on the top of the conduit and the velocity at the several sections are shown as circles and crosses, respectively, above the sections.

When the approach velocity is higher on the inside of the approach tangent, the effect of the bend is to increase still further the difference in velocity at the inner and outer walls; if the approach velocity is greater near the outer wall, the bend tends to make the velocity distribution more uniform.

The pressure distribution on the periphery of the cross sections for the 10- by 10-in. conduit at the bend and at various discharges is shown in Fig. 4. The variation in pressure along the radius of the bend for various sections is also shown.

## Abstract 34, Yarnell and Woodward

The head loss resulting from the bend was determined by taking the difference of the hydraulic grade lines upstream and downstream of the bend. The average bend coefficient for the 10- by 10-in. channel whose  $R/d = 1.0$  was 0.36; for the 10- by 5-in. bend with 5-in. inner radius,  $R/d = 1.5$ , the average bend coefficient was 0.23; and for the 5- by 10-in. bend with 10-in. inner radius,  $R/d = 2.5$ , the average bend coefficient was 0.12.

During the course of the experiments the secondary currents were observed by the use of yarns attached to a rod that could be shifted to different verticals through the cross section.

Experiments were also performed with the conduit as an open channel. The qualitative results were similar to those of the closed conduit, except that the free surface had a transverse slope.

The report presents a derivation of an equation for the difference in elevation of the water surface between two sides of an open channel in the form  $\Delta H = (v^2 b / gR)$ , where  $v$  is the mean velocity,  $b$  is the width of channel,  $R$  is the radius at center of channel, and  $g$  is the acceleration of gravity.

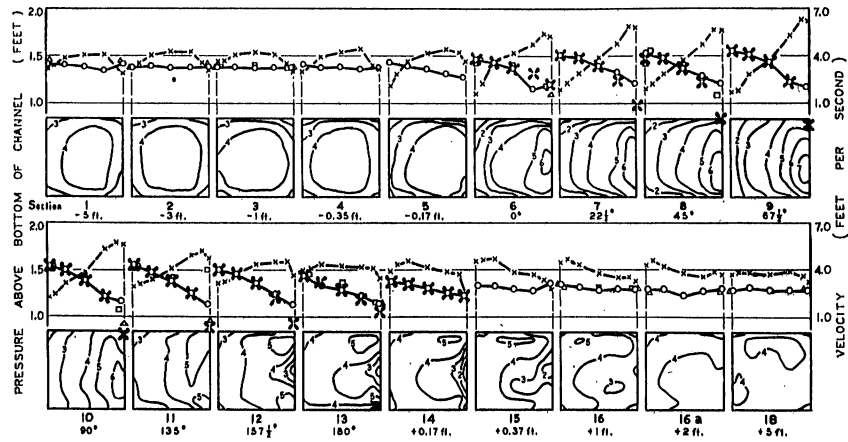


Fig.1—Velocity Distribution in 10- by 10-in. Channel Flowing Full; Discharge 2.67 cu ft per sec, Inner Radius of Bend 5 in.

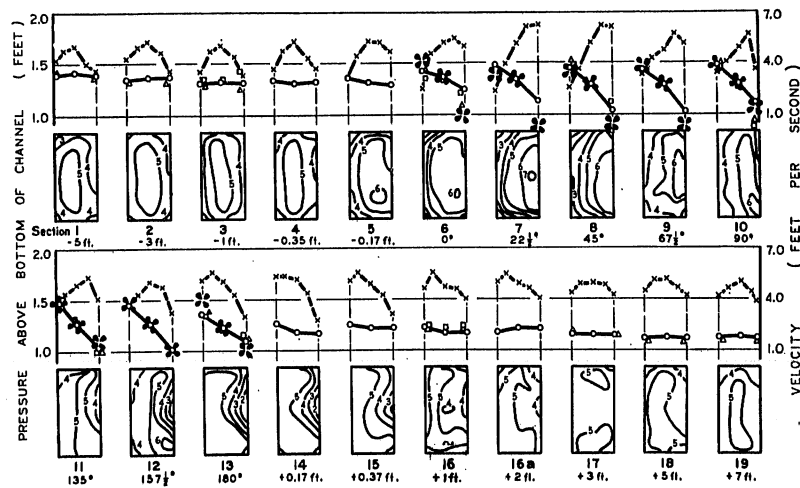


Fig.2—Velocity Distribution in 5- by 10-in. Channel Flowing Full; Discharge 1.71 cu ft per sec, Inner Radius of Bend 5 in.

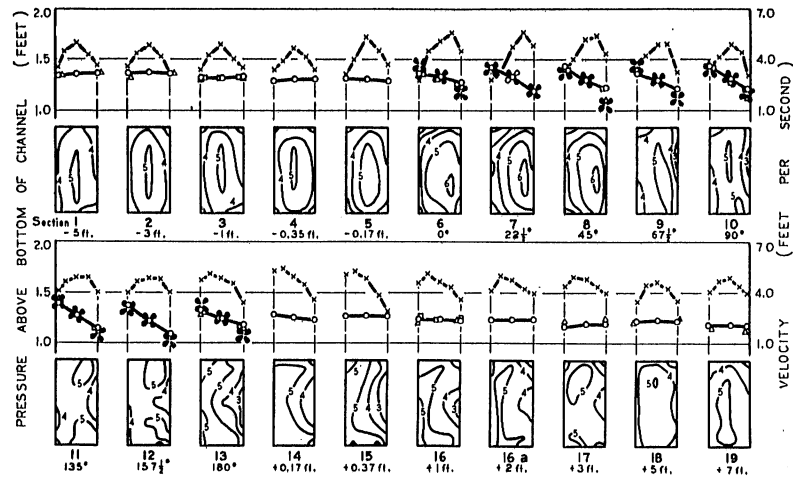


Fig. 3—Velocity Distribution in 5-by 10-in. Channel Flowing Full; Discharge 1.67 cu ft per sec, Inner Radius of Bend 10 in.

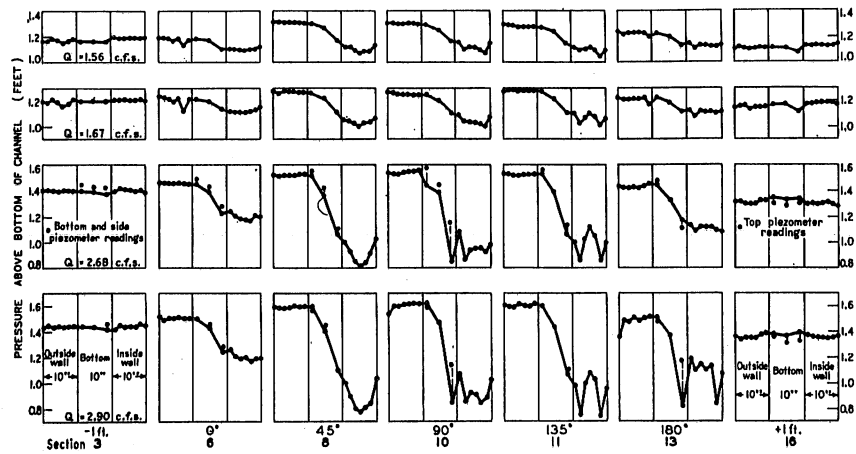


Fig. 4—Periphery Pressures in 10-by 10-in. Channel For Discharges from 1.56 to 2.9 cu ft per sec

## Abstract 35

Zur Nedden, F., "Induced Currents of Fluids," TRANSACTIONS OF THE AMERICAN SOCIETY OF CIVIL ENGINEERS, Vol. 80, Paper No. 1364, pp. 844-913, 1916, 36 figs.

This paper includes a discussion of transverse induced currents which the author states will occur wherever the direction of flow is altered. The most notable examples of this occur in bends and elbows. The discussion is based upon experimental data of various investigators on flow through bends.

Assuming potential flow through the bends, that is  $vr = \text{constant}$ , application of Bernoulli's theorem results in the pressure difference of the inside and outside walls of the bend of

$$\frac{\Delta P}{w} = \frac{v_i^2 - v_a^2}{2g}$$

where  $v_i$  = the velocity at the inside wall,

$v_a$  = the velocity at the outer wall, and

$\frac{\Delta P}{w}$  = the difference in pressure head.

The radius at which the mean velocity occurs is  $r_m$ .

$$r_m = \frac{d}{\log r_a/r_i}$$

where  $r_a$  and  $r_i$  are the radii of the outer and inner walls, respectively, and  $d$  is the duct diameter. On the basis of these equations, the author arrives at the relationship that, for a constant velocity, the total pressure difference between the outer and the inner walls and the maximum depression from the mean pressure depend only on the degree of curvature,  $R/d$ , where  $R$  is the radius of the centerline and  $d$  is the diameter of the conduit.

In a bend, the particles in the center will develop the greatest centrifugal force, or will have the greatest inertia to keep flowing in the same direction. They will dislodge the particles in their way which, in turn, must find a way to flow toward the center of curvature. Thus, by following a curved path of smaller radius, these particles gain in centrifugal force and flow again toward the outside of the bend. The path of any single particle is approximately spiral; that is, it is the resultant of the main flow and the transverse induced flow. The pressure varies in accordance with

the velocity. Figure 1 is a diagram based upon experimental results of von Cordier. It shows the area of high pressure near the outside of the bend and the area of minimum pressure on the inside just downstream of the bend.

The experiments of Lell on flow through a  $180^\circ$  rectangular bend revealed the formation of two symmetric induced currents. It was found that the induced currents originate in the strata near the upper and lower boundaries of the bend and gradually increase in volume and intensity as the main current flows forward. Near the upper boundary the friction along the outer and inner wall can be disregarded. Figures 3 and 4 are diagrams of the relative values of the energy terms for the flow near the upper boundary for straight and curved ducts. For the straight duct the energy lines B-B, C-C, D-D, and the resultant E-E are level, since all the particles travel with uniform speed. As the water enters the bend the velocities change, increasing at the inner wall and decreasing near the outer wall, while that at the so-called neutral vein remains constant. The elevations of the various energy terms change accordingly on both sides of the neutral vein, where the elevation will remain the same as for the straight pipe. Since the wall friction increases with the velocity, it will be greater near the inner wall. The resultant of the energy terms is now such that energy near the inner is less than that near the outer wall. On this basis the author points out that the fluid near the upper boundary, and similarly on the lower boundary, will flow inward toward the center of curvature. As the transverse flow progresses, the layer near the upper and lower boundaries in which it occurs grows in thickness.

The excess loss of head observed in the bends is the outcome of (1) the loss of head caused by the impact of the induced currents at the center of the inner wall, (2) the separation at the inner wall of the bend, and (3) the acceleration and retardation of the particles in traversing the bend.

On the basis of an analysis of experiments on the head loss in bends, the author arrives at the following general conclusions:

1. The disturbance caused by a bend extends a long way (up to 80 diameters and more) downstream.

## Abstract 35, Zur Nedden

2. The excess losses caused by the curvature of right-angled elbows are mainly influenced by the ratio between the radius of curvature and the width.

3. The roughness of the pipe apparently has no pronounced influence on the magnitude of these losses.

4. The relative values of the velocities prevailing in various concentric layers of a bend are, in fair approximation, inversely proportional to the respective radii.

Figure 2 is a chart of the excess loss caused by bends as deduced by the experiments of various investigators.

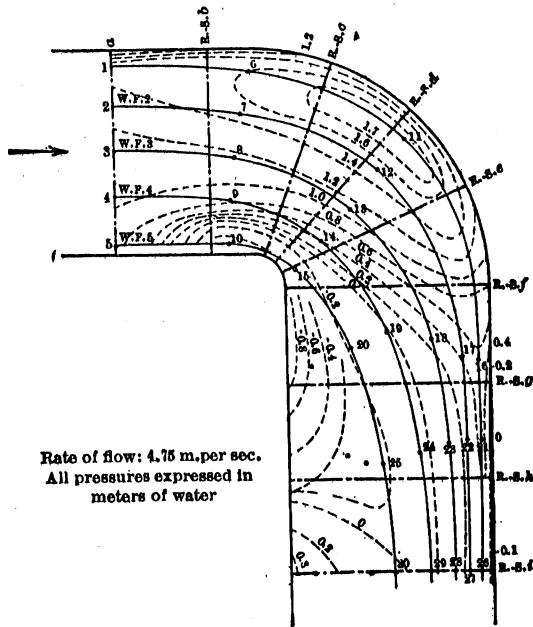


Fig. 1—Curves of Equal Pressure in Sharp Bend of Rectangular Cross Section (According to Von Cordier's Tests)

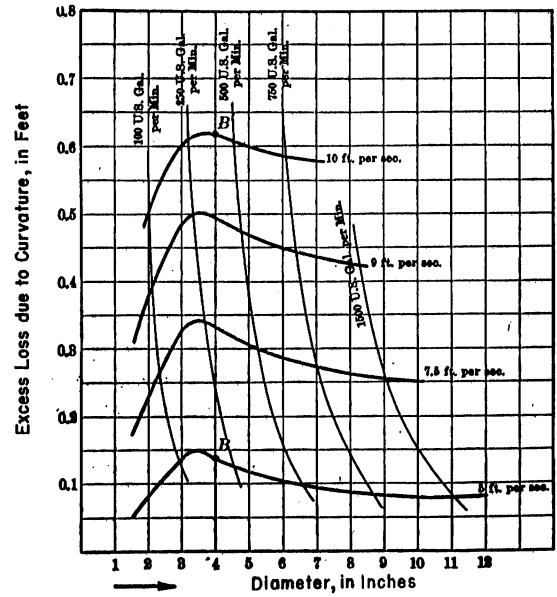


Fig. 2—Excess Loss Due to Bends. American Standard Long Turn Elbows (1912)

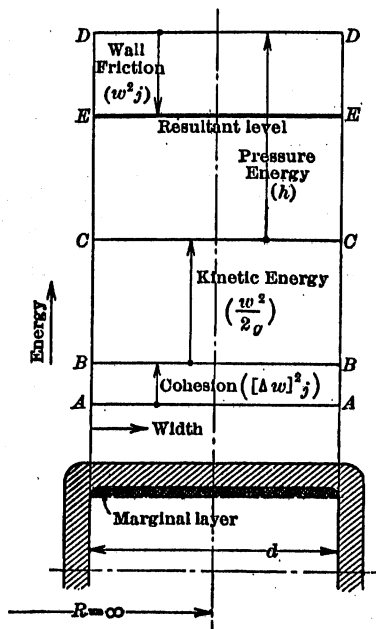


Fig. 3—Energy Diagram of Marginal Layer in Straight Duct

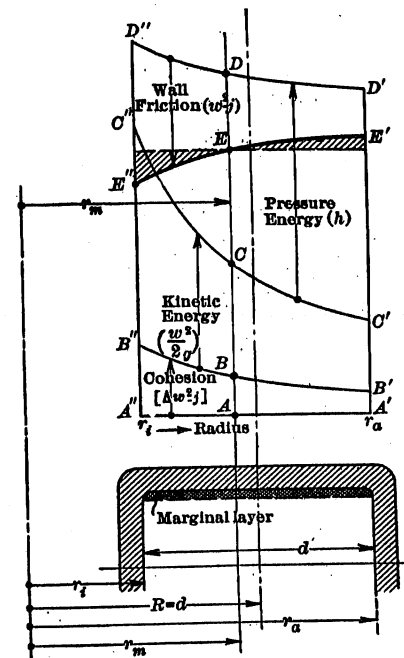


Fig. 4—Energy Diagram of Marginal Layer in Bend  $\frac{R}{d} = 1$

## Abstract 36

Collar, A. R., "Some Experiments with Cascades of Aerofoils," TECHNICAL REPORT OF THE AERONAUTICAL RESEARCH COMMITTEE, R. & M. 1768, Vol. II, pp. 1281-1287, 1937, 5 figs.

Experiments were performed on cascades of airfoils to determine the most suitable section for a proposed wind tunnel. The shape and dimensions of the airfoils used in the experiments are given in Figs. 1, 2, 3, and 4. Section A involves an area constriction at the turn of about 12 per cent. Section B was drawn from geometrical considerations to prevent the constriction. Both surfaces are circular arcs of  $90^\circ$ . The concave surface of one vane and the convex surface of the next vane have the same center of curvature. The remainder of the vane consists of two planes tangent to both the concave and convex surfaces. In practice the leading and trailing edges had finite thicknesses (Fig. 3). Section C was obtained from section B by rounding off the leading edge. The chord of sections A and B was about 2 inches. In all cases the spacing was 1 inch. Sections D and E (Fig. 5) were modifications of section B to provide for an expansion ratio at the corner of 1.2. The concave face was offset to provide a thicker tail.

The cascades were installed in a corner with the chord at  $45^\circ$  to the incident stream, and velocity distribution, angle of deflection, and resistance were measured. The relative resistance,  $r$ , was the ratio of the change of total head through the cascade to the total head downstream of the cascade. The total head was used since the static pressure downstream of the cascades was very nearly atmospheric. The results of observations at air velocities from 50 ft per sec to 190 ft per sec are tabulated in Table I. Section A improved with speed; the deflection increased to approximately  $90^\circ$  and the relative pressure loss fell rapidly to 0.11. Sections B and C both showed a decreased deflection angle as the speed increased. The relative pressure loss of section C, however, is only about half as large as that of sections A and B.

Experiments were performed in which the airfoils of section C were interlaced with horizontal steel strips of 1 1/2-in. chord and spaced 1-in. apart to form a honeycomb. The performance was quite satisfactory. The mean deflection angle was  $89.8^\circ$  and the mean speed was 47.5 ft per sec. The flow around the suction surfaces of the airfoils was not as steady as it was for the plain airfoils, and the relative resistance increased to 0.19.

## Abstract 36, Collar

Sections B, D, and E were installed in the corner with a 20 per cent expansion. With a cascade of vanes composed of section B, the deflection in the central section varied from  $89.7^\circ$  to  $90.5^\circ$ , with a mean value of  $90.1^\circ$ . There was a considerable separation from the suction surface of the vanes in the expanding duct as compared to the vanes in the non-expanding duct, and the relative pressure loss was 0.19. Both sections D and E caused an over-deflection of the air at the corner,  $96.0^\circ$  in the central portion for section D and  $94.2^\circ$  for section E. There was no appreciable increase in steadiness, and the relative pressure loss was 0.23.

The author concluded that, of the five sections tested, section C gave the most consistent deflection of nearly  $90^\circ$  over the range of Reynolds number used and had much less loss of pressure. An expansion of 20 per cent was considered too large because there was too much separation from the suction surface, with resulting unsteadiness of flow and increased relative pressure loss. The author also thought that, in those cases where structural considerations required support along the vane span, the cascade could also perform the duties of a honeycomb if flat ties were used at intervals along the span.

TABLE I  
Effect of Vane Shape on Deflection Angle and Pressure Loss

$V_T$ (approx.)	50	100	150	190
Reynolds No. (approx.)	$5 \times 10^4$	$9 \times 10^4$	$14 \times 10^4$	$18 \times 10^4$
Section A $\psi$ (deg.)	82.1	88.5	90.8	90.0
r	0.36 <sub>5</sub>	0.16 <sub>5</sub>	0.12	0.11
Section B $\psi$	91.1	89.9	89.0	88.7
r	0.13 <sub>5</sub>	0.11	0.10	0.09
Section C $\psi$	90.4	89.0	88.7	88.6
r	0.10 <sub>5</sub>	0.07	0.06	0.05

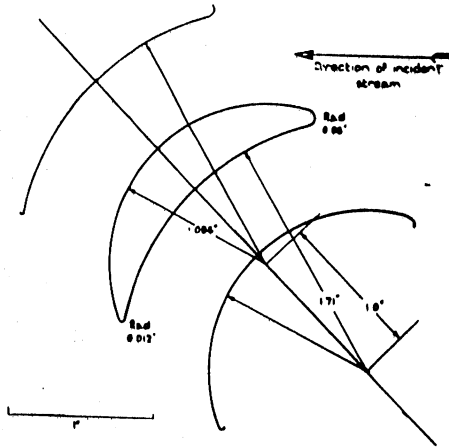


Fig. 1 - Profile of Section A.

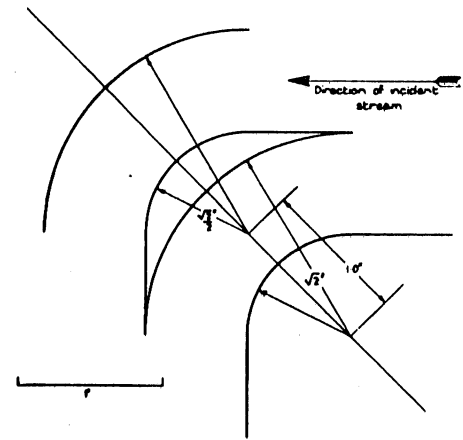


Fig. 2 - Profile of Section B. Geometrical Airfoil

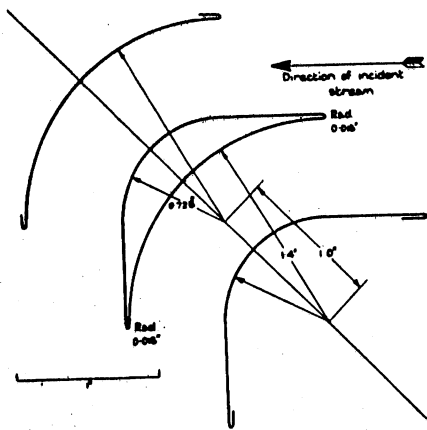


Fig. 3 - Profile of Section B. Practical Airfoil

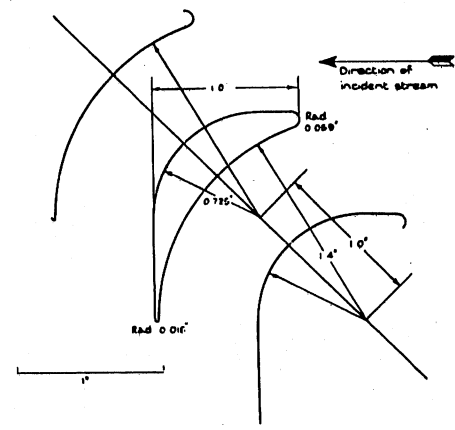


Fig. 4 - Profile of Section C.

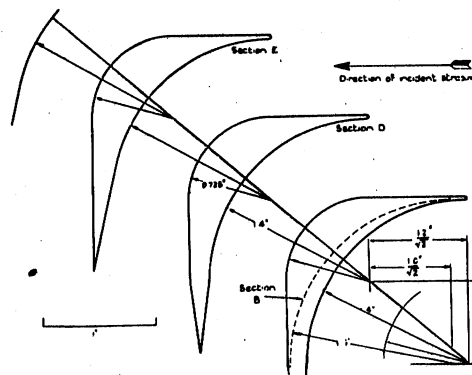


Fig. 5 - Profile of Sections D and E.

## Abstract 37

Collar, A. R., "Cascade Theory and the Design of Fan Straighteners," TECHNICAL REPORT OF THE AERONAUTICAL RESEARCH COMMITTEE, R. & M. 1885, 1940, 16 pp., 7 figs., 1 table.

Since an annulus of a ring of straighteners can be developed into an infinite two-dimensional cascade of airfoils, the investigations of the properties of cascades may be applied to the design of fan straighteners, the purpose of which is to remove the rotation from the slipstream of an air fan or blower. Part of such an infinite cascade of cambered and staggered airfoils is shown in Fig. 1. The chords  $c$  make an angle  $\sigma$  with the normal to the cascade. The direction of inflow at  $x = -\infty$  makes an angle  $\alpha_1$  with the x-axis, and the direction of outflow at  $x = +\infty$  makes a corresponding angle  $\alpha_2$ . The vector mean of the two velocities makes an angle  $\alpha_m$  with the x-axis and an angle  $\alpha$  with the chord of the airfoils.

The component of velocity  $U$  normal to the cascade is by continuity the same at  $x = \pm\infty$ , and the mass flowing through unit depth of the cascade is then  $\rho sU$  per airfoil, where  $\rho$  is the fluid density and  $s$  is the foil spacing. The rate of change of momentum parallel to the cascade is then  $\rho sU^2 (\tan \alpha_1 - \tan \alpha_2)$  and is thus the force on each airfoil in the positive direction of  $y$ . If  $C_{LC}$  is the lift coefficient for the airfoil in cascade, the force normal to the main flow is  $1/2 \rho c (U \sec \alpha_m)^2 C_{LC}$  so that the force parallel to the y-axis is  $1/2 \rho c U^2 \sec \alpha_m C_{LC}$ . Equating the two expressions for the force

$$C_{LC} = 2 \left(\frac{s}{c}\right) \cos \alpha_m (\tan \alpha_1 - \tan \alpha_2) \quad (1)$$

and, by definition of  $\alpha_m$ ,

$$2 \tan \alpha_m = \tan \alpha_1 + \tan \alpha_2 \quad (2)$$

If, for the range of  $\alpha_m$  considered, the curve of the lift coefficient versus angle of attack for an isolated airfoil of the type considered is linear and has a slope  $a_0$ , the lift coefficient for the single airfoil would be

$$C_{LF} = a_0 (\alpha_m - \sigma - \mu) \quad (3)$$

## Abstract 37, Collar

where  $\mu$  is the no-lift angle of attack, and  $\sigma$  is the angle between the chord and the normal to the axis of the cascade. Owing to the presence of other airfoils in the cascade, the lift coefficient for each airfoil is  $C_{LC}$ , therefore  $C_{LC} = fC_{LF}$  where  $f$  is the lift factor depending upon the spacing of the vanes in the cascade. It approaches zero as  $s/c$  approaches zero, and approaches unity as  $s/c$  becomes infinitely large. Therefore,

$$C_{LC} = fa_o (\alpha_m - \sigma - \mu) \quad (4)$$

The elimination of  $C_{LC}$  and  $\alpha_m$  from equations (1), (2), and (4) results, for small angles, in

$$4 \left(\frac{s}{c}\right) (\alpha_1 - \alpha_2) = fa_o (\alpha_1 + \alpha_2 - 2\sigma - 2\mu) \quad (5)$$

or

$$(p + 1) \alpha_2 = (p - 1) \alpha_1 + 2(\sigma + \mu) \quad (6)$$

where

$$p = \frac{4}{fa_o} \left(\frac{s}{c}\right) \quad (7)$$

The condition essential to straighteners is that  $\alpha_2 = 0$  for all values of  $\alpha_1$ . This can be satisfied if from equation (6)  $\sigma = -\mu$  and if  $p = 1$ . It is therefore necessary to determine a gap-chord ratio for a given setting  $\sigma = -\mu$  for which

$$f = \frac{4}{a_o} \left(\frac{s}{c}\right) \quad (8)$$

The linear portion of the lift curve resulting from experiments on an isolated airfoil, whose centerline was a circular arc, satisfied the equation

$$C_{LF} = 0.0925 (\alpha + 11.1) \quad (9)$$

from which  $C_{LF}$  can be determined for values of  $\alpha = (\alpha_m - \sigma)$  corresponding to  $C_{LC}$  as determined from experiments on a similar airfoil in cascade and from which the lift factor  $f$  can be determined.

## Abstract 37, Collar

Figure 2 is a plot of the lift factor  $\underline{f}$  in terms of  $s/c$  based upon experiment by Harris and Fairthorne [132] and includes equation (8) where  $a_0$  is the rate of increase of lift coefficient per radian determined from equation (9). Equation (8) takes the form

$$f = 0.755 \left(\frac{s}{c}\right) \quad (10)$$

The intersection of the straight line with the curves defines the value of  $s/c$  for which  $p = 1$  in equation (6). It appears that for  $\sigma = 0$ , the corresponding  $s/c$  would be close to 1.0 and  $\alpha_2$  would be independent of  $\alpha_1$ .

For fan straighteners, the subject of the paper, a symmetrical airfoil section was set radially with its chord parallel to the fan axis and had a gap-chord ratio equal to unity. For this arrangement, the chord of the airfoil is proportional to the radius. The paper also gives theoretical development of these experiments results on the basis of a conformal transformation of known flows.

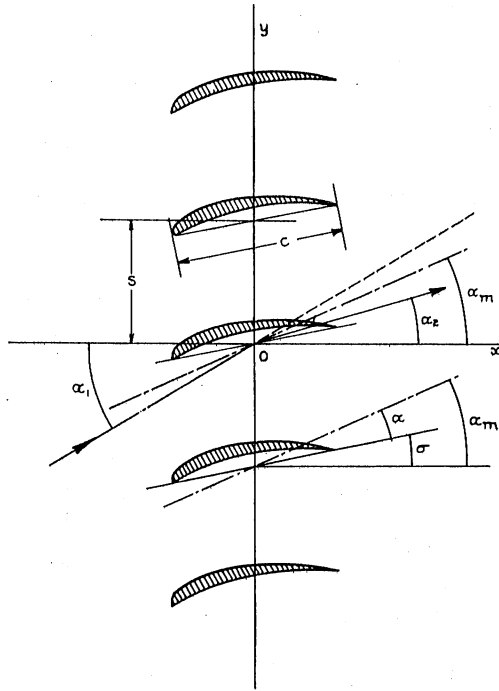


Fig.1—Airfoils Arranged in a Cascade

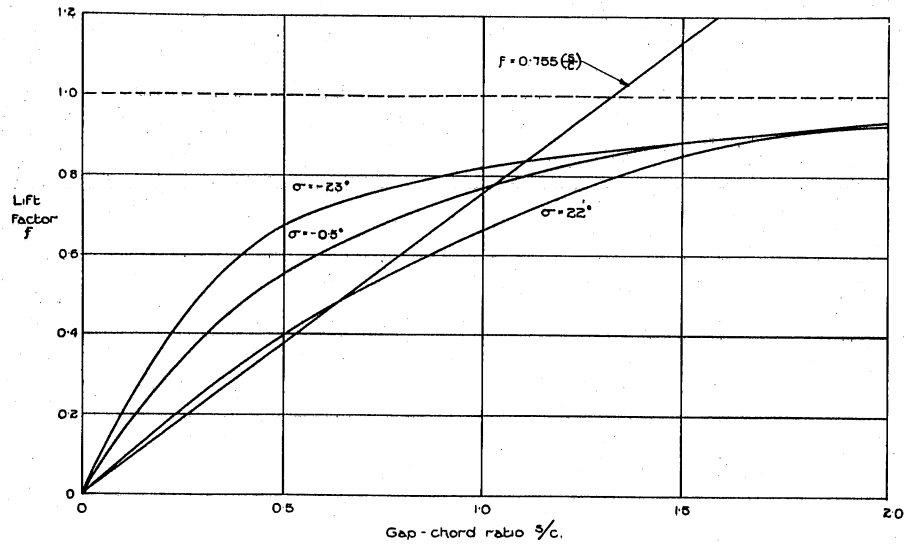


Fig.2—Relation of Lift Factor,  $f$ , to Gap-chord Ratio

## Abstract 38

Frey, Kurt, "Verminderung des Strömungs Widerstandes von Körpern Durch Leitflächen" (The Reduction of Flow Resistance of Bodies by Means of Guide Vanes), FORSCHUNG AUF DEM GEBIETE DES INGENIEURWESENS, Vol. 4, pp. 67-74, March/April, 1933, 21 figs.

This report describes experiments on the effect of judiciously placed guide vanes in reducing the resistance of blunt bodies. The experiments are restricted to plane flow about bodies without guide vanes, with "divided" guide vanes (cascades), and with "undivided" guide vanes. "Undivided" guide vanes are those arranged single or in multiples in the manner of splitters to direct the flow completely around the corner. "Divided" guide vanes are short vanes disposed in cascades in a manner somewhat similar to slotted wings.

The principal purpose of the experiments was to study the effect of cascades on the reduction of resistance and the sensitiveness of cascades to changes in arrangement, to changes in flow direction, and to discontinuities along the span as compared to undivided vanes.

Divided guide vanes used with bodies with a blunt nose and sharp or moderately round edges reduced the eddy resistance an average of 85 per cent. Cascades used at the downstream end of bodies with a blunt tail reduced the resistance about 70 per cent. The resistance of blunt bodies fitted with divided guide vanes was in general from 60 to 100 per cent higher than that of a comparable suitably shaped streamlined body without guide vanes. The same bodies without guide vanes, however, produced frontal resistances from 340 to 800 per cent higher and end resistances from 200 to 260 per cent higher than those produced by the streamlined body.

According to the experiments, the divided or cascaded vanes had a slightly lower resistance to flow than the corresponding undivided guide vanes. Of great importance was the fact that the resistance coefficients were much less sensitive to inaccurately chosen settings or changes in flow direction. Span discontinuities as well as greater roughness caused only slight increases in the resistance coefficients and their effect decreased as the Reynolds number increased.

## Abstract 39

Frey, Kurt, "Verminderung des Strömungsverlustes in Kanälen durch Leitflächen" (The Reduction of Flow Losses in Canals by Means of Guide Vanes). FORSCHUNG AUF DEM GEBIETE DES INGENIEURWESENS, Vol. 5, pp. 105-117, May/June, 1934, 26 figs., 24 tables.

This article describes experiments on the effectiveness of irregularly spaced guide vanes (Frey vanes) in reducing the flow losses in bends. The paper describes the experiments, discusses the results, and recommends guide vane arrangements in typical applications. The experiments were carried out in a wind tunnel. The flow losses were determined from the pressure drop across the model and presented in terms of coefficients,  $R = \zeta v^2/2g$ , where  $R$  is the energy loss between the points of measurement and  $\zeta$  is the corresponding loss coefficient.

Tests were made with and without guide vanes on  $90^\circ$  sharp bends of constant cross section. There was a 73 to 87 per cent decrease of energy loss in a bend with guide vanes over the loss in the same bend without guide vanes. Change of position of the vanes did not appreciably affect the losses and moderate changes in profile form caused no measurable increase in resistance. Comparative tests using the irregularly spaced (Frey) vanes and uniform corner cascades indicated that the reduction of flow losses in each case was similar. Each type of vane serves its particular purpose.

When a uniform distribution of velocity after a bend is essential, as in the case of a wind tunnel, the corner cascades or lattices are to be preferred. However, the irregularly spaced (Frey) vanes require less material and labor and are of simpler construction. They are also less likely to be damaged by foreign bodies carried by the stream. For  $180^\circ$  bends the loss is reduced approximately 82 to 85 per cent by the use of the guide vanes. Further experiments were carried out on diffusers.

Separation at the inner corner is the principal source of the loss for flow around sharp corners. The causes of flow separation in the case of a homogeneous fluid are:

1. Inability of the retarded boundary layer to advance under its own power into zones of higher pressure; the tendency toward separation of flow to increase with the magnitude of the pressure rise and with the boundary layer thickness at the place of minimum pressure.

2. Inertia effect in flow around sharp corners.
3. Lowering of fluid pressures to vaporization pressure (cavitation.)
4. For gases and vapors flowing at supersonic velocity strong separations occurring practically throughout when there are pressure increases along the walls as a result of compression waves and impulses.

The prevention of separation by the use of irregularly spaced (Frey) guide vanes follows from the causes of separation. Separation caused by boundary layer friction can be prevented by the installation of guide vanes to prevent sudden pressure increases from the relatively large quantity of boundary layer fluid present along the channel wall. The inertia effect can be overcome by the use of guide vanes to force the fluid around the corner. When there is danger of cavitation or when high flow velocities exist in the case of gases, excessively low pressures should be prevented at the channel walls as well as at the guide vanes.

## Abstract 40

Harris, R. G., and Fairthorne, R. A., "Wind Tunnel Experiments with Infinite Cascades of Aerofoils," TECHNICAL REPORT OF THE AERONAUTICAL RESEARCH COMMITTEE, R. & M. 1206, Vol. I, pp. 286-304, 1928-29, 11 pp. figs., 5 tables.

The object of the experiments was to provide data pertaining to the forces on the cascade blades and on the deflection of the stream caused by the cascade. The experiments were performed on a row of airfoils installed with the axis of the cascade at various angles to the tunnel axis. The measurement of deflection, total head, pressure, and air speed were made over a line in the plane of the center section covering a width of one gap. The airfoil used was disposed on a circular arc of 0.1 camber (i.e., an arc of  $45.2^\circ$ ) with the streamlining of an RAF 27-section superposed upon it. The dimensions of the airfoil are given in Table I.

In the tests the angle of the cascade axis to the tunnel axis, the angle of attack, and the spacing-chord ratio were varied. The arrangement of the cascade and a summary of the results are given in Table II.

TABLE I  
Aerofoil Dimensions in Terms of Unit Chord

Distance from leading edge	Distance above datum line	
	Upper surface	Lower surface
0	0	0
0.007	0.0176	-0.0056
0.029	0.0367	-0.0080
0.064	0.0585	-0.0051
0.113	0.0821	+0.0030
0.172	0.1042	0.0133
0.241	0.1227	0.0256
0.318	0.1368	0.0378
0.402	0.1441	0.0483
0.491	0.1444	0.0556
0.577	0.1367	0.0585
0.666	0.1223	0.0571
0.749	0.1021	0.0506
0.828	0.0770	0.0398
0.896	0.0507	0.0264
0.954	0.0251	0.0117
1.000	0	0

Radius at L.E. = 0.0075      Radius at T.E. = 0.0023

TABLE II  
Summary of Cascade Results

$\phi$	$\alpha$	s/c	U (ft/ sec)	$\epsilon$	$\frac{V}{U}$	$\frac{\Delta P}{\rho U^2}$	$\frac{\bar{\omega}}{\rho U^2}$	$\frac{k'_Q}{s/c}$	$\frac{k'_P}{s/c}$
35°	13°	1/2	57.6	24.3°	0.858	0.094	0.0346	0.410	0.118
45	23	1/2	58.7	35.7	0.755	0.188	0.0257	0.504	0.242
55	33	1/2	59.2	43.3	0.617	0.278	0.0295	0.590	0.338
35	13	1	57.5	22.2	0.859	0.118	0.0116	0.362	0.144
45	23	1	58.8	31.2	0.747	0.202	0.0147	0.408	0.228
55	33	1	58.8	32.6	0.630	0.192	0.101	0.330	0.234
35	13	1 1/2	58.6	20.0	0.867	0.116	0.0077	0.264	0.108
45	23	1 1/2	58.7	26.0	0.766	0.188	0.0136	0.328	0.194
55	33	1 1/2	58.3	20.8	0.674	+0.060	0.188	0.230	+0.158
12.5	13	1/2	58.7	29.9	1.054	-0.084	0.0251	0.536	-0.066
22.5	23	1/2	58.9	40.2	0.999	-0.024	0.0216	0.666	-0.002
32.5	33	1/2	58.7	47.7	0.907	+0.074	0.0178	0.720	+0.084
12.5	13	1	59.4	24.0	1.017	-0.032	0.0109	0.448	-0.020
22.5	23	1	58.5	34.7	0.979	+0.012	0.0105	0.540	+0.032
32.5	33	1	58.8	37.9	0.876	+0.090	0.0233	0.538	+0.120
12.5	13	1 1/2	59.3	21.0	1.010	-0.018	0.0074	0.362	-0.004
22.5	23	1 1/2	59.4	28.8	0.962	+0.028	0.0085	0.424	+0.052
+32.5	33	1 1/2	58.9	29.0	0.877	+0.028	0.096	0.374	+0.064
-10	13	1/2	58.6	28.9	1.269	-0.332	0.0314	0.704	-0.416
0	23	1/2	58.8	39.5	1.361	-0.458	0.0313	0.826	-0.422
+10	33	1/2	58.8	49.8	1.321	-0.414	0.0335	0.948	-0.394
-10	13	1	49.2	22.9	1.213	-0.258	0.0185	0.556	-0.264
0	23	1	49.0	33.2	1.210	-0.262	0.0190	0.708	-0.268
+10	33	1	49.0	40.0	1.186	-0.236	0.0269	0.846	-0.242
-10	13	1 1/2	39.2	19.0	1.168	-0.196	0.0140	0.440	-0.186
0	23	1 1/2	39.0	29.2	1.777	-0.208	0.0122	0.570	-0.194
+10	33	1 1/2	39.1	34.4	1.125	-0.168	0.0302	0.602	-0.126

$\phi$  = angle between the tunnel axis and the normal to the cascade axis,

$\alpha$  = angle of attack of the airfoil, the angle between the chord and the direction of the entering airstream,

s/c = spacing-chord ratio,  $s$  being the distance between airfoils, along the cascade axis and  $c$  the length of the airfoil chord,

U = velocity parallel to the tunnel axis upstream of the cascade,

V = velocity downstream of the cascade,

$\epsilon$  = the angle of deflection of the airstream caused by the cascade,

$\Delta P/\rho U^2 = (P_2 - P_1)/\rho U^2$  = pressure drop before and after the vanes;  $P_1$  being the pressure upstream and  $P_2$  the pressure downstream of the cascade,

$\bar{w}/\rho U^2$  = change in total head upstream and downstream of the cascade  
divided by the upstream velocity head,

$$\frac{k'_Q}{s/c} = \frac{1}{(\cot \epsilon + \tan \phi)} \quad \text{and}$$

$$\frac{k'_P}{s/c} = \left\{ \frac{1}{2} \left[ 1 - \frac{\cos \phi}{\cos (\phi - \epsilon)} \right]^2 \right\} - \frac{\bar{w}}{\rho U^2}$$

## Abstract 41

Klein, G. J., Tupper, K. F., and Green, J. J., "The Design of Corners in Fluid Channels," CANADIAN JOURNAL OF RESEARCH, Vol. 3, pp. 272-285, 1930, 24 figs.

An investigation of vane shapes, spacing, and setting was undertaken to establish the vane design for a 9-ft wind tunnel of the National Research Laboratory at Ottawa, Canada. A small wind tunnel, 18 in. by 36 in., incorporating a  $90^\circ$  corner was constructed so that it was capable of producing air velocities of 30 to 80 ft per sec, depending upon the resistance of the tested cascade of vanes in the corner.

The six vane shapes tested, all of which had a chord length of six inches, are shown in Fig. 1. Vanes 1 through 4 were constructed of 16 gauge sheet metal, and their shapes ranged from a  $90^\circ$  square corner to a  $90^\circ$  circular arc. Vane 5 was a thick section resembling the vanes employed in the Gottingen Tunnel. Vane 6 was a modification of a foreshortened RAF 30-section arranged along a circular arc, the thickest portion occurring approximately  $1/3$  chord length from the leading edge. One set of vanes was constructed similar to vane 4, with a  $1/16$ -in. chord, to study the nature of the scale effect.

Visual observations of the flow patterns were obtained by installing a thin metal sheet coated with lampblack and kerosene in a horizontal plane at the centerline just behind the vanes. Photographs of the resulting streak pattern of the plate showed that the presence of vanes eliminated the separation which occurred at the inner corner for flow without vanes. The presence of spacers between vanes at the centerline introduced inter-vane "swirls" manifested by transverse flow in the boundary layer as a result of pressure differentials set up in passing through the vanes.

The velocity distribution resulting from the use of vanes 1, 3, 4, and 5 at a spacing-chord ratio of 0.5 are shown in Fig. 2. The distribution pattern was similar for all vanes, but vanes 4 and 5 were somewhat superior since they produced a more uniform velocity distribution on the exit side of the tunnel. It was found that, as far as velocity distribution was concerned, better flow was obtained with the closer vane spacings.

Figure 3 shows the velocity distribution downstream of vane 5 for various angles of incidence. Zero incidence was taken as the position of the

Abstract 41, Klein, Tupper, and Green

vane when the chord is perpendicular to the plane of the corner. For a spacing-chord ratio of 0.375, observations were made at incidences of  $-4.0^\circ$ ,  $0^\circ$ ,  $+5^\circ$ , and  $+10^\circ$ . The velocity distribution remained uniform for the various angles of incidence, but evidence indicated that the change of incidence produced corresponding changes in direction of the emerging stream.

The resistance coefficient,  $\xi = \frac{\Delta P}{P \frac{V^2}{2}}$ , is defined as the ratio of

the drop in static pressure across the corner,  $\Delta P$ , to the upstream impact pressure,  $P(V^2/2)$ , and is taken as a measure of the resistance of the corner appurtenances. The pressure drop varied greatly with the spacing-chord ratio. Figure 4 shows that the resistance coefficient decreases from a high value at large spacing-chord ratios to a minimum value and then increases again as the vanes are placed still closer together. The pressure drop was a minimum for spacing-chord ratios in the region from 0.3 to 0.5. The spacing of the vanes was a critical factor in reducing the corner resistance. The effect of incidence of the vane had relatively less effect on the resistance than the spacing-chord ratio, as shown in Fig. 5.

For measuring the pressure distribution on the surface of the vane, piezometer holes and connecting tubes were installed in vane 5 and the pressures measured for vane incidences of  $0^\circ$ ,  $3^\circ$ , and  $6^\circ$ , and a spacing-chord ratio of 0.5. The pressure distribution for  $0^\circ$  incidence and a spacing-chord ratio of 0.5 are plotted in Fig. 6.

The research indicates that, in general, the thick and thin vanes have similar flow properties, a characteristic of considerable value where structural strength must be considered.

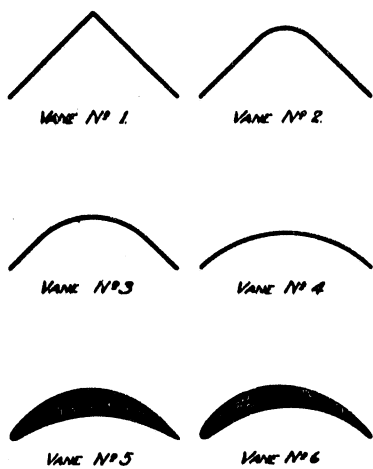


Fig. 1—Diagram of the Vane Sections Employed

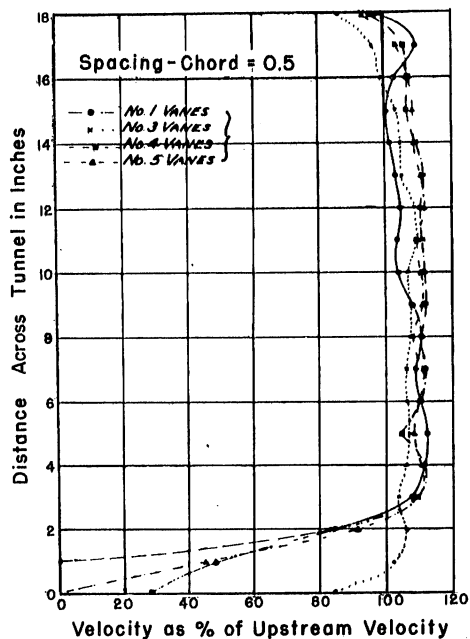


Fig. 2—Velocity Distribution Behind Vanes of Various Shape

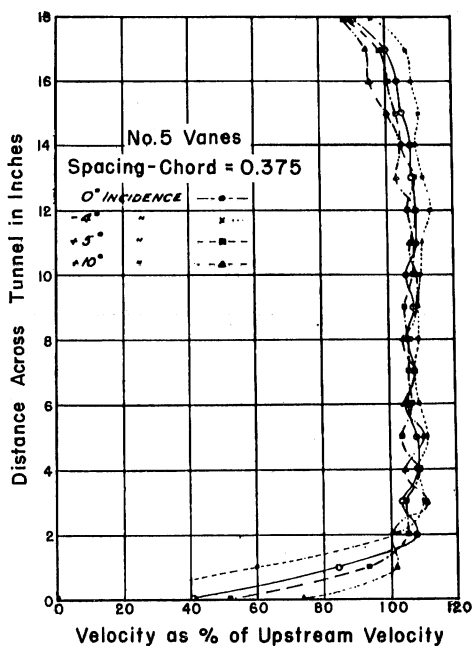


Fig. 3—Velocity Distribution Behind Vanes at Various Incidences

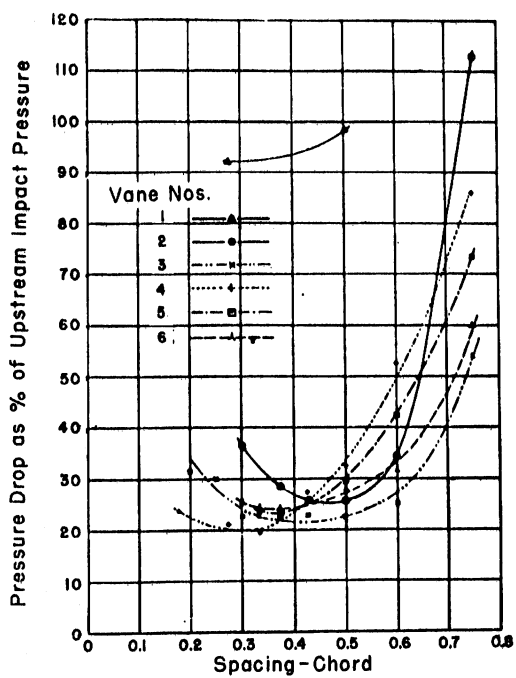


Fig. 4 - Corner Resistance Curves for all Vane Shapes

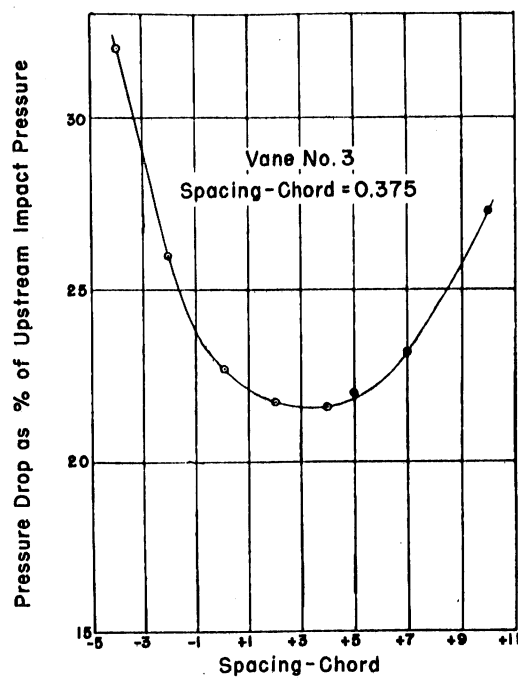


Fig. 5 - Variation of Corner Resistance with Incidence

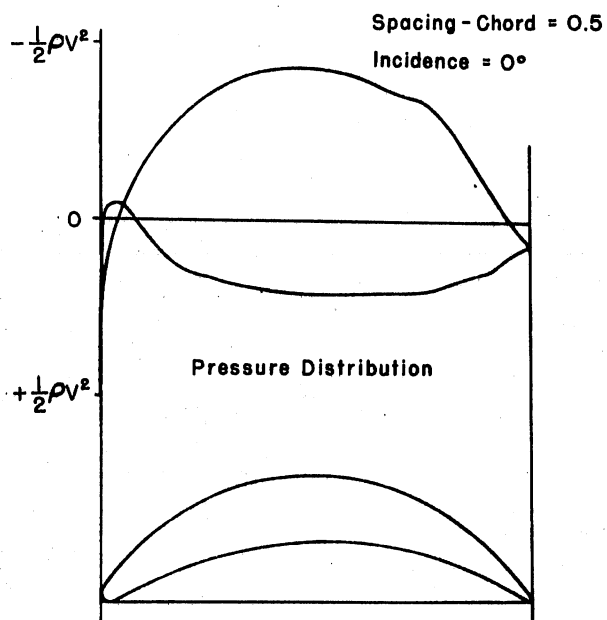


Fig. 6 - Pressure Distribution Curves for Vane 5

## Abstract 42

Kröber, G., "Guide Vanes for Deflecting Fluid Currents with Small Loss of Energy," *INGENIEUR ARCHIV*, Vol. III, pp. 516-541, 1932, trans. and pub. as Technical Memorandum No. 722, U. S. National Advisory Committee for Aeronautics, (n.d.), 43 pp., 42 figs.

The principal causes of large losses in bends with a small radius of curvature are the separation at the inside of the bend, the lost kinetic energy of the vortices of the secondary flow, and increased friction caused by uneven velocity distribution downstream of the bend. Vanes which divide the bend cross section into smaller parts serve to prevent separation and secondary flow and provide a more favorable  $R/d$  ratio (the ratio of the radius of curvature of the centerline of the bend to the width in the plane of the bend). The purpose of this paper was to describe a method by which a profile form with definite characteristics could be determined.

As a first approximation, the flow through the deflecting grid might be regarded as a potential flow consisting of a series of concentrated vortices equally spaced in the plane of the grid replacing the vanes and superposed upon a parallel planar flow perpendicular to the grid. The factor which determines the deflection of the fluid is the circulation about the vane. If the assumption is made that the circulation is concentrated at the center of pressure of the vane, the vane can be replaced by a vortex having its center coincident with the center of pressure and having a vortex strength equal to the circulation about the vane which it replaced. At a large distance before and after the grid, the velocity  $w_1$  approaching the grid has the components  $v_1$  and  $u_1$ , and the velocity  $w_2$  after the grid had the components  $v_2$  and  $u_2$ . The velocity components  $v_1$  and  $v_2$  are caused by the parallel flow only, and  $v_1 = v_2$  and the components  $u_1$  and  $u_2$  are caused by the vortex only, so that before and after the grid  $u_1 = -u_2$  (Fig. 1). The circulation,  $\Gamma$ , about a region enclosing one vortex whose width is  $s$ , the distance between vortices, and whose length,  $l$ , extends a great distance before and after the grid, is equal to the line integral of the velocity along the boundary, or

$$\Gamma = su_1 + \int_{-\frac{l}{2}}^{+\frac{l}{2}} v dl - su_2 + \int_{+\frac{l}{2}}^{-\frac{l}{2}} v dl$$

or

$$\Gamma = s(u_1 - u_2) = 2sw \sin \frac{\theta}{2}$$

where  $\theta$  is the deflection angle (Fig. 1), and  $w = /w_1/$  or  $/w_2/$ .

An airfoil moving in rectilinear flow is subjected to a "lift" of  $L = \rho U \Gamma' = C_a \frac{\rho}{2} U^2 t$ , where  $U$  is the velocity of the undisturbed flow,  $C_a$ , the lift coefficient,  $t$  the chord of the airfoil, and  $\rho$  the density of the flowing medium. The circulation about a vane is therefore  $\Gamma' = \frac{1}{2} C_a U t$ .

Since in the conformal transformation, between the plane of the vanes and the plane of the vortices, according to the method developed by Betz, the circulation remains constant  $\Gamma' = \Gamma$ , or

$$\frac{1}{2} C_a U t = 2 s w \sin \frac{\theta}{2} \text{ which, for a } 90^\circ \text{ deflection, is } \frac{1}{2} C_a U t = s w \sqrt{2}$$

The scale of coordinates in the  $z$  and  $\zeta$  planes were so chosen that  $U = w$  and the same coordinate systems are obtained in both planes at a great distance from the profile. In order that a minimum number of vanes be required and that the chord correspond somewhat to that of tested airfoils,  $C_a = 1.35$  was chosen for the lift coefficient, which is near the maximum for most airfoils.

The airfoil chosen for the transformation was that determined by Birnbaum (Hütte, Vol. 1, 26th edition, p. 401). The theoretical lift coefficient for this airfoil, shown in Fig. 2, is  $C_a = 2\pi \sin(\alpha + \beta - 1/2\gamma)$  and the moment coefficient is  $C_m = \frac{\pi}{2} \sin(\alpha + 2\beta - 5/4\gamma)$  where  $\beta = 1/4(\psi + \phi)$  and  $\gamma = 1/4(\psi - \phi)$ .  $\psi$  is the angle between the chord and the tangent at the leading edge,  $\phi$  is the angle between the chord and tangent at the trailing edge, and  $\alpha$  is the angle of attack of the airfoil. For  $\psi = 12^\circ$ ,  $\phi = 6^\circ$ , and  $C_a = 1.35$ , the angle of attack  $\alpha = 8^\circ 40'$ . The moment coefficient  $C_m = 0.428$  and the center of pressure  $X_m = (C_m/C_a)t = 0.317 t$ .

Figure 3 shows the basic profile superposed on the square mesh with an angle of attack of  $8^\circ 40'$  and the transformed profile superposed on a

system of the grid flow in such a way that the theoretical center of pressure coincides with the center of the vortex. The angle of attack of the transformed profile was  $64^{\circ} 45'$ .

Experimental tests on this transformed profile indicated that minimum pressure loss,  $\zeta = 0.134$ , occurred when the angle of incidence was  $56^{\circ} 30'$ . Furthermore, the tests showed that the center of pressure of the transformed profile was shifted rearward to point Z, (Fig. 3), instead of remaining at the theoretical point O. If the original profile is shifted so that the new center of pressure again coincided with O, the center of the superposed vortex, and transformed again, a new profile results in which the angle of incidence is  $59^{\circ}$ . Tests with this arrangement again resulted in  $\zeta = 0.134$ .

These transformations were carried out on the assumption that the center of pressure of the vane coincided with the center of the vortex. Kröber performed a third transformation in which, instead of using a single vortex, he used the theoretical distribution of the circulation along the airfoil. The result of this transformation was a new vane profile whose angle of incidence was  $56^{\circ}$ . Tests of this vane indicated that the best performance occurred at an angle of  $55^{\circ}$  for a resistance coefficient,  $\zeta$ , of 0.138. Kröber concluded that, considering low resistance and uniform velocity distribution behind the guide vanes, the two types of approximation may be regarded as practically equivalent. When the vanes were set as a result of the tests at their best angle of incidence, their performance was very similar.

Extensive tests of the transformed profiles were carried out to determine the velocity and pressure distributions. Figure 4(a) shows the velocity distribution and pressure distribution downstream of the grid and Fig. 4(b) shows the pressure distribution about a vane for  $90^{\circ}$  deflection. Similar transformations and tests were carried out for deflection angles of  $60^{\circ}$ ,  $45^{\circ}$ , and  $30^{\circ}$ , the results of which are given in Table I. In the transformation of  $45^{\circ}$  and  $30^{\circ}$  deflections, a lift coefficient,  $C_a = 1.00$ , was chosen in order that the spacing of the vanes be appropriate. The profiles determined

## Abstract 42, Kröber

by the first transformation are shown in Fig. 5, and the tabulated dimensions are given in Table II.<sup>1</sup>

---

<sup>1</sup>Table II was obtained from REPORTS and MEMORANDA NO. 1773, "Note on the Design of Corners in Duct Systems" by G. N. Patterson, and was included to make the abstract complete.

TABLE I

Summary of Experiments on Resistance of Guide Vanes

Angle of Deflection	Shape of Cross Section	Form of Grid	Angle of Attack		Coefficient of Resistance	
			Theoretical	Experimental	With Guide Vanes	Without Guide Vanes
90°	Square	Profile of 1st approximation	64° 15' and 59°	56° 30'	0.134	1.63**
90°	Square	Profile of 2nd approximation	56°	55°	0.138	1.63
90°	Circular	Profile of 1st approximation	59°	56° 30'	0.136	1.0
60°	Square	Profile of 1st approximation	43°*	38°	0.146	1.08
45°	Square	Profile of 1st approximation	33° 15'	33° 15'	0.142	0.53
30°	Square	Profile of 1st approximation	22° 30'*	22° 30'	0.100	0.15
2 x 90°	Square	Profile of 1st approximation	59°	56° 30'	0.260	
2 x 45°	Square	Profile of 1st approximation	33° 15'*	33° 15'	0.266	
2 x 60°	Square	Profile of 1st approximation	43°*	38°	0.304	
90° bend $\frac{R}{b} = 0.7$	Square	Partitions	--	--	0.24	1.10

\*Calculated without taking into account the displacement of the circulation e.g.

\*\*Too high, because of the inadequate length of the outlet channel.

TABLE II  
Profile Dimensions for the Vanes

x/c	y/c			
	90°	60°	45°	30°
0.00	0.000	0.000	0.000	0.000
0.05	0.087	0.041	---	---
0.10	0.154	0.074	0.044	0.031
0.15	0.200	0.100	---	---
0.20	0.236	0.124	0.075	0.051
0.25	0.262	0.140	---	---
0.30	0.277	0.153	0.094	0.067
0.35	0.284	0.161	---	---
0.40	0.284	0.166	0.105	0.071
0.45	0.283	0.168	---	---
0.50	0.273	0.164	0.103	0.071
0.55	0.260	0.157	---	---
0.60	0.242	0.151	0.094	0.067
0.65	0.219	0.142	---	---
0.70	0.192	0.129	0.078	0.055
0.75	0.167	0.111	---	---
0.80	0.137	0.096	0.058	0.043
0.85	0.104	0.072	---	---
0.90	0.071	0.048	0.030	0.024
0.95	0.037	0.026	---	---
1.00	0.000	0.000	0.000	0.000

x = distance along chord (c), and  
y = distance perpendicular to chord.



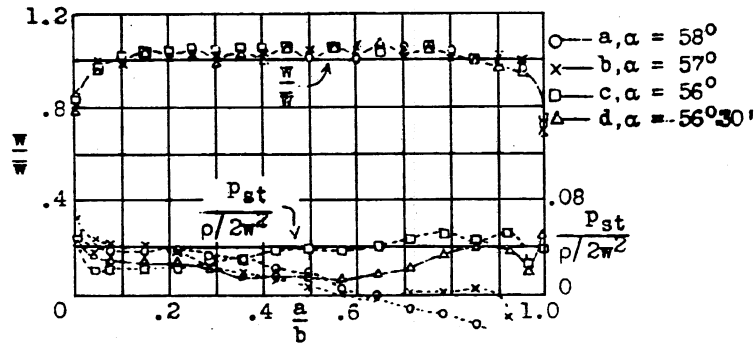


Fig.4(a)-Velocity and Pressure Distributions Downstream of the Cascade

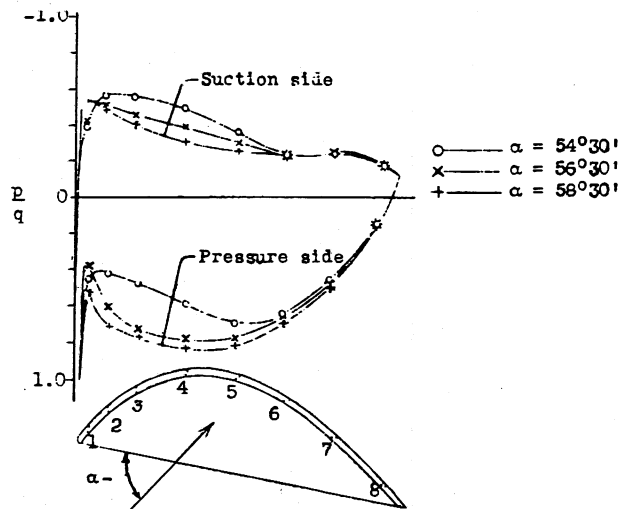


Fig.4(b)-Pressure Distribution on Profile of First Approximation

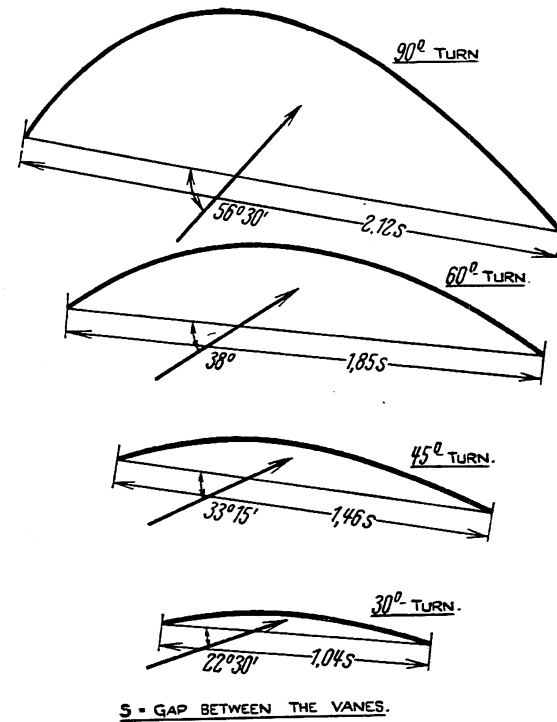


Fig.5-Vane Profiles for Various Corners Obtained by the First Transformation

## Abstract 43

MacPhail, D. C., "Experiments on Turning Vanes at an Expansion," TECHNICAL REPORT OF THE AERONAUTICAL RESEARCH COMMITTEE, R. & M. 1876, 1939, 11 pp., 15 figs.

Separation of the flow from the vane profile is more likely to occur when an expansion is incorporated in the corner. The separation produces a wavy velocity distribution downstream of the vanes. The high velocities occur downstream of the centerline between the vanes, and the low velocities occur downstream of the vanes themselves as shadows. This report describes the results of experiments in which the velocity downstream of turning vanes at an expansion was measured, and in which the effect of several types of screens on the velocity distribution was determined.

The experiments were performed in a channel with a free water surface in the apparatus shown in Fig. 1. The vanes shown in Fig. 2 were spaced 1/2 in. apart in one series of experiments and 1/4 in. apart in the second series of experiments. For the 1/2-in. spacing, separation occurred at both the inside and outside of the bend so that the central jet was slowed up very little. For the narrower spacing, the jet impinged on the outside wall of the vane and separation occurred principally at the inner wall.

The grids used downstream were classified by the constant,  $\underline{C}$ , which is defined as 
$$\underline{C} = \frac{p_1 - p_2}{1/2 \rho U^2}$$
 where  $p_1 - p_2$  is the pressure drop across the screen and  $1/2 \rho U^2$  is the dynamic pressure.

The velocity distributions were measured 0.4 in. upstream and 0.4 in. downstream of the screen. The measurements for the vanes 1/2 in. apart,  $d/r = 0.57$ , are shown in Figs. 3, 4, 5, and 6 for several values of  $\underline{C}$ . The curves are designated as  $\underline{C}$  for the distribution upstream of the screen and as  $\underline{D}$  for the distribution downstream of the screen. The results for the vane spacing of 1/4 in.,  $d/r = 0.29$ , are shown in Figs. 7, 8, 9, and 10, and the corresponding curves are designated A and B respectively. The effect of the screens in reducing large-scale variations is apparent from the figures.

The conclusion was that screens with values of  $\underline{C}$  between 1.4 and 3.0 smoothed the flow most effectively and caused a minimum drop in pressure.

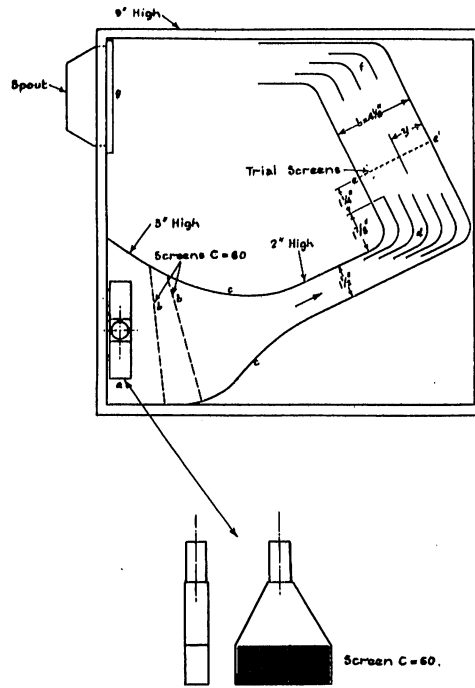


Fig. 1—Plan of Apparatus for Vane Experiments

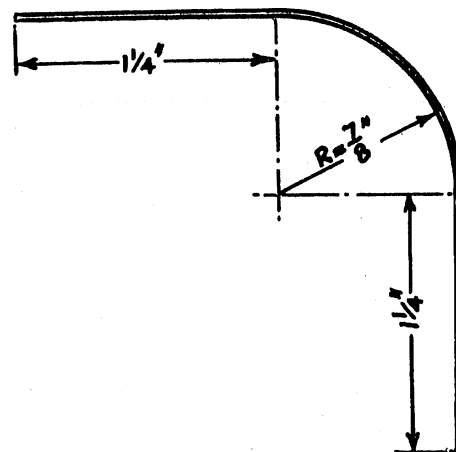


Fig. 2—Profile of Vane Used in Experiments

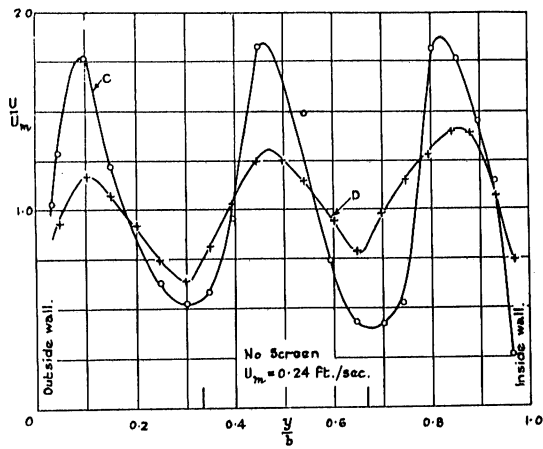


Fig. 3—Velocity Distribution with no Screen,  $\frac{d}{R} = 0.57$

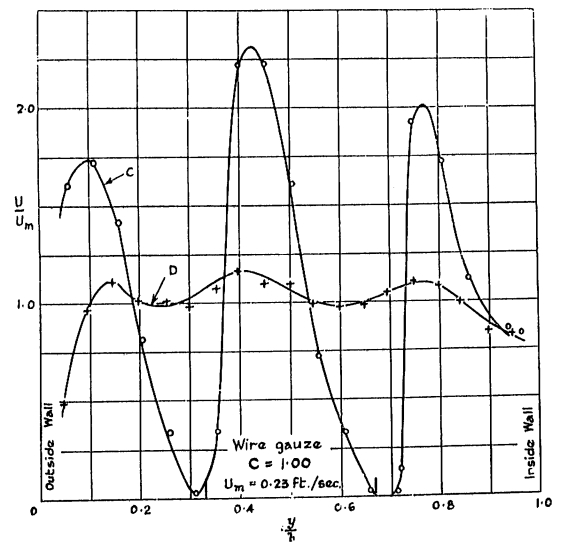


Fig. 4—Velocity Distribution with Screen  $C = 1.00$ ,  $\frac{d}{R} = 0.57$

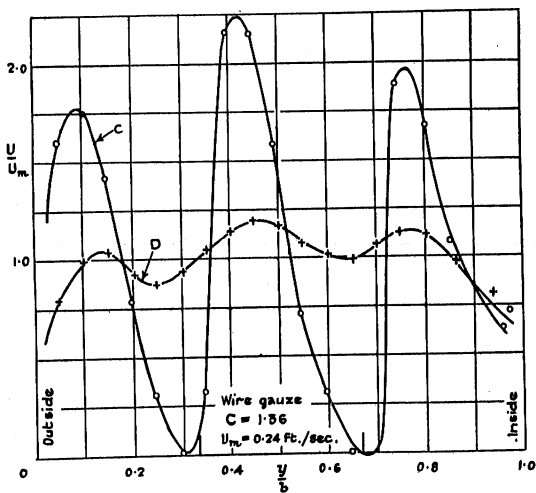


Fig. 5—Velocity Distribution with Screen  $C = 1.36$ ,  $\frac{d}{R} = 0.57$

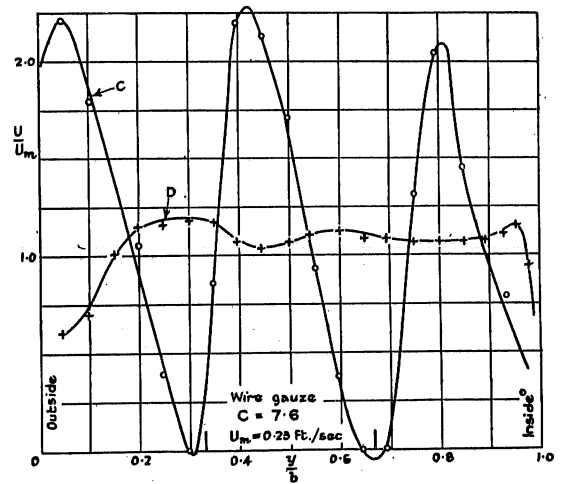


Fig. 6—Velocity Distribution with Screen  $C = 7.6$ ,  $\frac{d}{R} = 0.57$

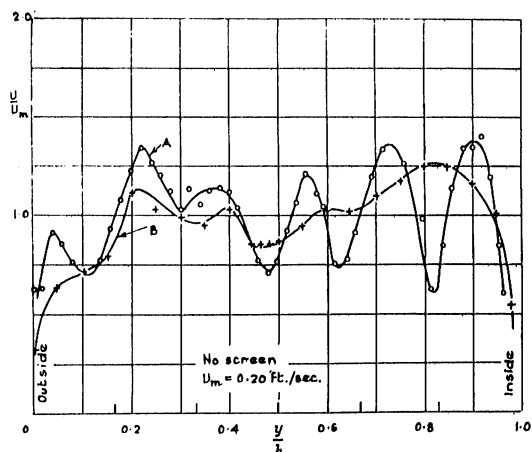


Fig. 7—Velocity Distribution with no Screen,  $\frac{d}{R}=0.29$

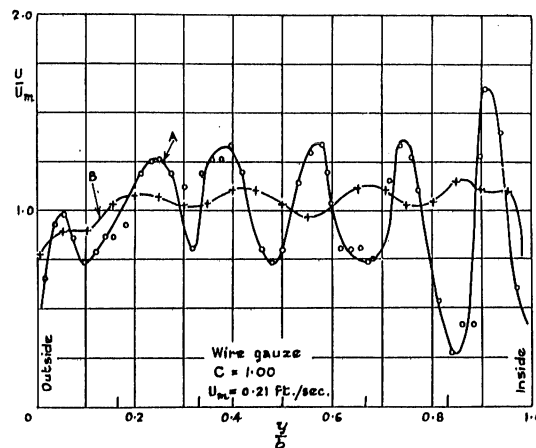


Fig. 8—Velocity Distribution with Screen  $C=1.00, \frac{d}{R}=0.29$

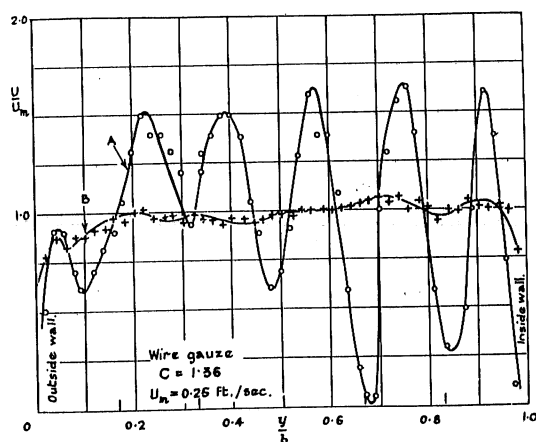


Fig. 9—Velocity Distribution with Screen  $C=1.36, \frac{d}{R}=0.29$

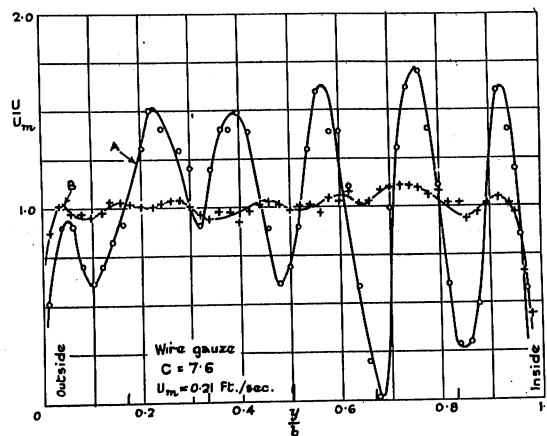


Fig. 10—Velocity Distribution with Screen  $C=7.6, \frac{d}{R}=0.29$

## Abstract 44

Marcinowski, H., "The Significance of the Measured Lattice Characteristics for Calculation and Design of Axial Flow Turbines and Compressors," trans. from German, published by Research and Standards Branch, Bureau of Ships, Navy Dept., May, 1946, 26 pp., 9 figs.

Although this article deals principally with the flow through lattices or cascades in connection with the design of axial flow turbines and compressors, the discussion of lattice characteristics applies also to flow through cascades for the purpose of deflecting the stream. The term, lattice, refers to any row or series arrangement of profiles.

The lift coefficient of a single profile is a linear function of the angle of attack so long as the latter is small. This is also true for profiles in cascades, except that the slope of the curve differs from that of a single profile and must be corrected by interference factors which depend principally upon the spacing ratio and the stagger of the profiles. A method for calculating the change in angle of attack for zero lift of a profile in a cascade as compared to the angle of attack for zero lift of a single profile has been developed by Weinig in the form

$$T = \left(\frac{l}{t}\right)^2 \left[ 18 \frac{d}{l} \sin 2\beta_w + 47 \left(\frac{f}{l}\right) \cos 2\beta_w \right]$$

where  $T$  = the angular change in angle of attack for zero lift,

$\left(\frac{l}{t}\right)$  = the pitch ratio,

$\left(\frac{d}{l}\right)$  = the thickness ratio,

$\left(\frac{f}{l}\right)$  = the camber, and

$\beta_w$  = the stagger angle minus the angle of attack.

The agreement between theory and measurement for the slope of the lift coefficient characteristic curve is best at a stagger angle of about  $15^\circ$ .

The use of lattice interference factors is useful when designing and calculating a blade arrangement by airfoil theory, but the results are valid only for light loading. For highly loaded blade lattices with narrow pitch and large camber, the effect of the boundary layer becomes so important because of the large pressure gradient that it is only possible to determine lattice characteristics by tests. The limits of the theory are due primarily

to the inability to predict (1) the point at which flow separation begins in the partial lattice, that is, the point which corresponds to the maximum lift coefficient of a single airfoil, and (2) the magnitude of the losses within the partial lattice corresponding to the selected values of the lattice parameters and the parameters of the lattice profiles.

Expressions for lattice characteristics must be introduced in order to analyze test data. The load of a lattice may be represented as

$$K = \frac{2\Delta C_u}{w_\infty}$$

where  $w_\infty$  is the geometrical mean value of the relative inlet velocity  $w_1$  and the relative outlet velocity  $w_2$ , and where  $\Delta C_u$  is the deflection of the streamlines parallel to the axis of the lattice.

The losses within the lattice may be expressed as

$$\zeta_v = \frac{2gh_v}{w_1^2 - w_2^2}$$

defined as the ratio of the pressure head loss,  $h_v$ , to the theoretically possible static head increase corresponding to perfect diffusion from the mean inlet velocity,  $w_1$ , to the mean outlet velocity,  $w_2$ . The object of a lattice test will be both the determination of the deflection triangle and the measurement of the loss of energy at various values of  $\beta_s$ . The test results may be presented as  $K = f(\beta_s)$  and  $\zeta_v = f(\beta_s)$ . These two characteristic numbers correspond to the lift coefficient and the drag-lift ratio of a single profile.

## Abstract 45

Merchant, W., "Flow of an Ideal Fluid Past a Cascade of Blades," Part I, TECHNICAL REPORT OF THE AERONAUTICAL RESEARCH COMMITTEE, R. & M. 1890, 1940, 10 pp., 4 figs.

This report deals with the general problem of the flow of an ideal fluid past a cascade of blades, and presents a general relationship which must hold for all types of blades. Since both the velocity potential  $\phi$  and the stream function  $\psi$  obey Laplace's equation for an ideal fluid,

$$\nabla^2 v = \frac{\partial^2 v}{\partial x^2} + \frac{\partial^2 v}{\partial y^2} = 0$$

and if any function of the complex variable is considered,  $w = f(z) = \xi + i\eta$ , where  $z = x + iy$ ,  $\xi$  and  $\eta$  can be identified with  $\phi$  and  $\psi$  and a solution to some flow problems can be obtained for every function of the complex variable. The plane of representation can be changed by using a conformal transformation, and corresponding flows in the new plane can be obtained.

In any cascade of blades there is a direction of flow for which there is no deviation of the fluid stream. If  $\phi$  is the angle of inclination of this direction with the normal to the cascade axis, and the flow net is known for this direction, it can be replotted in the  $\phi - \psi$  plane as a square mesh and the blades will transform into finite lengths of the  $\psi$  lines. Furthermore, if a flow past a uniformly distributed series of laminae on the  $x$ -axis, with no circulation around the laminae and having the angle  $\phi$  to the flow at infinity, is replotted as a simple square mesh in the  $\phi - \psi$  plane, and if the blades transform to the same lengths of the  $\psi$  lines, then we can use the  $\phi - \psi$  plane to transfer other known flows to flows around the actual series of blades in the cascade.

In the equation

$$u - iv = \frac{dw}{dz} = U + \frac{V\sqrt{2} \sin 1/2z}{\sqrt{r + \cos z}} + \frac{W\sqrt{2} \cos 1/2z}{\sqrt{r + \cos z}}$$

where  $(-1 \leq r \leq 1)$ .

The first term represents a uniform flow parallel to the axis of  $x$  and the velocity  $\underline{U}$ . The second term represents the flow of a uniform stream

normal to the cascade and of velocity  $\underline{V}$  at infinity. The third term represents the flow caused by equal circulations around the blades corresponding to velocities of  $\mp W$  parallel to the  $x$ -axis (Fig. 1).

From Joukowski's hypothesis, the stagnation points can be found by equating the above term to zero, if a direction of flow free from circulation is imposed upon the blades and the circulation is added.

If these are the same points as for  $\phi$  with no circulation, it follows that

$$\tan \alpha = \frac{U + W}{V} \tan \beta = \frac{U - W}{V} \tan \theta = \frac{U}{V}$$

Thus the general relationship applicable to all types of blades is given as,

$$\tan \beta = \frac{y \tan \alpha + 2 \tan \phi}{y + 2}$$

Therefore it is seen that the general problem of flow past a cascade becomes two partial problems, first to determine the neutral axis of the cascade and second to determine the length of the transformed laminae along the cascade axis.

For the complete solution for a cascade of straight blades at any angle to the axis and at any pitch-chord ratio,  $\phi$  is known to be the angle the blades make with the normal to the cascade axis, and  $\underline{r}$  can be determined as follows. When the flow is replotted in the  $\phi - \psi$  plane, the length of the laminae is equal to the change in  $\phi$  between the stagnation points. The width of the gap is the change in  $\psi$  between each lamina. Then it is seen that the ratio of change of coordinates is given by

$$\frac{s}{c} = \frac{\frac{\pi}{2} \sec \phi}{\tan \phi \tan^{-1} \left( \frac{\tan \phi}{1 + y} \right) + 1/2 \log \left( \frac{y + 2}{y} \right)}$$

An alternate proof of the general equation is given in the first appendix. In the second appendix, the effect of cascade interference on the lift coefficient of an isolated blade is calculated on the basis of the general

Abstract 45, Merchant

equation for flow through a cascade. The result is given in the form of a ratio

$$\frac{C_{LC}}{C_L} = \frac{2s}{\pi c} \frac{1}{(y + 1) \cos \phi}$$

where  $s/c$  is defined as above.

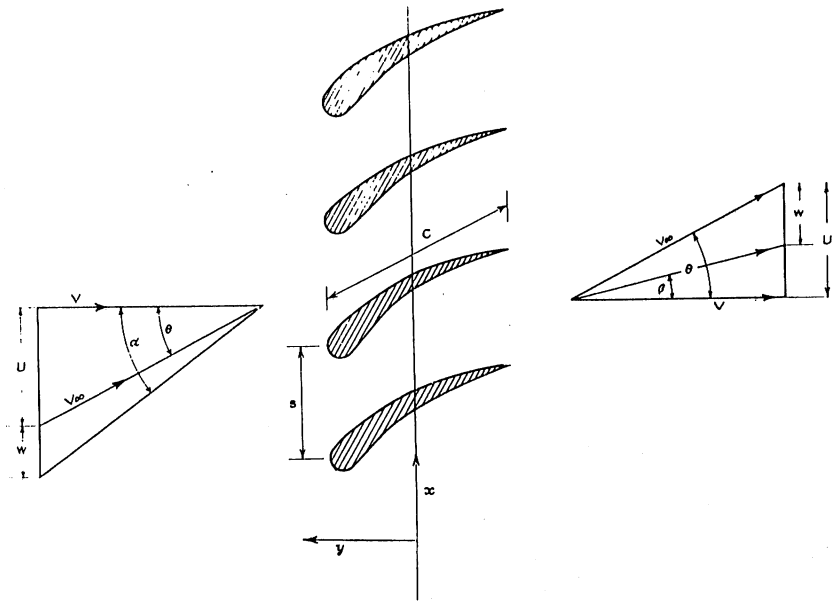


Fig.1—Flow through a Cascade of Airfoils with Circulation

## Abstract 46

Merchant, W., and Collar, A. R., "Flow of an Ideal Fluid Past a Cascade of Blades," Part II, TECHNICAL REPORT OF AERONAUTICAL RESEARCH COMMITTEE, R. & M. 1893, 1941, 6 pp., 2 figs.

This report is a continuation of an earlier report in which the general equation was derived for the flow through a cascade of blades and a complete solution was given for a cascade of straight blades at any angle to the cascade axis with any spacing-chord ratio. The present report gives a method of transforming a cascade of straight blades into a cascade of airfoils. The method is based upon the intermediate transformation of known flow through a cascade of straight blades to flow through a cascade of ovals. If any particular flow past a series of oval bodies on the axis of a complex plane is known, a transformation can be found which converts the ovals into a cascade of straight blades, since the corresponding flow past the latter is known. Moreover, by applying the reverse transformation to the general flow around the straight blades, the general flow around the ovals is obtained. The direct transformation can also be applied to an offset series of ovals, which can then be transformed into a cascade of airfoils.

The authors outline the method as follows:

1. The normal flow past a series of doublets on the imaginary axis is known and can be interpreted as the normal flow past a series of oval bodies.
2. The general flow past a series of laminae lying along the imaginary axis is known; in particular the normal flow is known, and a transformation can therefore be obtained which converts the laminae into the ovals.
3. Application of this transformation to the general flow around the laminae gives the general flow around the ovals.
4. A particular case of the general flow around the ovals is that for which the flow at infinity is inclined to the cascade axis but for which there is no circulation. In this case the ovals can immediately be transformed into a cascade of flat plates parallel to the direction of flow at infinity.
5. Application of the transformation of (4) to an offset series of ovals yields a cascade of airfoils. If the offset ovals

## Abstract 46, Merchant and Collar

pass through the points corresponding to the trailing edges of the inclined flat plates (which are stagnation points in the flow around the transformed ovals) the airfoils will have cusps at their trailing edges.

In the remainder of the report the authors carry out the transformations suggested and develop an airfoil based on the general equations. An illustrative example is also given.

## Abstract 47

Patterson, G. N., "Note on the Design of Corners in Duct Systems," TECHNICAL REPORT OF THE AERONAUTICAL RESEARCH COMMITTEE, R. & M. 1773, pp. 1288-1303, 1936, 12 figs., 2 tables.

This report is a resume of the research on bends with and without vanes. No new research data have been included.

Wirt's method of delineating the streamlines near the boundary by the use of flow casts is discussed. The flow lines were produced by the action of the air upon a mixture of lampblack and oil applied to the interior walls of the bend. These flow lines were preserved by making a plaster cast of the interior of the bend. The flow around a sharp corner was projected upon the outer wall at the turn, with part of it reversing and flowing back into the corner (Fig. 3a, p. 148). When the corner was rounded, the reversed flow did not occur, but the streamlines diverged at the outside wall and flowed toward the inner side along the wall, forming a pair of longitudinal vortices (Fig. 3b, p. 148). The spiral currents met at the center of the inner wall slightly downstream of the midpoint of a  $90^\circ$  bend, and an area of low velocity resulted. Below this point the flow gradually assumed a more uniform distribution.

The resistance of the bend is reduced by rounding the corner and increasing the radius of curvature. By reference to Hofmann (p. 98) and Wirt (p. 147), the author concluded that the resistance of a  $90^\circ$  corner of square or circular section can be made less than 30 per cent of the velocity head if  $R/d > 2.5$ . The radius ratio,  $R/d$ , is the ratio of radius of curvature ( $R$ ) to the width or diameter ( $d$ ) of the duct in the plane of the bend.

According to Wirt's experiments it is possible to reduce the loss by about 50 per cent by increasing the aspect ratio, (the ratio of width normal to the plane of the bend to the width in the plane of the bend), from one to 6. A large radius ratio and a high aspect ratio result in a corner loss of about 20 per cent.

For deflection angles of less than  $90^\circ$ , the loss decreases as the deflection angle decreases. For deflection angles of less than  $25^\circ$ , the loss is negligible.

On the basis of experimental data on corner losses, the author summarizes the properties of an efficient corner as follows:

## Abstract 47, Patterson

a. The corner should be rounded and not sharp. The radius ratio should be 3 or more.

b. A rectangular section of large aspect ratio is better than a circular section.

c. The duct should not be terminated immediately following the corner, but should extend at least four diameters beyond the bend.

d. A  $90^\circ$  corner designed according to the conditions above should have a corner loss of approximately 15 per cent of the velocity head.

The author discusses the use of vanes to reduce corner losses as presented by the experiments of Klein, Tupper, and Green (p. 175). Tests carried out on several types of vanes indicated that uniform velocity distribution on the exit side of the corner can be obtained with vanes of either thin or thick sections. The effect of incidence was the same for all the vanes. The incidence at which the minimum corner loss was obtained was not very critical and was approximately  $45^\circ$  between the chord of the vane and the direction of the incident air stream. Changes in incidence resulted mainly in changing the angle of deflection of the issuing stream.

The most important factor governing the uniformity of the velocity distribution and magnitude of the corner resistance is the gap-chord ratio, (the ratio of the spacing between vanes to the length of the vane chord). In general the velocity distribution improves as the gap-chord ratio decreases, but the corner resistance reaches a minimum value and then increases with further reduction of the gap-chord ratio.

The author discusses in considerable detail the work of Kröber (p. 179) pertaining to the development of vanes based upon aerodynamic theory, and presents a table of dimensions for the resulting vane shapes.

## Abstract 48

Shimoyama, Yoshinori, "Experiments on Rows of Aerofoils for Retarded Flow,"  
MEMOIRS OF THE FACULTY OF ENGINEERING, KYUSHU IMPERIAL UNIVERSITY,  
Fukuoka, Japan, Vol. 8; pp. 281-329, 1936-40, 51 figs.

This report describes experiments on a row of airfoils to determine the interference factor for the lift and drag, compared to that of isolated airfoils. The coefficient of lift for airfoils in cascade is given as

$$C_{LC} = kC_L$$

where  $C_{LC}$  is the lift of an airfoil when in a cascade, and  $C_L$  is the lift of a similar isolated airfoil at the same angle of attack. The experiments were performed principally on a cascade of five airfoils ( $z = 5$ ) arranged with the angle  $\theta$  between the cascade axis and the direction of the tunnel axis varying from  $10^\circ$  to  $27.5^\circ$ , and the angles of attack from  $-5^\circ$  to  $10^\circ$ . The spacing-chord ratio,  $t/\ell$ , varied from 0.75 to 2.0. The airfoil section used was similar to the Gottingen No. 549 profile.

The lift and drag on the airfoil in the cascade were determined by measuring the pressure distribution on the airfoil, and coefficients of lift were compared to the theoretical values obtained by Weinig and are shown in Fig. 1. The effect of the cascade on the drag of the airfoils is shown in Fig. 2, and compared to the drag of an isolated airfoil at corresponding setting. The author's conclusions based on the experiments are as follows:

1. Special care must be taken in estimating the value of the lift coefficient in the design of a propeller pump or propeller fan because the lift coefficient, based on the test result of an isolated airfoil, is too large for retarded flow through a row of the airfoils.

2. The inclination of the curves of lift coefficients for the airfoils in rows, as shown in Fig. 1, becomes steeper for small values of lift coefficient when  $t/\ell$  becomes smaller; and it seems that  $\theta$  has but a little effect upon the inclination.

3. It seems that the theoretical result obtained for the row of flat plates cannot be used directly for the row of airfoils with some thickness and camber if the variation of angle of attack at zero lift is ignored.

4. The inclination of lift coefficient curve, if the inclination alone is taken into consideration, coincides well with the theoretical value; strictly speaking, however, the coincidence is quite good only in the neighborhood of  $\theta = 15^\circ$  and becomes somewhat less favorable when  $\theta$  differs from  $15^\circ$ .

5. The lift coefficient curve for an airfoil in a row, the angle of attack being taken as the abscissa, moves to the right from that of the isolated airfoil. Accordingly, the angle of attack at zero lift varies with  $t/\ell$  and  $\theta$ .

6. The variation of angle of attack at zero lift for an airfoil with some thickness and camber in a row can be calculated approximately by substituting the doublets equivalent to the airfoils in a row. The result is compared with experimental results, both showing good agreement.

7. The results of the present experiment coincide quite well with experimental results on propeller pumps and propeller fans obtained by certain other investigators.

8. On the pressure side of the vane there exists a region of low pressure which is very near to the leading edge, and this negative pressure becomes much larger when  $t/\ell$  becomes smaller. When vanes in a row stand very close to each other, as in the case of  $t/\ell = 0.75$ , low pressure will also occur on the back side of the vane to which the nose of the adjacent vane approaches.

9. The drag coefficient for a row of airfoils of retarded flow is larger than that of the isolated airfoil in the greater part of the angle of attack, and varies with  $t/\ell$  and  $\theta$ .

10. The lift coefficients obtained for the row of nine airfoils for  $t/\ell = 1$  and for the row of seven airfoils for  $t/\ell = 1.5$  may show close agreement with those for the row of airfoils of infinite number. The lift coefficients for the row of five airfoils are entirely similar to those for the rows of seven and nine airfoils. The drag coefficients seem to have no appreciable effect, owing to the variation of the number of airfoils in a row, in the range of five, seven, and nine airfoils.

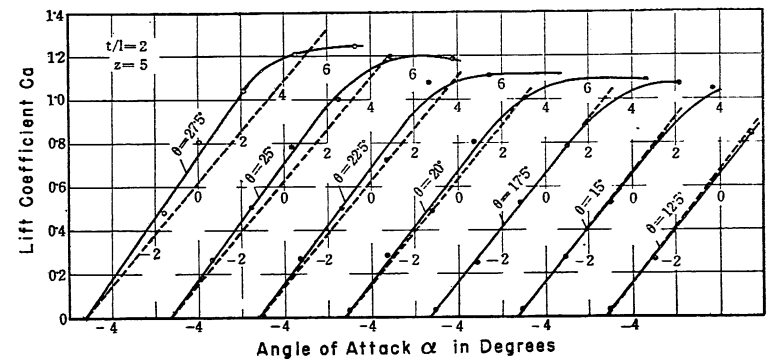
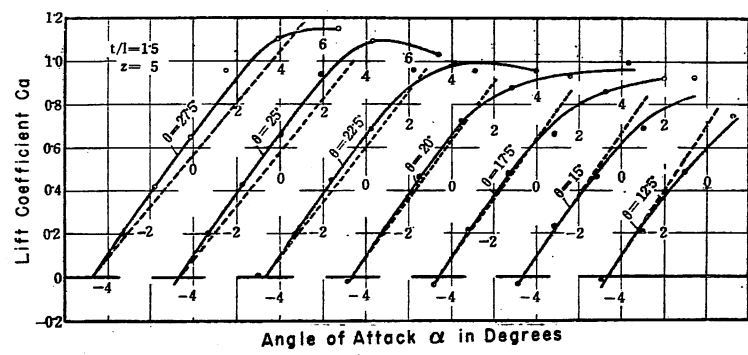
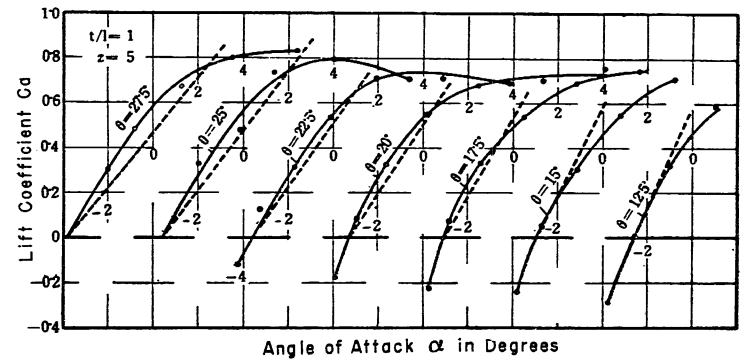
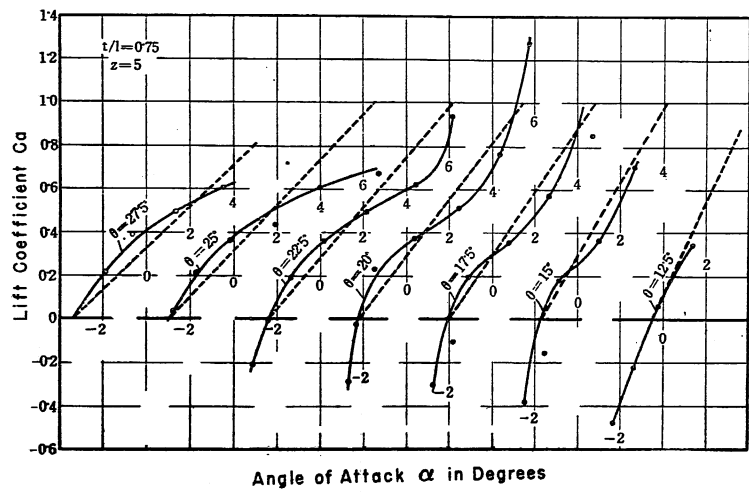


Fig.1-Relation of Lift Coefficient,  $C_a$ , to Angle of Attack,  $\alpha$ , for Airfoils in a Cascade - Theoretical Values are Shown by Dotted Lines

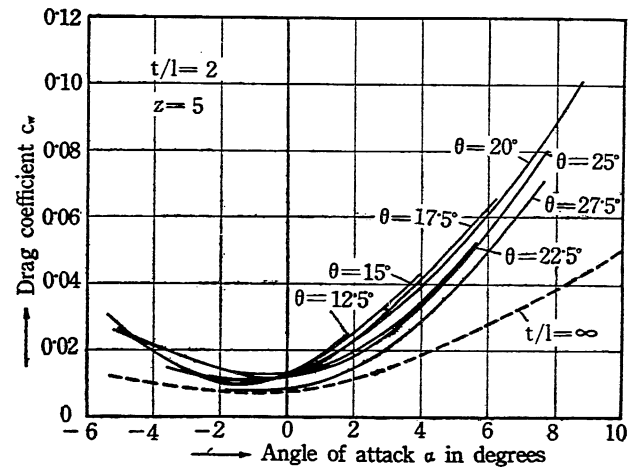
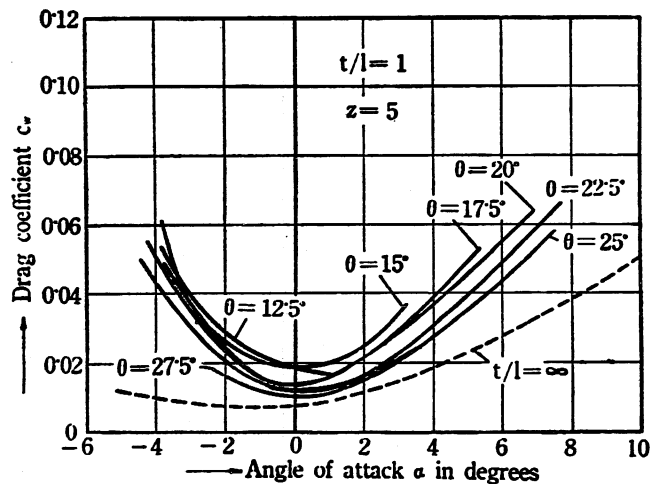
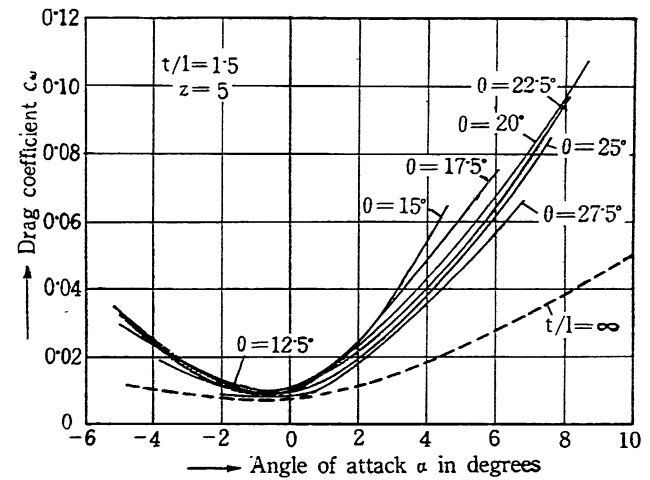
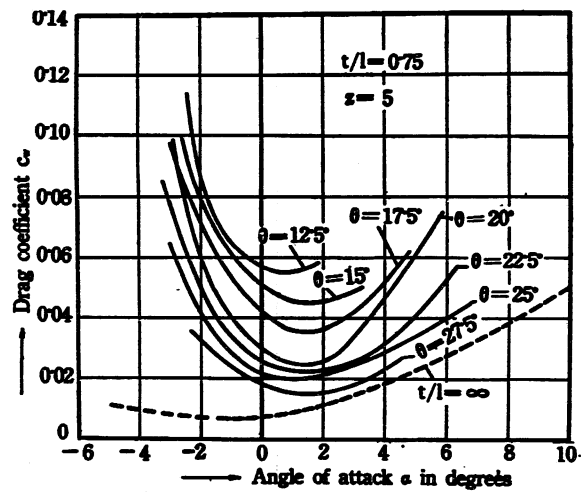


Fig.2-Relation of Drag Coefficient,  $C_w$ , to Angle of Attack,  $\alpha$ , for Airfoils in a Cascade

## Abstract 49

Stuart, M. C., Warner, C. F., and Roberts, W. C., "Effect of Vanes in Reducing Pressure Loss in Elbows in 7-Inch Square Ventilating Duct," TRANSACTIONS, AMERICAN SOCIETY OF HEATING AND VENTILATING ENGINEERS, Vol. 48, pp. 409-424, 1942, 46 figs.

Pressure losses in standard elbows of square cross section and with radius ratios from 0.5 to 4.5 were measured and are plotted in Fig. 1 in terms of equivalent length of straight duct. Additional equivalent length was defined as the length of straight duct having the same loss as that caused by the elbow. The total equivalent length was the sum of the additional equivalent length and the centerline length of the elbow. Fig. 1 compares the losses in elbows with curved outside walls to those with square outside corners and shows nearly double the loss for square corners.

The present investigation was directed largely to determine the effect of vanes and splitters in reducing the pressure loss. The arrangements tested and the results of the tests are shown in tabular form in Figs. 2 and 3. The pressure losses are given in terms of the total equivalent length of duct.

The flow patterns shown in Figs. 4 and 5 were obtained by using a model of the corner in which the upper and lower boundaries were of glass. The vanes were installed between the glass plates. The flow lines were made visible by the use of the "schlieren" apparatus. The flow pictures show the flow lines for elbows corresponding to those shown in Figs. 2 and 3.

The authors conclude from the experiments that:

1. The loss caused by an elbow may be reduced by increasing the radius until the radius ratio is about 2.6.
2. Elbows with square outside walls cause larger losses than do elbows with curved outside walls.
3. Splitters very materially reduce the loss of miter elbows.
4. The simple  $90^\circ$  arc splitter has almost as much effect on reduction of loss as do the more complicated vanes.
5. An "easy" or long radius elbow has less loss than a miter elbow equipped with the best vanes.

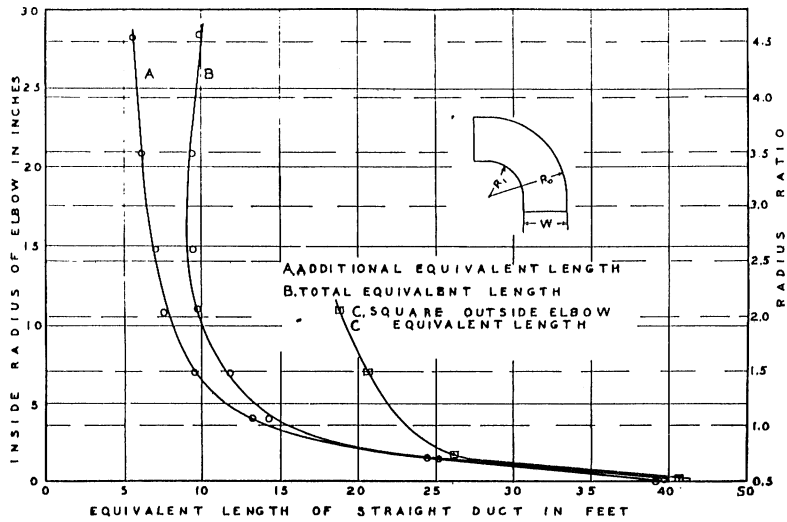


Fig. 1—Relation between Inside Radius of Elbows and Equivalent Length of Straight Duct

ELBOW TYPE	RATIO	TOTAL EQUIVALENT LENGTH OF DUCT							
		0	5	10	15	20	25	30	35
MITER	0	[Bar chart showing equivalent length values]							
	1	[Bar chart showing equivalent length values]							
	2	[Bar chart showing equivalent length values]							
	3	[Bar chart showing equivalent length values]							
	4	[Bar chart showing equivalent length values]							
	5	[Bar chart showing equivalent length values]							
	6	[Bar chart showing equivalent length values]							
	7	[Bar chart showing equivalent length values]							
	8	[Bar chart showing equivalent length values]							
	9	[Bar chart showing equivalent length values]							
COMMERCIAL A	2 4	[Bar chart showing equivalent length values]							
	3 5	[Bar chart showing equivalent length values]							
	2 4 6	[Bar chart showing equivalent length values]							
COMMERCIAL B	3 5 7	[Bar chart showing equivalent length values]							
	COMMERCIAL C	[Bar chart showing equivalent length values]							
SPLITTER 90° 1/4 TRAILING EDGE	4 6 8	[Bar chart showing equivalent length values]							
	5 7 9	[Bar chart showing equivalent length values]							
HEISEN VANES	4 6 8	[Bar chart showing equivalent length values]							
	5 7 9	[Bar chart showing equivalent length values]							

Fig. 2—Equivalent Length of Straight Duct of all Vanes When Tested in Miter Elbows

ELBOW TYPE	RATIO	TOTAL EQUIVALENT LENGTH OF DUCT							
		0	5	10	15	20	25	30	35
MITER	0	[Bar chart showing equivalent length values]							
	1	[Bar chart showing equivalent length values]							
	2	[Bar chart showing equivalent length values]							
	3	[Bar chart showing equivalent length values]							
	4	[Bar chart showing equivalent length values]							
	5	[Bar chart showing equivalent length values]							
	6	[Bar chart showing equivalent length values]							
	7	[Bar chart showing equivalent length values]							
	8	[Bar chart showing equivalent length values]							
	9	[Bar chart showing equivalent length values]							
192° I.R.	2 4	[Bar chart showing equivalent length values]							
	3 5	[Bar chart showing equivalent length values]							
	4 6	[Bar chart showing equivalent length values]							
	5 7	[Bar chart showing equivalent length values]							
	6 8	[Bar chart showing equivalent length values]							
	7 9	[Bar chart showing equivalent length values]							
	8 10	[Bar chart showing equivalent length values]							
	9 11	[Bar chart showing equivalent length values]							
	10 12	[Bar chart showing equivalent length values]							
	11 12	[Bar chart showing equivalent length values]							
4" I.R.	4 6 8	[Bar chart showing equivalent length values]							
	5 7 9	[Bar chart showing equivalent length values]							
	6 8 10	[Bar chart showing equivalent length values]							
	7 9 11	[Bar chart showing equivalent length values]							
	8 10 12	[Bar chart showing equivalent length values]							
	9 11 12	[Bar chart showing equivalent length values]							
	10 12	[Bar chart showing equivalent length values]							
	11 12	[Bar chart showing equivalent length values]							
	12	[Bar chart showing equivalent length values]							
	12	[Bar chart showing equivalent length values]							

Fig. 3—Equivalent Length of Straight Duct of Splitters When Tested in Standard Elbows of Various Radii

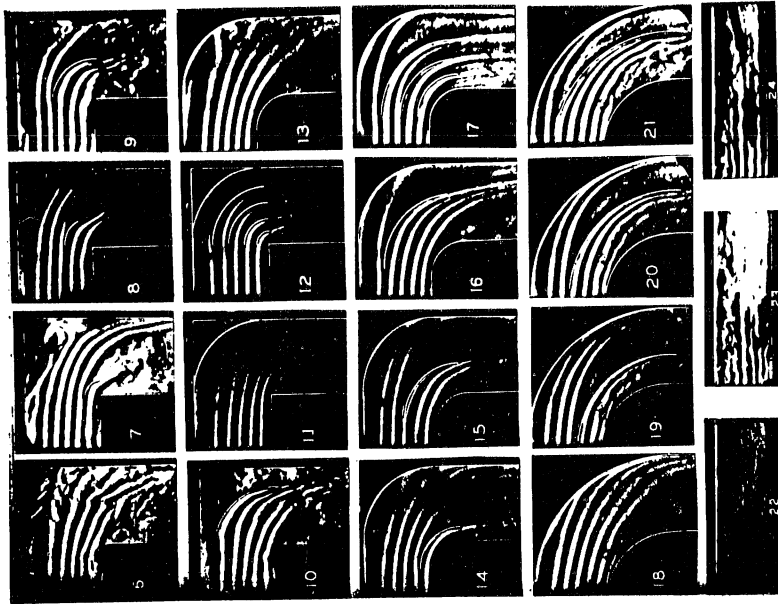


Fig.5-Photographs of the Flow through  
Various Bends

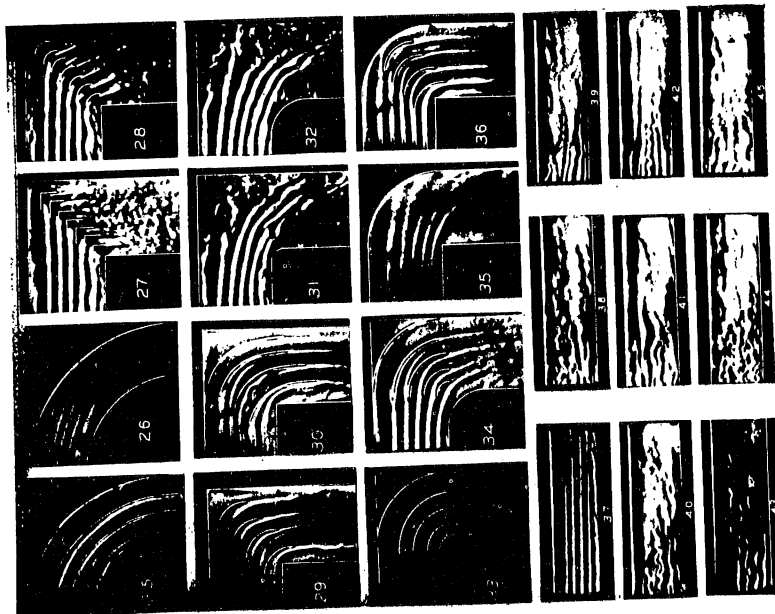


Fig.4 - Photographs of the Flow through  
Various Bends

## Abstract 50

Weinig, F., "The Flow around Turbine and Compressor Blades," trans. from German pub. by Research and Standards Branch, Bureau of Ships, Navy Department, May, 1946, 173 pp., 120 figs.

This paper is a treatise on the flow through grids of blades. It presents the basic mechanics of the flow through given blade profiles, and describes methods of obtaining profiles by conformal mapping to satisfy certain flow conditions.

The paper first discusses the mechanics of the flow through profile grids and past single airfoil sections. The purpose of a grid is to deflect the flow in a prescribed manner with resulting release of energy to the flow machine. The deflection of the flow depends upon the desired velocity triangles as determined from turbine theory.

The author develops the concept of an equivalent grid of straight line profiles for which the flow conditions are known when the profiles are placed at the no-lift angle of attack. A further condition of flow through a grid of straight profiles is obtained by mapping conformally the field of the straight profiles to the exterior of a unit circle at symmetrically located singularities. Initially, the relation of a given deflection triangle to the characteristics (length, angle of inclination, angle of attack) of a straight profile are developed. By conformal mapping and especially by use of the hodograph method, the flow about the straight profiles is analyzed in a picture plane as the flow about a unit circle deformed by the placing of sources or sinks and vortices outside and inside the circle. Curves for the determination of the straight profile parameters are presented. The principal parameters in the straight profile plane are  $t/l$ , the ratio of profile spacing along the grid axis to profile length, and  $\beta$ , the angle between the normal to the grid axis and the straight profile. In the conformal picture plane ( $\zeta$  plane) they are  $\alpha_{st}$ , the angle between the  $\zeta$ -axis and the front stagnation point, and  $R$ , the distance (in units of picture circle radius) along a parallel to the  $\zeta$ -axis from the origin to the required sources or sinks and vortices. A fifth parameter,  $k$ , represents the ratio of the lift coefficient in grid arrangement to that of a single straight profile.

On the basis of this transformation, the author derives the forces on a straight profile in a grid in relation to a single straight profile and

## Abstract 50, Weinig

draws the following conclusions: (1) In a grid with a small pitch ratio,  $t/\ell < 0.7$ , the outflow angle is independent of the inflow angle, (2) the outflow angle is equal to the grid angle of the equivalent straight profile grid, and (3)  $k$  approaches unity for large  $t/\ell$  and is approximately unity for  $\beta = 50^\circ$  and  $t/\ell \gg 1.4$ ; for  $t/\ell < 0.7$ ,  $k$  varies directly with  $t/\ell$  and inversely with  $\cos \beta$ . The equivalent straight profile grid can be determined from the prescribed flow changes and, upon establishment of the equivalent grids of straight profiles, it can be transformed to an equivalent grid of more appropriate profiles.

Given a grid of actual profiles, an equivalent grid of straight profiles can be found which will have the same characteristics and hence provide a means of determining the velocity distribution. In the case of a profile of the Joukowski type, the equivalent straight profile is obtained by mapping between the plane which contains the circle determining the actual profile and the plane which contains the unit circle and determines the straight profile. The basic points of comparison between the profiles are the zero lift direction, the lift on the profiles, and the deflection of the flow. By approximate methods the equivalent grid of straight profiles can be determined for profiles of any shape, including circular arcs of different pitch ratios. The results on the basis of calculation agree satisfactorily with test measurements made on grids.

The paper includes a discussion of the flow net method for determining the properties of a profile grid. It describes the procedure and explains methods of checking the resulting flow net for correctness. The development of pressure and velocity curves for the profile grid may also be based on the flow net method. Practical limits in selection of actual blade shapes to prevent cavitation and separation are also discussed. The paper concludes with an example of the treatment to determine a profile grid to meet prescribed conditions of inflow and outflow.

## Abstract 51

Hegly, V. M., "Flow in Earthen Canals of Compound Cross-Section," abridged trans. from ANNALES DES PONTS ET CHAUSSEES, Vol. 106, pp. 445-528, 1936, appearing in Proceedings, American Society of Civil Engineers, Vol. 63, pp. 36-48, November, 1937, 4 figs.

This paper reports experiments on models of a proposed earthen channel of compound cross section. Three experimental canals were used; the dimensions of the first were one-twentieth of the prototype dimensions, and the second and third were built to one-fiftieth scale. The first two were straight but the third was curved in plan on a 230-ft radius, with a length of 230 ft. All the models were made of clay soil, carefully tamped and rolled on a bed slope of 0.0001, except as later modified. The data and results pertaining to the curved channel are included in this abstract. The proportions of the curved channel cross section are shown in Fig. 1.

Longitudinal profiles of the water surface in each canal were taken on the centerline of each part and above the top of the slope connecting the two parts of the cross section. The curved channel was investigated with the deep part of the cross section, first against the concave side and then the convex side. Measurements were also made upon decelerating flow.

Typical cross sections of the curved canal showing velocity curves derived from Pitot tube observations are given in Figs. 1 (a) and 1 (b). The position of the maximum velocity for the curved channel was displaced toward the concave bank a distance ranging from 32 to 13 cm as compared to the similar straight canal. The author does not state where the measurements were made on the curve, but presumably they were made at the midpoint. The displacement was found to be somewhat less for experiments in which the deep part was against the convex bank. The ratio of the mean velocity in the shallow part of the channel to the mean velocity in the deep part of the channel was found to be 0.716 when the deep part was against the concave bank and 0.753 when the shallow part was against the concave bank, as compared to 0.688 for a comparable straight channel. The increase in the first case was due principally to the change in distribution of the velocity. The stronger velocities near the concave bank were partly reduced by friction along the bank, while the weaker velocities in the shallow part remained unchanged. In the second case the ratio was more marked because the higher velocity from the deep part invaded the shallow part and caused an increase in its velocity. Furthermore, the velocity in the deep part was reduced.

The slopes of the water surface for these experiments were considerably greater than those for the corresponding straight canal. This is explained as caused by the increased frictional resistance against the concave bank. The propelling force thus tends to be reduced and can be compensated for only by an increase in the slope of the water surface. The increase of slope was more marked when the deep part was near the concave bank.

The author presents Flamant's equation for the slope of a water-course on a smooth curve as (in metric units)

$$S = \frac{V^2}{d} \left( b + \tau \sqrt{\frac{\ell}{r}} \right) \quad (1)$$

where  $\tau$  is a coefficient of fluid friction against the bank resulting from centrifugal force,  $d$  is the depth,  $\ell$  is the average width of the bed at the curve, and  $r$  is the radius of curvature. Values of  $\tau$  were not definitely determined but apparently ranged between 0.0003 and 0.0005. In applying equation (1) to the curved canal the author replaced  $d$  by  $R$ , the mean hydraulic radius of the cross section. The first term of equation (1) then became  $S = V^2 b/R$ . This is another form of the Chezy formula where  $c = 1/\sqrt{b}$ . The value of  $c$  in the experiments averaged close to 50, corresponding to a value of  $b$  of 0.0004, the average value suggested by Flamant. Consequently, the second term of equation (1) must represent the loss of head caused by the effect of centrifugal force on the friction. In equation (1) the second term may be used for computing a close approximation to the additional loss of head caused by curvature.

The author concludes with respect to the curved canal that the region of maximum velocity in the deep part of the section is displaced practically an equal amount toward the concave bank regardless of whether the deep part is against the concave or convex bank. The reduction of the mean velocity in the shallow part was less than for a straight canal.

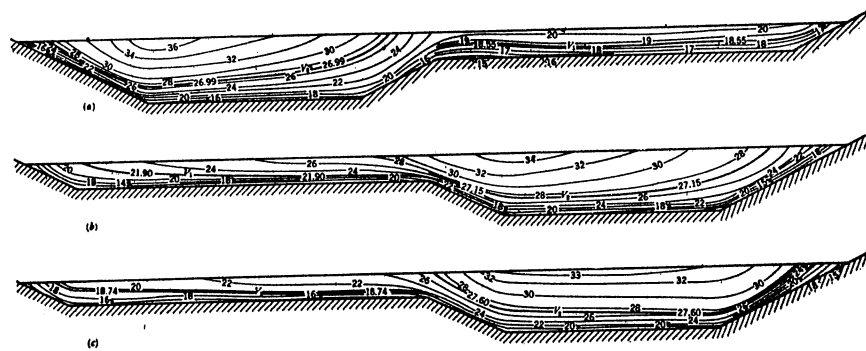


Fig.1—Velocity Distribution in Curved Canal, and Comparison with Straight Canal (a) Deep Part on Concave Side,  $Q=72.4$  liters per sec; (b) Deep Part on Convex Side,  $Q=76.0$  liters per sec; (c) Straight Canal,  $Q=75.2$  liters per sec

## Abstract 52

Mockmore, C. A., "Flow Around Bends in Stable Channels," TRANSACTIONS OF THE AMERICAN SOCIETY OF CIVIL ENGINEERS, Vol. 109, Paper No. 2217, pp. 593-628, 1944, 21 figs., 4 tables.

The purpose of these experiments was to study the flow phenomena around a stable curved channel. Transparent pyralin sections of a rectangular open channel 18 in. wide and 10 in. deep were built so that they could be assembled into various bends and tangents.

The channel was laid on a slope of 0.005 per cent and the depth of flow was controlled by a tailgate at the outlet. The rate of flow was measured by means of a calibrated concrete volumetric measuring tank, and the current velocities were measured by means of a midget current meter and were checked with a carefully calibrated Pitot tube. The effect on the particular phenomena under consideration of the backwater curve caused by the tailgate was considered to be negligible.

The experiments were divided into two distinct sets. In the first, the rate of flow was held constant at 0.449 cu ft per sec while the velocity was varied and, in the second, the mean velocity was held constant at 0.5 ft per sec while the discharge was varied.

In the experiments reported on, the equipment was arranged so that two 180° bends were connected by a 4-ft tangent. The inside walls of the bends were circular arcs of 1-ft radius and the cross sections through the bend were the same as those through the straight reaches. From a 2-to-1 contraction there were 12 ft of straight channel upstream of the first bend, but the effect of the bend could be seen the total length of the upstream tangent. The conditions at the entrance to the second bend did not repeat those of the first. This indicated that the tangent between the two bends was too short to isolate the second bend from the disturbance caused by the first.

Rice grains, fine sawdust, and a mixture of n. Butyl Plithalate and technical Xylol colored with a deep red oil dye having the same specific gravity as water were used to obtain a qualitative picture of the nature of the flow around the bend. Floats consisting of 3/8-in. hedgewood cubes, boiled in paraffin, were used to study the angular velocity of the water surface. A composite picture made from several frames of a 16-mm motion picture illustrates directions of the flow at different depths around the bend. The

existence of higher filamental velocities along the inside of the bend is substantiated and the formation of a turbulent eddy at the inside wall of the downstream end of the bend is illustrated. The cross currents were found to be more pronounced at the bottom of the stream.

The u-, v-, and w-components are defined as the velocities along the x-, y-, and z-axes respectively. The origin is at the base of the stream in the center, the y-axis extends positively upward, the x-axis extends across the channel, and the z-axis is positive in the primary direction of flow in the channel. The author made the following assumptions in his analysis of a frictionless fluid flowing around a bend:

1. Parabolic variation of the u-component of the velocity, starting with zero at each side wall and becoming a maximum on the y-axis midway between the two sidewalls; straight line variation of the u-component, starting with zero at the mid-depth of the channel and becoming a maximum at the top and bottom with opposite signs.

2. Straight line variation of the v-component of the velocity starting with zero on the y-axis and becoming maximum on each side wall, with opposite signs; parabolic variation of the v-component starting with zero at the top and bottom of the channel, with a maximum value at mid-depth.

3. Parabolic variation of the w-component of the velocity, starting with zero at the bottom of the channel and becoming maximum at the water surface; parabolic variation of the w-component starting with zero at each side wall and becoming a maximum on the y-axis midway between the two side walls.

These assumptions led to equations of motion that closely approximated the observed results. Diagrams are plotted to show the nature of the velocity profiles, both in cross section and along the direction of flow in the channel.

The author listed the following conclusions, which he believes are justified by the observations of bends in stable channels:

1. Spiral flow in the bends of open channels, as enunciated by James Thomson, certainly does exist, although the pattern is an exceedingly complex one.

2. The downstream components of the filamental velocities in the first half of the bend are greater at the convex bank than at the concave bank and vary across the channel in close agreement with the laws of a free vortex.

3. The angular velocities and accelerations inherent to the spiral motion constitute strong contributing factors to the movement of bed load, not only in a downstream direction but toward the inside of bends.

4. At about three-fourths the way around the bend there is a tendency for the development of an eddy or slack water along the inside bank caused by the spiral motion, which is conducive to the deposition of suspended matter and the formation of a bar.

## Abstract 53

Raju, Sanjiva P., "Resistance to Flow in Curved Open Channels," abridged trans. from MITTEILUNGEN DES HYDRAULISCHEN INSTITUTS DER TECHNISCHEN HOCHSCHULE, MUNCHEN, Vol. 6, pp. 45-60, 1933, appearing in Proceedings, American Society of Civil Engineers, Vol. 63, pp. 49-55, November, 1937, 5 figs.

Some experiments on open channel bends of  $R/B = 1$  and  $R/B = 5$ , in which the bend coefficient,  $\zeta$ , was determined for various conditions of flow, are described in this paper. Two bends were investigated--one having a uniform width,  $B$ , of 300 mm and a radius of curvature,  $R$ , of 1500 mm,  $R/B = 5$ ; and the other having the same width but a radius of curvature of 300 mm,  $R/B = 1$ . The bends were  $90^\circ$  deflections in rectangular channels with a horizontal bed throughout the entire length.

The total head loss was first determined for a straight channel section. Insertion of a bend created a disturbance that increased the head loss. The bend loss was obtained by subtracting the friction loss from the total head loss. The bend loss coefficient was calculated from the relationship

$$\zeta = \frac{h_b}{V_b^2/2g}$$

where  $V_b$  is the mean velocity in the bend and  $h_b$  is the head loss caused by the bend. The friction coefficient,  $\lambda$ , for the straight channel sections was evaluated from the Darcy-Weisbach equation

$$h_f = \lambda \frac{V_m^2}{2g} \frac{L}{4R_m}$$

where  $V_m$  is the mean velocity throughout the significant length of channel,  $R_m$  is the mean hydraulic radius through the entire length of channel, and  $L$  is the length of channel in which  $h_f$  occurs.

The friction loss in the straight channel was determined from the measurements by the following equation

$$h_f = (Z_3 - Z_{12}) - \frac{(V_{12}^2 - V_3^2)}{2g}$$

Abstract 53, Raju

in which  $Z_3$  and  $Z_{12}$  are the observed elevations of the water surface at stations 3 and 12 respectively, and  $V_{12} = Q/A_{12}$  and  $V_3 = Q/A_3$ . From measurements made with the bend in place, the bend loss was similarly determined by

$$h_b = (Z_3 - Z_{12}) - \frac{(V_{12}^2 - V_3^2)}{2g} - h_f$$

Figure 1 is a diagram of the test flume and Fig. 2 shows a smoothed curve of the variation of  $\lambda$ , with Reynolds number for the channel computed from  $Re = 4V_m R_m / \nu$ . The variation of the computed bend coefficient  $\zeta$  for the two bends and the corresponding depth-width ratio  $d/B$  are shown in terms of Reynolds number in Fig. 3. The computed  $\zeta$  for the bend,  $R/B = 5$ , did not deviate far from 0.04 throughout the observed range, but for  $R/B = 1$  varied considerably, first decreasing and then increasing. The values of  $\zeta$  lie between 0.31 and 0.17 and are five to nine times as large as they are for the bend,  $R/B = 5$ .

A comparison with the results of Hofmann (p. 98) shows equal values of  $\zeta$  for  $Re = 146,000$  and for  $R/B = 1$ , but only about half as large a value for  $R/B = 5$  (Fig. 4).

For the bend  $R/B = 1$ , the influence of the form of the cross section and the velocity on  $\zeta$  is indicated in Fig. 5. The value of  $\zeta$  decreases with  $d/B$ , but increases with the velocity.

In these experiments the bend caused a difference in elevation of the water surface on the outer and inner sides of the channel for a distance of  $1.3B$  before, and  $2B$  after the bend.

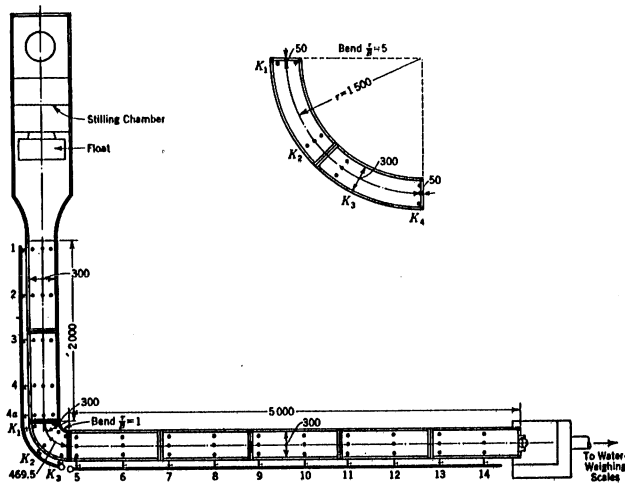


Fig. 1—The Test Flume (Diameters, in Millimeters)

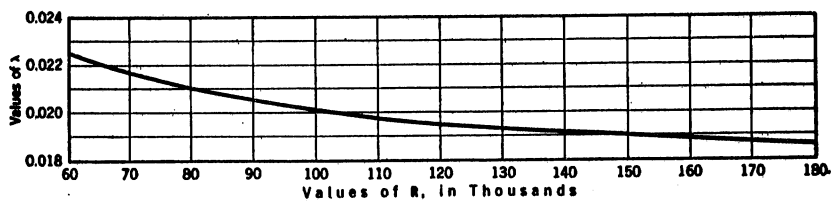


Fig. 2—Darcy-Weisbach Friction Coefficient,  $\lambda$ , as a Function of R

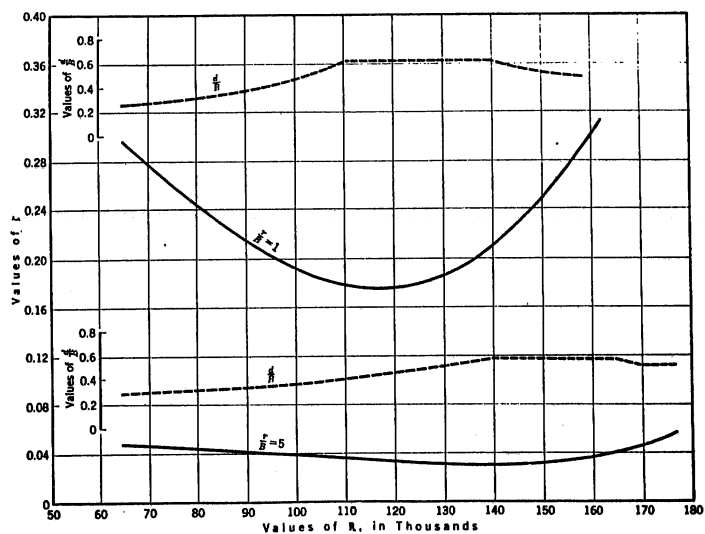


Fig. 3—Bend Resistance Coefficient,  $\zeta$ , as a Function of R

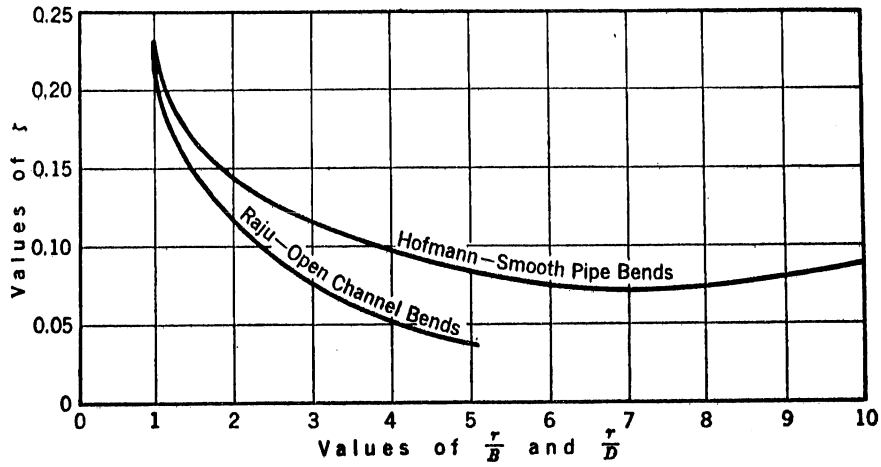


Fig.4-Bend Resistance Coefficient,  $\zeta$ , as a Function of  $\frac{r}{B}$  (in Open Channels) and  $\frac{r}{D}$  (in Smooth Pipes)

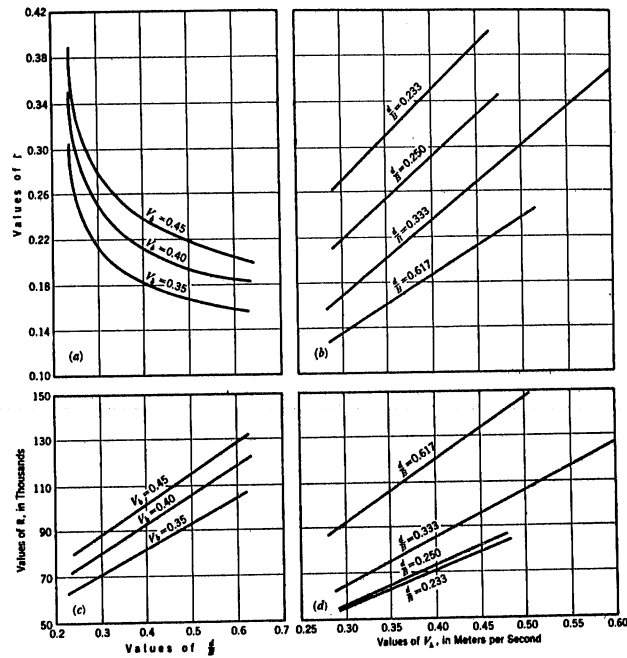


Fig.5-Bend Resistance Coefficient,  $\zeta$ , for the Bend  $\frac{r}{B} = 1$ , as a Function (a) of  $\frac{d}{B}$ , and (b) of  $V_b$ . Corresponding Values of  $R$  are Shown in (c) and (d)

## Abstract 54

Ripley, H. C., "Relation of Depth to Curvature of Channels," TRANSACTIONS OF THE AMERICAN SOCIETY OF CIVIL ENGINEERS, Vol. 90, Paper No. 1599, pp. 207-265, 1927, 16 figs., 35 tables.

The object of this paper is to record the results of the author's investigations pertaining to curvature of rivers. Presented in the paper are two empirical formulas by which the cross profile of a channel bend may be computed.

$$Y = D\left(1 - \frac{X^2}{W^2}\right) + D \frac{17.52}{R} \left(1 - \frac{X^2}{W^2}\right) X \quad (1)$$

$$Y = P\left(1 - \frac{X^2}{W^2}\right) + P \frac{26.28}{R} \left(1 - \frac{X^2}{W^2}\right) X \quad (2)$$

where  $D$  = the mean depth of the channel in feet, multiplied by 1.445,

$P$  = the mean depth of the channel in feet, multiplied by 1.65,

$W$  = the half width of the channel in feet,

$R$  = the radius of curvature in feet on the concave side of the channel, and

$X$  and  $Y$  = the coordinates of the cross profile of the channel, the origin being in the center of the channel at the surface of the water.

The author makes the following comments regarding the formulas:

1. Formula (1) is applicable to all streams of whatever size where the channel occupies the entire width of the waterway, with certain restrictions.

2. Formula (2) is applicable to channels not occupying the entire width of the waterway and to channels at entrances created by the action of a single curved jetty.

3. The algebraic sign of  $X$  must be recognized in the solution of the equations.

4. Whenever the radius of curvature is less than 40 times the square root of the area of the channel, no further deepening of the channel results from the increased curvature. Hence, in such cases the value to be given to  $R$  in the formula must be equal to  $40\sqrt{\text{area}}$ .

5. Whenever the radius of curvature is greater than about  $50\sqrt{\text{area}}$ , the shape of the cross-profile does not conform strictly to that caused by curvature.

6. Formula (2) is not applicable to straight channels nor to curved ones where the radius exceeds about  $110\sqrt{\text{area}}$ .

7. On a "cross-over bar" where the channel is neither on a curve nor in a straight reach, the maximum depth is about  $14\frac{1}{2}$  per cent less than its computed value.

8. Formula (2) gives a width of channel at mean depth about 20 per cent greater than the actual width; hence, the width of the channel at mean depth, as given by the formula, must be reduced by 20 per cent to obtain its exact value.

The author tested the formulas by comparing the computed cross-profiles with the measured cross-profiles for a large number of curves ranging in size from the Brazos River, with a cross-sectional area of 5000 sq ft, a width of 336 ft, and a radius of curvature of 1250 ft, to the Mississippi River, and a cross-sectional area of 153,000 sq ft, a width of 3000 ft, and a radius of curvature of 36,600 ft.

The discussion that followed the paper presented data pertaining to many further specific instances of bends where cross-profiles were available.

## Abstract 55

Schwarz, A. I., "Flow of Water in Channels Curved in Vertical Plane to an Arc of a Circle," (In Russian), TRANSACTIONS OF THE SCIENTIFIC RESEARCH INSTITUTE OF HYDROTECHNICS, Leningrad, Vol. 16, pp. 129-147, 1935.

This article reports a study of flow of water in channels whose longitudinal profile has considerable curvature.

The following assumptions have been made:

- a. The channel has the shape of a circular arc.
- b. The cross sections of the channel are rectangular.
- c. The depth of flow is small as compared with the radius of curvature of the channel.
- d. Velocities at all points of the cross section are equal.

Euler's theorem, concerning the relation between the change in the component of the momentum along any line and the components of external forces along the same line, may be applied to an elementary volume of the moving body of water which possesses the above-enumerated characteristics.

As a result of the application of this theorem to the flow under consideration, the following differential equation was obtained:

$$\frac{dh}{d\theta} = \frac{\frac{-q^2}{gh} \tan \theta - h^2 \sin \theta - \frac{q^2}{g(2R-h)} \tan \theta + Rh \sin \theta}{\frac{q^2}{gh^2} - h \cos \theta - \frac{q^2}{g(2R-h)^2}} + \frac{+ R \frac{2q^2}{(2R-h)h} \tan \theta + R \left(2 \frac{h}{b} + 1\right) \lambda \frac{q^2}{gh^2}}{\frac{q^2}{gh^2} - h \cos \theta - \frac{q^2}{g(2R-h)^2}} \quad (1)$$

where  $h$  = variable depth of the stream,

$\theta$  = angle which the cross section having the depth  $h$  makes with the vertical,

$R$  = radius of curvature of the channel

$q$  = discharge per unit width of the channel,

$b$  = width of the channel, and

$\lambda = g/C^2$  ( $g$  = acceleration of gravity;  $C$  = Chezy's coefficient).

Equation (1) could not be integrated. Therefore, in order to compute the curve of the free surface of a stream, recourse was had to the method of approximate integration.

By analysis of this equation, however, certain general conclusions may be drawn regarding the conditions of flow in cases studied in this paper. The most important of these conclusions is the following: when the depth of the stream reaches a certain depth ( $h_{lv}$ ), the value  $dh/d\theta$  tends to infinity, which shows that there is a break in continuity of flow. Thus an analogy exists between the conditions of flow usually considered in hydraulics (gradually varying) and those assumed in this paper. It is necessary to note, however, that there is a considerable difference between the depth  $h_{lv}$  and the critical depth  $h_k$ ; while the critical depth in steady flow is constant, the depth  $h_{lv}$  depends upon the values of  $R$  and  $\theta$ , and may be found from the following equation:

$$\left(\frac{h_k}{h_{lv}}\right)^3 - \cos \theta - \frac{\frac{h_k}{h_{lv}}}{\left(2 \frac{R}{h_k} - \frac{h_{lv}}{h_k}\right)^2} = 0 \quad (2)$$

in which the symbols and letters have the same significance as above.

For practical computations equation (2) can be replaced by a more simple one

$$h_{lv} = h_k / \sqrt[3]{\cos \theta} \quad (3)$$

which gives sufficiently accurate results.

In consideration of the above-mentioned difference between  $h_{lv}$  and  $h_k$ , the depth  $h_{lv}$  may be termed as the "limiting" depth. Using equations (1) and (2), or (1) and (3), a series of practical problems in connection with the design of various hydraulic structures can be solved.

One of such problems has been analyzed in this paper; namely, the determination of the limiting value of discharge over a spillway ending in a toe shaped to an arc of a circle, at which discharge the jet at the toe would be submerged. The solution of this problem is accomplished by determining

## Abstract 55, Schwarz

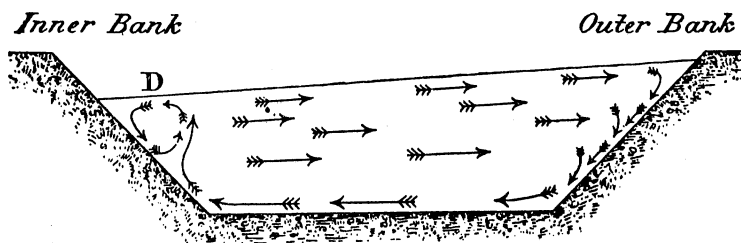
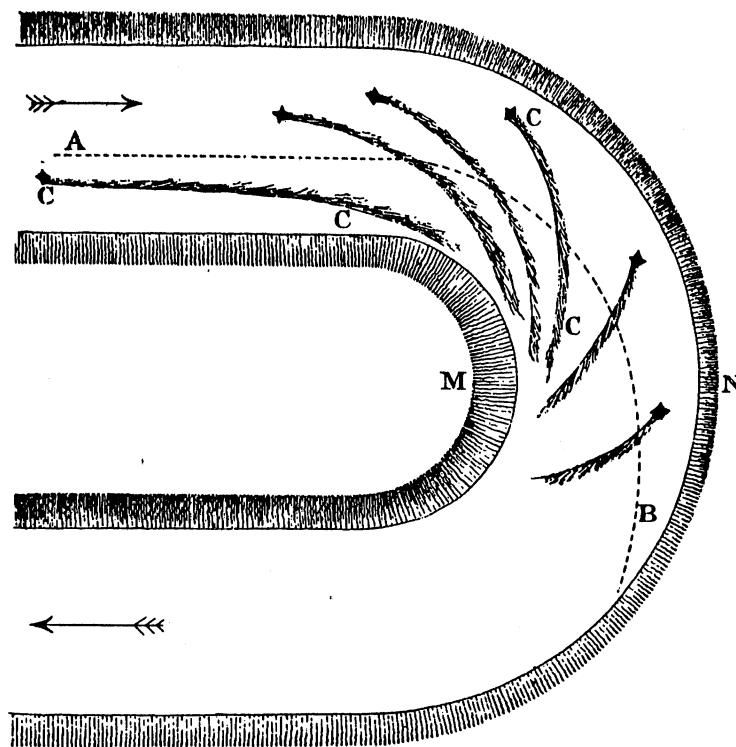
the discharge at which the depth at the end of the toe will be equal to the "limiting" depth. Such a solution involves a considerable amount of purely calculatory work. Therefore, an approximate solution of the same problem has been presented, based upon equations (2) and (3). In addition, this solution has been compared with the results of experiments which checked sufficiently close to the theoretical computations.

## Abstract 56

Thomson, J., "Experimental Demonstration in Respect to the Origin of Windings of Rivers in Alluvial Plains and to the Mode of Flow of Water Round Bends of Pipes," PROCEEDINGS OF THE ROYAL SOCIETY OF LONDON, Vol. 26, pp. 356-357, 1877.

This article describes experiments in a model to demonstrate the existence of spiral currents in the bend of an open channel. The author constructed a small open channel with a  $180^{\circ}$  bend about 8 in. wide and 1 to 2 in. deep. The paths of the streamlines were shown in several ways: by means of threads attached at various elevations to pins set in the stream bed; by means of granules of sand and seeds such as clover and poppy; and by means of specks of dye adhering to the bed. The threads and the seeds showed that the direction of the currents near and at the bottom were directed toward the inner bank at rather sharp angles with the main current, while the particles on the surface moved gradually toward the outer bank as shown in the sketch of Fig. 1. The velocity of the water toward the inner bank near the bed was relatively greater than the outward flow of the filament near the surface because the flow area near the bed was limited to a relatively small thickness while the outward flow encompassed a much larger area.

The reasoning advanced for this phenomena was based on the centrifugal force of the water flowing around the bend and the friction of the water on the bed of the stream. A transverse slope at the bend rising toward the outer bank is counterbalanced by the centrifugal force. Because of the friction of the bottom, however, the velocity near the bottom is decreased with a consequent lessening of the centrifugal force on the water in this area. Therefore, near the bottom the pressure gradient developed by the stream is greater than the opposing centrifugal force in this region. Consequently, water flows toward the inner side of the bend with a corresponding outward flow near the surface. The superposition of this circulation upon the main flow results in a spiral current being developed in the flow around the bend.



*Section at M N.*

Fig.1-Diagrammatic Sketch of Streamlines  
Around an Open Channel Bend

## Abstract 57

Yen, C. H., and Howe, J. W., "Effects of Channel Shape on Losses in a Canal Bend," CIVIL ENGINEERING, Vol. 12, pp. 28-29, January, 1942, 1 table, 2 photos.

The experiments reported in this article were undertaken to determine the effect of the channel shape on the loss of energy in the flow around a bend in an open channel. The major changes made in the channel shape consisted of shifting the inner and outer walls and the bottom, thus changing the proportions of the channel at the bend. The experiments were performed in a 10- by 11-in. channel having a  $90^\circ$  bend with a straight approach tangent of 24 ft and a straight discharge tangent of 48 ft. The water surface was determined by the use of bottom piezometers in the bend and tangents. Three methods were used to determine the head loss caused by the bend.

1. Two stations upstream and downstream of the bend were used as reference points. The measured loss of head between these two stations, minus that caused by a straight channel of equal length, was taken as the loss resulting from the bend.

2. The vertical difference between the hydraulic grade lines for the upstream approach tangent and the downstream discharge tangent was considered the loss of head caused by the bend.

3. The vertical difference between the average total head gradient upstream and downstream of the bend was taken to be the loss resulting from the bend.

All of the measured losses occurring as a result of changes in the shape of the bend were compared to those resulting from the so-called normal bend, that is, the bend with a constant cross section equal to the approach and discharge tangents.

The results of the experiments are tabulated in Table I, where the losses resulting from the several changes in cross section are listed for comparison with the normal channel.

The following conclusions are given as a result of the study:

1. Loss of head through a rectangular channel bend can be reduced either by (a) shifting the inner wall away from the centerline of the channel, or by (b) narrowing the width of the channel

and increasing the depth to provide a constant cross-sectional area for a given discharge.

2. If the loss of head is to be kept at a minimum, the width of the channel around the bend should never be narrowed without lowering the bed sufficiently to compensate for the loss in cross-sectional area.

3. In the  $90^\circ$  bend with a uniform width of 11 in. and a 5-ft radius of curvature, the head loss was found to follow the empirical formula  $H_b = 0.380 V^2/2g$  where  $H_b$  = head loss in ft caused by the bend,  $V$  = mean velocity in ft per sec in the approach channel, and  $g$  = acceleration resulting from gravity. The maximum deviation from this formula was about 10 per cent.

TABLE I. SUMMARY OF EXPERIMENTAL DATA  
Flows in Cu Ft Per Sec

Description of Model Bend	Width at Middle Section of Bend		Head Loss in Bend							
			Flow, 0.95		Flow, 0.77		Flow, 0.62		Flow, 0.38	
	In.	% Increase or Decrease	Ft	% Increase or Decrease	Ft	% Increase or Decrease	Ft	% Increase or Decrease	Ft	% Increase or Decrease
a. Normal bend with 5-ft radius of curvature.....	11.00	0	0.038	0	0.033	0	0.031	0	0.028	0
b. Both walls shifted toward centerline of channel.....	7.70	-30	0.188	+400	0.167	+400	0.156	+406	0.137	+385
c. Same as b. with bottom curved down.....	7.70	-30	0.033	-11.0	0.032	-7.5	0.032	+2.7	0.060	+112
d. Both walls shifted outward from centerline of channel.....	14.30	+30	0.036	-4.5	0.031	-7.5	0.030	-2.7	0.036	+26
e. Same as d. with bottom curved up....	14.30	+30	0.036	-4.5	0.032	-5.0	...	...	...	...
f. Outer wall shifted toward centerline of channel.....	9.35	-15	0.072	+93.0	0.068	+105	0.066	+116	0.062	+118
g. Outer wall shifted outward from centerline of channel.....	12.65	+15	0.038	+2.2	0.036	+7.5	0.035	+13.5	0.033	+18.0
h. Inner wall shifted toward centerline of channel.....	9.35	-15	0.071	+89.0	0.068	+103	0.066	+113	0.061	+115
i. Inner wall shifted outward from centerline of channel.....	12.65	+15	0.034	-9.0	0.030	-10.0	0.028	-8.0	0.032	-6.0

A D D E N D U M  
T O  
B I B L I O G R A P H Y

(November, 1950)

## I. Flow Through Conduit Bends

- (181) Carrier, G. F., "Elbows for Accelerated Flow," JOURNAL OF APPLIED MECHANICS, Vol. 14, No. 2, pp. 108-112, June, 1947. Applies conformal mapping to obtaining an elbow shape with given increase in velocity over a given distance.
- (182) Gregorig, Romano, "Turbulente Stromungen in geraden und gekrümmtten glatten Rohrleitungen bei hohen Reynoldschen Zahlen," (Turbulent Flow in Straight and Curved Smooth Conduits for High Reynolds Numbers), Eidgenössischen Technischen Hochschule, Zurich, Switzerland, Bulletin No. 695, 1933. Experiments on smooth bends 1.7 inch and 3.5 inches in diameter at high Reynolds numbers show an increase in bend loss for Reynolds numbers above about  $3 \times 10^5$ .
- (183) Hawthorne, W. R., "Secondary Circulation in Fluid Flow," Unpublished paper of Gas Turbine Laboratory of Massachusetts Institute of Technology. Demonstrates from vector equations for vorticity that secondary circulation is consequence of vorticity of mean flow in boundary layer. Contains verification of equations with experimental data.
- (184) "Hydraulic Model Studies of Green Mountain Penstock," U. S. Bureau of Reclamation, Hydraulic Machinery Laboratory Report No. HM-6, June, 1941, 9 pp., 10 figs. Several different elbow shapes, including one with vanes, were studied for relative efficiency in a  $90^\circ$  penstock bend.
- (185) Krantz, A. P., MacIntire, H. J., and Gould, R. E., "Flow of Liquids in Pipes of Circular and Annular Cross Sections," University of Illinois Bulletin No. 222, 1931, 26 pp. Head losses measured in  $1\frac{1}{4}$  in. and 2 in. standard cast iron  $90^\circ$  elbows for Reynolds numbers between  $Re = 1000$  and  $Re = 40,000$ .
- (186) Schoder, E. W., and Vanderlip, A. M., "Long Versus Short Body Fittings for Water Supply," Cornell University, Bulletin No. 20, September, 1935, 102 pp., 30 figs., 24 tables. Contains results of experiments, on 6- and 12-in. diameter long and short radius cast-iron elbows, and a discussion of results.
- (187) Silberman, E., "The Nature of Flow in an Elbow," University of Minnesota, St. Anthony Falls Hydraulic Laboratory Project Report No. 5, December, 1947, 61 pp., 43 figs. This is a report of experimental measurements and discussion of results in a radius elbow of square cross section.
- (188) Watkins, Franklin M., "Hydraulic Loss in Pipe Bends," Bureau of Reclamation, Denver, Colo., 1936. An analysis of head loss was made by means of the rebound polygon method using published experimental data.

- (189) Weske, J. R., "Investigation of the Flow in Curved Ducts at Large Reynolds Number," JOURNAL OF APPLIED MECHANICS, Vol. 15, No. 4, pp. 344-348, December, 1948. An investigation is reported which attempts to relate the pressure drop in a radius elbow to the momentum deficiency in a boundary layer near the inside of the bend.
- (190) Young, A. D., Green, G. L., and Owen, R. R., "Tests of High-speed Flow in Right-angled Pipe Bends of Rectangular Cross-section," TECHNICAL REPORT OF THE AERONAUTICAL RESEARCH COMMITTEE, R. & M. 2066, October, 1943, 28 pp. This is a study of compressible flow in a bend observed by means of shadowgraphs.

## II. Flow Through Conduit Bends With Guide Vanes

Note: In the years during and since World War II, a great deal of work was done on guide vane systems or cascades in connection with gas turbine and compressor work. Only a few of the resulting reports which are applicable to guide vane bends were selected for inclusion in this addendum and the original bibliography.

- (189) Carter, A. D. S., "Three-Dimensional Flow Theories for Axial Compressors and Turbines," PROCEEDINGS OF THE INSTITUTION OF MECHANICAL ENGINEERS, Vol. 159, No. 4, pp. 255-268, 1948. Discusses secondary currents in bends provided with guide vanes.
- (190) Carter, A. D. S., and Cohen, E. M., "Preliminary Investigation into the Three-Dimensional Flow Through a Cascade of Aerofoils," TECHNICAL REPORT OF THE AERONAUTICAL RESEARCH COMMITTEE, R. & M. 2339, 1946. Discusses secondary currents and losses in a three-dimensional flow through guide vanes. Contains theoretical analysis and experimental verification.
- (191) Davis, H., "A Method of Correlating Axial-Flow Compressor Cascade Data," TRANSACTIONS, AMERICAN SOCIETY OF MECHANICAL ENGINEERS, Vol. 70, No. 8, pp. 951-955, November, 1948. Introduces charts relating the cascade characteristics to the deflection angle and expansion or contraction of the flow.
- (192) de Haller, P., "Application of Electrical Analogy to the Investigation of Cascades," PROCEEDINGS, SIXTH INTERNATIONAL CONGRESS OF APPLIED MECHANICS, Paris, September, 1946. Describes electrolytic tank and compares pressure distributions obtained in tank and in wind tunnel.
- (193) Erwin, J. R., and Emery, J. C., "Effect of Tunnel Configuration on Cascade Performance," NATIONAL ADVISORY COMMITTEE FOR AERONAUTICS, Technical Note 2028, February, 1950. Discusses effect of end wall boundary layers and number of blades on experimental measurements.
- (194) Garrick, I. E., "On the Plane Potential Flow Past a Lattice of Arbitrary Airfoils," NATIONAL ADVISORY COMMITTEE FOR AERONAUTICS, Report No. 788, 1944, 16 pp. This is a conformal mapping method of computing flow past a cascade applicable to small combs. It requires a great deal of labor.

- (195) Hausmann, G. F., "The Theoretical Induced Reflection Angle in Cascades Having Wall Boundary Layers," JOURNAL OF AERONAUTICAL SCIENCE, Vol. 15, No. 11, pp. 686-690, November, 1948. This is a theoretical discussion of the secondary currents in guide vane cascades and the reason different installations give deflection angles for a given cascade.
- (196) Holdhusen, J. S., and Lamb, O. P., "Model Experiments for the Design of a Sixty-Inch Water Tunnel, Part V, Vaned Elbow Studies," University of Minnesota, St. Anthony Falls Hydraulic Laboratory Project Report No. 14, September, 1948. Experimental data on a specific water tunnel bend equipped with guide vanes are given.
- (197) Howell, A. R., "A Theory of Arbitrary Airfoils in Cascade," PHILOSOPHICAL MAGAZINE, Vol. 39, pp. 913-927, December, 1948. This is a conformal mapping method of computing flow through guide vanes of arbitrary profile but limited to small spacing-chord ratio and small combs.
- (198) Katzoff, S., Finn, R. S., and Laurence, J. C., "Interference Method for Obtaining the Potential Flow Past an Arbitrary Cascade of Airfoils," NATIONAL ADVISORY COMMITTEE FOR AERONAUTICS, Technical Note No. 1252, 1947. An approximate method for computing theoretical flow past guide vanes of arbitrary shape is reported.
- (199) Lighthill, M. J., "A Mathematical Method of Cascade Design," TECHNICAL REPORT OF THE AERONAUTICAL RESEARCH COMMITTEE, R. & M. 2104, June, 1945. This is a conformal mapping method of designing guide vane profiles with a given velocity distribution. It requires a great deal of labor.
- (200) Mutterperl, W., "A Solution of the Direct and Inverse Potential Problems for Arbitrary Cascades of Airfoils," NATIONAL ADVISORY COMMITTEE FOR AERONAUTICS, Wartime Report L4K22b, December, 1944. Presents a theoretical method for obtaining the flow past given guide vane shapes or the shapes required to produce a given flow. The method is sensitive to small changes and lacks accuracy.
- (201) Silberman, E., "Fluid Flow Diversion by Guide Vanes in Miter Bends," University of Minnesota, St. Anthony Falls Hydraulic Laboratory Project Report No. 8, April, 1949. These are results of experiments and discussion based on tests with several shapes of thick and thin guide vanes in a 90° bend in a square duct.

- (202) Traupel, W., "Calculation of Potential Flow Through Blade Grids," SULZER TECHNICAL REVIEW, No. 1, pp. 28-42, 1945. A conformal mapping method of calculating flow through thick, highly-cambered guide vanes is given.
- (203) "Water Tunnel Vaned-Turn Studies," Pennsylvania State College, Serial 1947 No. 7958-64, September 10, 1947. Results of experimental measurements on a specific water tunnel elbow with guide vanes are presented.
- (204) Westphal, W. R., and Dunavant, J. C., "Application of the Wire-Mesh Plotting Device to Incompressible Cascade Flows," NATIONAL ADVISORY COMMITTEE FOR AERONAUTICS, Technical Note No. 2095, May, 1950. Describes a mechanical device for obtaining the two-dimensional flow past guide vanes.

## III. Flow in Open Channel Bends

- (205) Shukry, Ahmed, "Flow Around Bends in an Open Flume," PROCEEDINGS OF THE AMERICAN SOCIETY OF CIVIL ENGINEERS, Vol. 75, No. 6, 1941, pp. 713-741, June, 1941. Experimental data and discussion pertaining to measurements of secondary flows in an open channel are detailed.